

1984

Synthetic, stereochemical, and electronic studies of organophosphorous ligands and their transition metal complexes

James Timothy Spencer
Iowa State University

Follow this and additional works at: <https://lib.dr.iastate.edu/rtd>

 Part of the [Inorganic Chemistry Commons](#)

Recommended Citation

Spencer, James Timothy, "Synthetic, stereochemical, and electronic studies of organophosphorous ligands and their transition metal complexes" (1984). *Retrospective Theses and Dissertations*. 7727.
<https://lib.dr.iastate.edu/rtd/7727>

This Dissertation is brought to you for free and open access by the Iowa State University Capstones, Theses and Dissertations at Iowa State University Digital Repository. It has been accepted for inclusion in Retrospective Theses and Dissertations by an authorized administrator of Iowa State University Digital Repository. For more information, please contact digirep@iastate.edu.

INFORMATION TO USERS

This reproduction was made from a copy of a document sent to us for microfilming. While the most advanced technology has been used to photograph and reproduce this document, the quality of the reproduction is heavily dependent upon the quality of the material submitted.

The following explanation of techniques is provided to help clarify markings or notations which may appear on this reproduction.

1. The sign or "target" for pages apparently lacking from the document photographed is "Missing Page(s)". If it was possible to obtain the missing page(s) or section, they are spliced into the film along with adjacent pages. This may have necessitated cutting through an image and duplicating adjacent pages to assure complete continuity.
2. When an image on the film is obliterated with a round black mark, it is an indication of either blurred copy because of movement during exposure, duplicate copy, or copyrighted materials that should not have been filmed. For blurred pages, a good image of the page can be found in the adjacent frame. If copyrighted materials were deleted, a target note will appear listing the pages in the adjacent frame.
3. When a map, drawing or chart, etc., is part of the material being photographed, a definite method of "sectioning" the material has been followed. It is customary to begin filming at the upper left hand corner of a large sheet and to continue from left to right in equal sections with small overlaps. If necessary, sectioning is continued again—beginning below the first row and continuing on until complete.
4. For illustrations that cannot be satisfactorily reproduced by xerographic means, photographic prints can be purchased at additional cost and inserted into your xerographic copy. These prints are available upon request from the Dissertations Customer Services Department.
5. Some pages in any document may have indistinct print. In all cases the best available copy has been filmed.

**University
Microfilms
International**
300 N. Zeeb Road
Ann Arbor, MI 48106

8423673

Spencer, James Timothy

SYNTHETIC, STEREOCHEMICAL, AND ELECTRONIC STUDIES OF
ORGANOPHOSPHORUS LIGANDS AND THEIR TRANSITION METAL
COMPLEXES

Iowa State University

PH.D. 1984

**University
Microfilms
International** 300 N. Zeeb Road, Ann Arbor, MI 48106

PLEASE NOTE:

In all cases this material has been filmed in the best possible way from the available copy. Problems encountered with this document have been identified here with a check mark ✓.

1. Glossy photographs or pages _____
2. Colored illustrations, paper or print _____
3. Photographs with dark background _____
4. Illustrations are poor copy _____
5. Pages with black marks, not original copy _____
6. Print shows through as there is text on both sides of page ✓
7. Indistinct, broken or small print on several pages _____
8. Print exceeds margin requirements _____
9. Tightly bound copy with print lost in spine _____
10. Computer printout pages with indistinct print _____
11. Page(s) _____ lacking when material received, and not available from school or author.
12. Page(s) _____ seem to be missing in numbering only as text follows.
13. Two pages numbered _____ . Text follows.
14. Curling and wrinkled pages _____
15. Other _____

University
Microfilms
International

Synthetic, stereochemical, and electronic studies
of organophosphorus ligands and their
transition metal complexes

by

James Timothy Spencer

A Dissertation Submitted to the
Graduate Faculty in Partial Fulfillment of the
Requirements for the Degree of
DOCTOR OF PHILOSOPHY

Department: Chemistry
Major: Inorganic Chemistry

Approved:

Signature was redacted for privacy.

~~In~~ Charge of Major Work

Signature was redacted for privacy.

~~For the Major Department:~~

Signature was redacted for privacy.

For the Graduate College

Iowa State University
Ames, Iowa

1984

TABLE OF CONTENTS

	Page
LIST OF COMPOUNDS	xvii
LIST OF ABBREVIATIONS	xxvi
DEDICATION	xxvii
PREFACE	1
PART I. PREPARATION, STRUCTURE, AND TRANSITION METAL COMPLEXES OF DIOXAPHOSPHORUS LIGANDS	3
INTRODUCTION	4
EXPERIMENTAL	29
Materials	29
Techniques	30
Preparations	35
Reactions	62
RESULTS AND DISCUSSION	68
Reactions of \geq P-X Compounds with X Acceptors	68
Reactions of \geq P(X)-Transition Metal Complexes with X Acceptors	73
Reactions of \geq P(NR ₂) Compounds with Acids	74
Reactions of \geq P(NR ₂)-Transition Metal Complexes with Acids	85
Reactions of \geq P-Cl Compounds with Transition Metal Nucleophiles	90
Dimeric Iron Complexes	92
PART II. CRYSTALLOGRAPHIC STUDIES OF THE CIS AND TRANS COMPLEXES OF [Fe(η^5 -Cp)(CO)(μ -5,5-Dimethyl-1,3,2- dioxaphosphorinane)] ₂	171
INTRODUCTION	172

EXPERIMENTAL	174
Structural Determination of the cis-[Fe(η^5 -Cp)(CO)(μ -5,5-DMP)] ₂	174
Structural Determination of the trans-[Fe(η^5 -Cp)(CO)(μ -5,5-DMP)] ₂	177
RESULTS AND DISCUSSION	222
PART III. CRYSTALLOGRAPHIC STUDY OF [Fe(η^4 -C ₅ H ₆)(CO)(μ -4,4,5,5-tetramethyl-1,3,2-dioxaphospholane) ₂ Fe(CO) ₃]	251
INTRODUCTION	252
EXPERIMENTAL	264
Synthesis of [Fe(η^4 -C ₅ H ₆)(CO)(μ -P(OC(Me) ₂ C(Me) ₂ O)) ₂ Fe(CO) ₃]	264
Structural Determination	265
RESULTS AND DISCUSSION	284
PART IV. STEREOCHEMICAL STUDIES OF ORGANOPHOSPHORUS TRIESTERS WITH PHOSPHORUS AS THE PRIMARY CHIRAL SITE	300
INTRODUCTION	301
EXPERIMENTAL	311
Materials	311
Techniques	311
Preparations	314
RESULTS AND DISCUSSION	336
Chiral Triesters	336
Diastereomeric Organophosphorus Esters	346
Chiral Stationary Phase HPLC	355
Diastereomeric Platinum(II) Complexes	357
CONCLUSIONS	366
REFERENCES	369
ACKNOWLEDGMENTS	383
APPENDIX I	385
Stereopair Drawings and Unit Cell Drawing of cis-[Fe(η^5 -Cp)(CO)-(μ -5,5-dimethyl-1,3,2-dioxaphosphorinane)] ₂	

APPENDIX II	389
Stereopair Drawings and Unit Cell Drawings of trans-[Fe(η^5 -Cp)(CO)(μ -5,5-dimethyl-1,3,2-dioxaphosphorinane)] ₂	
APPENDIX III	394
Stereopair Drawings and Unit Cell Drawing of [Fe(η^4 -C ₅ H ₆)(CO)(μ -4,4,5,5-tetramethyl-1,3,2-dioxaphospholane) ₂ Fe(CO) ₃]	

LIST OF TABLES

Table 1.	^{31}P NMR data for free phosphonium ions	12
Table 2.	^{31}P NMR data for phosphonium ion-transition metal complexes	23
Table 3.	Infrared data for phosphonium ion and precursor iron carbonyl complexes	25
Table 4.	R_f values for $[\text{Fe}(\eta^5\text{-Cp})(\text{CO})\text{L}]_2$ complexes on alumina	60
Table 5.	^{31}P NMR data for the reactions of $\text{M}(\text{CO})_5(\text{Cl-P} \lt)$ (M = Cr, W) with AlCl_3	73
Table 6.	Aminophosphorus(III) compounds reacted with HSO_3CF_3 by Dahl	74
Table 7.	^1H NMR chemical shifts and coupling constants data for $\text{Me}_2\text{N-P}$ systems	75
Table 8.	^{31}P NMR data for $\text{Me}_2\text{N-P} \lt + \text{HB}$ reactions	77
Table 9.	Conductance data for $(\text{Me}_2\text{N})\text{PX}_2 + \text{HSO}_3\text{CF}_3$ and standard systems	82
Table 10.	^1H NMR data for $\text{Me}_2\text{N-P} \text{---} \text{M}(\text{CO})_x$ systems	86
Table 11.	^{31}P NMR data for $\text{M}(\text{CO})_x(\text{Me}_2\text{N-P} \lt) + \text{HB}$ reactions	87
Table 12.	^{31}P NMR data for the $\text{Fe}(\text{CO})_4(\underline{8}) + \text{HSO}_3\text{CF}_3$ system	88
Table 13.	^{31}P NMR data of the intermediates from the $\text{M}(\text{CO})_x(\underline{8}) + \text{HB}$ system	89

Table 14.	Selected metal nucleophiles and rate constants for alkylation	90
Table 15.	Mass spectral data for <u>26</u> and cis and trans- $[\text{Fe}(\eta^5\text{-Cp})(\text{CO})(\mu\text{-5,5-DMP})]_2$	99
Table 16.	^1H NMR data for precursor chlorophosphorus compounds	104
Table 17.	^1H NMR data for $[\text{Fe}(\eta^5\text{-Cp})(\text{CO})(\text{L})]_2$ systems	117
Table 18.	^{13}C NMR data for precursor chlorophosphorus(III) compounds	142
Table 19.	^{13}C NMR data for $[\text{Fe}(\eta^5\text{-Cp})(\text{CO})(\text{L})]_2$ systems	145
Table 20.	^{31}P NMR data for $[\text{Fe}(\eta^5\text{-Cp})(\text{CO})(\text{L})]_2$ systems	148
Table 21.	Infrared data for $[\text{Fe}(\eta^5\text{-Cp})(\text{CO})(\text{L})]_2$ systems	161
Table 22.	Experimental crystallographic data for cis- $[\text{Fe}(\eta^5\text{-Cp})(\text{CO})(\mu\text{-5,5-DMP})]_2$	175
Table 23.	Fractional atom coordinates for cis- $[\text{Fe}(\eta^5\text{-Cp})(\text{CO})(\mu\text{-5,5-DMP})]_2$ with estimated standard deviations	178
Table 24.	Hydrogen fractional coordinates for cis- $[\text{Fe}(\eta^5\text{-Cp})(\text{CO})(\mu\text{-5,5-DMP})]_2$	179
Table 25.	Anisotropic thermal parameters for cis- $[\text{Fe}(\eta^5\text{-Cp})(\text{CO})(\mu\text{-5,5-DMP})]_2$	180
Table 26.	Structure factor tables for cis- $[\text{Fe}(\eta^5\text{-Cp})(\text{CO})(\mu\text{-5,5-DMP})]_2$	182

Table 27.	Experimental crystallographic data for trans- $[\text{Fe}(\eta^5\text{-Cp})(\text{CO})(\mu\text{-5,5-DMP})]_2$	198
Table 28.	Fractional atom coordinates for trans- $[\text{Fe}(\eta^5\text{-Cp})(\text{CO})(\mu\text{-5,5-DMP})]_2$ with estimated standard deviations	200
Table 29.	Hydrogen fractional coordinates for trans- $[\text{Fe}(\eta^5\text{-Cp})(\text{CO})(\mu\text{-5,5-DMP})]_2$	202
Table 30.	Anisotropic thermal parameters for trans- $[\text{Fe}(\eta^5\text{-Cp})(\text{CO})(\mu\text{-5,5-DMP})]_2$	204
Table 31.	Structure factor tables for trans- $[\text{Fe}(\eta^5\text{-Cp})(\text{CO})(\mu\text{-5,5-DMP})]_2$	206
Table 32.	Bond distances (A°) in cis- $[\text{Fe}(\eta^5\text{-Cp})(\text{CO})(\mu\text{-5,5-DMP})]_2$ with estimated standard deviations	223
Table 33.	Selected non-bonded distances (A°) in cis- $[\text{Fe}(\eta^5\text{-Cp})(\text{CO})(\mu\text{-5,5-DMP})]_2$	224
Table 34.	Bond angles (degrees) in cis- $[\text{Fe}(\eta^5\text{-Cp})(\text{CO})(\mu\text{-5,5-DMP})]_2$	225
Table 35.	Least-squares planes in cis- $[\text{Fe}(\eta^5\text{-Cp})(\text{CO})(\mu\text{-5,5-DMP})]_2$	226
Table 36.	Dihedral angles between planes (degrees) in cis- $[\text{Fe}(\eta^5\text{-Cp})(\text{CO})(\mu\text{-5,5-DMP})]_2$	227
Table 37.	Bond distances (A°) in trans- $[\text{Fe}(\eta^5\text{-Cp})(\text{CO})(\mu\text{-5,5-DMP})]_2$ with estimated standard deviations	228
Table 38.	Selected non-bonded distances (A°) in trans- $[\text{Fe}(\eta^5\text{-Cp})(\text{CO})(\mu\text{-5,5-DMP})]_2$	229

Table 39.	Bond angles (degrees) in trans-[Fe(η^5 -Cp)(CO)(μ -5,5-DMP)] ₂	231
Table 40.	Least-squares planes in trans-[Fe(η^5 -Cp)(CO)(μ -5,5-DMP)] ₂	233
Table 41.	Dihedral angles between planes (degrees) in trans-[Fe(η^5 -Cp)(CO)(μ -5,5-DMP)] ₂	233
Table 42.	Crystallographic and $\delta^{31}\text{P}$ NMR data for diiron- μ -phosphorus systems	242
Table 43a.	η^4 -complexes selected crystallographic parameters	255
Table 43b.	Selected crystallographic parameters of η^4 -complexes	260
Table 44.	R_f values for the reaction products of the Fp^- anion with <u>18</u>	265
Table 45.	Experimental crystallographic data for [Fe(η^4 -C ₅ H ₆)(CO)(μ -P(OC(Me) ₂ C(Me) ₂ O)) ₂ Fe(CO) ₃]	267
Table 46.	Atom coordinates [$\times 10^4$] and average temperature factor [$\text{\AA}^3 \times 10^3$] for [Fe(η^4 -C ₅ H ₆)(CO)(μ -P(OC(Me) ₂ C(Me) ₂ O)) ₂ Fe(CO) ₃]	270
Table 47.	Atom coordinates [$\times 10^4$] and temperature factor [$\text{\AA}^3 \times 10^3$] for hydrogen atoms in [Fe(η^4 -C ₅ H ₆)(CO)(μ -P(OC(Me) ₂ C(Me) ₂ O)) ₂ Fe(CO) ₃]	272
Table 48.	Anisotropic thermal parameters for [Fe(η^4 -C ₅ H ₆)(CO)(μ -P(OC(Me) ₂ C(Me) ₂ O)) ₂ Fe(CO) ₃] with estimated standard deviations	274
Table 49.	Structure factor tables for [Fe(η^4 -C ₅ H ₆)(CO)(μ -P(OC(Me) ₂ C(Me) ₂ O)) ₂ Fe(CO) ₃]	276

Table 50.	<u>Bond distances (Å)</u> in $[\text{Fe}(\eta^4\text{-C}_5\text{H}_6)(\text{CO})(\mu\text{-P}(\text{OC}(\text{Me})_2\text{C}(\text{Me})_2\text{O}))_2\text{Fe}(\text{CO})_3]$ with estimated standard deviations	285
Table 51.	<u>Bond angles (degrees)</u> in $[\text{Fe}(\eta^4\text{-C}_5\text{H}_6)(\text{CO})(\mu\text{-P}(\text{OC}(\text{Me})_2\text{C}(\text{Me})_2\text{O}))_2\text{Fe}(\text{CO})_3]$ with estimated standard deviations	286
Table 52.	<u>Least squares planes</u> in $[\text{Fe}(\eta^4\text{-C}_5\text{H}_6)(\text{CO})(\mu\text{-P}(\text{OC}(\text{Me})_2\text{C}(\text{Me})_2\text{O}))_2\text{Fe}(\text{CO})_3]$	288
Table 53.	<u>Dihedral angles (degrees)</u> between planes in $[\text{Fe}(\eta^4\text{-C}_5\text{H}_6)(\text{CO})(\mu\text{-P}(\text{OC}(\text{Me})_2\text{C}(\text{Me})_2\text{O}))_2\text{Fe}(\text{CO})_3]$	289
Table 54.	Chromatographic and spectroscopic data of product from method A for $\text{P}(\text{OC}_6\text{H}_5)(\text{OC}_6\text{H}_4\text{-p-Cl})(\text{OC}_6\text{H}_4\text{-p-Me})$ <u>84</u>	317
Table 55.	Chromatographic retention times (R_f) ^a of some diastereomeric organophosphorus compounds on silica gel	318
Table 56.	Product dependence on the reaction conditions of <u>86</u> with paratolyltrifluoroacetate	326
Table 57.	Spectroscopic and yield data for $\text{cis-}[\text{Cl}_2\text{PtL}_2]$ complexes from method B	330
Table 58.	Spectroscopic and physical data for cis- platinum-phosphite complexes, $\text{cis-}[\text{X}_2\text{PtL}_2]$	331
Table 59.	Chromatographic separation and NMR data for diastereomeric $\text{cis-}[\text{I}_2\text{Pt}(\text{84})(\text{81})]$ complexes	334
Table 60.	Spectroscopic and yield data for the resolved enantiomeric phosphite triesters <u>84</u>	335

Table 61.	Expected random distribution values for the $P(OR)_x(OR')_y(OR'')_z$ systems from the $(RO)PCl_2 + R'OH/R''OH$ reaction with and without substituent redistribution	342
Table 62.	Preparation of <u>84</u>	343

LIST OF FIGURES

	Page
Figure 1.	5
Historical synthesis of phosphonium ions	
Figure 2.	7
Typical ^{31}P NMR chemical shifts of phosphorus compounds	
Figure 3.	9
Chemical shift correlation with coordination number in chloro- and aminophosphorus compounds	
Figure 4.	15
Stabilization of phosphonium ions from N \rightarrow P π -conjugation	
Figure 5.	17
Molecular orbital energy level diagram for $[\text{P}(\text{NH}_2)_2]^+$	
Figure 6.	18
Back-bonding in metal carbonyls and metal-phosphonium ion complexes	
Figure 7.	21
Examples of the preparations of phosphonium ion-transition metal complexes	
Figure 8.	62
Apparatus for the reaction of chlorophosphorus(III) compounds with chloride abstractors	
Figure 9.	70
Plot of phosphorus coordination number versus ^{31}P chemical shift for $[\text{P}(\text{OEt})_n]^x$ systems ($x = 0, +1$)	
Figure 10.	71
Product dependence on time of the reaction of <u>26</u> with aluminum trichloride	
Figure 11.	84
Intermediates in the reaction of <u>27</u> with HSO_3CF_3	
Figure 12.	92
Possible structures of the product from $[\text{Mo}(\eta^5\text{-Cp})(\text{CO})_3]^-$ and <u>26</u>	

Figure 13.	^{31}P NMR of the reaction mixture of $[\text{Fe}(\eta^5\text{-Cp})(\text{CO})_2]^-$ with <u>26</u>	94
Figure 14.	^{31}P NMR of the once-chromatographed reaction mixture of $[\text{Fe}(\eta^5\text{-Cp})(\text{CO})_2]^-$ with <u>26</u>	96
Figure 15.	Mass spectrum of $\text{trans-}[\text{Fe}(\eta^5\text{-Cp})(\text{CO})(\mu\text{-5,5-DMP})]_2$	100
Figure 16.	Mass spectrum of $\text{cis-}[\text{Fe}(\eta^5\text{Cp})(\text{CO})(\mu\text{-1,3,2-dioxaisophosphindolane})]_2$	102
Figure 17.	^1H NMR spectrum of <u>26</u>	109
Figure 18.	Schematic spin-spin splitting diagram for the ^1H NMR of <u>26</u>	111
Figure 19.	"W" coupling in <u>26</u>	113
Figure 20.	Computer simulated ^1H NMR spectrum of <u>26</u>	115
Figure 21.	Proton NMR of $\text{cis-}[\text{Fe}(\eta^5\text{-Cp})(\text{CO})(\mu\text{-5,5-DMP})]_2$	120
Figure 22.	Diagram showing the equivalent methylene protons in $\text{cis-}[\text{Fe}(\eta^5\text{-Cp})(\text{CO})(\mu\text{-5,5-DMP})]_2$	122
Figure 23.	Schematic spin-spin splitting diagram for the ^1H NMR of $\text{cis-}[\text{Fe}(\eta^5\text{-Cp})(\text{CO})(\mu\text{-5,5-DMP})]_2$	124
Figure 24.	Decoupling experiments on $\text{cis}[\text{Fe}(\eta^5\text{-Cp})(\text{CO})(\mu\text{-5,5-DMP})]_2$; a. ^1H NMR spectrum in CDCl_3 , b. irradiation of the upfield methylene resonance, c. irradiation of the downfield methylene resonance, d. enlarged methylene region, and e. ^{31}P decoupled ^1H spectrum in the methylene region	127

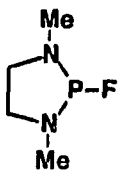
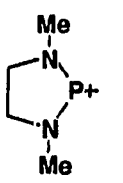
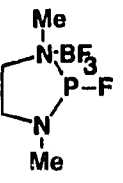
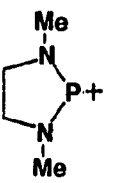
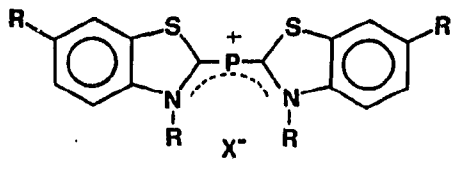
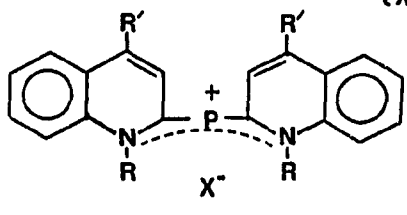
Figure 25.	Computer simulated ^1H NMR spectrum in the methylene region of $\text{cis-}[\text{Fe}(\eta^5\text{-Cp})(\text{CO})(\mu\text{-5,5-DMP})]_2$	128
Figure 26.	Proton NMR of $\text{trans-}[\text{Fe}(\eta^5\text{-Cp})(\text{CO})(\mu\text{-5,5-DMP})]_2$ in the methylene region	130
Figure 27.	Diagram showing the equivalent methylene protons in $\text{trans-}[\text{Fe}(\eta^5\text{-Cp})(\text{CO})(\mu\text{-5,5-DMP})]_2$	133
Figure 28.	Schematic spin-spin splitting diagram for the ^1H NMR of $\text{trans-}[\text{Fe}(\eta^5\text{-Cp})(\text{CO})(\mu\text{-5,5-DMP})]_2$	134
Figure 29.	Decoupling experiments on $\text{trans-}[\text{Fe}(\eta^5\text{-Cp})(\text{CO})(\mu\text{-5,5-DMP})]_2$; a. ^1H NMR of the methylene region in CDCl_3 , b. irradiation at the upfield methylene resonance, c. irradiation at the downfield methylene resonance, and d. ^{31}P NMR decoupled ^1H spectrum of the methylene region	135
Figure 30.	Computer simulated ^1H NMR spectrum in the methylene region of $\text{trans-}[\text{Fe}(\eta^5\text{-Cp})(\text{CO})(\mu\text{-5,5-DMP})]_2$	138
Figure 31.	^1H NMR spectrum of $\text{trans-}[\text{Fe}(\eta^5\text{-Cp})(\text{CO})(\mu\text{-P(OEt)}_2)]_2$	140
Figure 32.	^1H undecoupled ^{31}P NMR spectrum and schematic splitting diagram for $\text{trans-}[\text{Fe}(\eta^5\text{-Cp})(\text{CO})(\mu\text{-5,5-DMP})]_2$	151
Figure 33.	Solid state ^{31}P NMR of $\text{cis-}[\text{Fe}(\eta^5\text{-Cp})(\text{CO})(\mu\text{-5,5-DMP})]_2$	153
Figure 34.	Solid state ^{31}P NMR of $\text{trans-}[\text{Fe}(\eta^5\text{-Cp})(\text{CO})(\mu\text{-5,5-DMP})]_2$	155
Figure 35.	Plot of ^{31}P chemical shifts of cis and $\text{trans-}[\text{Fe}(\eta^5\text{-Cp})(\text{CO})(\text{L})]_2$ complexes versus the $\Delta^{31}\text{P}$ chemical shifts	158
Figure 36.	Plot of the ^{31}P chemical shifts of cis and $\text{trans-}[\text{Fe}(\eta^5\text{-Cp})(\text{CO})(\text{L})]_2$ complexes versus the infrared carbonyl stretching frequencies	159

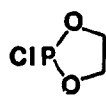
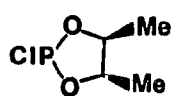
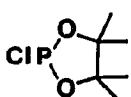
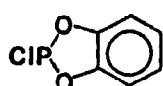
Figure 37.	Plot of $\Delta^{31}\text{P}$ chemical shifts of cis and trans- [Fe($\eta^5\text{-Cp}$)(CO)(L)] ₂ complexes versus infrared stretching frequencies	164
Figure 38.	³¹ P NMR of [Fe($\eta^4\text{-C}_5\text{H}_6$)(CO)($\mu\text{-P}(\text{OC}(\text{Me})_2\text{C}(\text{Me})_2\text{O})_2\text{-}$ (OC) ₃ Fe]	167
Figure 39.	³¹ P NMR stack plot of cis-[Fe($\eta^5\text{-Cp}$)(CO)($\mu\text{-5,5-}$ DMP)] ₂ reacted with water over 18 hours	169
Figure 40.	ORTEP drawing of cis-[Fe($\eta^5\text{-Cp}$)(CO)($\mu\text{-5,5-DMP}$)] ₂	234
Figure 41.	ORTEP drawing of cis-[Fe($\eta^5\text{-Cp}$)(CO)($\mu\text{-5,5-DMP}$)] ₂	236
Figure 42.	ORTEP drawing of trans-[Fe($\eta^5\text{-Cp}$)(CO)($\mu\text{-5,5-DMP}$)] ₂	238
Figure 43.	ORTEP drawing of trans-[Fe($\eta^5\text{-Cp}$)(CO)($\mu\text{-5,5-DMP}$)] ₂ viewing down the iron-iron axis	240
Figure 44.	Iron orientations with respect to the bridging dioxaphosphorinane ring systems	247
Figure 45.	Angles within the Fe ₂ P ₂ subunit	248
Figure 46.	ORTEP computer drawing of [Fe($\eta^4\text{-C}_5\text{H}_6$)(CO)($\mu\text{-}$ $\text{P}(\text{OC}(\text{Me})_2\text{C}(\text{Me})_2\text{O})_2\text{Fe}(\text{CO})_3$)] showing atom labeling scheme	290
Figure 47.	ORTEP computer drawing of [Fe($\eta^4\text{-C}_5\text{H}_6$)(CO)($\mu\text{-}$ $\text{P}(\text{OC}(\text{Me})_2\text{C}(\text{Me})_2\text{O})_2\text{Fe}(\text{CO})_3$)] showing the orientation of the $\eta^4\text{-C}_5\text{H}_6$ ring and carbonyls	292
Figure 48.	Dihedral angles in the $\eta^5\text{-cyclohexadienyl}$ and the $\eta^4\text{-}$ cyclopentadiene ligand systems	294
Figure 49.	σ -donation and π -backbonding schemes for metal- olefin and metal-carbonyl systems	295

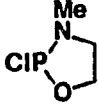
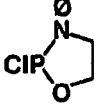
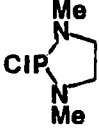
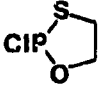
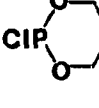
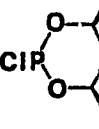
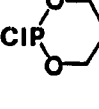
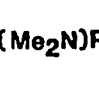
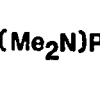
Figure 50.	Highest occupied molecular orbital (HOMO) for $[\text{Fe}_2(\text{CO})_6[\mu\text{-PR}_2]_2$ systems	299
Figure 51.	Stereospecific synthesis of <u>72</u>	303
Figure 52.	Synthesis of chiral phosphinites in the presence of a chiral amine (230,231)	305
Figure 53.	Preparation of chiral <u>75</u> and <u>76</u>	305
Figure 54.	Preparation of chiral <u>79</u>	306
Figure 55.	Optical resolution of phosphines by asymmetric platinum(II) complexes	308
Figure 56.	Resolution of triphosphamide <u>68</u> via platinum diastereomers	309
Figure 57.	^{31}P chemical shift dependence upon aromatic substitution in triesters	337
Figure 58.	Proposed four-center interaction to account for the observed phosphite product distribution	338
Figure 59.	Preparation of chiral triaryl phosphites	339
Figure 60.	^{31}P NMR spectrum of <u>84</u> after two months at room temperature	344
Figure 61.	^{31}P NMR spectrum of <u>85</u> after four days at room temperature	347
Figure 62.	Resolution scheme via chiral amine substituted phosphites	349

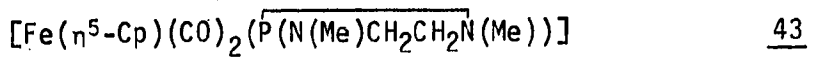
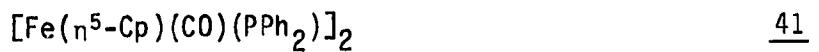
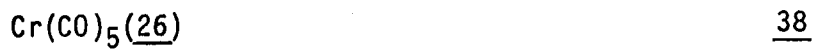
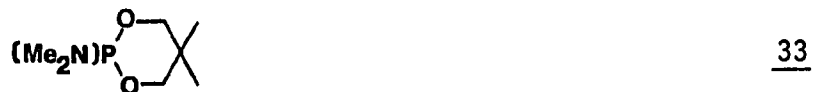
Figure 63.	^{31}P NMR of <u>87</u>	351
Figure 64.	Preparation of "CSP XIII"	356
Figure 65.	Preparation of ligands for the platinum phosphite resolution	359
Figure 66.	Resolution of <u>84</u> via platinum diastereomers	361

LIST OF COMPOUNDS

	<u>1</u>
	<u>2</u>
	<u>3</u>
	<u>4</u>
	<u>5</u>
<p>(X⁻ = BF₄⁻, ClO₄⁻)</p> 	<u>6</u>
$\text{Mo}(\text{CO})_2(\overline{\text{P}(\text{N}(\text{Me})\text{CH}_2\text{CH}_2\text{N}(\text{Me}))})$	<u>7</u>

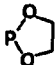
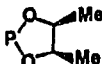
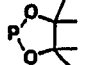
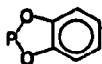

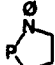

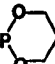
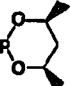
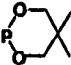
$P(NMe_2)_3$	<u>8</u>
$CIP\emptyset_2$	<u>9</u>
$CIPMe_2$	<u>10</u>
Fp_2	<u>11</u>
$CIP(OEt)_2$	<u>12</u>
$CIP(O\emptyset)_2$	<u>13</u>
$CIP-(O-C_6H_4)_2$	<u>14</u>
$CIP(NMe_2)_2$	<u>15</u>
	<u>16</u>
	<u>17</u>
	<u>18</u>
	<u>19</u>

	<u>20</u>
	<u>21</u>
	<u>22</u>
	<u>23</u>
	<u>24</u>
	<u>25</u>
	<u>26</u>
$(\text{Me}_2\text{N})_2\text{P}(\text{OMe})$	<u>27</u>
$(\text{Me}_2\text{N})\text{P}(\text{O}-\text{C}_6\text{H}_2(\text{X})_2)_2$	<u>28</u>
	<u>29</u>
	<u>30</u>



$$[\text{Fe}(\eta^5\text{-Cp})(\text{CO})(\text{L})]_2$$

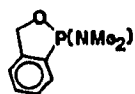
L

$\text{P}(\text{OEt})_2$	<u>44</u>
$\text{P}(\text{O}^\ominus)_2$	<u>45</u>
$\text{P}-(\text{C}_6\text{H}_4\text{-X})_2$	<u>46</u>
	<u>47</u>
	<u>48</u>
	<u>49</u>
	<u>50</u>
	<u>51</u>
	<u>52</u>
	<u>53</u>
	<u>54</u>
	<u>55</u>
	<u>56</u>
$\text{Fe}(\text{CO})_3$ (26)	<u>57</u>
$\text{P}(\text{NMe}_2)_2(\text{Ph})$	<u>58</u>

$P(NMe_2)(Ph)_2$ 59

$P(NMe)_2Cl$ 60

$P(NMe_2)Cl_2$ 61

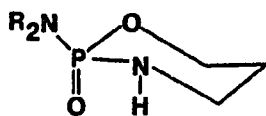


62

$[(OC)_xM-\overset{+}{P}-N(H)(Me)_2](B^-)$ 63

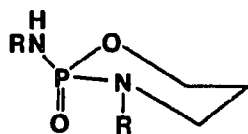
$[Fe(\eta^5-Cp)(CO)(\overline{P(OCH_2C(Me)_2CH_2O)})]$ 64

$[Fe(CO)_3(\overline{P(OCH_2C(Me)_2CH_2O)})_2]$ 65



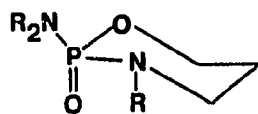
66

$R = (CH_2CH_2Cl)$



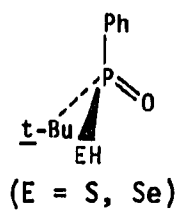
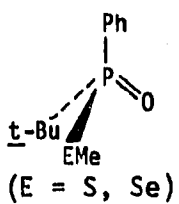
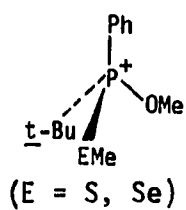
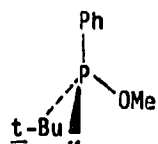
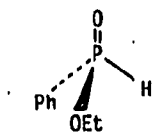
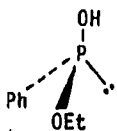
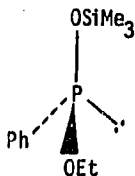
67

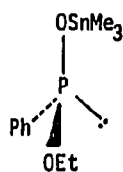
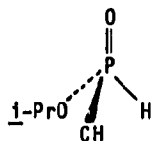
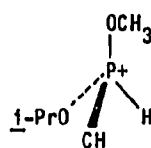
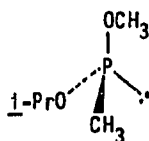
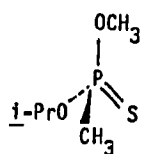
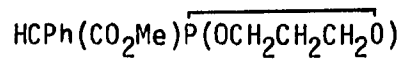
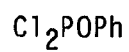
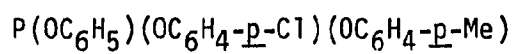
$R = (CH_2CH_2Cl)$



68

$R = (CH_2CH_2Cl)$

69707172737475

767778798081828384

P(O- <u>t</u> -Bu)(OEt)(OMe)	<u>85</u>
P(OPh)(OC ₆ H ₄ - <u>p</u> -Cl)(L-ethylprolinate)	<u>86</u>
P(OPh)(OEt)(L-ethylprolinate)	<u>87</u>
P(OPh)(OCH ₂ CH ₂ C ₆ H ₅)(L-ethylprolinate)	<u>88</u>
P(OPh)(OEt)(D-methamphetamine)	<u>89</u>
P(OPh)(OEt)(L-ethylprolinate)·BH ₃	<u>90</u>
O=P(OC ₆ H ₅)(OC ₆ H ₄ - <u>p</u> -Cl)(OC ₆ H ₄ - <u>p</u> -Me)	<u>91</u>
P(OC ₆ H ₅)(Cl)(L-ethylprolinate)	<u>92</u>
cis[Cl ₂ Pt(<u>84</u>) ₂]	<u>93</u>
cis-[Cl ₂ Pt(<u>81</u>) ₂]	<u>94</u>
cis-[I ₂ Pt(<u>84</u>) ₂]	<u>95</u>
cis-[I ₂ Pt(<u>81</u>) ₂]	<u>96</u>
cis-[I ₂ Pt(<u>84</u>)(<u>81</u>)]	<u>97</u>

LIST OF ABBREVIATIONS

Ar	Aryl group
Bu	Butyl
COD	Cyclooctadiene
Cp	Cyclopentadienyl, $C_5H_5^-$
CSP	Chiral stationary phase
5,5-DMP	5,5-dimethyl-1,3,2-dioxaphosphorinane
ee	Enantiomeric excess
Et	Ethyl
Fc	Ferrocenyl
FID	Free induction decay
Fp ₂	$[Fe(\eta^5-Cp)(CO)_2]_2$
h	hour(s)
HPLC	High performance (pressure) liquid chromatography
J	Coupling constant, in Hertz
L	Ligand
Me	Methyl
Ph, ϕ	Phenyl
Pr	Propyl
R	Alkyl or aryl group
THF	Tetrahydrofuran
TLC	Thin layer chromatography
Å	Angstroms, 10^{-10} meter
β	Beta, anisotropic thermal parameter
δ	Delta, chemical shift
Δ	Delta, (δ product - δ starting material)
Θ	Theta, crystallographic orientation
ϕ	Phi, crystallographic orientation
ψ	Psi, crystallographic orientation
ω	Omega, crystallographic orientation
°	Degrees centigrade

xxvfi

DEDICATION

TO MY PARENTS

AND TO MY WIFE

PREFACE

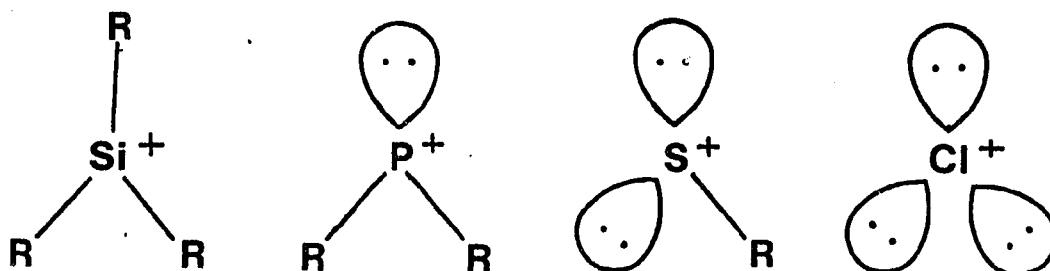
Recently, a great deal of work has been done on the synthesis, characterization, and reactivity of divalent aminophosphine cations. In this dissertation are presented studies to determine if these types of compounds can be prepared with oxygen substituted systems. During the course of this work, a number of quite interesting new diiron complexes were prepared and studied by a variety of techniques including multinuclear NMR and X-ray crystallography.

Chiral phosphines have recently found very important applications as ligands for a variety of catalytic processes and it is well-known that changes in the electronic environment of phosphorus can greatly affect its donor properties. In this dissertation is described the first successful resolution into enantiomers of a trivalent phosphorus triester with the primary chiral site at phosphorus.

PART I.
PREPARATION, STRUCTURE, AND TRANSITION
METAL COMPLEXES OF DIOXAPHOSPHORUS LIGANDS

INTRODUCTION

Higher and lower valent cations of many of the non-metallic elements have been well-recognized and studied for a number of years with particular attention centered recently on the divalent nitrogen ions (1,2). Until quite recently, however, research involving lower valent species of phosphorus have been for the most part neglected. These dicoordinate phosphorus cations belong to an interesting family of main-group, second row cations containing six valence electrons around the central atom. Included in this group, along with phosphorus, are the silicon (3), sulfur (4), and chlorine cations shown below:



The electron-deficient phosphorus species are commonly referred to as phosphonium ions, after the system of nomenclature introduced by Olah (1).

The first literature reports of the successful synthesis of true phosphonium ions by Flemming, Lupton, and Jekot (5) and by Maryanoff and Hutchins (6) showed independently that these ions could indeed be prepared as stable species by relatively straightforward but yet somewhat

unexpected synthetic procedures. Previous to these works, the appearance of $+PCl_2$ had been reported as the most abundant positive ion in the electron-impact mass spectrum of phosphorus trichloride (7). This species is, however, apparently unstable and was not isolated and has not been synthesized to date by any other synthetic procedure. In the first work cited, the authors were investigating the modes of bonding in adduct formation with compounds of the type F_2PNR_2 and $FP(NR_2)_2$. It had been known previously that in adducts of acyclic compounds of this type with BH_3 , the bonding occurs at the phosphorus while with BF_3 evidence suggested nitrogen bonding (8). The reaction of the cyclic diaminofluorophosphine 1 with an equivalent amount of BF_3 was found to yield the nitrogen-bonded system from conclusive NMR analyses. Upon further addition of BF_3 , a unique monomeric cation was reversibly formed rather than the expected diadduct. These results are shown in Figure 1. The structure of 2 was initially unambiguously verified as the monomeric

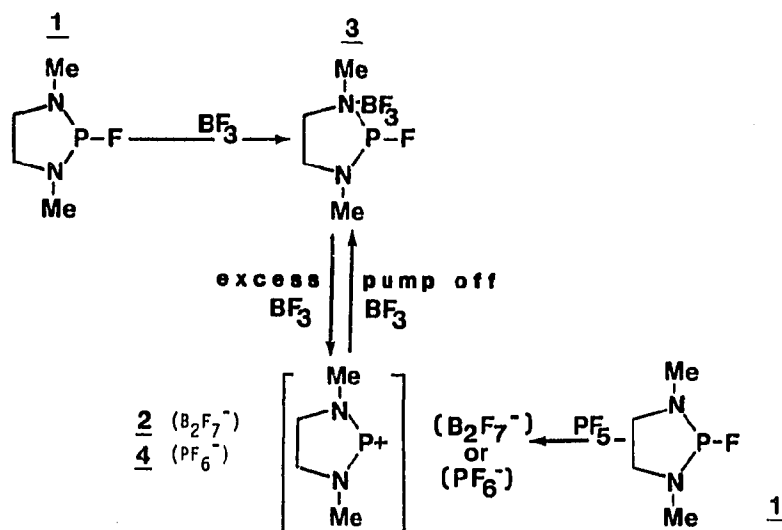


Figure 1. Historical synthesis of phosphonium ions

cation by multinuclear NMR techniques with particular emphasis on the spin-spin coupling data. Similar results were further obtained by reacting the precursor diaminofluorophosphine with phosphorus pentafluoride. In this reaction, however, only one equivalent of the phosphorus pentafluoride was required to form the ion and the reaction was furthermore found to be irreversible. Very similar observations were made by Maryanoff and Hutchins using 2-chloro-2-phospha-1,3,-diazacyclohexanes with phosphorus pentachloride as the halide acceptor. The most important and conclusive early observations verifying the monomeric structure of these ions came from ^{31}P NMR spectroscopy. The ^{31}P chemical shifts of both 2 and 4 were located quite close to one another and the spectra did not show any P-F coupling as had been observed in the precursor compounds. The chemical shifts of these ions appeared at extremely low applied fields and well outside the range normally observed in ^{31}P NMR spectroscopy, as summarized in Figure 2. The values of the ^{31}P chemical shifts are not consistent with the changes in the chemical shifts usually observed upon phosphorus-adduct bond formation. Normal variation in δ values upon coordination with a wide variety of acceptor molecules range from +40 to -11 ppm (δ free ligand - δ coordinated species) (9). In dicoordinate phosphonium ions, however, the change in chemical shift from the free tricoordinate ligands to the ions are greater than +105 ppm, shifted downfield. These values are indicative of phosphorus in a highly deshielded environment as suggested by the localization of the positive charge on the phosphorus. Dimroth

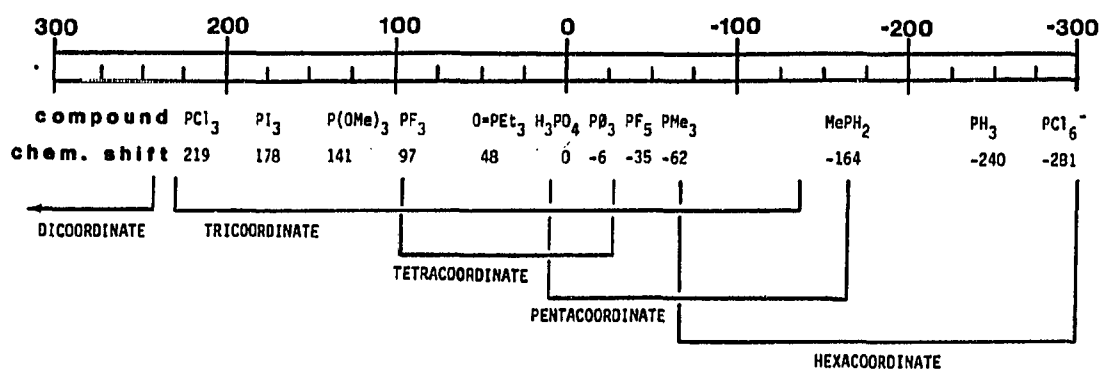
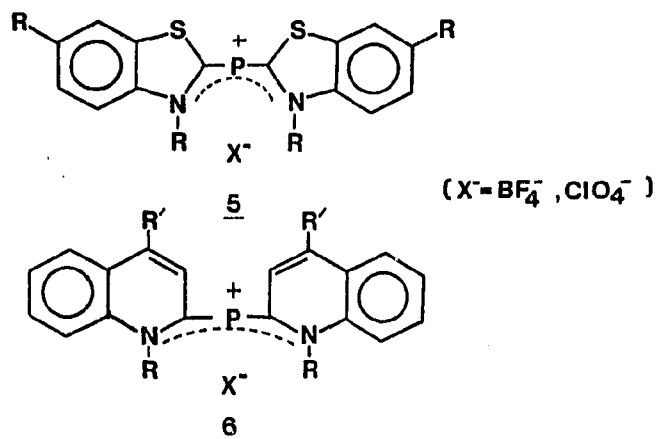
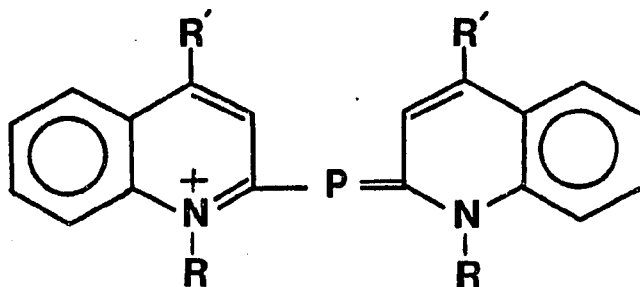


Figure 2. Typical ^{31}P NMR chemical shifts of phosphorus compounds.

and Hoffman (10) have reported the synthesis of the two coordinate cations 5 and 6. However, the physical and spectroscopic properties of these cations differ strikingly from the cations prepared by Flemming and Maryanoff. These crystallographically characterized (11) phosphamethinecyanines were isolated as quite stable salts having nearly planar geometries. The ^{31}P NMR chemical shifts of 5 and 6 occur at much higher field strengths (+24.9 and +48.8 ppm, respectively). Furthermore,



5 and 6 are weakly basic and can be protonated, whereas cations of the type $+P(NR_2)_2$ are very strong Lewis acids and exhibit basic character only toward π -electron donors such as metal carbonyls (12). This indicates that these phosphamethinecyanines truly exhibit very little phosphonium character and are more accurately represented as phosphorus ylides which place the positive charge at the heterocyclic atoms as shown in the resonance form below.



Parry reported a noteworthy relationship between the ^{31}P NMR chemical shifts and the coordination number of phosphorus (9). When the ^{31}P chemical shift values of the series of compounds PCl_6^- , PCl_5 , PCl_4^+ , and PCl_3 are plotted against the phosphorus coordination number, an approximately linear plot is obtained. If the value for $P(NMe_2)_3$ is then plotted and a similar line drawn through it parallel to that of the phosphorus-chloride system and extrapolated to the two coordinate species, the expected ^{31}P value from this treatment for $+P(NMe_2)_2$ would be $+260 \pm 20$ ppm. This is in remarkable agreement with the experimentally

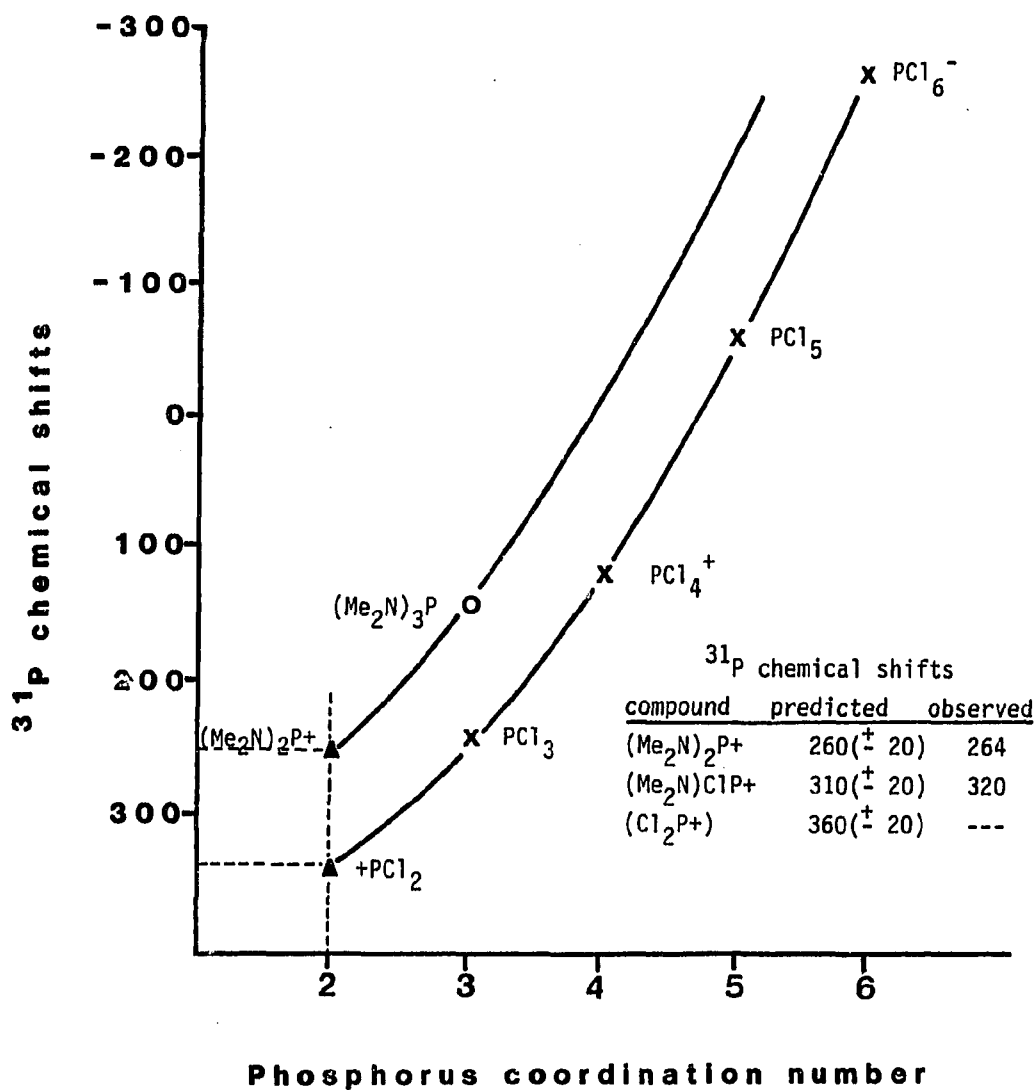
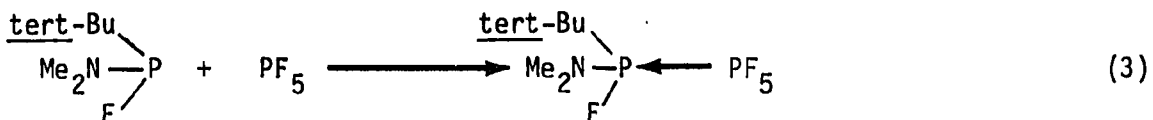
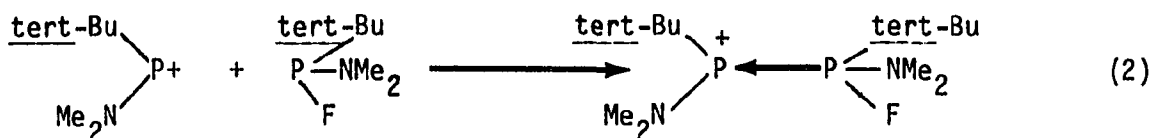
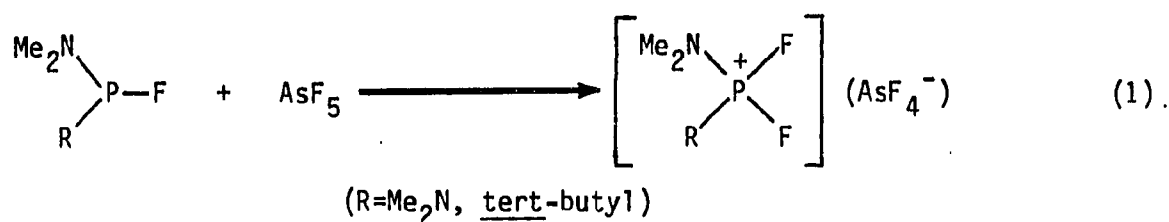


Figure 3. Chemical shift correlation with coordination number in chloro- and aminophosphorus compounds (9)

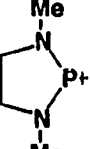
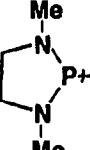
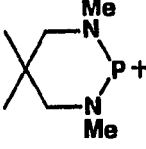
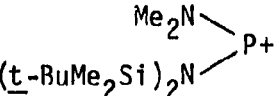
observed values of +264 and +269.4 ppm. These plots are shown in Figure 3. The value for the two-coordinate mixed ligand cation $+PCl(NMe_2)$ is predicted to be halfway between the extrapolated values for $+P(NMe_2)_2$ and $+PCl_2$ at a value of $+310 \pm 20$ ppm. Again this is in excellent agreement with the observed chemical shift of 320 ppm. The value for $+PCl_2$ would be expected to be $+360 \pm 20$ ppm, however, this cation has not been experimentally synthesized to date. Proton NMR and conductivity measurements have also been helpful in elucidating the structures of these compounds (9). In the proton NMR spectrum of $+P(NMe_2)_2$ at -35° , two sets of doublets are observed. This indicates inequivalence of the two methyl groups, presumably due to a barrier to rotation about the N-P bond. Upon warming to $+35^\circ$, rotation around this bond occurs and the spectrum collapses to a single doublet. The ΔG value in methylene chloride for this process has been calculated to be $+14.6 \pm 0.5$ kcal/mole (9). The chemical shifts of the methyl groups for the cation are shifted upfield from the trivalent analogue, from +2.9 to +2.01 ppm. Conductivity data further support the cationic nature of the species. Since the original reports, other halide acceptors producing counteranions such as $AlCl_4^-$ (13), $GaCl_4^-$, and $FeCl_4^-$ (9) have been successfully used to prepare phosphonium ions. As discussed previously, ^{31}P nmr has been the primary tool for the identification of phosphonium ions with observed chemical shift values ranging from +260 to +600 ppm. Table 1 presents a summary of the known free phosphonium ions, along with their counteranions and the ^{31}P chemical shift data. Although simple halide abstraction from a precursor halophosphine is usually a relatively

straightforward procedure, it does not always lead to the desired products. There appear to be at least three important side reactions which occur under various conditions to produce species other than phosphonium ions (13). These are formation of four-coordinate phosphonium salts (eq. 1), reaction of the initially formed phosphonium ion with a Lewis base present (such as the starting material (eq. 2)), and adduct formation with the reactant halide abstractor (eq. 3).



One or more of these side reactions are usually present (and detectable in the ³¹P nmr spectrum) but they can usually be greatly reduced or even eliminated under the appropriate experimental conditions and proper choice of reagents.

Table 1. ^{31}P nmr data for free phosphonium ions

Cation	Anion	^{31}P chemical shift ^a	Reference
	B_2F_7^-	+274	5
	PF_6^-	+264	5
	PCl_6^-	+222	6
$(\text{Me}_2\text{N})_2\text{P}^+$	AlCl_4^-	+264	9
$(\text{Me}_2\text{N})_2\text{P}^+$	SO_3CF_3^-	+269.4	14
$(\text{Me}_2\text{N})\text{ClP}^+$	AlCl_4^-	+322	9
$(\text{Me}_2\text{N})\text{ClP}^+$	GaCl_4	+329	9
$(\text{Et}_2\text{N})_2\text{P}^+$	AlCl_4^-	+263	12
$(i\text{-Pr}_2\text{N})_2\text{P}^+$	AlCl_4^-	+313	12
$(i\text{-Pr}_2\text{N})(\text{Me}_2\text{N})\text{P}^+$	AlCl_4	+290	13
$(\text{Me}_2\text{N})(t\text{-Bu})\text{P}^+$	AlCl_4^-	+513.2	15
	AlCl_4^-	+370.1	15

^aRelative to 85% phosphoric acid.

Table I (continued)

Cation	Anion	^{31}P chemical shift ^a	Reference
$\begin{array}{c} \text{Me}_2\text{N} \\ \diagdown \\ \text{P}^+ \\ \diagup \\ (\text{Me}_3\text{Si})_2\text{N} \end{array}$	AlCl_4^-	+354.3	15
$((\text{Me}_3\text{Si})_2\text{N})_2\text{P}^+$	AlCl_4^-	+450.3	15
$\begin{array}{c} \text{t-Bu} \\ \\ \text{N} \\ / \quad \backslash \\ \text{ClP} \quad \text{P}^+ \\ \backslash \quad / \\ \text{N} \\ \\ \text{t-Bu} \end{array}$	AlCl_4^-	+365.7	15
$(\text{Fc})_2\text{P}^+$	AlCl_4^-	+183	16
$(\text{Fe})(\text{Me}_2\text{N})\text{P}^+$	AlCl_4^-	+258.5	4
$(\text{Me}_3\text{Si})_2\text{C-P}^+)^2$ ^b	---	+599.6	17,18

^bNot a true phosphonium ion; for other examples of this type of compound, see reference 18.

Recently, a second method for the synthesis of the free ions (besides the halide abstraction procedure) was reported by Dahl (14). In this procedure, a precursor aminophosphine is reacted with two equivalents of a protic acid to precipitate the quaternary amine salt and produce the free phosphonium ion by the following reaction:



$\text{R} = \text{Me}$

$\text{R}' = -\text{NMe}_2, -\text{N}(\text{Me})\text{CH}_2\text{CH}_2\text{N}(\text{Me})-$

$\text{B}^- = \text{SO}_3\text{CF}_3^-$

Trifluoromethanesulfonic acid was selected because of the known low nucleophilicity of the anion. Other acids such as HCl are known to give trivalent substitution products rather than the formation of the desired dicoordinate cation (19). It appears from ^{31}P and ^1H nmr studies that the mechanism operating here involves the initial protonation of the phosphorus followed by proton shift to the nitrogen and subsequent reaction with an additional acid molecule to eliminate the amine salt and form the phosphonium ion.

By comparison between these "true" phosphonium ions with the ylide-like ions reported by Dimroth and Hoffman (5 and 6), it is clear that the best criterion for the identification and determination of whether a species is truly a phosphonium ion is ^{31}P nmr spectroscopy. This criterion will be employed throughout this thesis.

It appeared from the work reported to date, as seen in the data presented in Table 1, that at least one amino substituent on the phosphorus is required to isolate or even detect a phosphonium ion (with the notable exception of $+\text{P}(\text{Fc})_2$). This observation has been attributed to the potential thermodynamic stabilization arising from the interaction of the lone pair of electrons on the nitrogen atoms with the formally vacant p orbital on the phosphorus in the cation, leading to a significant degree of $\text{N} \rightarrow \text{P} \pi$ -conjugation. This type of interaction is depicted in Figure 4. This observed stability is similar to the situation in carbenes in that they are best stabilized when the substituent group can serve as a π -electron donor to the carbon (20).

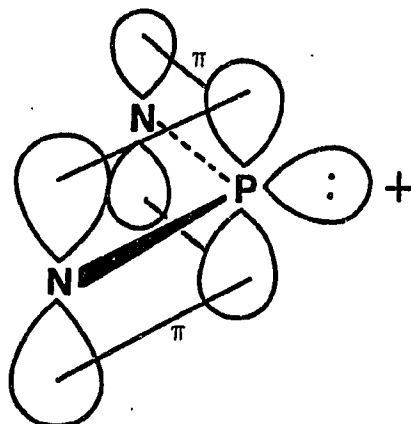


Figure 4. Stabilization of phosphonium ions from $N \rightarrow P$ π -conjugation

For this reason, amino and alkoxy groups are very commonly found in carbene complexes.

A number of structural implications are of primary concern for bonding of this sort and thus maximize stabilization. Maximum overlap of the proper orbitals on both the nitrogen and phosphorus atoms requires that all the non-hydrogen atoms within the $+P(NMe_2)_2$ framework be coplanar. Furthermore, the bond order of the phosphorus-nitrogen bond would be expected to be greater than one because of this conjugation. Since the bond then has some multiple character, the resulting bond distance observed should be shorter than a singly bonded analogue. An X-ray crystallographic study has been done on $[(i-Pr_2N)_2P^+][AlCl_4^-]$ by Cowley to confirm some of these speculations (21). From this work, it was found that, within experimental error, the phosphorus and the two nitrogen atoms indeed have planar geometries with a slight decrease in the N-P-N bond angle from the expected 120° to 114.8° , due to lone pair-

bond pair repulsions. The importance of planarity on the cation stability can also be seen by comparing $+P(NMe_2)_2$ with $+P(N(SiMe_3)_2)_2$. When the bulky trimethylsilyl group replaces the much smaller methyl substituent, the observed increase in the intramolecular interactions would suggest a significant deviation from coplanarity within the cation, thereby decreasing the effectiveness of the $N \rightarrow P \pi$ conjugation. This trend is reflected in the much larger downfield chemical shift in the ^{31}P NMR spectrum of $+P(N(SiMe_3)_2)_2$ relative to $+P(NMe_2)_2$ (+450.3 ppm versus +264 ppm). This indicates a more deshielded electronic environment about the phosphorus in the silyl compound resulting from a decrease in the amount of $N \rightarrow P \pi$ stabilization. In addition to the planarity, the average N-P bond distance of 1.613 Å was found to be slightly shorter than those for neutral aminophosphines (22), as expected from the predicted increase in the N-P bond order. Further confirmation of the multiple N-P bond character in these ions comes from theoretical and dynamic NMR studies in which barriers to rotation about this bond were calculated (13). MNDO calculations indicate that the barrier for N-P single bond rotation should be approximately 8.5 kcal/mole for $+P(NMe_2)_2$ while the experimental value was found to be 14.6 kcal/mole (13). This further confirms the existence and importance of the $N \rightarrow P \pi$ conjugation upon the stabilization of the cation.

Ab initio molecular orbital calculations have provided further information on the electronic properties of phosphonium ions (21). The orbital energy level diagram for $+P(NH_2)_2$ is shown in Figure 5 (13). The

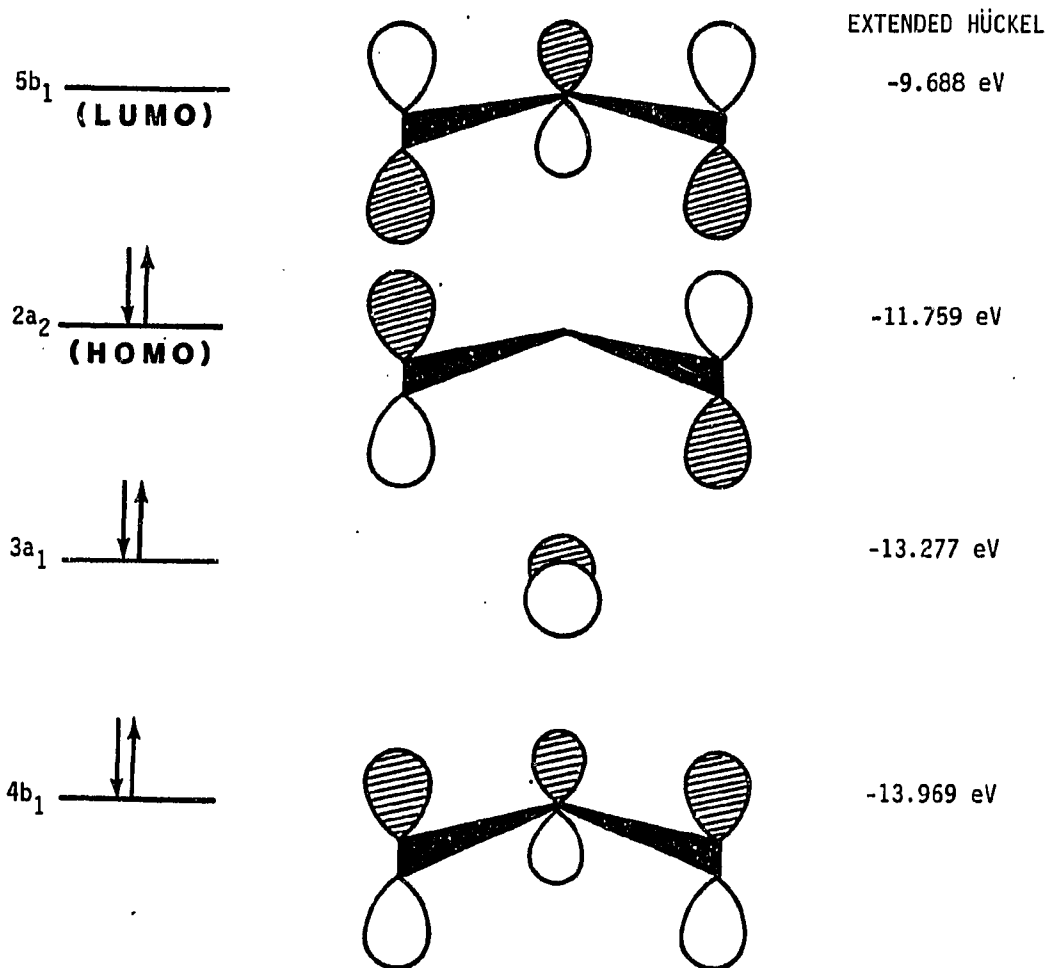


Figure 5. Molecular orbital energy level diagram for $[P(NH_2)_2]^+$ (21)

four molecular orbitals shown in this figure are particularly important in understanding some of the chemistry of these ions, especially as it applies to their ligation in metal complexes. The third highest occupied molecular orbital, with b_1 symmetry, represents the π -N-P-N bonding molecular orbital which, as described previously, accounts for, in large part, the stability of these species. The next highest occupied orbital,

with a_1 symmetry, is essentially a non-bonding lone pair of electrons located on the phosphorus atom. It is this orbital which accounts for the observed donor capabilities of these ions, especially with respect to their transition metal complexes. The highest occupied orbital (HOMO) is an out of phase a_2 orbital involving primarily the p orbitals on the nitrogen atoms. The lowest unoccupied molecular orbital (LUMO), with b_1 symmetry, is an N-P π -antibonding orbital. This orbital is particularly important in the bonding in transition metal complexes of these ions since they permit back donation of electron density from filled metal d orbitals. This bonding situation is quite similar to that proposed by Chatt for back-bonding of CO in metal carbonyl complexes (23). Both of these situations are shown in Figure 6.

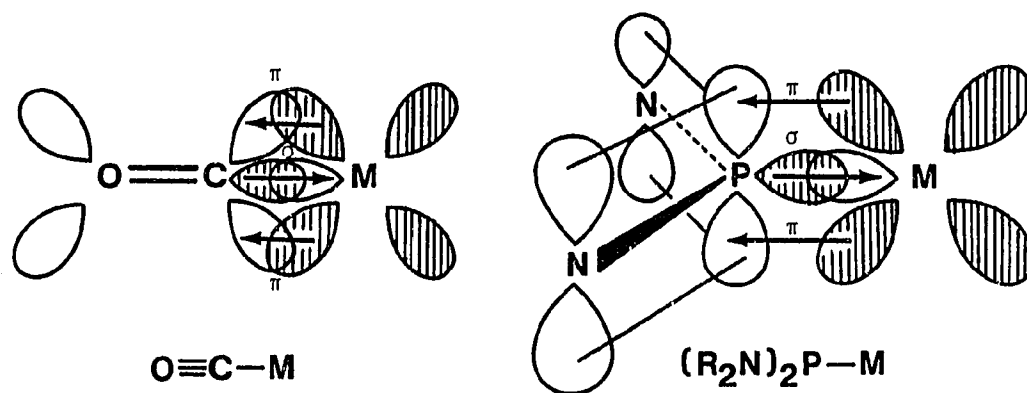
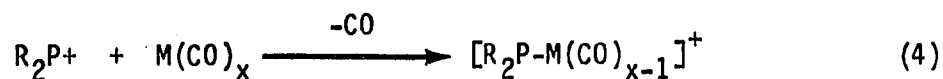


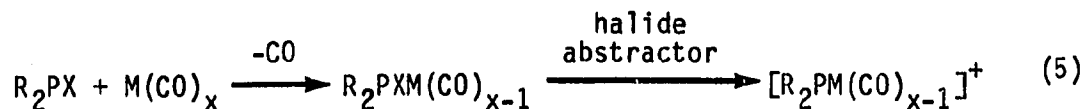
Figure 6. Back-bonding in metal carbonyls and metal-phosphonium ion complexes

As expected from the structures and the molecular orbital calculations of phosphonium ions, they can act both as Lewis acids and bases: Acting as Lewis acids, they have been found to react irreversibly with a variety of Lewis bases such as trimethylphosphite, pyridine, triethylamine, triphenylphosphine and methanol (9). They have also been found to react reversibly with diethylether. In many cases, the initial acid-base reaction is followed by secondary reactions which appear to be quite complicated. In their capacity as Lewis acids, these ions are thought to utilize primarily the vacant p orbital on the phosphorus. None of these adduct compounds have been structurally characterized to date to verify this scheme of bonding. The most interesting aspect of the reaction chemistry of phosphonium ions, however, lies in their ability to act as Lewis bases toward transition metals. As discussed previously, centered on the phosphorus is a lone pair of electrons which can effectively serve in a σ -donating capacity to a metal center. In addition to this feature, there is also the π -antibonding orbital appropriately situated to allow back-donation from the metal. This orbital is again primarily p in character and since a positive charge resides on the phosphorus center, this orbital should be suitably contracted to make it more effective in the formation of the π -system interaction. Free phosphonium ions have been found to exhibit no Lewis base behavior with compounds which are unable to π -backbond, indicating the relative importance of this type of π -stabilization in such transition metal complexes.

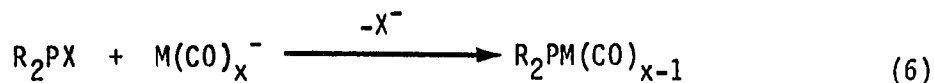
Three general methods have been developed for the formation of phosphonium ion transition metal complexes. The first procedure involves the direct interaction of a free phosphonium ion and a neutral metal carbonyl complex. This synthetic route is summarized in equation 4 (24).



This method, although conceptually straightforward, has received little attention primarily because of the difficulties involved with the preparation, purification, and handling of the free ion. The second method requires the initial formation of a precursor halophosphine-metal complex followed by halide ion abstraction to yield the complex as seen in equation 5 (12). A wide variety of cationic complexes have been

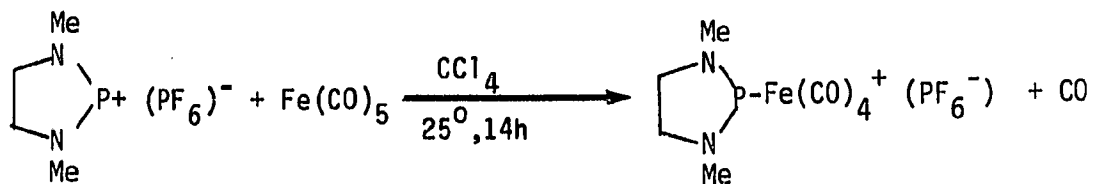


prepared using this procedure. A major advantage is that the precursor halophosphine-complex can usually be easily prepared, isolated, and purified as a relatively stable compound. The third procedure involves the reaction of the precursor halophosphine with a metal nucleophile. This method is shown in equation 6. This route has been used extensively

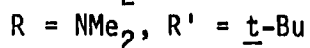
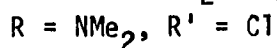
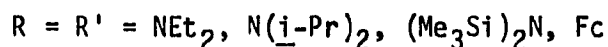
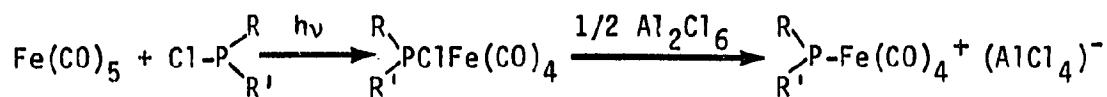


to prepare many neutral phosphonium complexes. Specific examples of each of these three procedures are shown in Figure 7.

1. Direct interaction;



2. Preparation of precursor halophosphine complex followed by halide abstraction;



3. Reaction of halophosphine with metal nucleophiles;

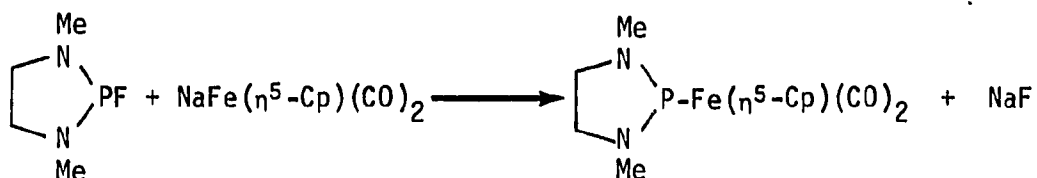
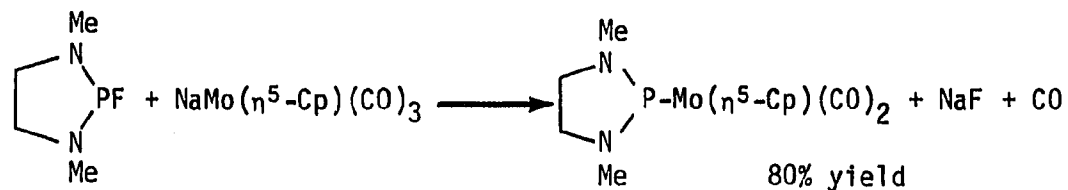


Figure 7. Examples of the preparations of phosphonium ion-transition metal complexes

A wide variety of phosphonium ion complexes have been prepared and the known complexes are summarized along with their ^{31}P NMR data in Table 2. As can be clearly seen from the data in this table, ^{31}P NMR chemical shifts occur at very low applied fields and are again diagnostic for phosphonium ion-complex formation. A variety of other techniques have also been used to characterize these complexes including mass spectroscopy, infrared spectroscopy, multinuclear NMR spectroscopy (^1H , ^{13}C , ^{19}F , and ^{27}Al), X-ray crystallography, Mössbauer spectroscopy, and conductivity measurements. All the data obtained fully support the structures proposed for these complexes as will now be briefly discussed.

To study the π -acidity of these ions in their complexes, a ^{13}C NMR and ^{13}C isotope exchange study was done (30). It was found that in the $\text{Fe}(\text{CO})_4\text{L}$ complexes, the CO ligands showed an extreme degree of lability compared both with the precursor halophosphine complex before halide abstraction and with iron pentacarbonyl. This suggests that the phosphorus ligand competes very favorably with CO as a strong π -acid by back-donation from the metal and in the process weakens the M-CO bond. This effect is due to the positive charge and appropriate orbitals for interaction with the metal as discussed previously. Infrared carbonyl stretching frequencies also show the expected trend. The frequencies significantly shift to higher energies in the phosphonium complexes compared with the precursor complexes as shown in Table 3. This is again due to back donation into the carbonyl π^* orbitals and therefore higher stretching frequencies correspond to a lower degree of M-C π bonding from the competition with the phosphonium ligand.

Table 2. ^{31}P NMR data for phosphonium ion-transition metal complexes

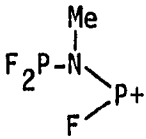
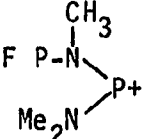
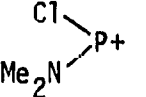
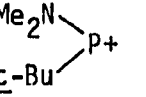
Phosphonium ligand	Metal Group	Anion	Phosphonium ion ^{31}P chem. shift	Reference
	$\text{Mo}(\eta^5\text{-Cp})(\text{CO})_3^-$	---	+275.2	25
	$\text{Mo}_2(\eta^5\text{-Cp})_2(\text{CO})_4^-$	---	+404.1	25
	$\text{Fe}(\text{CO})_4$	AlCl_4^-	+268.8	12
$(\text{Me}_2\text{N})_2\text{P}^+$	$\text{Fe}(\text{CO})_4$	PF_6^-	+311	24
$(\text{Et}_2\text{N})_2\text{P}^+$	$\text{Fe}(\text{CO})_4$	AlCl_4^-	+307.6	12
$(i\text{-Pr}_2\text{N})_2\text{P}^+$	$\text{Fe}(\text{CO})_4$	AlCl_4^-	+311.3	12
$((\text{Me}_3\text{Si})_2\text{N})_2\text{P}^+$	$\text{Fe}(\text{CO})_4$	AlCl_4^-	+349.7	12
	$\text{Fe}(\text{CO})_4$	AlCl_4^-	+441.5	12

Table 2 (continued)

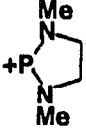
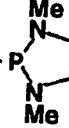
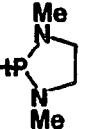
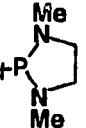
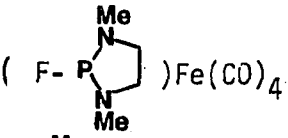
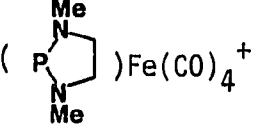
Phosphenium ligand	Metal Group	Anion	Phosphenium ion ^{31}P chem. shift	Reference
	$\text{Fe}(\text{CO})_4$	PF_6^-	+300	24
$(\text{Fc})_2\text{P}^+$	$\text{Fe}(\text{CO})_4$	AlCl_4^-	+280	16,4
$2 \mu^- +$ 	$\text{Co}_2(\text{CO})_5^{-2}$	---	+307	26
	$\text{Me}(\eta^5\text{-Cp})(\text{CO})_2^-$	---	+271	27,28
	$\text{Fe}(\eta^5\text{-Me}_5\text{C}_5)(\text{CO})_2^-$	---	+285.9	29

Table 3. Infrared data for phosphonium ion and precursor iron carbonyl complexes^a

Complex	IR (ν_{CO} , cm^{-1})			E
	A ₁	A ₁	A ₂	
Fe(CO) ₅	(2114) ^b	2031	2027	1994, (1884)
 (F-P(NMe) ₂)Fe(CO) ₄ ⁺	2061	1996	----- ^c	1956, 1939
 (P(NMe) ₂)Fe(CO) ₄ ⁺	2121	2070	-----	2018, 1955
((Et ₂ N) ₂ PCl)Fe(CO) ₄	2055	1975	-----	1955, 1940
((Et ₂ N) ₂ P)Fe(CO) ₄ ⁺	2105	2030	-----	1965, 1940

^aReference 30.

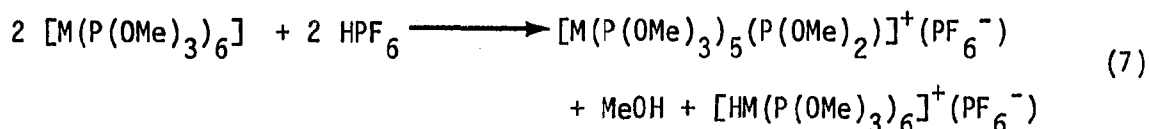
^bValues in parentheses were from the Raman spectrum.

^cThe A₂ mode does not exist for this species.

The single crystal X-ray structure of [Mo(CO)₂(P(N(Me)CH₂CH₂N(Me)))]7 has been determined (28) along with those of several other complexes (26, 29). In 7 the Mo-P multiple bond character expected is seen in a shorter-than-usual bond distance of 2.213 Å (usual Mo + P single bonds range from 2.40 to 2.57 Å (31)). Within the planar phosphorus ligand itself, the P-N bond distances are still shorter (1.645 Å) than the normal single bond distance (1.78 Å) but yet longer than in the free ion (1.613 Å) as expected.

Several metal nucleophiles have been reacted with a number of organophosphorus compounds other than halodiaminophosphines. Two preliminary reports have been published involving the interaction of metal carbonyl anions with halodioxaphosphorus(III) compounds to prepare either the bridged dinuclear or the mononuclear complexes (32, 33). In this report, the $M(\eta^5\text{-Cp})(\text{CO})_3^-$ anions ($M=\text{Cr, Mo, W}$) were reacted with cyclic chlorodioxaphospholanes to prepare the complexes mentioned above. These complexes were then further reacted with a variety of other phosphorus(III) compounds to yield a number of compounds substituted either at the metal or at the phosphorus centers. In the monomeric complexes of this type, however, the phosphorus ligand is serving as only a one electron donor with a free uncomplexed electron pair still on the phosphorus, giving the phosphorus a presumably pyramidal structure, as contrasted with 7.

Very recently, Muettertides has reported the preparation of what appears to be a true dioxaphosphenium ion complex (34, 35, 36). The method of synthesis involved the reaction of the zero-valent $[\text{M}(\text{P}(\text{OMe})_3)_6]$ ($M= \text{Mo, W}$) with hexafluorophosphoric acid to yield both the phosphonium ion complex and the protonated starting material as shown in equation 7.



This procedure has been tried by these authors on a number of other systems but it was found that only in the cases of molybdenum and

tungsten are phosphonium ion-complexes generated. In the other cases, only simple protonation or methyl group transfer occurred, unfortunately making this approach apparently limited to the two examples reported. A crystal structure determination was carried out showing the expected feature of the planar phosphonium ligand with a shortened M-P bond. Somewhat surprising, however, is that the ^{31}P chemical shift of the phosphonium ligand is not as far downfield as expected, although it is significantly downfield from the other trimethylphosphite ligand resonances in the complex. The coupling patterns and the number of resonances are what would be expected based upon the pseudo-octahedral coordination around the metal.

The interaction of the previously discussed metal nucleophile $[\text{Fe}(\eta^5\text{-Cp})(\text{CO})_2]^-$ with halophosphines was first reported by Hayter (37) to yield dimeric species with bridging phosphine linkages. Recently, this approach has been successfully extended to other metal-phosphine systems (M= nickel, cobalt (38), and platinum (39)). These complexes have received a great deal of attention because of their potential use in binuclear and cluster catalysis since the phosphorus bridge can stabilize a wide variety of angles and distances (and hence oxidation states) within the Fe_2P_2 framework (39).

As discussed previously, alkoxy substituents on phosphorus should be able to stabilize phosphonium ions as in carbenes in a manner analogous to that of the amino substituted compounds. Attempts reported in the literature to prepare these compounds have been sparse. It was found early in our work, however, that in the electron-impact mass spectrum of

several chloro-alkoxy substituted phosphorus compounds, that a major peak was observed corresponding to the $+P(OR)_2$ species. We have undertaken studies to develop synthetic procedures for oxaza- and dioxaphosphenium ion systems as both the free ions and their transition metal complexes. A variety of techniques was investigated. Through the attempted preparation of transition metal complexes of this type by the reaction of chloro-phosphorus(III) compounds with metal nucleophiles, a new route for the facile synthesis of dioxaphosphorus bridged iron dimers with phosphorus in a highly deshielded electronic environment was developed. These compounds were found to exhibit some unusual and very interesting physical and spectroscopic properties.

EXPERIMENTAL

Materials

All solvents used were reagent grade or better and were distilled from the appropriate drying agents under a dry nitrogen atmosphere: tetrahydrofuran, benzene, diethylether (sodium-potassium alloy, NaK); acetone, chloroform (4 Å molecular sieves); methylene chloride, acetonitrile (phosphorus pentoxide); methanol (calcium hydride). Ethyl acetate and methylcyclohexane were used as received. All organic solvents were degassed with a dry nitrogen stream and stored over 4 Å molecular sieves prior to use. Deuterated solvents were purchased from the Aldrich Chemical Company and stored over 4 Å molecular sieves.

The following reagents which are not commonly used were purchased from the Aldrich Chemical Company and used as received: 2-anilinoethanol ($C_6H_5NHCH_2CH_2OH$), 2,3-butanediol ($CH_3CH(OH)CH(OH)CH_3$), dicyclopentadiene ($C_{10}H_{12}$), diiron nonacarbonyl ($Fe_2(CO)_9$), 2,2-dimethyl-1,3-propanediol ($HOCH_2C(CH_3)_2CH_2OH$), ironpentacarbonyl ($Fe(CO)_5$), 2-mercaptoethanol (HSC_2H_4OH), 2-methylaminoethanol ($CH_3NHCH_2CH_2OH$), pinacol ($HOC(CH_3)_2C(CH_3)_2OH$), propionyl chloride (C_2H_5COCl), pyrocatechol ($C_6H_4-1,2-(OH)_2$), silvertetrafluoroborate ($AgBF_4$), tetrafluoroboric acid-diethylether complex ($BF_4 \cdot O(C_2H_5)_2$), triethylphosphite ($P(OC_2H_5)_3$), trifluoroacetic acid (CF_3CO_2H), trifluoromethanesulfonic acid (CF_3SO_3H), triirondodecacarbonyl ($Fe_3(CO)_{12}$), tris(dimethylamino)-phosphine, 8, ($P(N(CH_3)_2)_3$) and 2,4,6-tri-tert-butylphenol ($((CH_3)_3C)_3C_6H_2OH$).

The following reagents were purchased from the Aldrich Chemical Company and purified prior to use by vacuum distillation: chlorodiphenylphosphine 9 ($\text{ClP}(\text{C}_6\text{H}_5)_3$), N,N'-dimethylethylenediamine ($\text{CH}_3\text{NHCH}_2\text{CH}_2\text{NHCH}_3$); ethyleneglycol ($\text{HOCH}_2\text{CH}_2\text{OH}$), phosphorus trichloride (PCl_3), 1,3-propanediol ($\text{HO}(\text{CH}_2)_3\text{OH}$), and triphenylphosphite ($\text{P}(\text{OC}_6\text{H}_5)_3$).

The following organometallic and organophosphorus reagents were purchased from the Strem Chemical Company and used as received: hexacarbonylchromium, molybdenum, and tungsten ($\text{M}(\text{CO})_6$), dimanganesedecacarbonyl ($\text{Mn}_2(\text{CO})_{10}$), chlorodimethylphosphine 10 ($\text{ClP}(\text{CH}_3)_2$).

The following reagents were obtained from the listed commercial sources and were used as received: (cyclopentadienyl)(dicarbonyl)iron dimer 11 ($[(\text{Fe}(\eta^5\text{-Cp})(\text{CO})_2)_2]$; Pressure Chemical Company), anhydrous dimethylamine ($\text{HN}(\text{CH}_3)_2$; Kodak), hexafluorophosphoric acid-diethylether complex ($\text{HPF}_6 \cdot \text{O}(\text{C}_2\text{H}_5)_2$; Columbia Chemicals), and diisopropylether ($\text{O}(\text{C}_3\text{H}_7)_2$; Fisher Chemicals).

Techniques

NMR spectroscopy

Proton NMR spectra were obtained on either a Varian Associates EM-360A or a Bruker WM-300 spectrometer interfaced with an Aspect 2000 computer system. Spectra of all compounds were taken in either d_6 -benzene or d_1 -chloroform solution in 5mm (o.d.) tubes as specified. Chemical shifts are given in parts per million (ppm) relative to internal tetramethylsilane (TMS), with a positive shift indicating a resonance at

a lower applied field than that of the standard. All coupling constants (J) are given throughout in cycles per second (Hz). Routine spectra for identification and purity assessment were obtained on the Varian EM-360A operating at 60 MHz. Spectra recorded on the Bruker WM-300 spectrometer were obtained at an operating frequency of 300.133 MHz with a spectral sweep width of 4000.0 Hz (13.3 ppm) and a calculated acquisition time of 2.048 seconds per scan operating in the FT mode while locked on the deuterium resonance of the solvent. Double resonance and variable temperature spectra were all obtained on the WM-300. Phosphorus decoupled proton spectra were also obtained on the WM-300 spectrometer in 10 mm (o.d.) tubes. The frequency of the phosphorus resonance was first determined by observing the ^{31}P spectrum and calculating the phosphorus single resonance frequency. The instrument was then switched over to observe the proton NMR spectrum. The sample was then irradiated at the previously calculated resonance frequency by a PTS-160 frequency synthesizer interfaced to the spectrometer through a standard amplifier. Using an irradiating power of about 5 watts, a significant change was observed in the proton FID, verifying phosphorus decoupling. The system was initially checked and found to be operating successfully on several model compounds (e.g., $\text{P}(\text{OMe})_3$).

^{13}C NMR spectra were obtained on either a JEOL FX 90Q spectrometer operating at 22.50 MHz or a Bruker WM-300 operating at 75.473 MHz and interfaced with an Aspect 2000 computer system. Both spectrometers were operated in the FT mode while locked on the deuterium resonance of the solvent of samples in 5mm (o.d.) tubes. The reference was set relative

to TMS from the known chemical shifts of the carbon atoms of the solvent. A great deal of difficulty was encountered in observing the ^{13}C resonance of the carbonyl carbons in the transition metal complexes due to their long relaxation time. This problem was overcome in several cases by employing a small amount of $\text{Cr}(\text{acac})_3$ as a shiftless relaxation agent (40) to reduce the normally very long relaxation times of quaternary carbons and using pulse delays of 12 seconds. All spectra were broad-band proton decoupled.

Solution ^{31}P NMR spectra were obtained in 10mm (o.d.) tubes on a Bruker WM-300 spectrometer interfaced with an Aspect 2000 computer system operating at 121.513 MHz and employing a spectral sweep width of 71428.571 Hz (587.83 ppm). The instrument was operated in the FT mode while locked on the deuterium resonance of the solvent and using a 0.4 to 0.8 second delay between pulses. The external standard used was 85% phosphoric acid sealed in a 1 mm capillary tube held coaxially in the sample tube by a Teflon vortex plug. Downfield (lower applied field) chemical shifts are given as positive values. The field offset was adjusted such that an effective range of +530 to -57 ppm was routinely observed. Both proton broad-band decoupled and undecoupled spectra were routinely observed for each sample with a decoupling power of about 5 watts. Solid state ^{31}P NMR spectra were run on the Colorado State University Regional NMR center's spectrometers operating at 60.754 MHz with a spectral sweep width of 41666.6 Hz and employing the technique of magic angle spinning. Spectra were obtained both with and without cross polarization.

Mass spectrometry

High resolution mass spectra were obtained on an AE1 MS-902 high resolution mass spectrometer. Exact masses were determined by peak matching.

Low resolution nominal scan and low EV mass spectra were obtained on a Finnigan 4000 mass spectrometer interfaced with a gas chromatograph utilizing a temperature-programmable six foot 3% OV-101 column. Chemical ionization mass spectra were also obtained on the Finnigan using either isobutane or methane as the bulk reactant gas.

Infrared spectroscopy

Routine infrared spectra in the range of 4000 to 600 cm^{-1} and carbonyl stretching frequencies in the range of 1700 to 2100 cm^{-1} were measured on either a Beckman IR-4250 programmable spectrometer or a Perkin-Elmer 681 programmable spectrometer. All complexes were measured in solution. Frequencies reported are accurate to $\pm 3 \text{ cm}^{-1}$. Both instrumental systems employed NaCl optics and were operated in the double beam mode with pure solvent in a matched cell placed in the reference cell. Spectra were obtained in 1 mm NaCl cells with Teflon spacers. Absorption bands were referenced to the 1601.8 cm^{-1} band of polystyrene.

Conductivity measurements

Conductivities were measured on a Markson 4400 series Selectromark analyzer using the 1100 conductivity cell which is temperature compensating over a range of 0 to 100°.

Chromatography

Thin-layer chromatography was performed on Baker-flex aluminum oxide IB-F 20 cm x 5 cm precoated strips. The spots were visualized either by the visual color of the complexes or by exposure to either iodine vapor or ultraviolet irradiation.

Column chromatography was accomplished using Baker 60-200 mesh alumina powder and the locations of the bands were monitored either by thin-layer chromatography or by their visual colors. Both the thin-layer chromatography plates and the chromatographic powders were dried in an oven at 110°C for three days prior to use.

Melting points

The melting points of organic compounds and melting/decomposition points of other compounds were measured with a Thomas-Hoover capillary melting point apparatus and are uncorrected.

Preparations

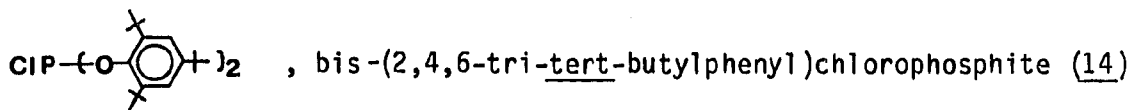
CIP(OCH₂CH₃)₂, chlorodiethylphosphite (12)

This compound was prepared and purified from the redistribution reaction of phosphorus trichloride and triethylphosphite by the modification of a procedure previously described (41, 42). The modified procedure used is described in detail below.

Under a dry nitrogen atmosphere, 118.7 grams (0.7146 mol) of triethylphosphite was placed in a 250 mL round bottom flask equipped with a water-cooled reflux condensor and a magnetic stirrer. To this was added in one portion 49.07 grams (0.3573 mol) of phosphorus trichloride. The reaction mixture was then heated to and held at reflux for 45 minutes by an oil bath. The reaction was allowed to cool slowly to room temperature and the crude product vacuum distilled at 15 torr, collecting the fraction which boiled over the range of 45-55°C. The pure product was obtained by redistilling this material on a 16" platinum spinning band column operating at 25 torr with a 30:1 reflux ratio. The first fraction, collected at 32°C, consisted of pure dichloroethyl phosphite. The second fraction, which distilled at 56°C, consisted of the pure desired product which was obtained in a 38.8% overall yield (lit. yield = 59%, lit. bp (25) = 54.5°C (42)). The ³¹P NMR chemical shifts of these pure compounds corresponded with those reported in the literature (43, 44). ¹H, ¹³C, and ³¹P NMR data are in agreement with what would be expected based upon the structure and are reported in Tables 16 and 18, respectively.

C1P(OPh)₂, chlorodiphenylphosphite (13)

The reaction of propionyl chloride with triphenylphosphite yields chlorodiphenylphosphite as reported in the literature (45). A second synthetic method reported involves the reaction of phosphorus trichloride with triphenylphosphite, which is analogous to that used for the preparation of chlorodiethylphosphite 12 except that it requires the use of a sealed tube reaction system (46). The former method above was used here with the addition of several modifications which were found to make the method more convenient. The heated reaction mixture required 28 hours to reach 195°C (the criterion used to indicate the completion of the reaction) rather than the reported 8 hrs. The desired product was separated from the other reaction products (primarily dichloro-phenylphosphite) and obtained in a pure form by a spinning band distillation at 6 torr. The fraction containing the desired product was collected at 157°C (lit. bp (0.5) = 115-116°C (45)) in a 45% overall yield (lit. yield = 62% (45)). The ¹H and ³¹P nmr data were consistent with that previously reported (44) and are given in Tables 16 and 20, respectively.



This phosphorochloridite has been reported previously in the literature as being prepared in very low yields from the interaction of phosphorus trichloride and the trisubstituted phenol in the presence of triethylamine (47). This procedure was found to be unsuitable for this

work, so a new procedure was developed to obtain larger amounts of the purified compound.

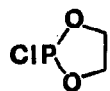
Under a dry argon atmosphere, 19.81 grams (0.1442 mol) of phosphorus trichloride was placed in an oven dried 1 L, three-necked flask equipped with an addition funnel and a mechanical stirrer. The phosphorus trichloride was then dissolved in 500 mL of dry toluene. The addition funnel was then charged with 125.25 grams (0.4921 mol) of 2,4,6-tri-tert-butylphenol and 113.09 grams (1.1176 mol) of triethylamine and dissolved in 100 mL of dry toluene. This solution was then added dropwise to the phosphorus trichloride solution over two hours. After the addition was complete the reaction was gently refluxed for 24 hours. The reaction was then cooled to room temperature, filtered, and the solid washed with 300 mL of dry hexanes. The solutions were combined and the solvents removed in vacuo to yield a black solid which was further dried in vacuo for an additional 24 hours. This solid was then stirred well with 400 mL of a 10% (weight by weight) aqueous sodium hydroxide solution and filtered. The collected solid was washed well with 500 mL of water and recrystallized twice from a hot acetone solution to yield in 38% yield a light tan, highly crystalline material. The observed melting point of 165-168°C corresponded well with that previously reported (lit. mp. = 173-174°C) (47). ^1H , ^{13}C , and ^{31}P NMR data agreed well with those expected based upon the structure and are given in Tables 16, 18, and 20, respectively. The mass spectrum showed the expected parent peak at 588.4 m/e⁻ (0.07% of the base peak) and the base peak corresponding to the trisubstituted phenoxy residue at 261 m/e⁻. This phosphorochloridite is

extremely resistant to neutral and basic hydrolysis as well as being stable toward air oxidation at room temperature.

CIP(NMe₂)₂, chlorobis(dimethylamino)phosphine (15)

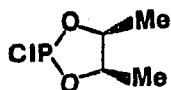
This compound was prepared from the redistribution reaction of phosphorus trichloride with tris(dimethylamino)phosphine (8, TDP) by a procedure significantly modified from that reported (48, 49).

Under a dry nitrogen atmosphere, 77.23 grams (0.5574 mol) of freshly distilled TDP was placed in a 250 mL round bottom flask equipped with an addition funnel and a magnetic stirrer. The addition funnel was then charged with 38.28 grams (0.2787 mol) of phosphorus trichloride which was slowly added dropwise over one hour to the aminophosphine. The reaction mixture was first stirred at room temperature for one hour and then refluxed at 100°C for 45-60 minutes. Caution when heating at this point is strongly advised since if the temperature is allowed to rise above 110°C an uncontrollable exothermic reaction takes place with complete decomposition of all products to a highly air-sensitive, pyrophoric orange solid. After heating, the mixture was allowed to cool slowly to room temperature and the product vacuum distilled at 3.5 torr and 47-50°C (lit. bp₍₁₀₎ = 64°C (48)). The purified product was obtained in a 73.1% yield as a clear, colorless liquid which is readily flammable on exposure to air or moisture (no yield was reported in the literature). The ¹H and ³¹P spectra were consistent with those previously reported (50) and are given in Tables 16 and 20, respectively.



, 2-chloro-1,3,2-dioxaphospholane (16)

This compound was prepared by the method reported by Cason et al. (51) from the reaction of dry ethylene glycol with phosphorus trichloride and purified prior to use by vacuum distillation ($bp_{(10)} = 41-43^{\circ}\text{C}$). The ^1H and ^{31}P nmr data corresponded with those previously reported (44) and are given in Tables 16 and 20, respectively.

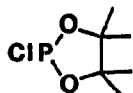


, meso-2-chloro-4,5-dimethyl-1,3,2-dioxaphospholane (17)

The preparation of this chlorophosphite has been previously reported from the reaction of meso-2,3-butanediol and phosphorus trichloride (52, 53). It was found that an improvement in both yield and purity of the product could be obtained by substantially modifying this procedure as described below. The pure meso form of the diol was obtained by repeated recrystallizations of the commercially available mixture of the meso and dl forms (however, mostly meso) from diisopropyl ether at dry ice/acetone temperature.

Under a dry nitrogen atmosphere, 81.66 grams (0.5947 mol) of phosphorus trichloride, which was dissolved in 100 mL of diethyl ether, was placed in a 250 mL flask equipped with an addition funnel and ice bath. The addition funnel was charged with 53.59 grams (0.5947 mol) of the 2,3-butanediol dissolved in 75 mL of ether. The diol solution was then added dropwise to the phosphorus trichloride solution over 1.5 hours while maintaining the 0°C temperature. After the addition was complete, the reaction was allowed to warm slowly to room temperature and nitrogen

bubbled through the solution for 2 hours to remove any remaining HCl. The solvent was then removed in vacuo and the product vacuum distilled at 12 torr and 47-48°C (lit. bp₍₁₅₎ = 66-67°C (53)) to give an 80.77% overall yield (lit. yield = 69% (52)). The ¹H and ³¹P data agreed well with those previously reported (54, 44) and are given in Tables 16 and 20, respectively.

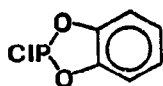


, 2-chloro-4,4,5,5-tetramethyl-1,3,2-dioxaphospholane (18)

This phosphorochloridite was synthesized by the reaction of 2,3-dimethyl-2,3-butanediol (pinacol) with phosphorus trichloride in the presence of two equivalents of N,N-dimethylaniline by a procedure reported by Denney et al. (55) and Goldwhite (56). Since the modification was substantial, a complete description of the method used here is given below.

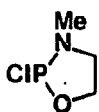
Under a dry nitrogen atmosphere, 56.84 grams (0.4263 mol) of phosphorus trichloride in 500 mL of dry ether was placed in a 1 L, 3-necked flask equipped with an ice bath, mechanical stirrer, and addition funnel. The funnel was charged with 50.38 grams (0.4263 mol) of the diol and 103.33 grams (0.8527 mol) of the N,N-dimethylaniline dissolved in 100 mL of ether. This solution was then added dropwise over 3 hours to the phosphorus trichloride solution while maintaining the 0°C temperature and vigorous stirring. Upon completion of the addition, the reaction was allowed to warm slowly to room temperature and stirred for an additional 18 hours. The amine hydrochloride was then filtered off and the solvent

removed in vacuo. The product was vacuum distilled at 12 torr and 77-78°C to yield a colorless, air-sensitive, mobile liquid in approximately a 90% overall yield (no bp or yield data were reported in the literature). The ^1H , ^{13}C , and ^{31}P NMR data are in agreement with what would be expected based upon the structure and are given in Tables 16, 18, and 20, respectively.



, 2-chloro-1,3,2-dioxaisophosphindolane (19)

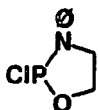
This compound was prepared using the previously reported procedures (57, 58) involving the reaction of pyrocatechol with a stoichiometric quantity of phosphorus trichloride in diethyl ether. The product was purified by vacuum distillation at 10 torr and 80-82°C (lit. bp. (10) = 80°C (57)) and it solidified on cooling to room temperature to a colorless, crystalline, air-sensitive material in 42% yield. The ^1H , ^{13}C and ^{31}P NMR data agreed well with what would be expected based on the structure of this compound and are given in Tables 16, 18, and 20, respectively (no NMR or yield data were reported in the literature).



, 2-chloro-N-methyl-1,3,2-azaioxaphospholane (20)

This compound was prepared by the reaction of phosphorus trichloride with a stoichiometric amount of the appropriate amino-alcohol. In a typical experimental, 75.11 grams (1.00 mol) of N-methylaminoethanol, 202.38 grams (2.00 mol) of triethylamine, and 137.33 grams (1.00 mol) of phosphorus trichloride were reacted in 500 mL of dry diethyl ether at 0°C

over 2 hours. After filtration and removal of the solvent, the pure product was isolated by a vacuum distillation at 8 torr and 60-63°C. This chlorophospholane was obtained in a 38.1% overall yield as an air-sensitive, mobile liquid. The ^1H and ^{31}P NMR data were consistent with those predicted by the structure and are given in Tables 16 and 20, respectively.

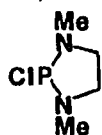


, 2-chloro-N-phenyl-1,3,2-azaioxaphospholane (21)

The preparation of this cyclic phosphorochloridite has been previously reported in the literature (59). The synthetic method used here, however, did not follow this published procedure because a more convenient and a higher yield method was developed which is described in detail below.

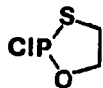
Into a flame dried 1 L 3-neck flask equipped with a dry nitrogen flush, ice bath, addition funnel and mechanical stirring device was placed 108.6 grams (0.7907 mol) of phosphorus trichloride and 150 mL of dry diethyl ether. The addition funnel was then charged with 108.5 grams (0.7909 mol) of freshly vacuum distilled 2-anilinoethanol and 160.06 grams (1.582 mol) of triethylamine dissolved in 175 mL of dry diethyl ether. The amine mixture was then added to the phosphorus trichloride solution dropwise over 1.5 hours while maintaining the temperature throughout the addition below 5°C. The reaction was then allowed to warm slowly to room temperature and stir for an additional 8 hours. The white amine hydrochloride precipitate which had formed was filtered off under

nitrogen and the solvent removed in vacuo to yield a colorless, viscous oil. The product was obtained in pure form by vacuum distillation at 8 torr and 135-137°C (no bp data were reported in the literature). Upon cooling to room temperature the product solidified to a white, crystalline, air-sensitive material which constituted a 56.3% overall yield. The ^1H and ^{31}P NMR data were consistent with that expected and are given in Tables 16 and 20, respectively. The toxicity warning for compound 22 (vide infra) should also be applied here.



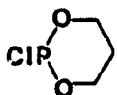
, 2-chloro-N,N'-dimethyl-1,3,2-diazaphospholane (22)

This compounds was prepared by the method of Ramirez et al. (60, 61) and Hayter (62) from the reaction of phosphorus trichloride and N,N'-dimethyl-ethylenediamine with the modification that the triethylamine was added simultaneously with the diamine to the phosphorus trichloride solution rather than at the end of the addition. It was found that the addition of the triethylamine in this modified manner greatly increased the yields of the cyclic aminophosphine in our hands. The product was distilled each time prior to use at 0.2 mm and 70°C. A 40% overall yield was obtained (lit. yield = 52% (60)). The ^1H and ^{31}P NMR data corresponded with those previously reported (60) and are reported in Tables 16 and 20, respectively. As a note of warning, cyclic aminophosphines should be handled with great care. Exposure to the vapors has resulted in reported cases of acute nausea and other severe symptoms (63).



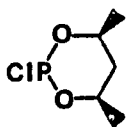
, 2-chloro-1,3,2-oxathiaphospholane (23)

The preparation of this compound was accomplished by the reaction of 2-mercaptoethanol with phosphorus trichloride using 2 equivalents of triethylamine as the HCl acceptor as previously reported in the literature (64). The product was obtained in pure form in 42% yield (no lit. yield reported) by vacuum distillation at 0.5 torr and 55-57°C (lit. bp(0.4) = 57°C (64)). The ^1H and ^{31}P NMR data corresponded well with those predicted based on the structure and are given in Tables 16 and 20, respectively.



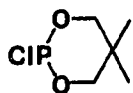
, 2-chloro-1,3,2-dioxaphosphorinane (24)

The preparation of this compound was accomplished by the reaction of 1,3-propanediol and phosphorus trichloride in methylene chloride using the apparatus and procedure described previously by Lucas et al. (65, 52). The product was vacuum distilled at 12 torr and 62-63°C (lit. bp(15) = 45.5-47.0°C (65)). Heating the bath above 100°C during the course of the distillation results in a significant amount of decomposition to an orange, pyrophoric solid. The product was obtained pure in an 88% yield (lit. yield = 63% (52)) and the ^1H NMR spectrum agreed well with that previously reported (44) and is given in Table 16. The ^{13}C and ^{31}P data support the proposed structure and are given in Tables 18 and 20, respectively.



, meso-2-chloro-4,6-dimethyl-1,3,2-dioxaphosphorinane (25)

The preparation of this compound requires the initial synthesis and purification of the meso form of 2,4-pentanediol followed by its reaction with phosphorus trichloride. The diol was synthesized and the dl and meso isomers separated by the initial sodium borohydride reduction of acetylacetonate followed by the reaction of this diol with thionyl chloride to yield both the isomeric cyclic sulfites by the procedure of Pritchard and Vollmer (66). Following the modification of White et al. (67), the isomeric sulfites were separated via a spinning band distillation at 12 torr and the meso isomer collected at 72-73°C (lit. bp₍₁₂₎ = 72°C (66)). The free diol was obtained by reaction with aqueous sodium hydroxide followed by a final vacuum distillation at 3 torr and 74-75°C (lit. bp₍₃₎ = 73°C (66)). The product was identified as greater than 95% pure of the meso isomer by ¹H NMR (66). The meso-phosphorochloridite was then obtained by the method previously reported (67) by the reaction of the diol with phosphorus trichloride, without an amine base present and the final product vacuum distilled at 12 torr and 72-73°C (same as reported in the literature (67)). The ¹H and ³¹P NMR data agreed well with those reported (67) and are given in Tables 16 and 20, respectively.



, 2-chloro-5,5-dimethyl-1,3,2-dioxaphosphorinane (26)

This phosphorochloridite was prepared from the reaction of 2,2-dimethyl-1,3-propanediol with phosphorus trichloride by a procedure

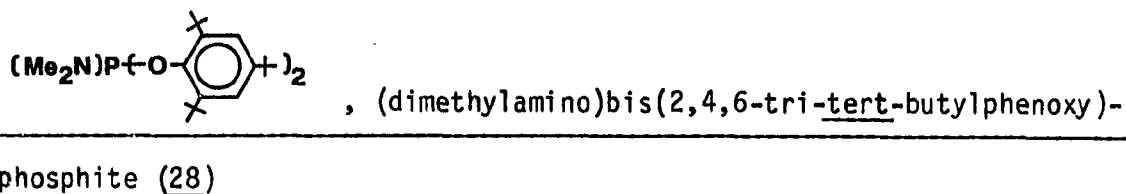
previously described by Edmundson (68) and modified by White et al. (67). Several further modifications to the above procedure were used in this work as described below. During the addition of the diol to the phosphorus trichloride solution, no amine base was employed as an HCl acceptor. Following the completion of the addition, dry nitrogen was bubbled through the reaction solution for several hours to aid in driving off any HCl remaining in solution. The product was purified by vacuum distillation at 12 torr and 72-73°C (lit. bp₍₁₃₎ = 66°C (68), bp₍₁₂₎ = 70°C (67)) and obtained in a 62% overall yield. The ¹H and ³¹P data corresponded well with those previously reported (67) and are given in Tables 16 and 20, respectively.

(Me₂N)₂P(OMe), bis(dimethylamino)methoxyphosphine (27)

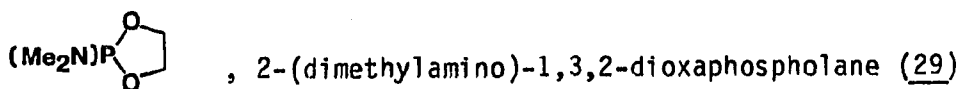
The preparation of this phosphinite has not been reported in the literature; however, the synthesis of a close analogue, bis(dimethylamino)ethoxyphosphinite, has been reported from the redistribution reaction between tris(dimethylamino)phosphine and trimethylphosphite (69). The method used here to prepare 27, however, uses an entirely different synthetic route which was found to be more convenient and is described in detail below.

Into a 250 mL, 2 necked flask equipped with an ice bath, mechanical stirrer, and addition funnel was placed 17.11 grams (0.1108 mol) of chlorobis(dimethylamino)phosphine 15 dissolved in 100 ml of dry ether. The addition funnel was charged with 3.544 grams (0.1108 mol) of dry

methanol and 11.21 grams (0.1108 mol) of triethylamine dissolved in 75 ml of ether. This solution was then added dropwise over 1 hour to the solution of 15. After the addition was complete, the reaction was warmed to room temperature and the amine hydrochloride filtered off. The solvent was removed in vacuo and the product purified by vacuum distillation at 22 torr and 147-148°C. The product was obtained in a 68.4% overall yield as a colorless liquid. The ^1H and ^{31}P NMR data were in agreement with those expected for the structure and are given in Tables 7 and 8, respectively.



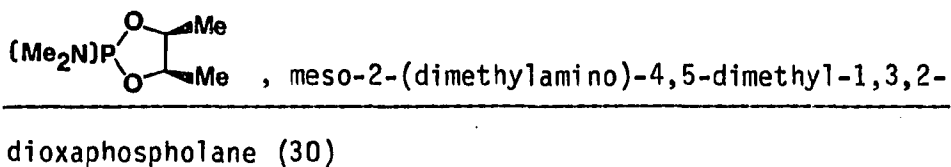
This compound was prepared by the method used for the synthesis of 27. The mass spectrum showed a parent ion at 597 m/e (0.5% rel. int). The ^1H and ^{31}P NMR spectra were consistent with the expected structure (data presented in Tables 7 and 8).



The preparation of this compound has been previously reported (70); however, a more convenient procedure was developed which is described in detail below.

The apparatus used for this preparation consisted of a 2-necked, 500 mL, round bottomed flask equipped with a nitrogen inlet, ice bath, and a nitrogen outlet which was in turn connected with tigon tubing to an inlet into a 3-necked, 1 L, round bottomed reaction flask and fitted onto a gas

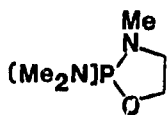
dispersion tube which extended to within 3 cm of the bottom of the flask. This 1 L flask was further equipped with a mechanical stirring device, ice bath, and nitrogen outlet connected to a bubbler. Into the 1 L flask was then placed 48.06 grams (0.3801 mol) of the 2-chloro-1,3,2-dioxaphospholane 16, dissolved in 600 mL of dry diethyl ether, and cooled to 0°C. To the 500 mL flask was added 45 grams (1.0 mol) of anhydrous dimethylamine. Nitrogen was then flushed through the entire system at a rate of about 5 mL/min until all the dimethylamine had evaporated (approximately 6 hours), while maintaining to 0°C temperature and rapid stirring. The reaction was then allowed to warm slowly to room temperature and to stir for an additional 12 hours. The amine hydrochloride was then filtered off and dry nitrogen gas was bubbled through the ethereal solution for 1 hour to remove any excess dimethylamine. The solvent was removed in vacuo and the product distilled at 11 torr and 60-62°C (lit. bp₍₁₂₎ = 65°C(70)) to obtain a 68.1% overall yield of the colorless liquid product (lit. yield = 67.7% (70)). ¹H and ³¹P NMR data were in agreement with the expected structure (no NMR data were reported in the literature) and are given in Tables 7 and 8, respectively.



The preparation of this dimethylaminophosphite has been reported previously in the literature (71). The synthetic method employed here,

however, was similar to that given for compound 29 and not the reported procedure of Edmundson because it was found to be synthetically more convenient.

Using the apparatus described for the preparation of 29, 25.857 grams (0.1673 mol) of meso-2-chloro-4,5-dimethyl-1,3,2-dioxaphospholane 17 and 40 grams of anhydrous dimethylamine were reacted under a nitrogen atmosphere in the manner described for 29. After filtration of the precipitated amine hydrochloride and removal of the solvent in vacuo, the product was vacuum distilled at 5.5 torr and 52-54°C (lit. bp. (8.5) = 65.5°C (71)). The product was obtained in an 82.4% yield as a clear, colorless liquid (lit. yield = 69% (71)). The ^1H and ^{31}P NMR spectra agreed well with those expected for the structure and are given in Tables 7 and 8, respectively (no NMR data were reported in the literature).

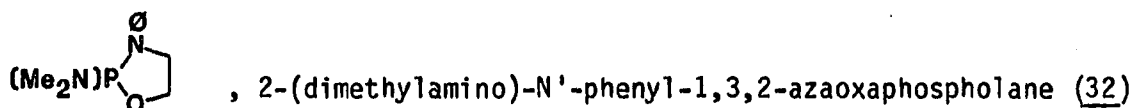


, 2-(dimethylamino)-N'-methyl-1,3,2-azaoxaphospholane (31)

The synthesis of this compound has been reported (72), however, this procedure was not used here. Instead, the method chosen for this work was found to be synthetically more convenient and is similar to that given for the synthesis of compound 32 (vide infra).

In a typical experiment involving the use of the apparatus previously described for the preparation of compound 29, 22.304 grams (0.1598 mol) of 2-chloro-N-methyl-1,3,2-azaoxaphospholane 20 and 25.0 grams of anhydrous dimethylamine were reacted in 600 mL of dry diethylether at 0°C over 6 hours. After stirring for an additional 12

hours at room temperature and filtration of the amine hydrochloride, the product was vacuum distilled at 8 torr and 40-43°C (lit. bp₍₁₆₎ = 66-68°C (72)). A 51.6% overall yield of a clear, colorless liquid was obtained (lit. yield = 63% (72)). The ¹H and ³¹P NMR data agreed well with those expected for the structure and are given in Tables 7 and 8, respectively (no NMR data for this compound were reported in the literature).



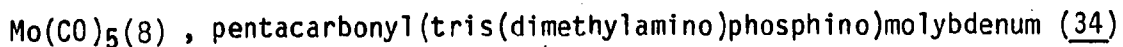
The preparation of this compound has been previously reported in the literature (72); however, the procedure used in this work was not similar to the reported method in which the amino alcohol was reacted with tris(dimethylamino)phosphine 8. For this study, it was found to be more convenient to first react phosphorus trichloride with the amino-alcohol followed by the reaction with dimethylamine as described below.

The apparatus used for this preparation was the same as that used for compound 29. Under a dry nitrogen atmosphere, 15.886 grams (0.07886 mol) of 2-chloro-N-phenyl-1,3,2-azaioxaphospholane 21 was dissolved in 600 mL of dry diethyl ether and placed in the reaction flask. The other flask was charged with 25 grams of anhydrous dimethylamine and nitrogen flushed through the entire system until all the dimethylamine had evaporated. The reaction mixture was then allowed to warm slowly to room temperature and stirred for an additional 12 hours, after which time the amine hydrochloride was filtered off. The solvent was removed in vacuo and the product vacuum distilled at 8 torr and 122-124°C. Note: during

the distillation, it is important that the bath temperature not be allowed to rise above 140°C or else significant decomposition occurs. The product was isolated in a 52.1% overall yield as an odiferous, clear, colorless liquid (no lit. bp or % yield data reported). The product was stored under nitrogen at -78°C to avoid decomposition. The NMR spectra agreed well with those expected from the structure and are given in Tables 7 and 8, respectively (no NMR data were given in the literature).



The synthesis of this compound has been previously reported from the reaction of excess anhydrous dimethylamine with the phosphorochloridite 26 using the apparatus described in the preparation of 29 (73, 74, 75). The product was purified prior to use by sublimation at 0.5 torr and 50°C. The ¹H and ³¹P NMR data agreed with those previously reported (75) and are given in Tables 7 and 8, respectively.



The preparation of this complex has been previously reported by King from the reaction of tris(dimethylamino)phosphine 8 with hexacarbonylmolybdenum in refluxing methylcyclohexane (76). The synthesis for this work involved the same reactants; however, the procedure employed was significantly modified from that reported as described in detail below.

Under a dry nitrogen atmosphere, 7.92 grams (30.0 mmol) of $\text{Mo}(\text{CO})_6$ and 6.00 grams (36.9 mmol) of tris(dimethylamino)phosphine 8 were mixed in 100 mL of dry methylcyclohexane. The reaction was refluxed for 9 hours, during which time the color changed from colorless to yellow and finally to black. The reaction was then allowed to cool to room temperature, filtered, and the solvent removed under vacuum. The resulting black residue was extracted with 110 mL of dry hexane which was filtered and stored at 0°C for 18 hrs. The colorless crystals which had formed upon standing were then filtered and washed with a small amount of cold hexane followed by drying in vacuo. The product was sublimed twice at 0.5 torr and 75°C to give a 28.1% yield of the colorless, crystalline product (lit. yield = 33.5% (76)). The melting point (observed mp = 148-151°C, lit. mp = 152-152°C (76)) and the ^1H NMR spectrum agreed well with the published values (76) and the ^{31}P NMR spectra agreed well with that expected. The ^1H and ^{31}P data are given in Tables 10 and 11, respectively.

$\text{Fe}(\text{CO})_4$ (8), tetracarbonyl(tris(dimethylamino)phosphino)iron (35)

The preparation of this complex was first reported by King (76). A more convenient synthesis was developed in this work by extending the procedure of Butts and Shriver (77) involving the reaction of pentacarbonyliron with tris(dimethylamino)phosphine in the presence of a catalytic amount of polynuclear iron carbonyl anions generated in situ. The procedure employed is given below.

Under a dry nitrogen atmosphere, 60 mL of a blue solution of sodium benzophenone ketyl in tetrahydrofuran (prepared by adding 0.2 grams of metallic sodium chunks to a 0.1M solution of benzophenone in 100 mL of dry, oxygen-free tetrahydrofuran) was added to 10.00 grams (0.0761 mmol) of pentacarbonyliron in a flask equipped with a magnetic stirrer, heating bath and condenser. This solution was then brought to reflux and 4.65 grams (0.0285 mmol) of tris(dimethylamino)phosphine 8 added at once. The reaction was then refluxed for an additional 4 hours followed by cooling to room temperature and removal of the solvent in vacuo. The resulting yellow, pasty residue was chromatographed on an alumina column (30 cm x 2.0 cm) by eluting with pure hexane. The solvent was removed to yield a light yellow crystalline product in approximately a 28% yield (lit. yield = 22% (76)). The melting point (observed mp = 54-62°C, lit. mp = 48.85°C (76)) and ^1H NMR spectrum agreed well with reported values (76) and the ^{31}P spectrum agreed with the expected spectrum. The ^1H and ^{31}P data for this complex are given in Tables 10 and 11, respectively.

$\text{Fe}(\text{CO})_4$ (30), tetracarbonyl(2-(dimethylamino)-4,5-dimethyl-1,3,2-dioxaphospholano)iron (36)

This complex was prepared using a modified procedure of Bratermen (78) which was found to give better yields of the product.

Under a dry nitrogen atmosphere, 2.47 grams (6.78 mmol) of diironnonacarbonyl was suspended with rapid stirring in 200 mL of dry hexane. To this was added 2.21 grams (13.6 mmol) of 2-(dimethylamino)-

4,5-dimethyl-1,3,2-dioxaphospholane 30 and the reaction mixture refluxed for 24 hours. The solvent was removed and the residue extracted with 100 mL of pentane which was then cooled to -78°C for 12 hrs. The solid yellow product which had formed was collected by filtration and was washed with a small portion of cold pentane. Final purification was accomplished by column chromatography on alumina eluting with hexane. A mobile yellow band was collected which was found to contain the desired product. The ^{31}P spectrum showed a single resonance and the ^1H NMR data agreed well with those expected based upon the structure. These data are given in Tables 11 and 10, respectively.

$\text{Fe}(\text{CO})_4$ (31), tetracarbonyl(2-(dimethylamino)-N'-methyl-1,3,2-
azaoxaphospholano)iron (37)

This complex was prepared by the reaction of 1.02 grams (2.80 mmol) of diironnonacarbonyl with 0.830 grams (5.6 mmol) of 2-(dimethylamino)-N'-methyl-1,3,2-azaoxaphospholane 31 in 200 mL of dry hexane while under a dry nitrogen atmosphere. The reaction was refluxed for 24 hrs followed by the removal of the solvent, extraction of the residue with pentane, and cooling to -78°C . The yellow solid product obtained was further purified in a manner similar to that used for complex 36. The ^1H and ^{31}P spectra agreed well with those expected based upon the structure and are given in Tables 10 and 11, respectively.

Cr(CO)₅ (26), pentacarbonyl(2-chloro-5,5-dimethyl-1,3,2-dioxaphosphorinano)chromium (38)

This complex was prepared using a modification of the procedure of Bartish and Kraihanzel (79) from the reaction of 5.347 grams (24.30 mmol) of hexacarbonylchromium with 4.094 grams (24.30 mmol) of 2-chloro-5,5-dimethyl-1,3,2-dioxaphosphorinane 26 in 100 mL of methylcyclohexane. The reaction mixture was refluxed for 12 hrs and the product purified by fractional sublimation at 0.05 torr and 40°C (unreacted hexacarbonylchromium) and 70°C (product) (observed yield = 42%, lit. yield = 50% (79)). The ¹H NMR spectrum agreed well with that previously reported in the literature (79) and both the ¹H and ³¹P NMR data are given in Tables 10 and 11, respectively.

Mo(CO)₅ (26), pentacarbonyl(2-chloro-5,5-dimethyl-1,3,2-dioxaphosphorinano)molybdenum (39)

This complex was prepared similarly to 38 in that 4.613 grams (17.48 mmol) of hexacarbonylmolybdenum and 2.945 grams (17.48 mmol) of 2-chloro-5,5-dimethyl-1,3,2-dioxaphosphorane 26 were reacted in refluxing methylcyclohexane for 3 hours. The product was purified, however, by first removing the unreacted hexacarbonylmolybdenum by sublimation at 0.1 torr and 45°C followed by recrystallization of the product from hexane (observed yield = 68%, lit. yield = 90% (79)). The ¹H NMR spectrum obtained for the product agreed well with that previously reported (79)

and both the ^1H and ^{31}P data are given in Tables 10 and 11, respectively.

$[\text{Mo}(\eta^5\text{-Cp})(\text{CO})_3]_2$, cyclopentadienylmolybdenum tricarbonyl dimer (40)

This complex was prepared by the reaction of hexacarbonylmolybdenum with dicyclopentadiene using the published method of Hayter (62). The excess hexacarbonylmolybdenum was sublimed out and the dark red-violet crystalline pure product obtained by recrystallization from a chloroform-hexanes mixture by the method of King (80). The ir spectrum of the product agreed with the literature (81) and the ^1H NMR spectrum agreed with that expected for the structure.

$[\text{Fe}(\eta^5\text{-Cp})(\text{CO})(\text{PPh}_2)]_2$, cis and trans-di- μ -(diphenylphosphido)-di- π -cyclopentadienyldicarbonyldiiron (40)

The cis and trans isomers of this complex were prepared by the method of Hayter (37) in which chlorodiphenylphosphine 9 was reacted with $\text{Na}[\text{Fe}(\eta^5\text{-Cp})(\text{CO})_2]$ in refluxing toluene. The two isomers were separated by column chromatography and further purified by recrystallization from a 10:90 benzene/hexane mixture to give crystalline products. The infrared and ^1H NMR data agreed with the reported values and the ^{13}C and ^{31}P NMR spectra agreed with those expected for the structure and all are given in Tables 21, 17, 19, and 20, respectively.

$[\text{Fe}(\eta^5\text{-Cp})(\text{CO})(\text{PMe}_2)]_2$, cis and trans-di- μ -(dimethylphosphido)-di-
 π -cyclopentadienyldicarbonyldiiron (42)

These complexes were prepared by the method of Hayter (37) by the reaction of chlorodimethylphosphine and $\text{Na}[\text{Fe}(\eta^5\text{-Cp})(\text{CO})_2]$ in refluxing toluene and purified in a manner similar to that of cis and trans - 41. The ir and ^1H NMR spectra agreed with the reported values and the ^{13}C and ^{31}P NMR data agreed with those expected based upon the structure. These data are given in Tables 21, 17, 19, and 20, respectively.

$[\text{Fe}(\eta^5\text{-Cp})(\text{CO})_2(\text{P}(\text{NMeCH}_2\text{CH}_2\text{N}))]$, (η^5 -cyclopentadienyl)(N,N'-dimethyl-
 1,3,2-diazaphospholano)dicarbonyliron (43)

This complex was prepared by the procedure described in the literature by Hutchins et al. (29) from the reaction of the chloro-aminophosphine 22 with $\text{Na}[\text{Fe}(\eta^5\text{-Cp})(\text{CO})_2]$ in THF. Its ^1H and ^{31}P NMR spectra agreed well with those reported (29) (ir (ν_{CO} , Nujol) 2202 (m) 1969 (s), 1954 (s), 1914 (s) cm^{-1} ; ^1H NMR (d_6 -benzene) δ 3.07 (4H, m), 2.63 (6H, d, $^3J_{\text{HCNP}} = 13.3$ Hz); ^{13}C { ^1H } (d_6 -benzene) δ 217.9 (d, $^2J_{\text{CFeP}} = 3.0$ Hz), 95.89 (s), 54.78 (d, $^2J_{\text{CNP}} = 10.1$ Hz), 35.23 (d, $^2J_{\text{CNP}} = 21.3$ Hz); ^{31}P { ^1H } (d_6 -benzene) δ 285.9).

$[\text{Fe}(\eta^5\text{-Cp})(\text{CO})\text{L}]_2$, cis and trans-bis- μ -L-dicarbonyldicyclopentadienyl-
diiron (41, 42, 44-56)

These complexes were all prepared in similar manners in which the chlorophosphorus compound is reacted with a stoichiometric amount of $\text{Na}[\text{Fe}(\eta^5\text{-Cp})(\text{CO})_2]$ in tetrahydrofuran. The procedure used is described below.

In a typical experiment, 15.0 grams of triple distilled mercury were placed in a flame dried 250 mL flask with a stopcock at the bottom and equipped with a magnetic stirrer and a dry nitrogen flush. While rapidly stirring the mercury, 2.10 grams (0.0913 mol) of sodium was added in very small pieces against a countercurrent of nitrogen. After the amalgam had cooled to room temperature, 50 mL of dry tetrahydrofuran were added followed by 10.00 grams (0.02825 mol) of $[\text{Fe}(\eta^5\text{-Cp})(\text{CO})_2]_2$ 11. The reaction mixture was allowed to stir for two hours followed by the removal of the amalgam via the bottom stopcock. To this solution was then added 0.0565 mol of the chlorophosphite dropwise via syringe over twenty minutes. Vigorous CO evolution started immediately upon addition and continued for several hours. The reaction was then allowed to stir for an additional 12 hours after the addition was complete. The tetrahydrofuran was removed in vacuo and the resulting red solid was dissolved in a minimum amount of benzene and chromatographed on an alumina column (25 x 2.5 cm) by eluting with benzene and employing nitrogen pressure to aid elution. The eluate was continuously collected until no further orange-red material was eluted. The benzene was then

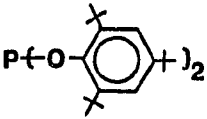
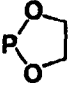
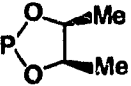
removed under vacuum leaving a red-brown powder. This material was then rechromatographed on alumina (50 x 2.5 cm) to separate and purify the isomers using either benzene or chloroform as the eluate. The R_f values for these complexes are listed in Table 4. After removal of the solvent, the complexes were recrystallized from a 50:50 benzene/methylene chloride mixture.

The cis and trans isomers were collected in 10-30% yields as microcrystalline, air-stable solids. Solutions of the trans isomers were quite stable on standing while those of the cis isomer decomposed much more rapidly (complete decomposition within 24 hours). The ir, ^1H , ^{13}C and ^{31}P NMR data for these compounds are tabulated in Tables 21, 17, 19, and 20, respectively.

$[\text{Fe}(\text{CO})_3(\underline{26})]_2$, bis(μ -5,5-dimethyl-1,3,2-dioxaphosphorinano)-
hexacarbonyldiiron (57)

This complex was prepared by the corrected procedure (the lit. report presumably has an error in the reported stoichiometric quantities of reactants) of Bartish and Kraihanzel (82) from the reaction of 7.9 grams of triiron dodecacarbonyl with 7.9 grams of 2-chloro-5,5-dimethyl-1,3,2-dioxaphosphorinane 26 in 50 ml of refluxing benzene. The product was purified by column chromatography on alumina eluting with benzene followed by recrystallization from a 50:50 methylene chloride/hexane mixture. The ^1H NMR and ir spectra agreed with those reported (82) and

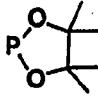
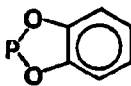
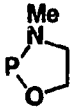
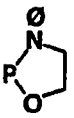
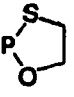
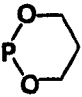
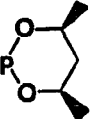
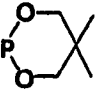
Table 4. R_f values for $[\text{Fe}(\eta^5\text{-Cp})(\text{CO})\text{L}]_2$ complexes on alumina

Bridging ligand	Cl-P<	Complex isomer	Complex	Chloroform	Benzene
CO	---	Fp_2	<u>11</u>	0.97	0.94
PPh ₂	<u>9</u>	cis	<u>41</u>	0.99	0.73 ^a
		trans	<u>41</u>	0.99	0.96 ^a
PMe ₂	<u>10</u>	cis	<u>42</u>	0.77	0.48 ^b
		trans	<u>42</u>	0.91	0.55 ^b
P(OEt) ₂	<u>12</u>	cis	<u>44</u>	0.87	0.67
		trans	<u>44</u>	0.96	0.94
P(OPh) ₂	<u>13</u>	cis	<u>45</u>	0.76	0.85
		trans	<u>45</u>	0.91	0.89
	<u>14</u>	cis	<u>46</u>	0.96	0.62 ^b
		trans	<u>46</u>	0.98	0.72 ^b
	<u>16</u>	cis	<u>47</u>	0.60	0.22
		trans	<u>47</u>	0.79	0.43
	<u>17</u>	cis	<u>48</u>	0.76	0.48
		trans	<u>48</u>	0.95	0.76

^a50:50 benzene/pentane mixture as eluate.

^b30:70 benzene/pentane mixture as eluate.

Table 4 (continued)

Bridging ligand	C1-P<	Complex isomer	Complex	Chloroform	Benzene
	<u>18</u>	cis	<u>49</u>	0.93	0.87
		trans	<u>49</u>	0.96	0.94
	<u>19</u>	cis	<u>50</u>	0.90	0.87
		trans	<u>50</u>	0.95	0.92
	<u>20</u>	cis	<u>51</u>	0.65	0.36
		trans	<u>51</u>	0.85	0.59
	<u>21</u>	cis	<u>52</u>	0.75	0.46
		trans	<u>52</u>	0.89	0.56
	<u>23</u>	cis	<u>53</u>	0.56	0.45 ^b
		trans	<u>53</u>	0.65	0.55 ^b
	<u>24</u>	cis	<u>54</u>	0.70	0.33
		trans	<u>54</u>	0.95	0.65
	<u>25</u>	cis	<u>55</u>	0.52	0.46
		trans	<u>55</u>	0.66	0.66
	<u>26</u>	cis	<u>56</u>	0.71	0.47
		trans	<u>56</u>	0.89	0.63

the ^{31}P NMR spectrum agreed with those expected based upon the structure (ir (ν_{CO} , hexane) 2066 (m), 2026 (vs), 2005 (s), 1978 (m), 1954 cm^{-1} (m); ^1H NMR (d_6 -acetone) δ 1.10 ppm (6H, s), 4.13 ppm (2H, 5 ($^3\text{J}_{\text{HP}} + ^5\text{J}_{\text{HP}} = 10.9$ Hz), 3.99 ppm (2H, 5 ($^3\text{J}_{\text{HP}} + ^5\text{J}_{\text{HP}} = 12.5$ Hz); ^{31}P { ^1H } (d_6 -acetone) δ 305.7 (s)).

Reactions

Reactions of chlorophosphorus(III) compounds with chloride abstractors

In these reactions, various chlorophosphorus(III) compounds 22, 26, 38, 39 were reacted with a variety of chloride abstractors (aluminum trichloride, phosphorus pentachloride, antimony pentachloride and silver (I) ions) and under a variety of conditions. The apparatus used in each case was that shown in Figure 8. All reactions were monitored via ^{31}P NMR spectroscopy. A brief description of each case is given below.

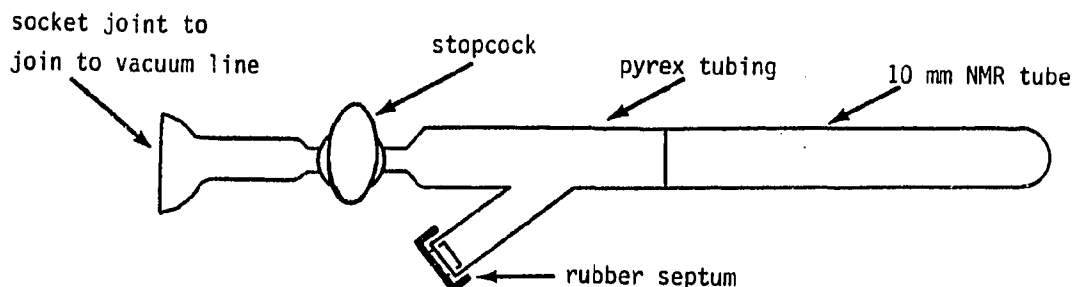


Figure 8. Apparatus for the reaction of chlorophosphorus(III) compounds with chloride abstractors

Reactions with aluminum trichloride

Into the flame-dried apparatus shown in Figure 8 was placed 15.26 mmol of 22 or 26 followed by 1 mL of dry, deoxygenated methylene chloride as solvent. This solution was then frozen to liquid nitrogen temperature. The system was evacuated under dynamic vacuum for 5 minutes. On top of this frozen solution was syringed in 0.2540 grams (17.55 mmol which is a 1:1.15 mol ratio of (22, 26) to aluminum trichloride) of freshly sublimed aluminum trichloride in 2.5 mL of tetrahydrofuran and this solution was also frozen. The system was allowed to warm to room temperature under dynamic vacuum, allowing all the solvent to evaporate. The system was then isolated from the vacuum line and 2 mL of tetrahydrofuran and 0.5 mL of deuterated benzene added via syringe. The solution was frozen, the system evacuated and the NMR tube sealed with a torch. The tube was then allowed to warm slowly to room temperature.

Reactions with phosphorus and antimony pentachlorides

The same procedure was used here as that used in the reaction with aluminum trichloride with the exception that nitromethane was used instead of methylene chloride as the solvent.

Reactions with silver(I) ion

The procedure used here was similar to that used for aluminum trichloride reactions except for some slight modifications. The silver (I) tetrafluoroborate was placed into the apparatus, dissolved in 0.5 mL

of methylene chloride and frozen. To this was then added a solution of an equimolar amount of 22 or 26 in 1.0 mL of dry methylcyclohexane. The remainder of the procedure was unchanged.

Reactions of (chlorophosphorus(III))-metal carbonyl complexes with aluminum trichloride

In a typical experiment, 5.227 mmol of 38 or 39 were placed in the apparatus and dissolved in 1.5 mL of dry methylene chloride. This solution was then frozen and evacuated. On top of this solution was placed via syringe 6.795 mmol of aluminum trichloride in 2.0 mL of tetrahydrofuran and this solution similarly frozen. The reaction was then allowed to warm slowly to room temperature under dynamic vacuum during which time all the solvent was evaporated. The apparatus was isolated from the vacuum line by means of the stopcock and 2.0 mL of methylene chloride and 0.5 mL of deuterated benzene added and frozen. The tube was then evacuated and flame sealed.

Reactions of chlorophosphorus(III) compounds with metal nucleophiles

Reaction with $\text{Na}[\text{Mo}(\eta^5\text{-Cp})(\text{CO})_3]$

The metal nucleophile, $[\text{Mo}(\eta^5\text{-Cp})(\text{CO})_3]^-$, was prepared by the method of Hayter (62). In a typical experiment, 3.69 mmol of $[\text{Mo}(\eta^5\text{-Cp})(\text{CO})_3]\text{Na}$ in 50 mL of tetrahydrofuran was placed in a 3 necked flask equipped with a dry ice/acetone bath, addition funnel, nitrogen purge, and magnetic stirrer. To this was then slowly added 3.69 mmol of 26 dropwise over 5

minutes via syringe. The reaction was allowed to warm slowly to room temperature and to stir for an additional 24 hours. The course of the reaction was monitored by observation of the ^{31}P NMR spectra over 48 hours. ^{31}P NMR data will be presented in the Results and Discussion portion of this chapter.

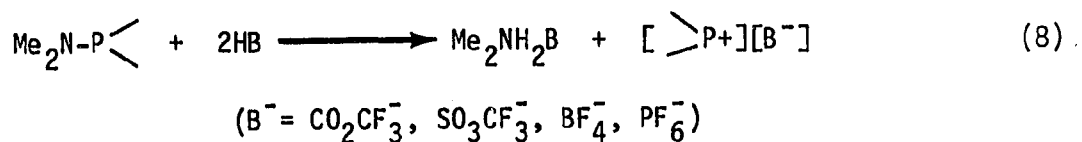
Reaction with $\text{Na}[\text{Mn}(\text{CO})_5]$

The metal anion, $[\text{Mn}(\text{CO})_5]^-$, was prepared by the method previously described in the literature (83). In a typical experiment, 7.69 mmol of 26 was dissolved in 50 mL of dry tetrahydrofuran and placed in a dry, 3 necked flask equipped with an addition funnel, ice bath, and magnetic stirrer. The addition funnel was charged with 7.69 mmol of $[\text{Mn}(\text{CO})_5]^-$ dissolved in 50 mL of tetrahydrofuran. This solution was then added dropwise over 1 hr to the chlorophosphorus ligand. After completion of the addition, the reaction was allowed to warm to room temperature and to stir for 12 hours.

The reaction of dimethylaminophosphorus(III) compounds with acids

In a typical experiment, under a dry nitrogen atmosphere, 35.49 mmol of a dimethylaminophosphorus(III) ligand (compounds 8, 27-33) were dissolved in 40 mL of dry chloroform and placed in a 3 neck flask equipped with a magnetic stirrer. This solution was cooled to and maintained at 0°C throughout the reaction by means of an external ice bath. To this solution was then slowly added dropwise over 15 minutes

70.98 mmol of the anhydrous acid via syringe. The acids used were; trifluoroacetic, trifluoromethanesulfonic acid, tetrafluoroboric (as the diethylether complex), and hexafluorophosphoric acid (as the diethylether complex). Within five minutes after the beginning of the acid addition, a white, highly crystalline precipitate began to form from the exothermic reaction. After completion of the addition, the reaction was allowed to warm slowly to room temperature and to stir for an additional 12 hours. Using Schlenk techniques, the crystalline ammonium salt which had formed was then filtered, dried, and weighed. In all cases, except for the reactions of compound 33, greater than a 90% theoretical yield of $\text{Me}_2\text{NH}_2\text{B}$ was recovered, based upon the stoichiometry shown in equation 8.



Throughout the course of the reaction, aliquots were periodically removed via syringe and the ^{31}P NMR spectrum observed (this data will be presented in the following section).

Reactions of (dimethylaminophosphorus(III) ligand)-metal carbonyl complexes with acid

The procedures followed here were similar to those for the reaction of the free ligand with acid, with a few modifications.

In a typical experiment, under a dry nitrogen atmosphere, 15.20 mmol of the metal complex (compounds 34-37) were dissolved in 50 mL of dry chloroform at 0°C. To this was then added 30.40 mmol of the acid dropwise by syringe (the acids used here were the same as those used in the reaction of the free ligand with acid). The color of the iron complexes (35-37) immediately lightened and all the complexes evolved a small amount of a gas (the molybdenum complex remained colorless). Within 15 minutes, a highly crystalline white precipitate of the ammonium salt began to form. The reaction was then warmed to room temperature and stirred for an additional 12 hours, after which time the ammonium salt was filtered off using Schlenk techniques. In all reactions, a greater than 90% of the theoretical yield of salt was recovered.

RESULTS AND DISCUSSION

The interest in broadening the scope of the phosphonium ion work reported previously in the literature to other than the amino substituted systems stems from several considerations, most of which have been presented already. In addition to these reasons, it is important to see how the substituents directly affect the π -acidity, σ -donation, and NMR spectroscopic properties of these ions. Also, it has been speculated that at least one amino group is required for sufficient stabilization of the cation to occur to allow its detection and it would be quite interesting to see if other groups can also stabilize this type of species. Finally, perhaps by changing the electronic environment of the phosphorus, the resulting compounds might show some new and interesting properties.

Reactions of $>P-X$ Compounds with X Acceptors

The most generally useful method for the preparation of phosphonium ions reported in the literature has been through the reaction of a precursor haloaminophosphine (primarily chlorides) with a halide acceptor (usually aluminum trichloride) and this was the first method investigated in the present work. The four halide abstractors used here were aluminum trichloride, phosphorus pentachloride, antimony pentachloride, and silver(I) ion. As discussed previously, ^{31}P NMR has proven to be the most valuable tool for following the course of these reactions and it was the primary method of identification used in this work. Upon the

reaction of a wide variety of chlorophosphites with phosphorus and antimony pentachlorides, and silver(I) ion, no downfield shift in the δ values from the starting materials was observed. If a phosphonium ion had been formed, it would have been expected that a large downfield chemical shift would have occurred. This is based upon the correlation presented by Parry (9) (shown in figure 3) between the phosphorus coordination number and the observed ^{31}P chemical shift in amino and chloro substituted systems. This relationship is readily extendable to oxygen substituted systems as shown in Figure 9. Plotting the known δ ^{31}P values for the 3, 4, and 5 coordinate $\text{P}(\text{OEt})_n$ systems versus the coordination number and extrapolating to the divalent case, the predicted δ ^{31}P for $+\text{P}(\text{OEt})_2$ should be approximately + 238 ppm (± 10 ppm).

In the reaction of aluminum trichloride with the chlorophosphite 26, a product somewhat downfield from the precursor compound was observed, but not far enough downfield to be considered a truly free ion. The starting material, 26, has a ^{31}P chemical shift of 146.64 ppm. Upon reaction, the gradual growth of a peak at 179.68 ppm and a decrease in the intensity of the peak at 146.64 ppm is observed. A plot of the ratios of the intensities of the peak at 146.64 to the one at 179.68 versus time is shown in Figure 10. Attempts at the isolation or further characterization of this downfield material were unsuccessful. This product probably has some degree of phosphonium ion character but is most likely tightly ion paired with the AlCl_4^- counteranion, resulting in a smaller than expected downfield shift. In the ^{27}Al NMR spectrum of the

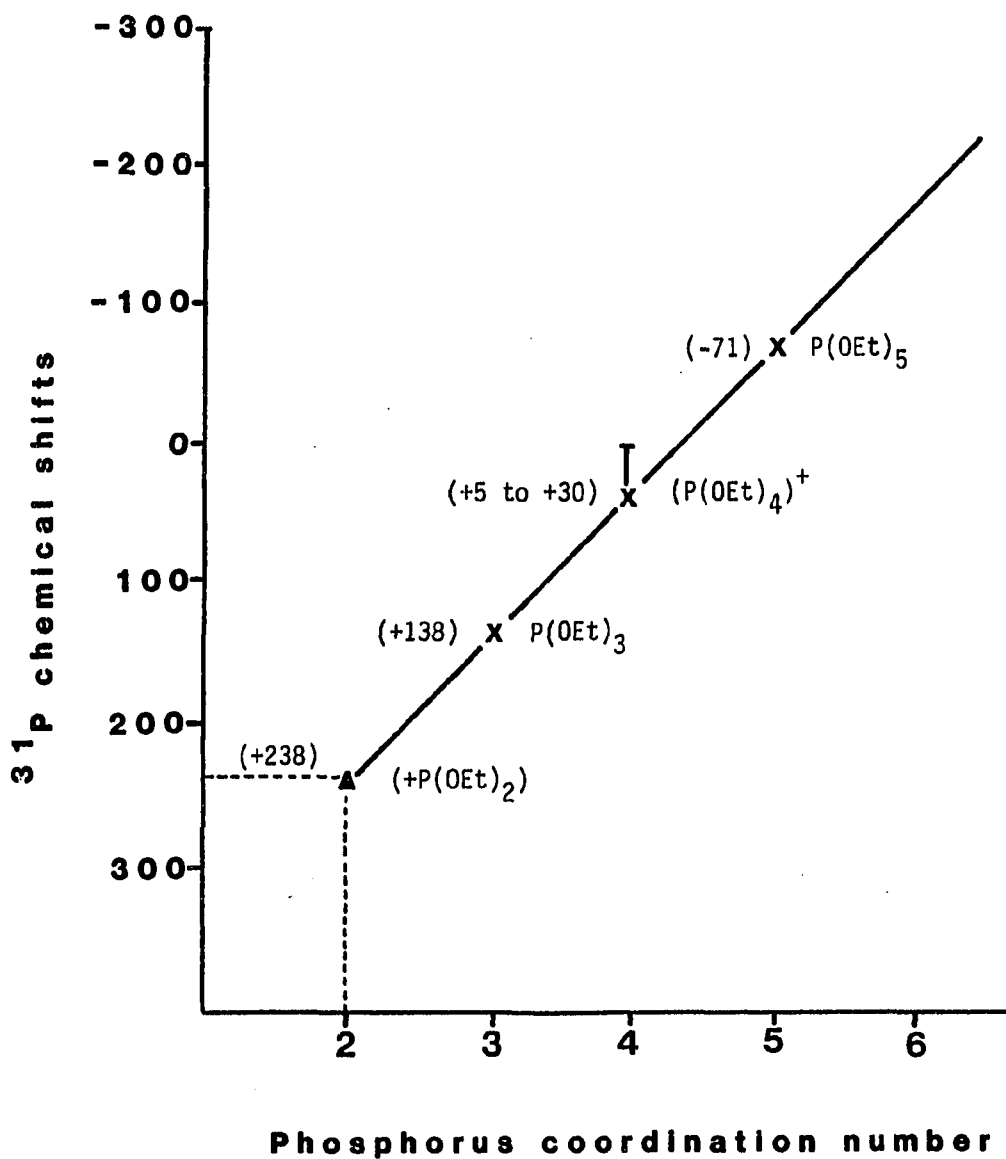
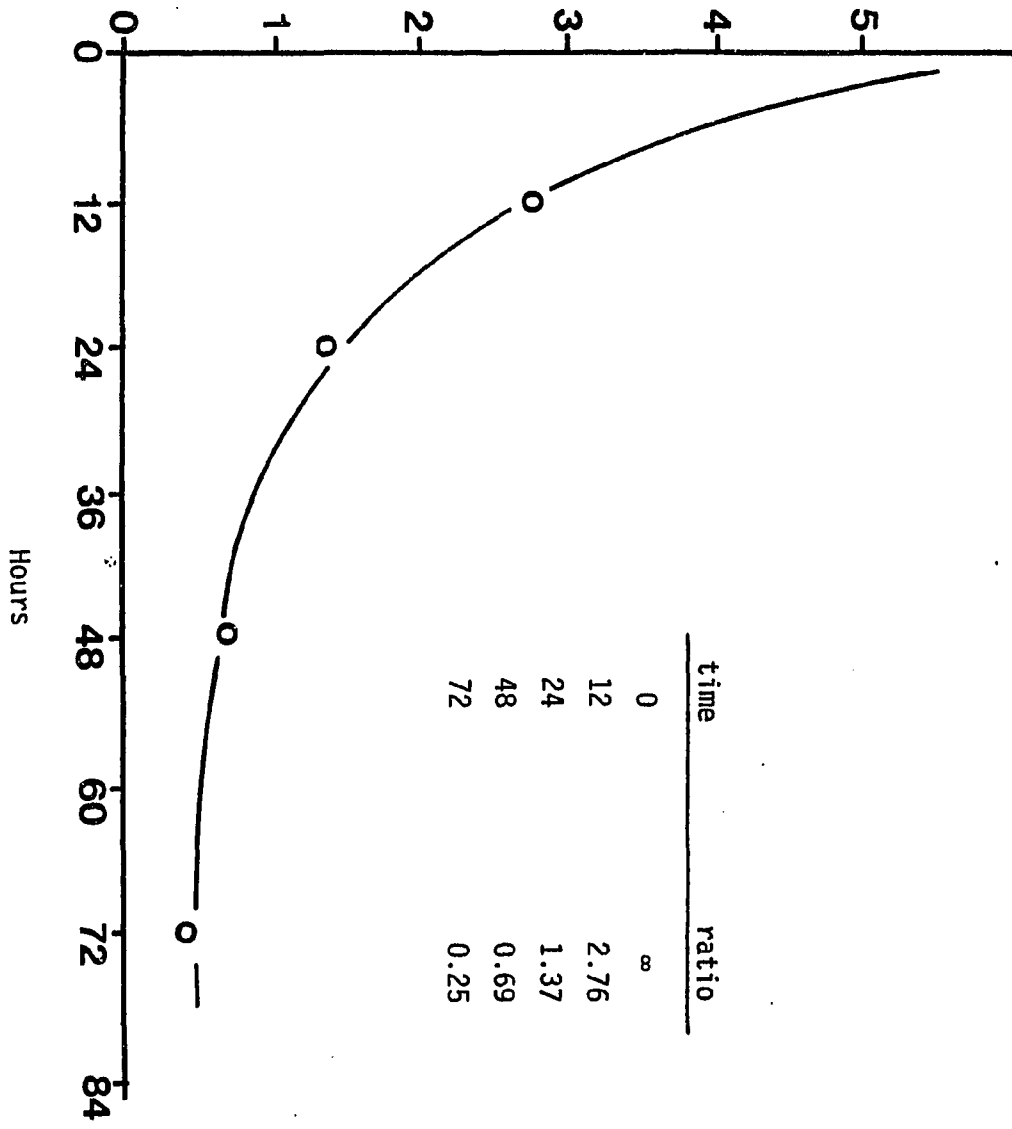


Figure 9. Plot of phosphorus coordination number versus ^{31}P chemical shift for $[\text{P}(\text{OEt})_n]^X$ systems ($X = 0, +1$)

Figure 10. Product dependence on time of the reaction of 26 with aluminum trichloride

Ratio of the $\delta^{31}\text{P}$ of starting material
to product (peaks at $\frac{146 \text{ ppm}}{179 \text{ ppm}}$)



reaction mixture, a peak at 101.1 ppm was observed corresponding to the AlCl_4^- anion (lit. value is +102 ppm (84)). This point will be discussed in more detail in subsequent sections.

Reactions of $>\text{P}(\text{X})$ -Transition Metal Complexes with X Acceptors

It has been reported that another valuable route to phosphonium ions involves the preparation of a precursor halophosphorus(III) transition metal complex followed by halide abstraction (12). Several complexes of the type $\text{M}(\text{CO})_5(\text{Cl}-\text{P}<)$ ($\text{M}=\text{Cr}, \text{W}$) were prepared and these were reacted with aluminum trichloride using standard techniques. Data for these reactions are given in Table 5. From these data, it can be seen that no significantly downfield shift was observed indicating the failure to produce any of the desired species.

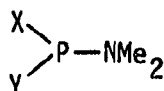
Table 5. ^{31}P NMR data for the reactions of $\text{M}(\text{CO})_5(\text{Cl}-\text{P}<)$ ($\text{M} = \text{Cr}, \text{W}$) with AlCl_3

Complex	$\delta^{31}\text{P}$	
	Starting complex	AlCl_3 reaction
$\text{Cr}(\text{CO})_5(26)$	186.45	194.30
$\text{W}(\text{CO})_5(26)$	160.47	174.20

Reactions of $>P(NR_2)$ Compounds with Acids

As discussed previously, a recent method for preparing $+P(NMe_2)_2$ has been reported by Dahl from the reaction of tris(dimethylamino)phosphine with trifluoromethanesulfonic acid (14). In this investigation, the author further reported the reactions of the six additional amino-phosphorus(III) compounds shown in Table 6 with trifluoromethanesulfonic acid.

Table 6. Aminophosphorus(III) compounds reacted with HSO_3CF_3 by Dahl (14)



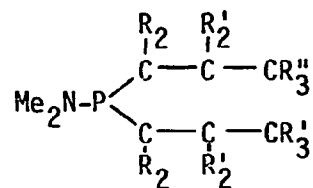
	<u>8</u>	<u>58</u>	<u>59</u>	<u>60</u>	<u>61</u>	<u>62</u>	<u>30</u>
X	NMe ₂	NMe ₂	Ph	NMe ₂	Cl		
Y	NMe ₂	Ph	Ph	Cl	Cl		

From these reactions, it was found that compound 8 clearly did form a phosphonium ion, compounds 58, 61, and 30 showed some evidence for phosphonium ion formation and the remaining compounds showed no evidence of the products having phosphonium ion character.

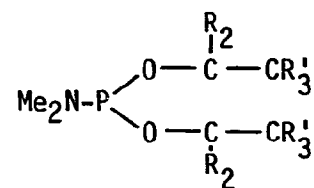
In our work, a number of dimethylamino substituted phosphorus(III) compounds were prepared and characterized for reaction with a variety of acids. Proton and ^{31}P NMR data for these compounds are given in Tables 7 and 8. All were prepared from their corresponding chlorides by reaction with excess anhydrous dimethylamine in diethyl ether. After purification

Table 7. ^1H NMR chemical shifts^a and coupling constants^b data for $\text{Me}_2\text{N}-\text{P}<$ systems

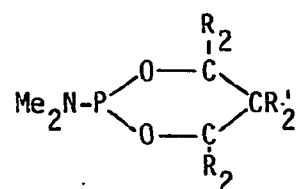
labeling scheme:



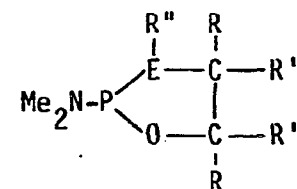
aminophosphines



aminophosphites



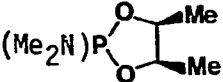
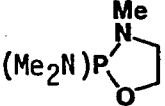
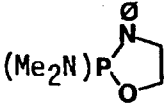
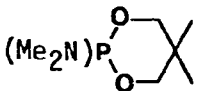
amino-1,3,2-phosphorinanes



(E = N, O)

amino-1,3,2-phospholanes

Me_2NP	R	J^c	R'	J^d	R''	NMe_2	J^e
$(\text{Me}_2\text{N})\text{P}(\text{NMe}_2)_2$	---	---	---	---	---	2.52(d)	8.9
$(\text{Me}_2\text{N})\text{P}(\text{NMe}_2)(\text{OMe})$	3.38(3H,d)	$^3J_{\text{POCH}} = 12.2$	---	---	---	2.58(12,d)	8.7
$(\text{Me}_2\text{N})\text{P}(\text{O}-\text{C}_6\text{H}_4)_2$	1.31(9H, p-t-Bu) 1.50(18H, o-t-Bu)	---	7.18 (2H, s)	---	---	2.53(6H,d)	8.2
$(\text{Me}_2\text{N})\text{P}(\text{O}-\text{CH}_2)_2$	3.73-4.16 (4H,m)	v. complex	---	---	---	2.59(6H,d)	8.4

	4.48(2H,m)	v. complex	1.16(6H,d)	$^3J_{HH} = 6.2$	---	2.67(6H,d)	8.4
	4.02-4.32 (2H,m, -O-CH ₂ -)	v. complex	---	---	2.73(3H,m)	2.58(6H,d)	8.1
	2.88-3.28 (2H, m, N-CH ₂)	v. complex					
	4.07-4.43 (2H, m, -O-CH ₂ -)	v. complex	---	---	6.66-7.34 (5H, m)	2.63(6H,d)	8.4
	3.21-3.59 (2H, m, N-CH ₂ -)	v. complex					
	3.26-4.01 (4H, m)	v. complex	0.80(3H, s, equatorial) 1.24 (3H, s, axial)	---	---	2.74(6H,d)	9.0

a Chemical shifts in ppm (in CDCl₃).

d = doublet

m = multiplet

s = singlet

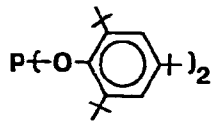
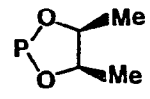
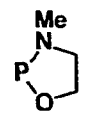
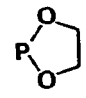
b J = coupling constant in Hertz

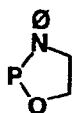
c $^3J_{POCH}$

d $^3J_{HH}$

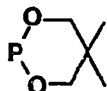
e $^3J_{PNCH}$

Table 8. ^{31}P NMR data for $\text{Me}_2\text{N}-\text{P} < + \text{HB}$ reactions^a

Ligand	Me_2NP	$\text{HCO}_2\text{CF}_3^{\text{b}}$	Δ^{c}	HSO_3CF_3	Δ	HBF_4	Δ	HPF_6	Δ
$\text{P}(\text{NMe}_2)_2$	121.43	--- ^d	---	262.55	+141.12	154.68	+33.25	154.97	+33.54
$\text{P}(\text{NMe}_2)(\text{OMe})$	136.14	146.17	+10.03	189.14	+53.00	153.50	+17.36	153.37	+17.23
	147.87	--- ^d	---	--- ^d	---	142.39	-5.48	142.45	-5.42
	138.85	128.02	-10.83	135.92	-2.93	132.98	-5.87	138.96	+0.11
	138.37	129.76	-8.61	137.41	-0.96	128.19	-10.18	145.63	+7.26
	129.97	139.66	+9.69	169.16	+39.19	150.92	+20.95	167.94	+37.97



117.88 129.79 +11.91 150.51 +32.63 132.25 +14.37 ---^d ---



143.16 ---^d --- N.R.^e --- ---^d --- ---^d ---

^aAll spectra were run in CDCl₃.

^bThe major products from this reaction occur from -10 to +30 ppm with only a small fraction as the downfield product.

^c $\Delta = (\delta^{31}\text{P for HB reaction product}) - (\delta^{31}\text{P for Me}_2\text{N-P} < \text{precursor})$

^dNo downfield (> + 100 ppm) product observed.

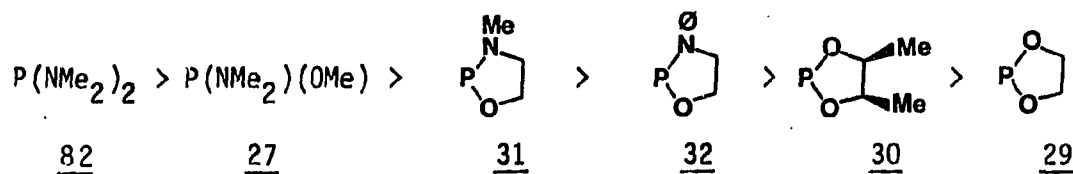
^eNo reaction observed.

by distillation, the ^1H NMR spectrum in each case showed the expected addition of the methyl resonance as a phosphorus spin-spin coupled doublet for the dimethylamino group. ^{31}P NMR showed a single product in each case with chemical shifts in the range of +117 to +139 ppm, shifted upfield by 27 to 37 ppm from the corresponding chlorides.

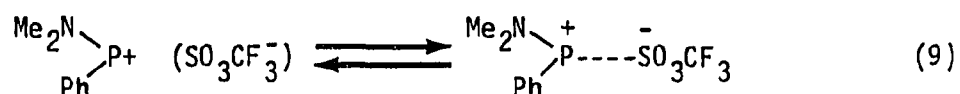
The four acids selected for use in the reactions with the dimethylamino substituted phosphorus compounds were trifluoromethanesulfonic acid, trifluoroacetic acid, hexafluorophosphoric acid, and tetrafluoroboric acid. These were chosen as the proton donors primarily because of the relatively low nucleophilicity of the corresponding anions and their availability in anhydrous form. Each of these acids were reacted with the aminophosphorus compounds under similar conditions and monitored periodically by the removal of aliquots from the reaction mixture and observing the ^{31}P spectrum. It was found that ^1H NMR was not a particularly useful tool to follow the courses of these reactions due to the complexity and similarity of the spectra before and after the reaction. A number of very interesting results and trends were obtained as seen in the ^{31}P NMR data summarized in Table 8.

The observation of the $+\text{P}(\text{NMe}_2)_2$ cation from the reaction of 8 and trifluoromethanesulfonic acid supported the work of Dahl discussed previously and served as a check on the experimental conditions and techniques employed here. In each reaction with an acid, a nearly stoichiometric amount of the appropriate amine salt precipitated within the first thirty minutes. For a given acid, the magnitude of the

downfield shift in the ^{31}P NMR upon reaction with the aminophosphorus compound follows the order shown below:



The positions of the observed chemical shift values of the product species, except in the case of 8, are not generally far enough downfield to be considered as truly free phosphonium ions. The smaller-than-expected Δ values (δ product species - δ starting compound) may be due to a combination of effects, especially increased ion pairing between the anion and the cation and solvent interactions. Dahl has suggested that an equilibrium exists in the case of 58 as shown in Equation 9 and that this equilibrium could be substantially shifted toward the "coordinated" form resulting in an upfield ^{31}P resonance.



Conductivity measurements were not very useful in these systems probably because a small amount of unreacted acid interferes with measurement of accurate values based upon the phosphonium species. These data are shown in Table 9.

The observed sequence of compounds in the Δ trend in Table 8 can be understood in terms of the relative donating properties of the substituent atoms on the phosphorus based primarily upon electro-

negativity arguments. As the electronegativity of the substituent attached to the phosphorus increases, the less the substituent can help stabilize the positive charge generated on the phosphorus by π -electron donation. If the π -donation to the phosphorus is reduced, a corresponding reduction in the stability of the divalent species would be expected and the equilibrium between the divalent and trivalent forms would be shifted toward the trivalent species. Therefore, nitrogen substituents (nitrogen Allred-Rochow electronegativity = 3.07 (85)) should stabilize these ions better than oxygen substituents (oxygen Allred-Rochow electronegativity = 3.50 (85)) and correspondingly shift the equilibrium toward the free divalent cationic form as observed in a farther downfield ^{31}P chemical shift. The experimentally observed ordering bears these expectations out. When a dimethylamino group in $+\text{P}(\text{NMe}_2)_2$ is replaced by a methoxy group, the ^{31}P chemical shift moves upfield. Changing the configuration to a cyclic species still containing one nitrogen and one oxygen linkage moves the chemical shift location further upfield because of the constraints imposed by the ring system. This observation can be rationalized in light of the relationship between molecular constraint and the electronic environment of phosphorus proposed by Verkade (86). It has been shown that upon increasing the molecular constraint in a system, such as going from an acyclic to a cyclic system, increases the positive charge localization on the phosphorus. This is primarily due to a change in the hybridization of the ring oxygens from sp^2 toward sp^3 as required by the ring constraint effects in decreasing the P-O-C bond angles. The decrease in the π -bonding capability of these oxygens with

Table 9. Conductance data for $(\text{Me}_2\text{N})\text{PX}_2 + \text{HSO}_3\text{CF}_3$ and standard systems

Sample	Resistivity ^a	Concentration ^b	Conductance
KCl ^c	3.80×10^3	0.0200	1.9×10^5
$\text{HSO}_3\text{CF}_3/\text{Et}_2\text{O}$	4.80	0.1043	46.0
$\text{HSO}_3\text{CF}_3/\text{Et}_2\text{O}$	930.	0.7132	1.30×10^3
$\text{HSO}_3\text{CF}_3/\text{Et}_2\text{O}$	2.32×10^3	1.0833	2.14×10^3
$\text{Me}_2\text{NH}_2\text{SO}_3\text{CF}_3^{\text{d}}$	0.005	7.238×10^{-3}	6.9×10^{-1}
$(\text{Me}_2\text{N})_3\text{P} + \text{HSO}_3\text{CF}_3$	0.174	0.7000	0.249
$(\text{Me}_2\text{N})\text{P}(\text{N}(\text{Ph})\text{CH}_2\text{CH}_2\text{O}) + \text{HSO}_3\text{CF}_3$	10.8	0.7008	15.41
$(\text{Me}_2\text{N})\text{P}(\text{OCH}_2\text{CH}_2\text{O}) + \text{HSO}_3\text{CF}_3$	150.	0.6990	214.6

^aIn micromhos (1/microohms).

^bMolarity.

^cCalculated cell constant $k = 0.7284$ from these data.

^dSaturated solution.

the phosphorus from an increase in the hybridization of the p lone pair orbitals on the oxygen results in a greater positive charge on the phosphorus, which would shift the equilibrium away from the divalent form. Replacing the relatively electron rich methyl group on the nitrogen with the electron withdrawing phenyl group causes the electron density for π -stabilization to be even further restricted resulting in an even smaller downfield shift in the phenyl substituted species. Finally, by replacing the last nitrogen linkage with an oxygen substituent, the smallest downfield shifts are observed.

The somewhat unexpected trend involving the magnitude of Δ among the various acids for a particular ligand is shown below:



It would be expected based solely upon the known coordination abilities of the various anions that tetrafluoroboric and hexafluorophosphoric acids would cause the greatest Δ values. This would be expected because of the low nucleophilicity of the tetrafluoroboric and hexafluorophosphoric anions and these would therefore favor the divalent over the trivalent coordinated species. In most cases, however, trifluoromethanesulfonic acid causes the greatest observed Δ values. This could be potentially due to the larger steric requirements of the trifluoromethanesulfonate anion which would cause an attenuation of the ion-pairing interaction relative to the tetrafluoroboric and hexafluorophosphoric anions. The position of trifluoroacetic acid in this sequence would be expected based upon its known coordination tendencies (14).

During the course of several of these reactions, various intermediates were observed in the ^{31}P NMR spectra. In the reaction of 27 with trifluoromethanesulfonic acid, the reactant had a ^{31}P chemical shift of 136.14 ppm. Upon addition of the acid, this resonance was quickly replaced by two peaks located at 111.76 and 145.4 ppm. These two peaks were in turn replaced over two hours by a single resonance at 189.14 ppm. Similar results were reported by Dahl in the reaction of 58

with the same acid. The intermediates observed in the reaction of 27 were assigned as shown in Figure 11 based on analogy to Dahl's work.

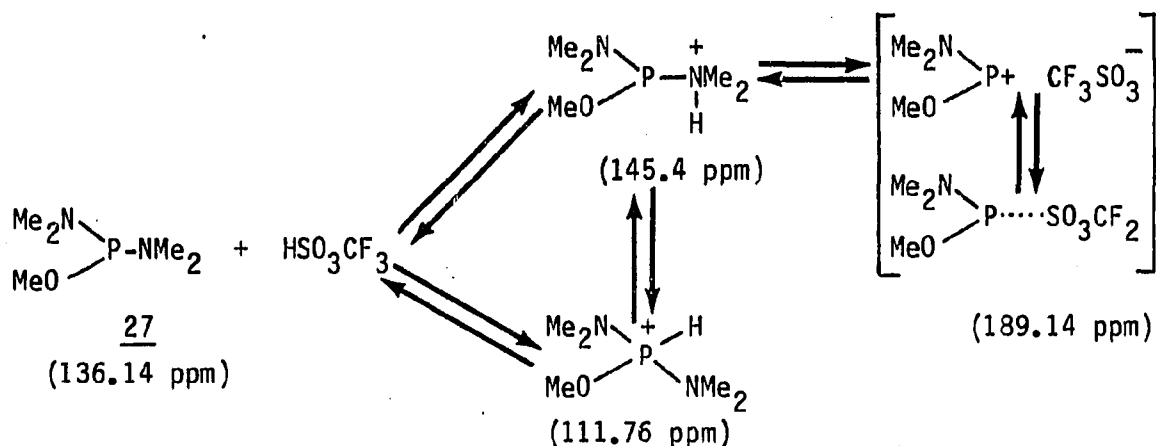


Figure 11. Intermediates in the reaction of 27 with HSO_3CF_3

Variable temperature ^{31}P studies were done on the final equilibrium product of 27 with trifluoromethanesulfonic acid. Over the temperature range observed (+40 to -40°C), no change in the spectrum was observed. A wider temperature range was not available due either to the decomposition of the sample at elevated temperatures or the solidification of the NMR tube contents.

It was observed that 23 did not react with the acids tried and no amine salt was precipitated. There is no apparent reason for this result.

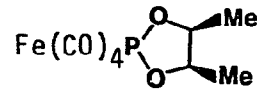
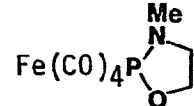
It does appear from these reactions that phosphonium-like species are indeed formed from compounds containing either nitrogen or oxygen

linkages, however, the presence of oxygen linkages tends to shift the equilibrium away from the divalent form toward the strongly ion paired system. In the compounds containing one nitrogen and one oxygen linkage, the ^{31}P chemical shifts of the products are outside of the region generally associated with normal trivalent systems, although not far enough downfield to be fully considered as free divalent ions. In these products, the equilibrium must lie between the two forms but perhaps having a significant amount of the free divalent character.

Reactions of $\text{>P}(\text{NR}_2)$ -Transition Metal Complexes with Acids

Transition metal carbonyl complexes are well known to stabilize phosphonium ions by π -back donation from the metal into the π -system of the ion as previously described (Figure 6). In an extension of the work presented in the previous section, a number of transition metal-aminophosphorus(III)-carbonyl complexes were prepared for reactions with acids to potentially obtain the phosphonium complexes. The synthesis of the tris(dimethylamino)phosphine complexes of iron and molybdenum carbonyls have been reported previously (83). Complexes of the other ligands were prepared using modifications of standard techniques. The ^1H and ^{31}P NMR data for these complexes are shown in Tables 10 and 11, respectively. In the reactions of these complexes with the four acids used in the previous section, ^{31}P NMR spectroscopy was again found to be the best method to follow the reactions as the ^1H spectra were very complicated. The ^{31}P data from the reactions of each complex with the

Table 10. ^1H NMR data for $\text{Me}_2\text{N}-\text{P}-\text{M}(\text{CO})_x$ systems^a

Complex	R	J ^b	R ¹	J ^c	R ^{''}	NMe ₂	J ^d
$\text{Mo}(\text{CO})_5\text{P}(\text{NMe}_2)_3$	---	---	---	---	---	2.62(d)	10.1
$\text{Fe}(\text{CO})_4\text{P}(\text{NMe}_2)_3$	---	---	---	---	---	2.68(d)	9.8
	4.55-5.85 (2H, m)	v. complex	1.39(6H, d)	$^3J_{\text{HH}}=5.8$	---	2.84(6H, d)	10.6
	4.10-4.39 (2H, m, -O-CH ₂ -) 3.15-3.54 (2H, m, N-CH ₂ -)	v. complex	---	---	2.78(3H, d) (J = 10.1) ^d	2.62(6H, d)	12.0

^aLabeling scheme used here is the same as that presented in Table 7 (spectra run in CDCl_3).
d = doublet
m = multiplet

^b $^3J_{\text{POCH}}$

^c $^3J_{\text{HH}}$

^d $^3J_{\text{PNCH}}$

Table 11. ^{31}P NMR data for $\text{M}(\text{CO})_x(\text{Me}_2\text{N-P} <) + \text{HB}$ reactions^a

Complex	δ	HCO_2CF_3	Δ^b	HSO_3CF_3	Δ	HBF_4	Δ	HPF_6	Δ
$\text{Mo}(\text{CO})_5\text{P}(\text{NMe}_2)_3$	143.92	181.28	+37.36	218.09	+74.17	195.93	+52.01	195.74	+51.82
$\text{Fe}(\text{CO})_4\text{P}(\text{NMe}_2)_3$	154.33	192.65	+38.32	232.38	+78.05	195.72	+41.39	183.60	+29.27
$\text{Fe}(\text{CO})_4\text{P} \begin{array}{c} \diagup \text{O} \text{Me} \\ \diagdown \text{O} \text{Me} \end{array}$	187.17	197.48	+10.31	201.82	+14.65	201.42	+14.25	201.66	+14.49
$\text{Fe}(\text{CO})_4\text{P} \begin{array}{c} \text{Me} \\ \\ \text{N} \\ \\ \text{O} \end{array}$	185.73	185.01	-0.72	174.46	-11.27	208.11	+22.38	206.06	+20.33

^aAll spectra in CDCl_3/THF .

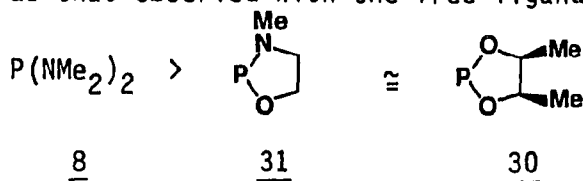
^b $\Delta = (\delta^{31}\text{P}$ for HB reaction product) - ($\delta^{31}\text{P}$ for $\text{M}(\text{CO})_x(\text{Me}_2\text{N-L})$ complex).

acids are shown in Table 11. It appears from these data that most of the complexes do exhibit some degree of phosphonium ion character. All the reactions were observed to precipitate an amine salt quantitatively within thirty minutes of the addition. In the tris(dimethyl-amino)phosphine complexes, the Δ values are relatively large, indicating substantial phosphonium-like behavior but these values are only one half as large as those reported in the literature for these complexes (24) where PF_6^- is the anion. These data are shown in Table 12. This result may again be explained in terms of an equilibrium existing between the metal coordinated divalent phosphonium ion and the species with some degree of SO_3CF_3^- anion pairing.

Table 12. ^{31}P NMR data for the $\text{Fe}(\text{CO})_4(\underline{8}) + \text{HSO}_3\text{CF}_3$ system

	δ ^{31}P	Δ (ppm)	Ref.	Solvent
unreacted complex	154.3	---	this work	CDCl_3
observed (SO_3CF_3^-)	232.4	78.1	this work	CDCl_3/THF
literature (PF_6^-)	311.0	156.7	24	CH_2Cl_2

The trend in the Δ values for the complexes with a given acid is basically the same as that observed with the free ligand as shown below:



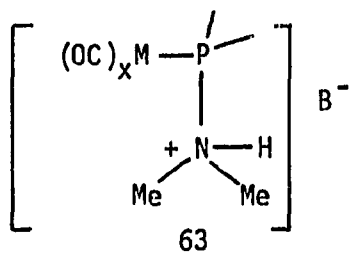
As the phosphonium species is relatively destabilized by replacing an amino group with an alkoxy group, the equilibrium is shifted away from the metal-coordinated divalent form resulting in a smaller Δ value. The reasons for this ordering, therefore, appears to be similar to those presented in the previous section in detail. Also, the same ordering in the trend in Δ values as a function of the acid used is the same as that observed for the free ligands ($\text{HSO}_3\text{CF}_3 > \text{HBF}_4 \cong \text{HPF}_6 > \text{HCO}_2\text{CF}_3$).

In the reactions of the complexes of 8, an intermediate was detected in the ^{31}P NMR spectra which gradually decreased in intensity over several hours relative to the further downfield peak. The ^{31}P NMR data for these intermediates are shown in Table 13.

Table 13. ^{31}P NMR data of the intermediates from the $\text{M}(\text{CO})_x(\text{8}) + \text{HB}$ system

	HCO_2CF_3	HSO_3CF_3	HBF_4	HPF_6
$\text{Fe}(\text{CO})_4(\text{8})$	180.59	166.33	186.89	172.60
$\text{Mo}(\text{CO})_5(\text{8})$	172.09	156.71	187.49	187.30

These intermediates were not isolable from the reaction mixture. Based upon the work with the free ligand plus acids in the previous section, these intermediates are perhaps similar to 63; however, this has not been substantiated.



Reactions of $>\text{P-Cl}$ Compounds with Transition Metal Nucleophiles

The technique of reacting chlorodiaminophosphorus compounds with transition metal nucleophiles to prepare phosphonium ion complexes has apparently met with good success in the literature (25, 26, 29). In our work, attempts were made to extend this synthetic scheme to systems containing alkoxy substituted phosphorus compounds. The three metal nucleophiles selected for study here are shown in Table 14, along with their second order rate constants for alkylation, which gives an indication of their relative nucleophilicities (87).

Table 14. Selected metal nucleophiles and rate constants for alkylation (87).

$$\text{Z}^- + \text{CH}_3\text{CH}_2\text{Br} \xrightarrow[250]{0.1\text{M Bu}_4\text{NClO}_4} \text{Z-CH}_2\text{CH}_3 + \text{Br}^-$$

Z^-^{a}	$k_2 \text{ (M}^{-1}\text{sec}^{-1})^{\text{b}}$
$\text{Fe}(\eta^5\text{-Cp})(\text{CO})_2^-$	7×10^7
$\text{Mn}(\text{CO})_5^-$	77
$\text{Mo}(\eta^5\text{-CP})(\text{CO})_3^-$	67

^aPrepared electrochemically ($\sim 2 \times 10^{-3}$ M).

^bSecond order rate constants normalized relative to $\text{Co}(\text{CO})_4^-$ ($k_2=1$), refs. 87, 88.

These were selected because of their widely differing nucleophilicities and their synthetic availability. The discussion of the reactions of the $\text{Fe}(\eta^5\text{-Cp})(\text{CO})_2^-$ anion will be reserved until the subsequent section. The reactions of the other nucleophiles with chlorodioxaphosphorus compounds have met with only limited success. These reactions were again followed primarily by ^{31}P NMR spectroscopy. In the reaction of 26 with the $\text{Mo}(\eta^5\text{-Cp})(\text{CO})_3^-$ anion, a large number of products were observed. Proton decoupled and undecoupled ^{31}P NMR spectra showed a proton coupled doublet with a downfield resonance at 377.94 ppm ($J_{\text{PH}} = 44.40$ Hz). Numerous attempts at isolating this product by procedures such as chromatography and crystallization were made but unfortunately they proved unsuccessful. Based upon the observation and magnitude of the J_{PH} value, the very far downfield ^{31}P chemical shift, the air sensitivity, and the lack of chromatographic movement (very small R_f values) this complex may be an ionic metal hydride with the hydrogen cis to the phosphorus ligand. The phosphorus ligand is perhaps acting as a true phosphonium ion (3 electron donor). A ^1H NMR resonance doublet ($J_{\text{PH}} = 44.5$ Hz) was observed from the filtered reaction mixture at -6.11 ppm, indicating the possible presence of a metal hydride. It is noteworthy that no other ^1H coupled species was observed in the ^{31}P spectrum of the reaction mixture. The complex is probably monomeric based on the far downfield position of the ^{31}P resonance (32). Two possible structures for this product which obey the eighteen electron rule are shown in Figure 12.

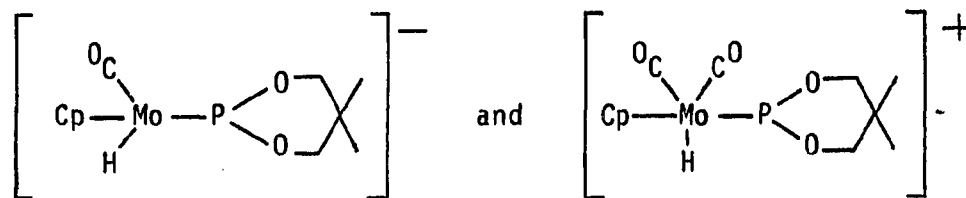


Figure 12. Possible structures of the product from $[\text{Mo}(\eta^5\text{-Cp})(\text{CO})_3]^-$ and 26

The reaction of the $\text{Mn}(\text{CO})_5^-$ anion with chlorophosphorus compounds 26 and 12 did not yield any detectable products with downfield ^{31}P chemical shifts.

Dimeric Iron Complexes

In a continuation of our studies on the interactions of transition metal nucleophiles with $\text{ClP} <$ compounds to form phosphonium ion complexes, the reactions of the very potent Fp anion were investigated. As previously discussed, the interaction of halophosphines with these nucleophiles tends to form dimeric species, which are currently of great interest for use in catalytic systems (37, 38). Paine, however, has recently reported the preparation of a monomeric, air sensitive, crystalline metallophosphonium ion complex in the reaction of the Fp nucleophile with the cyclic halodiaminophosphine 2-chloro-N,N'-dimethyl-1,3,2-dioxaphospholane 22 (83). To date, no reports involving the application of this approach to oxygen substituted systems, to potentially form metallophosphonium ion complexes, have been found in the

literature. Through this approach, a valuable synthetic procedure was developed leading to a series of interesting organophosphorus complexes.

The $[\text{Fe}(\eta^5\text{-Cp})(\text{CO})_2]^-$ anion was conveniently prepared by reduction of the dimeric starting complex with sodium amalgam under inert conditions. The anion thus prepared was reacted with a stoichiometric amount of the appropriate Cl-P< compound liberating CO from the reaction. In the reaction with 26, the ^{31}P NMR spectrum showed several peaks in the far downfield region (>200 ppm) as seen in Figure 13. Major downfield peaks were observed at 370.19, 351.72, 270.08, 265.49 and 220.20 ppm. The major products, as identified by ^{31}P NMR, corresponded to the two peaks at 270.08 and 265.49 ppm. Numerous attempts at the isolation, purification, and identification of each of these components were made using a variety of techniques. Repeated column chromatographic procedures were found to successfully separate each of the two major products from the reaction mixture and from each other in highly purified forms as stable crystalline materials. A ^{31}P NMR of this reaction mixture after one chromatographic separation is shown in Figure 14. The other downfield components were not isolable in pure form by any of the recrystallization or chromatographic methods tried.

The mass spectra of these two complexes were quite similar and showed the highest mass unit observed at 564 m/e, which corresponds to the molecular ion for a dimeric complex of the type $[\text{Fe}(\eta^5\text{-Cp})(\text{CO})(\mu\text{-5,5-DMP})]_2$. Other prominent fragments corresponded to the loss of one and two carbon monoxide units from the parent molecule. The mass spectral data for these two complexes and the precursor chlorophosphite 26 are

Figure 13. ^{31}P NMR of the reaction mixture of $[\text{Fe}(\eta^5\text{-Cp})(\text{CO})_2]^-$ with 26

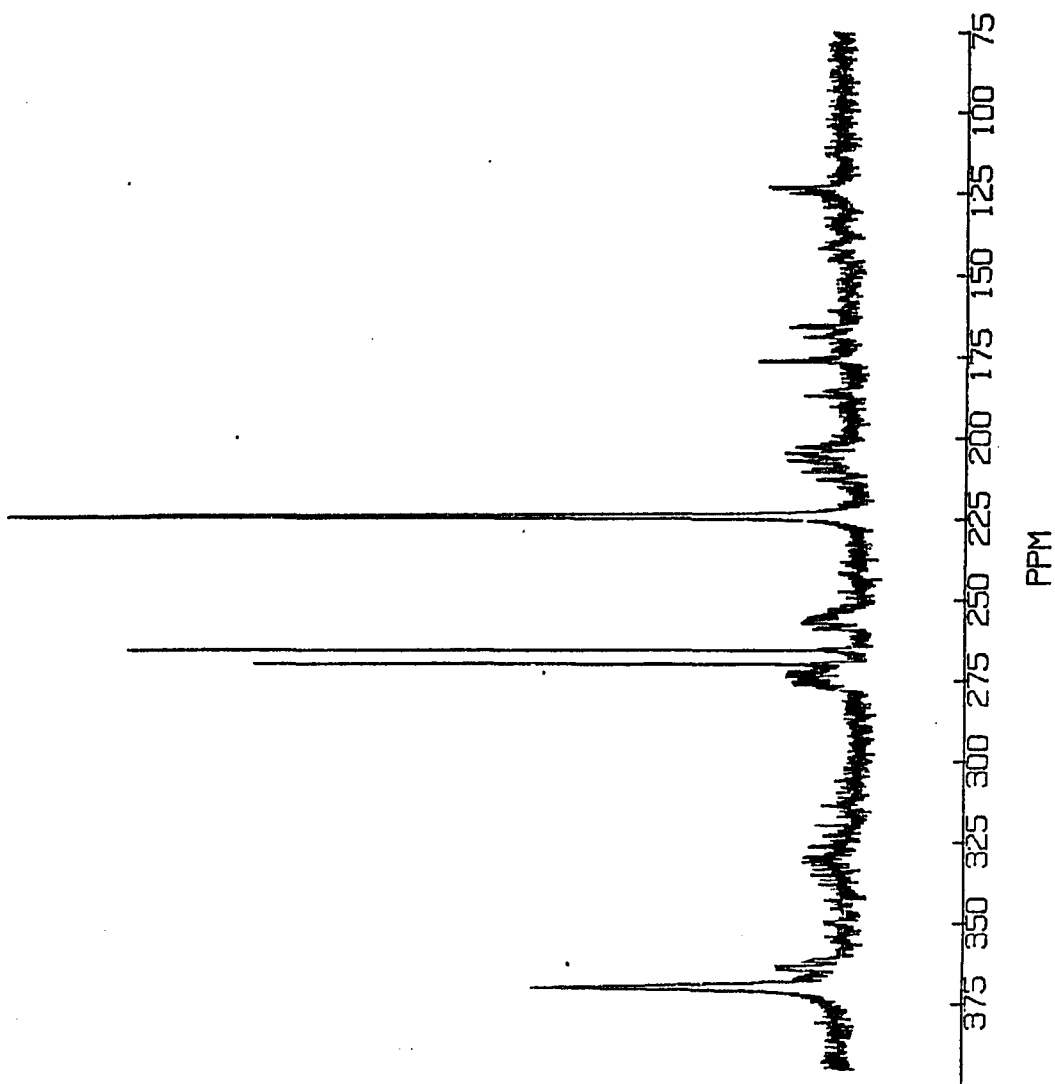
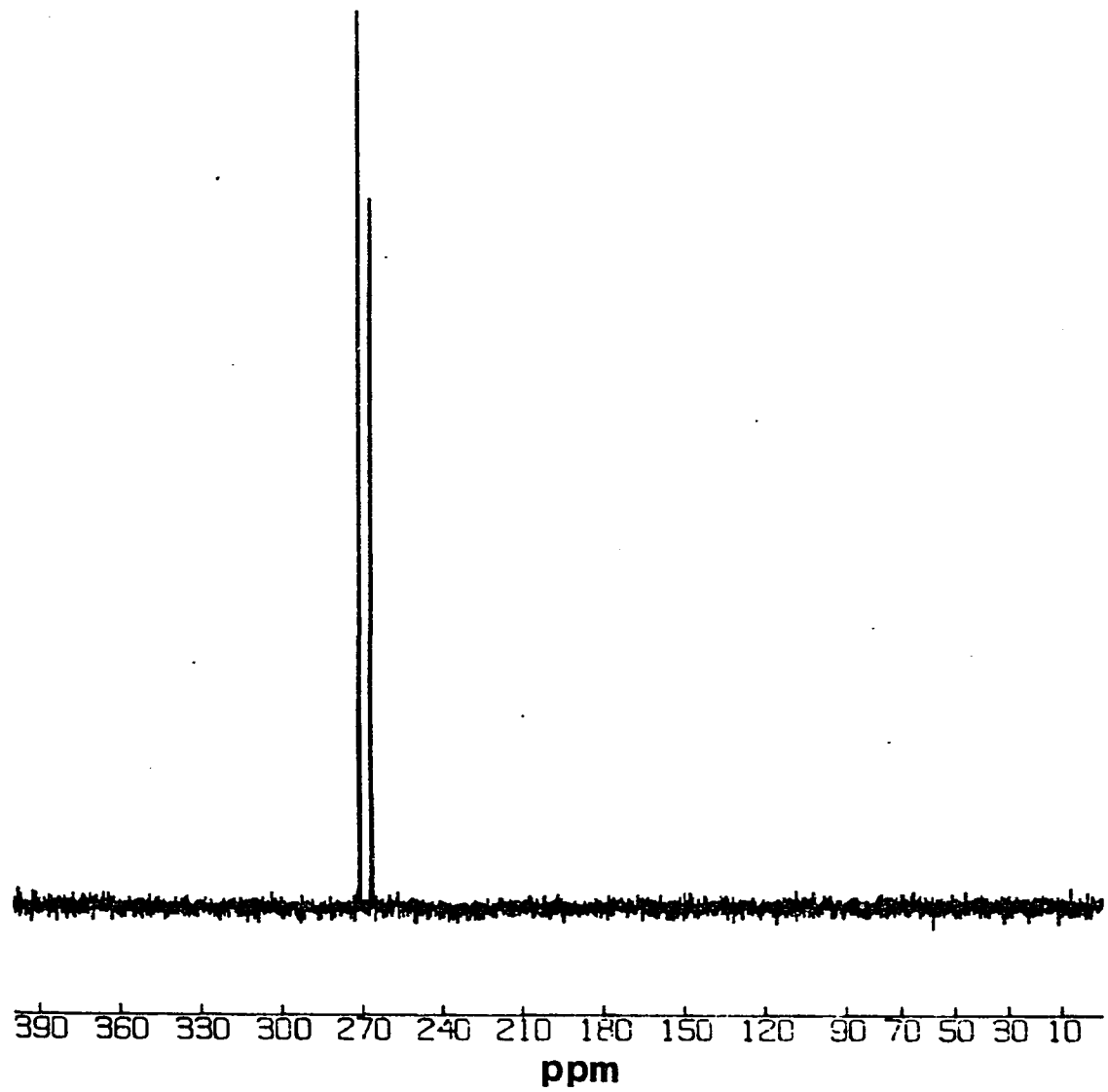


Figure 14. ^{31}P NMR of the once-chromatographed reaction mixture of $[\text{Fe}(\eta^5\text{-Cp})(\text{CO})_2]^-$ with 26



given in Table 15. The mass spectrum of trans-[Fe(η^5 -Cp)(CO)(μ -5,5-DMP)]₂ is shown in Figure 15. Cis and trans isomerism with respect to the orientation of the cyclopentadienyl groups is consistent with the ³¹P NMR and mass spectral data as well as the ¹H NMR, infrared, and X-ray spectral data to be discussed. A large number of other precursor chlorophosphorus compounds containing both nitrogen and oxygen substituents were reacted analogously and the dimeric complexes purified by column chromatography. These cis and trans complexes and their R_f values are given in Table 4 of the experimental section. The mass spectra of these other complexes typically showed similar fragmentation patterns to the ones previously discussed, in that a characteristic parent ion was displayed as well as peaks corresponding to the loss of one and two carbon monoxide units. A generally intense peak corresponding to ferrocene presumably arising from rearrangement while in the molecular beam was also observed. The spectrum of cis-[Fe(η^5 -Cp)(CO)(μ -1,3,2-dioxaisophosphindolane)]₂ is shown in Figure 16. An important peak was also observed in the spectra which corresponded to the cationic phosphonium ion fragment of the free ligand. Other peaks corresponded to complex fragmentation and rearrangement patterns. Only one other diiron complex with bridging phosphorus units containing other than alkyl or aryl phosphine linkages has been reported in the literature. This compound, namely [Fe(CO)₃(μ -5,5-DMP)]₂, was prepared by a very different synthetic route which was reported to be quite restrictive in scope (82).

Table 15. Mass spectral data for 26 and cis and trans-[Fe(η^5 -Cp)(CO)(μ -5,5-DMP)]₂

Peak	Mass ^a (m/e)	Intensities ^b		Identification	
		<u>26</u>	cis complex		trans complex
1	564	---	1.68	9.93	molecular ion (Fe isotope of mass 56)
2	536	---	7.65	18.45	loss of CO
3	508	---	36.09	100.00	loss of two CO
4	305	---	55.40	85.10	complex fragmentation (loss of 2 CO, 2 Cp, 4 Me, CH)
5	186	---	100.00	52.94 ^c	ferrocene
6	168	15.00	---	---	molecular ion ^d (chlorine isotope of mass 35)
7	133	34.92	8.90	4.26	+P(O ₂ C ₅ H ₁₀)
8	121	---	17.12 ^c	5.66	Fe-Cp
9	119	33.10	---	---	+P(O ₂ C ₄ H ₈) fragment
10	69	100.00	18.66	16.13	ligand fragmentation (H ₂ C1O ₂)
11	56	47.24	43.60	32.40	ligand fragmentation (C ₄ H ₈ ?)

^aAt 18 eV.

^bRelative to the base peak in percent.

^cBase peak at 70 eV.

^dA peak at 170 (P+2, int. = 5.00) was observed for the chlorine isotope of mass 37.

Figure 15. Mass spectrum of $\text{trans-}[\text{Fe}(\eta^5\text{-Cp})(\text{CO})(\mu\text{-5,5-DMP})_2]$

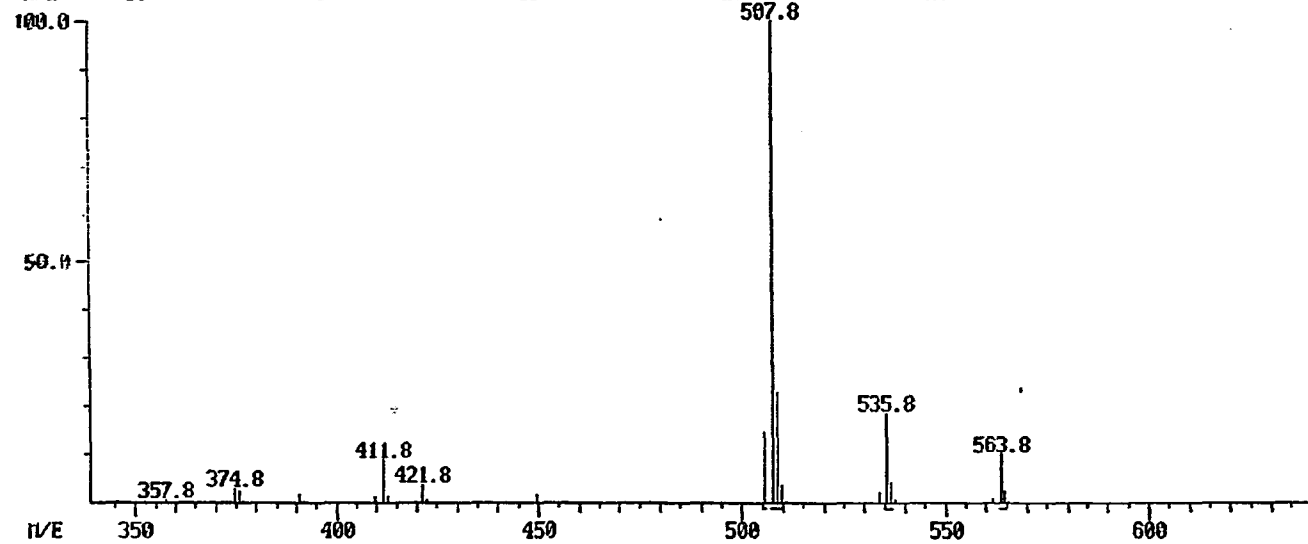


Figure 16. Mass spectrum of $\text{cis-[Fe}(\eta^5\text{-Cp})(\text{CO})(\mu\text{-1,3,2-dioxaisophosphindolane)]}_2$

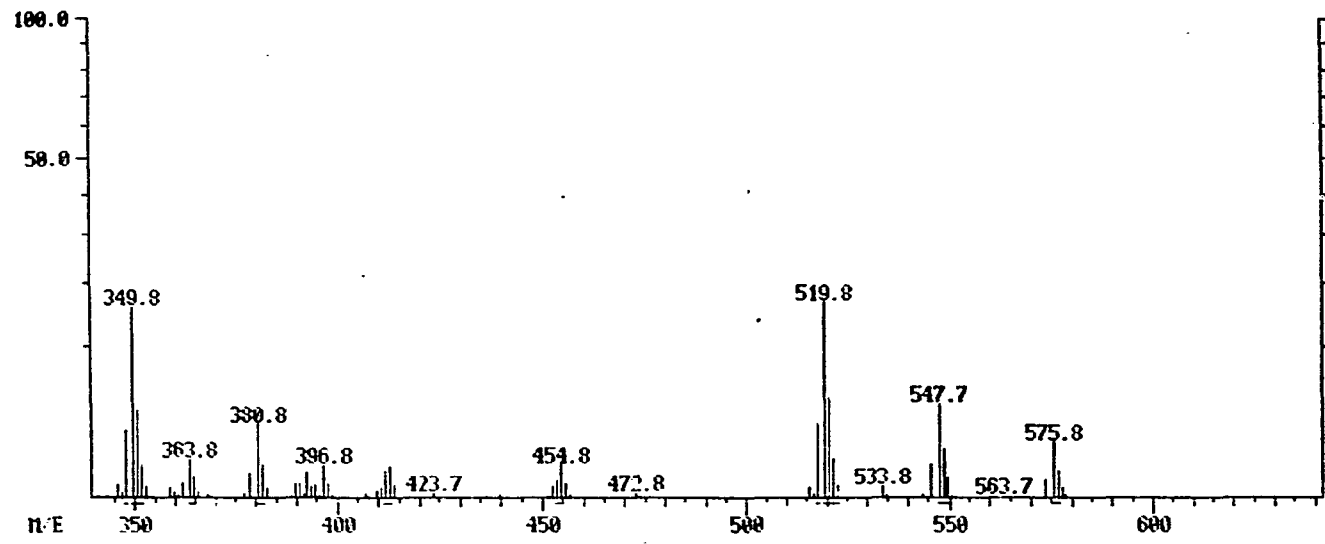
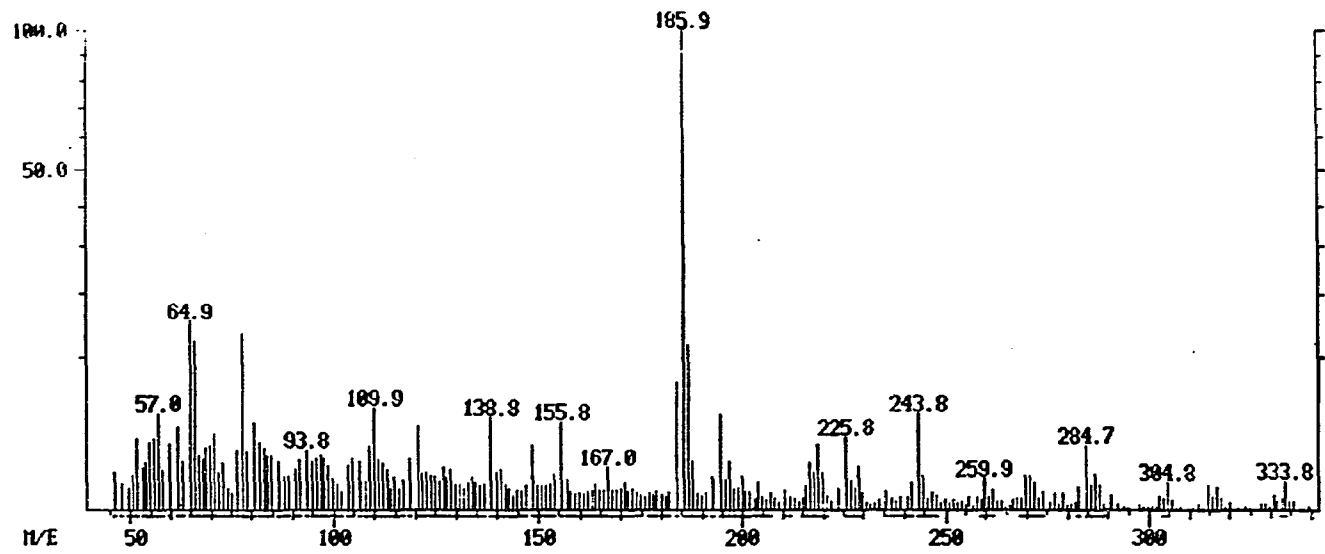
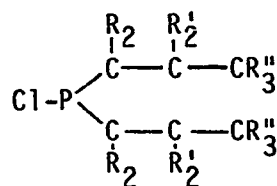
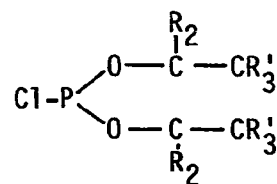


Table 16. ^1H NMR data for precursor chlorophosphorus compounds^a

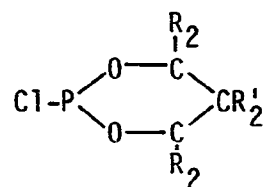
labeling scheme:



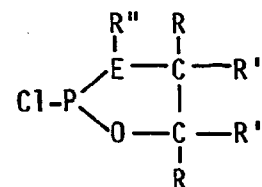
chlorophosphines



chlorophosphites



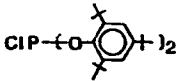
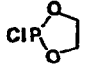
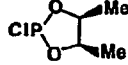
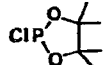
chloro-1,3,2-phosphorinanes



(E = N, O)

chloro-1,3,2-phospholanes

Ligand	R	J^b	R'	J^c	R''	Solvent
ClPMe_2	1.65(d)	$^2J_{\text{PCH}} = 8.2$	---	---	---	CDCl_3
ClPPh_2	7.43(m)	v. complex	---	---	---	CDCl_3
ClP(OEt)_2	4.07(2H, qd)	$^3J_{\text{HH}} = 7.04$ $^3J_{\text{POCH}} = 1.74$	1.32(3H, t)	$^3J_{\text{HH}} = 7.10$	---	CDCl_3
ClP(OPh)_2	6.84(m)	v. complex	---	---	---	CDCl_3

	7.28(2H, s) (aromatic)	---	1.50(18H, s) (<u>o-tert-butyl</u>)	---	1.34(9H, s) (<u>p-tert-butyl</u>)	CDCl ₃
CIP(NMe ₂) ₂	2.73(d, Me-N-)	³ J _{PNCH} = 12.5	---	---	---	CDCl ₃
	4.33(m)	v. complex ^d (J _{PH} = 9.8)	---	---	---	CDCl ₃
	4.81(2H, m)	v. complex	1.28(6H, d)	³ J _{HH} = 6.4	---	CDCl ₃
	1.41(s)	---	---	---	---	CDCl ₃

^aRelative to TMS in ppm.

d = doublet

ddt = doublet of doublets of triplets

ddtd = doublet of doublets of triplets of doublets

m = multiplet

qd = quintet of doublets

s = singlet

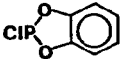
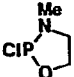
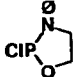
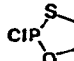
t = triplet

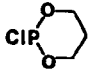
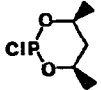
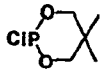
^bJ = coupling constant (Hz) as indicated.

^cJ_{HH}.

^dReference 89.

Table 16 (continued)

Ligand	R	J ^b	R ^c	J ^c	R ^d	Solvent
	7.12(m)	v. complex	---	---	---	CDCl ₃
	4.28-4.61 (2H, m, -O-CH ₂)	v. complex	---	---	2.77(3H,d) CDCl ₃ ³ J _{PNCH} = 15.6	
	2.95-3.40 (2H, m, N-CH ₂)	v. complex				
	4.36-4.74 (2H, m, -O-CH ₂)	v. complex	---	---	6.71-7.33 CDCl ₃ (5H, m)	
	3.26-3.62 (2H, m, N-CH ₂)	v. complex				
	4.21(2H, m, -O-CH ₂)	v. complex	---	---	---	CDCl ₃
	3.00-3.74 (2H, m, -S-CH ₂)	v. complex				

	3.98(2H, m, equatorial)	v. complex ^e	1.69(1H, m, equatorial)	v. complex	---	C ₆ D ₆
	4.59(2H, m, axial)	v. complex	2.48(1H, m, axial)	v. complex	---	C ₆ D ₆
	4.03(2H, m, 4,6-C-H)	v. complex ^d	1.41(1H, m, equatorial)	v. complex	---	CDCl ₃
	1.31(6H, d, 4,6 methyls)	³ J _{HH} = 6.2	1.47(1H, m, axial)	v. complex		
	3.19(2H, ddt, equatorial)	³ J _{POCH} = 10.90 ² J _{AB} = -10.90 ^f ⁴ J _{AA'} + ⁴ J _{BB'} = 2.92	0.27(3H, s, equatorial)	---	---	C ₆ D ₆
	4.14, 4.11(2H, 2 ddt, axial)	² J _{AB} = -10.90 ^f ³ J _{POCH} = 5.84 ⁴ J _{AA'} + ⁴ J _{BB'} = 2.92 ⁴ J _{ACH(ax. methyl)} = 1.24	0.97(3H, s, axial)			

^eReference 90.

^fReference 91.

The ^1H NMR spectra of these complexes have proven to be quite interesting and informative. The ^1H NMR data for each of the precursor chlorophosphorus compounds used as reactants in this study are shown in Table 16. Peak assignments and relative intensities all agreed well with what would be expected based upon their structures. The spectrum of the chlorodioxaphosphorinane 26 was found to be particularly interesting and a detailed understanding of its splitting patterns will be important in later discussions concerning the ^1H spectra of its complexes. It had been found in previous studies that 26 is a rigid system in the chair conformation, resulting in the observation of two separate resonances in the ^1H NMR for the inequivalent methyl groups in the 5 position (92). These signals are usually separated by 0.4 to 0.8 ppm (depending upon the solvent system employed). The splitting patterns reported previously for the methylene protons within the ring system were much more complicated. In the course of our studies, the 300 MHz spectrum of 26 was measured and it is shown in Figure 17. The rigidity of the structure on the NMR time scale was again confirmed by the observation of two methyl resonances. The assignment of these two resonances to the axial and equatorial positions was by analogy to work in the literature (92). The complexity of the methylene region, however, was relatively simplified in the 300 MHz spectrum so as to allow an analysis of the observed splitting pattern. Shown in Figure 18 is a schematic diagram depicting the probable origins of the observed spin-spin splitting. The two sets of methylene resonances centered at 4.12 and 3.19 ppm are due to the inequivalent sets of axial and equatorial protons, respectively. The

Figure 17. ^1H NMR spectrum of 26 (* solvent resonance)

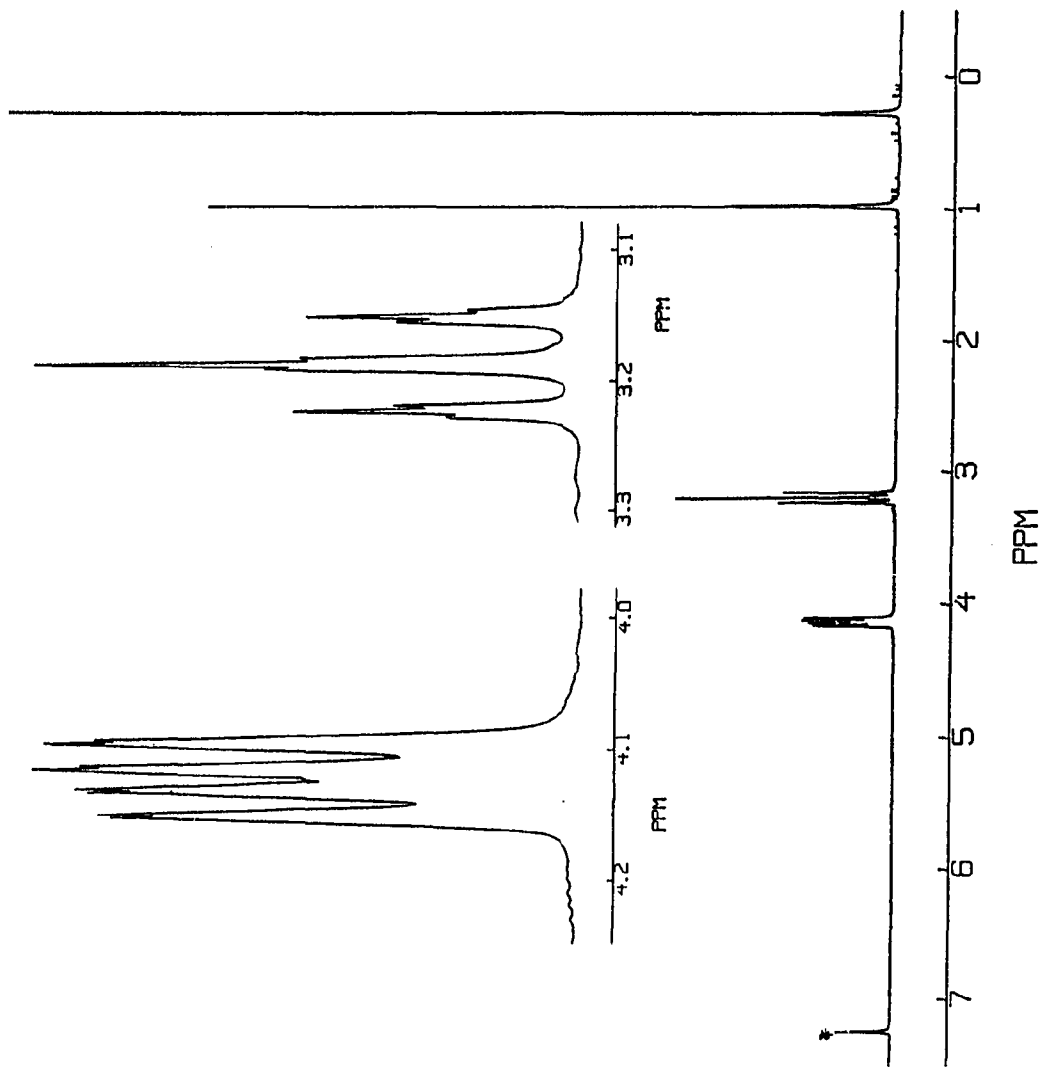
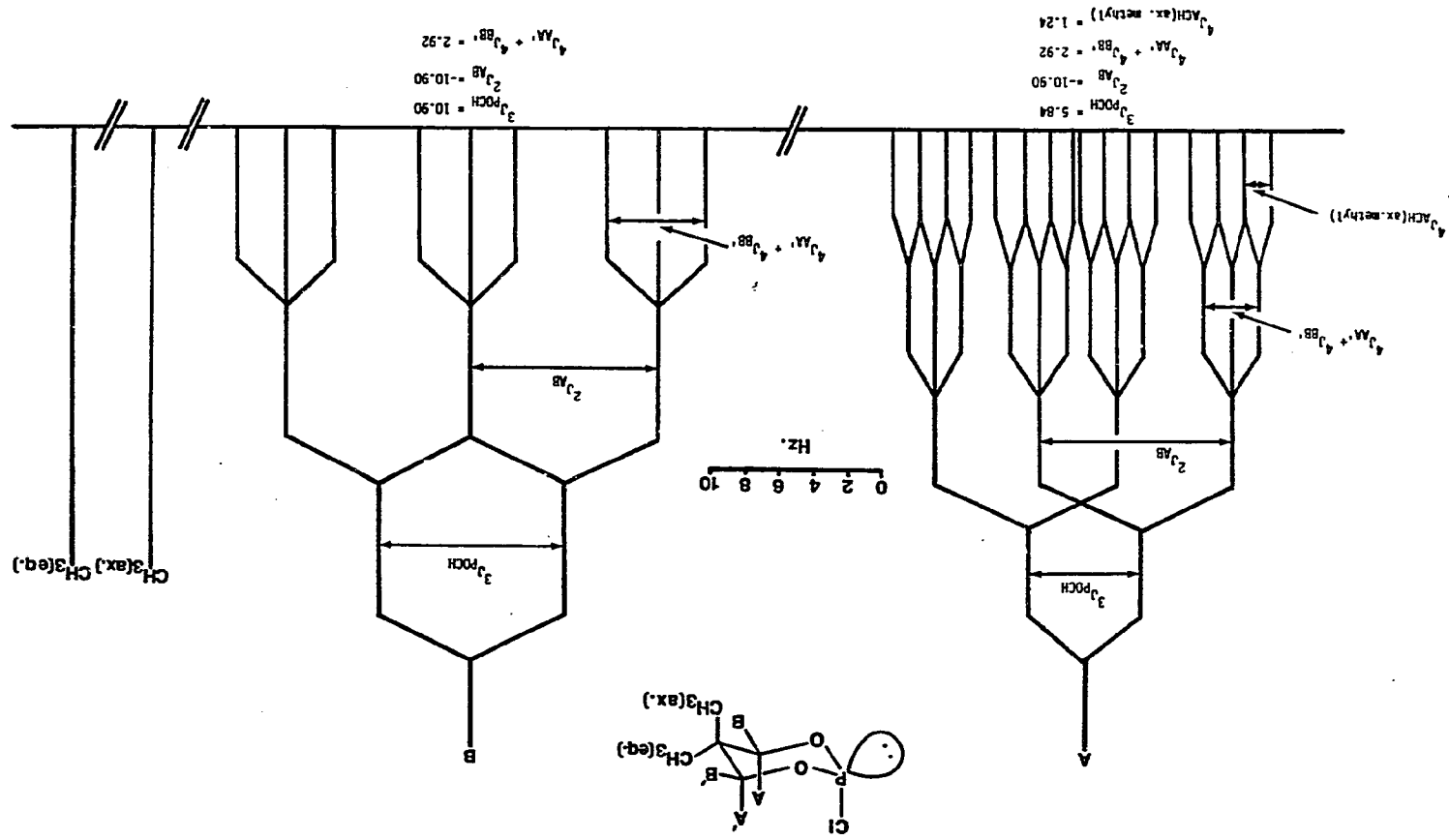


Figure 18. Schematic spin-spin splitting diagram for the ^1H NMR of 26



spectrum may be analyzed as part of an AA'MM'X spin system. The downfield multiplet consists of what appears to be two doublets of doublets. This splitting pattern arises from the axial methylene protons being split first into a doublet by coupling to the phosphorus and then each member of this doublet being split further into doublets by coupling to the geminal equatorial proton. The fine splitting of each of the two sets of doublets is due to two types of long range coupling. Each member of the doublets is first split into triplets from cross ring HCCC coupling of the type (${}^4J_{AA'} + {}^4J_{BB'}$). From other cyclic compounds, it has been shown that this type of long range coupling is associated primarily with the BB' pair (93). Each of the members of these triplets are finally further split into overlapping doublets from coupling with the axial methyl group on the 5 position to obtain the observed spectrum (the lower intensity outside lines are not resolved well in the spectrum). The axial methylene protons are only coupled to one of the axial methyl group's protons to yield the doublet splitting. This type of "W" coupling has been observed previously (94) and is diagrammed in Figure 19.

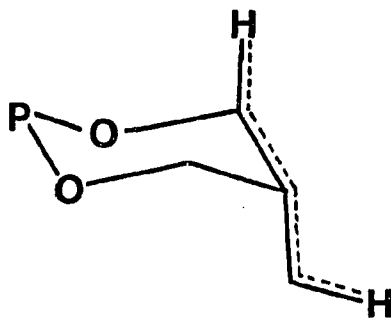


Figure 19. "W" coupling in 26

Irradiation at the axial methyl resonance caused the axial methylene resonance to collapse to the expected pattern of four sets of triplets. No change was observed upon irradiation of the equatorial methyl resonance, again as expected. In the case of the equatorial (upfield) proton resonances, some similar types of splitting are observed to occur. Since the value of ${}^3J_{\text{POCH}}$ equals that of ${}^2J_{\text{AB}}$ in this case, an apparent triplet results from the overlap of two doublets. Each member of this apparent triplet is further split into triplets from long range HCCCCH coupling as observed for the axial methylene protons (${}^4J_{\text{AA}'} + {}^4J_{\text{BB}'}$). The magnitude of (${}^4J_{\text{AA}'} + {}^4J_{\text{BB}'}$) is the separation between the outer lines of each of the triplets. No "W" coupling pathway to the 5 position methyl groups exists as was possible for the axial methylene protons. As expected, no change in the equatorial methylene splitting was observed upon irradiation of the methyl resonances. The computer simulated ${}^1\text{H}$ NMR spectrum of 26 shown in Figure 20 (${}^4J_{\text{ACH(ax. methyl)}}$ coupling was not included in the simulation) supported this rationalization of the observed spectrum. The chemical shift and coupling constant data for this system is given in Figure 18 and Table 20.

The ${}^1\text{H}$ NMR data for the cis and trans complex isomers isolated from the reaction of the chlorophosphorus precursor compounds with the $[\text{Fe}(\eta^5\text{-Cp})(\text{CO})_2]^-$ anion are given in Table 17. All the complexes showed resonances characteristic of cyclopentadienyl protons in the region of 4.15 to 4.59 ppm. The spectrum of cis- $[\text{Fe}(\eta^5\text{-Cp})(\text{CO})(\mu\text{-5,5-DMP})]_2$ is shown in Figure 21. The ${}^1\text{H}$ NMR of dimeric complexes arising from 26 are

Figure 20. Computer simulated ^1H NMR spectrum of 26 (without $^4J_{\text{ACH(axial methyl)}}$ included for the axial methylene proton peaks)

4.2 4.0 3.8 3.6 3.4 3.2 3.0 ppm

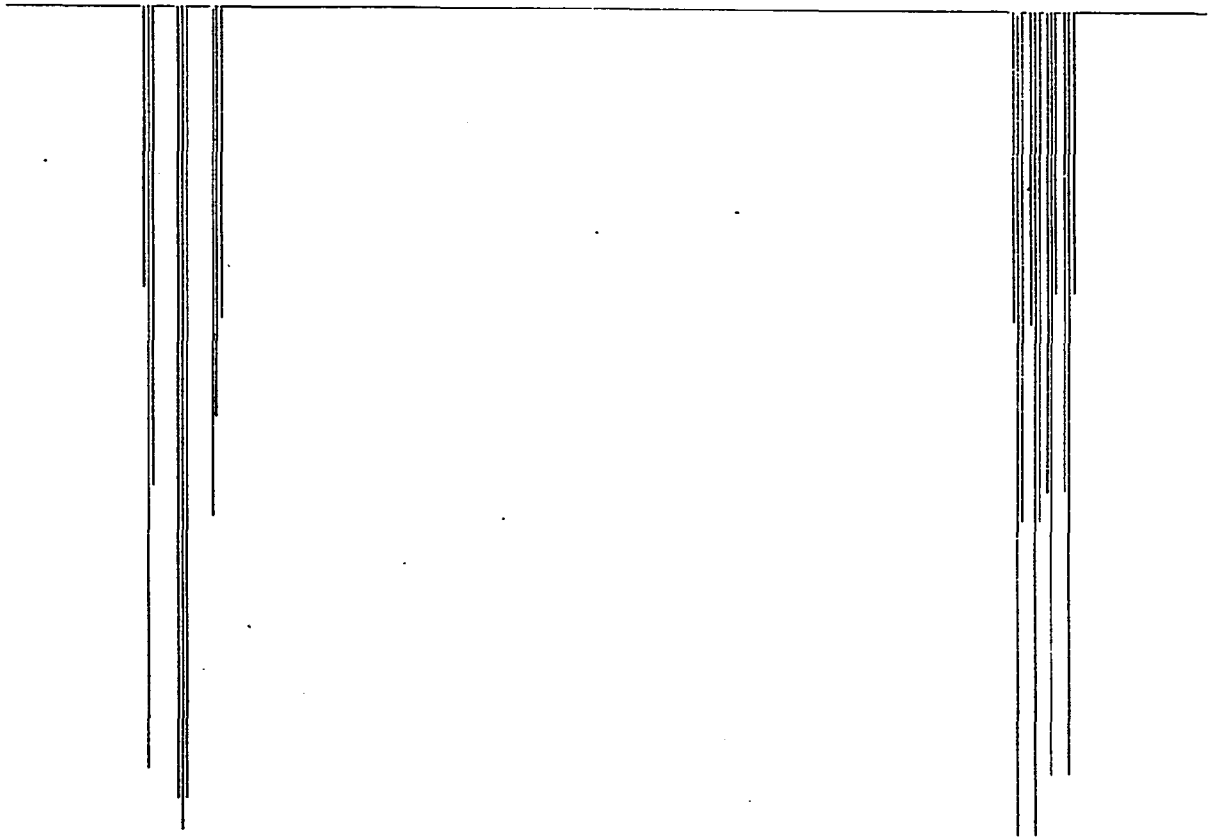
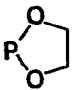
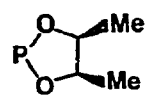
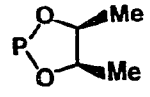
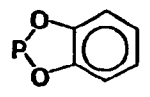
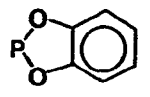
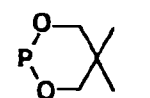


Table 17. ^1H NMR data for $[\text{Fe}(\eta^5\text{-Cp})(\text{CO})(\text{L})]_2$ systems^a

Ligand	Isomer	R	J^b	R'	J^c	R''	Cp	Solvent
Fp ₂	---	---	---	---	---	---	4.77	CDCl_3
PMe ₂	cis ^d	1.44(3H,t)	$^2J_{\text{PCH}}=7.9$	---	---	---	4.15(5H,s)	CS_2
		1.70(3H,t)	$^2J_{\text{PCH}}=6.2$					
PMe ₂	trans ^d	1.55(6H,t)	$^2J_{\text{PCH}}=7.0$	---	---	---	4.15(5H,s)	CS_2
PPh ₂	cis	7.24(10H,s)	---	---	---	4.37(5H,s)		CDCl_3
PPh ₂	trans	7.31(10H,s)	---	---	---	---	4.15(5H,s)	CDCl_3
P(OEt) ₂	cis	3.90(4H,m)	v.complex	1.43(6H,t)	$^3J_{\text{HH}}=7.0$	---	4.40(5H,s)	CDCl_3
P(OEt) ₂	trans	3.93(2H,m) (cis to Cp ring)	v.complex	1.35(6H,t)	$^3J_{\text{HH}}=7.03$	---	4.41(5H,s)	CDCl_3
		3.75 (2H,m) (trans to Cp ring)	v.complex					
	trans	2.38(2H,m)	v.complex	---	---	---	4.21(5H,s)	CDCl_3
		1.76(2H,m)	v.complex					

	cis	4.44(2H,m)	v.complex	1.09(6H,m)	v.complex	---	4.23(5H,s) CDCl ₃
	trans	3.83-4.43 (2H,m)	v.complex	1.26(6H,t)	³ J _{HH} =6.2	---	4.25(5H,s) CDCl ₃
	cis	6.89(4H,m)	v.complex	---	---	---	4.33(5H,s) CDCl ₃
	trans	7.11(2H,m) 7.12(2H,m)	v.complex v.complex	---	---	---	4.42(5H,s) CDCl ₃
	cis	3.89(2H,t) (endo to Cp ring)	J = 11.26 ^d	101.(6H,s)	---	---	4.45(5H,s) CDCl ₃

^aLabeling scheme used here is the same as that presented in Table 16.

m = multiplet

pd = pentet of doublets

s = singlet

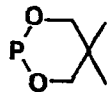
t = triplet

^bJ = coupling constant (Hz) as indicated.

^cJ_{HH}

^dData from reference 37.

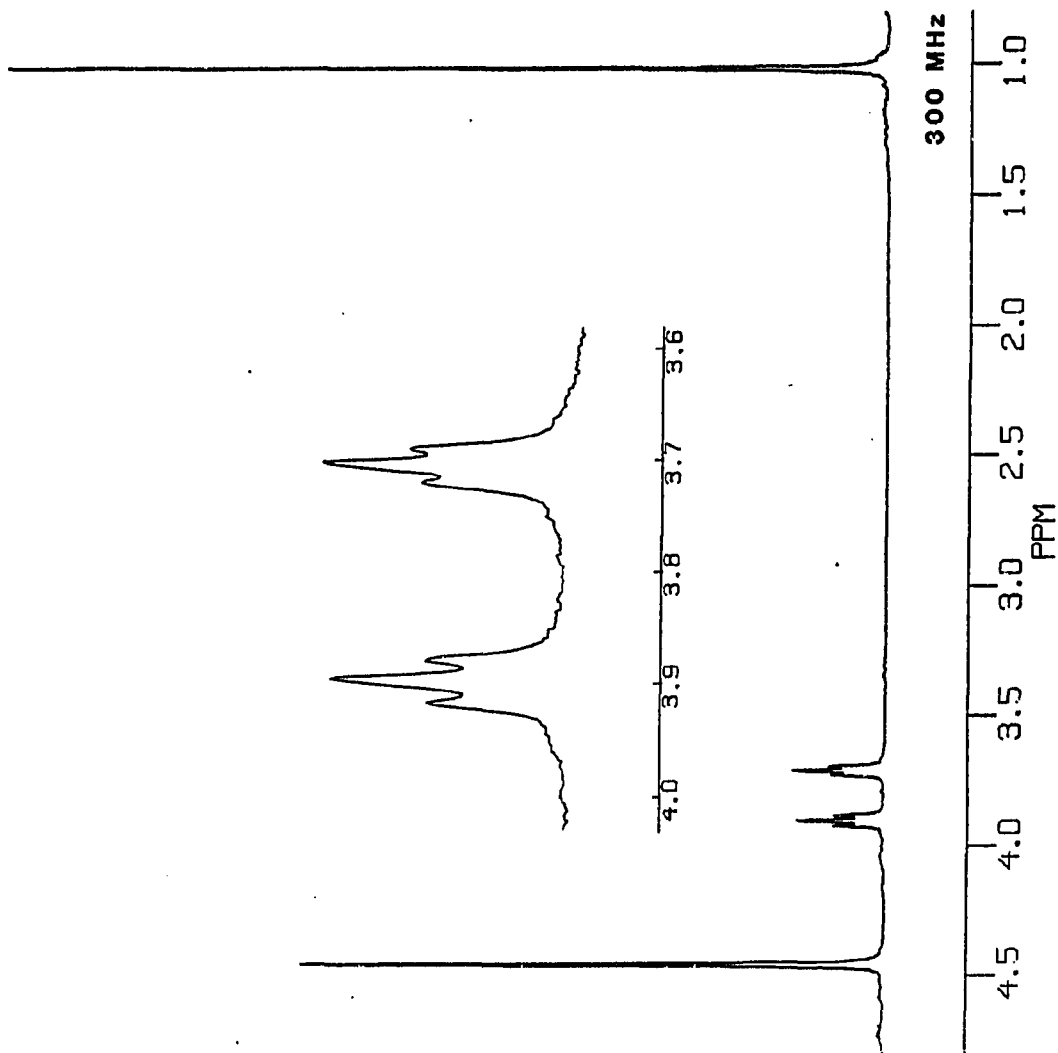
Table 17 (continued)

Ligand	Isomer	R	J ^b	R'	J ^c	R''	Cp	Solvent
		3.71 (2H,t) (exo to Cp ring)	J = 8.92 ^b					
	trans	3.91(2H,pd) (cis to Cp ring)	² J _{HH} =10.80 J=10.80 ^e ⁴ J _{HH} =1.08 ^f	0.88(6H,s)	---	---	4.59(5H,s)	CDCl ₃
		3.71(2H,pd) (trans to Cp ring)	² J _{HH} =10.80 J=10.80 ^e ⁴ J _{HH} =0.98 ^f					

$${}^e 3J_{POCH} + {}^5J_{POCH}$$

^fEqual values within experimental error ± 0.08 ("w" coupling).

Figure 21. Proton NMR of $\text{cis-}[\text{Fe}(\eta^5\text{-Cp})(\text{CO})(\mu\text{-5,5-DMP})]_2$



particularly interesting. In most transition metal complexes of 26, the dioxaphosphorane ring is usually a rigid system similar to that for the chlorophosphorinane (92). In the case of the $\text{cis-}[\text{Fe}(\eta^5\text{-Cp})(\text{CO})(\mu\text{-5,5-DMP})]_2$ complex, however, only a single methyl resonance is observed in a variety of solvents and over a wide range of temperatures. This indicates that in solution the ring system is rapidly interconverting between chair conformations so as to make the two methyl groups equivalent on the NMR time scale. This is in contrast with what is observed in the precursor chlorodioxaphosphorinane. The methylene region consists of two triplets at 3.91 and 3.71 ppm. This splitting pattern may be accounted for by considering the equivalent protons as shown in Figure 22. By inversion of the six-membered 1,3,2-dioxa-

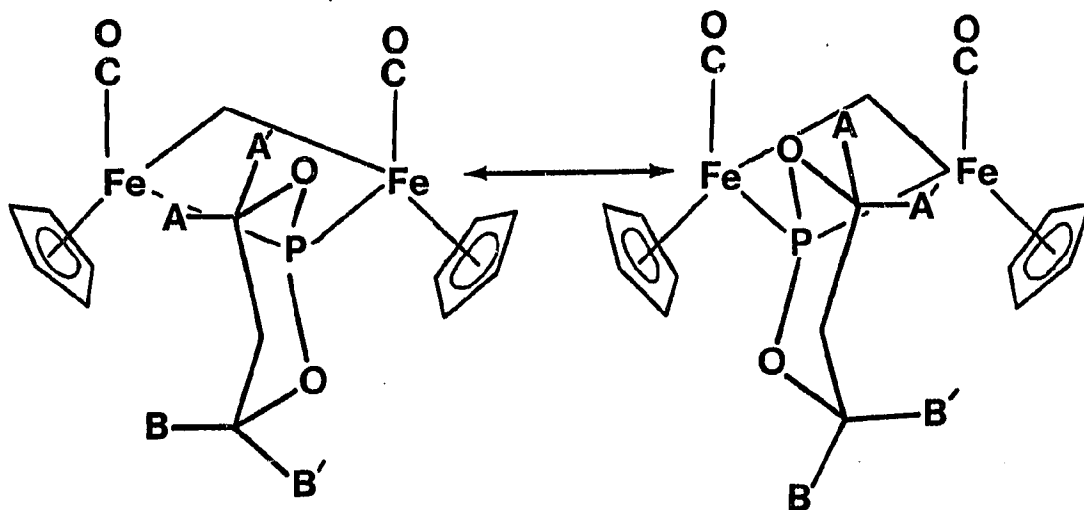


Figure 22. Diagram showing the equivalent methylene protons in $\text{cis-}[\text{Fe}(\eta^5\text{-Cp})(\text{CO})(\mu\text{-5,5-DMP})]_2$

phosphorinane ring system, as required by the observed equivalence of the methyl groups, the two protons of each methylene unit are chemically and magnetically equivalent to one another. The two methylene units are, however, not equivalent to each other because of the cis configuration of the cyclopentadienyl rings on the iron. Therefore, the proton labeled A is equivalent to A' by ring inversion and likewise B with B'. This arrangement would lead to the observed spectrum as schematically shown in Figure 23. The observed triplet for each methylene unit arises from a virtually coupled diphosphorus system in which the two phosphorus atoms in the complex are chemically equivalent but magnetically inequivalent (95). This indicates that ${}^2J_{PP}$ is significantly larger than ${}^3J_{POCH}$, which has been observed in other diphosphorus complexes (62). No ${}^4J_{AB}$ coupling across the ring was observed probably due to the fact that the magnitude of ${}^4J_{AB}$ was smaller than the resolution obtained in the spectrum. The assignment of the upfield triplet to the protons cis to the two carbonyl groups is based upon comparing the 60 MHz spectra taken in $CDCl_3$ with that taken in C_6D_6 . In C_6D_6 , the downfield triplet has approximately the same chemical shift as that observed in $CDCl_3$. The upfield triplet, however, shifts downfield by 0.37 ppm on going from $CDCl_3$ to C_6D_6 , indicating a side on interaction between the aromatic solvent and the methylene protons (96). Since there is spatially more room for the solvent molecules to interact with those protons cis to the carbonyl groups, the resonance which showed the greatest solvent dependence was tentatively assigned to these protons. The foregoing analysis of the spectrum was partially confirmed by the decoupling

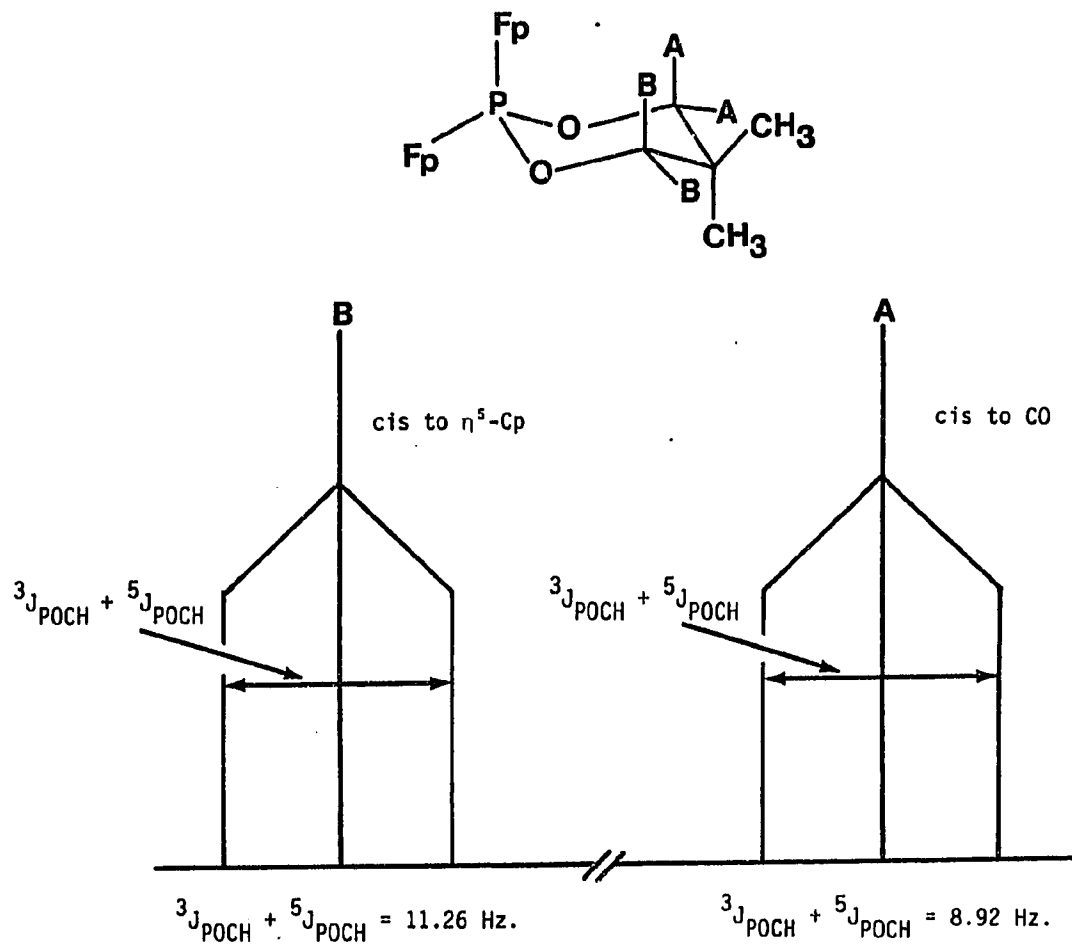


Figure 23. Schematic spin-spin splitting diagram for the ^1H NMR of $\text{cis-}[\text{Fe}(\eta^5\text{-Cp})(\text{CO})(\mu\text{-5,5-DMP})]_2$

experiments shown in Figure 24. Irradiation at either of the two triplets did not affect the appearance of the other. This result is expected since the triplet pattern is not due to any proton spin-spin coupling component but rather to virtual coupling involving the phosphorus atoms. The ^{31}P decoupled ^1H spectrum did, however, result in the collapse of each of the triplets to singlets as expected. Further support of this analysis came from a computer ^1H NMR spectrum (97) shown in Figure 25, which showed a very good agreement with the observed spectrum. Variable temperature ^1H NMR studies were done to determine if coalescence could be observed for this system. In the only other dioxaphosphorus bridged diiron complex, namely, $[\text{Fe}(\text{CO})_3(\mu\text{-5,5-DMP})]_2$; coalescence of the two inequivalent methylene signals to a single triplet occurs at 54°C (82). This was explained in terms of a flexing of the Fe_2P_2 ring which leads to the equivalence of these signals on the NMR time scale. Upon raising the temperature of *cis*- $[\text{Fe}(\eta^5\text{-Cp})(\text{CO})(\mu\text{-5,5-DMP})]_2$ to 75°C , no change in the spectrum was observed. This indicates that the Fe_2P_2 ring in this complex is probably quite rigid over the temperature range studied. Moreover, no change was observed upon cooling to 216°K , which indicates that the fluxionality of the phosphorinane ring system could not be "frozen out" under these conditions.

The ^1H NMR of *trans*- $[\text{Fe}(\eta^5\text{-Cp})(\text{CO})(\mu\text{-5,5-DMP})]_2$ appears to be similar in some respects to that of the *cis* isomer but quite different in others. The resonances for the cyclopentadienyl and methyl protons again appear as singlets indicating rapid ring inversion. The spectrum in the methylene region, which is shown in Figure 26, however, is substantially

Figure 24. Decoupling experiments on $\text{cis-}[\text{Fe}(\eta^5\text{-Cp})(\text{CO})(\mu\text{-5,5-DMP})]_2$; a. ^1H NMR spectrum in CDCl_3 , b. irradiation of the upfield methylene resonance, c. irradiation of the downfield methylene resonance, d. enlarged methylene region, and e. ^{31}P decoupled ^1H spectrum in the methylene region (asterisk indicates irradiation frequency)

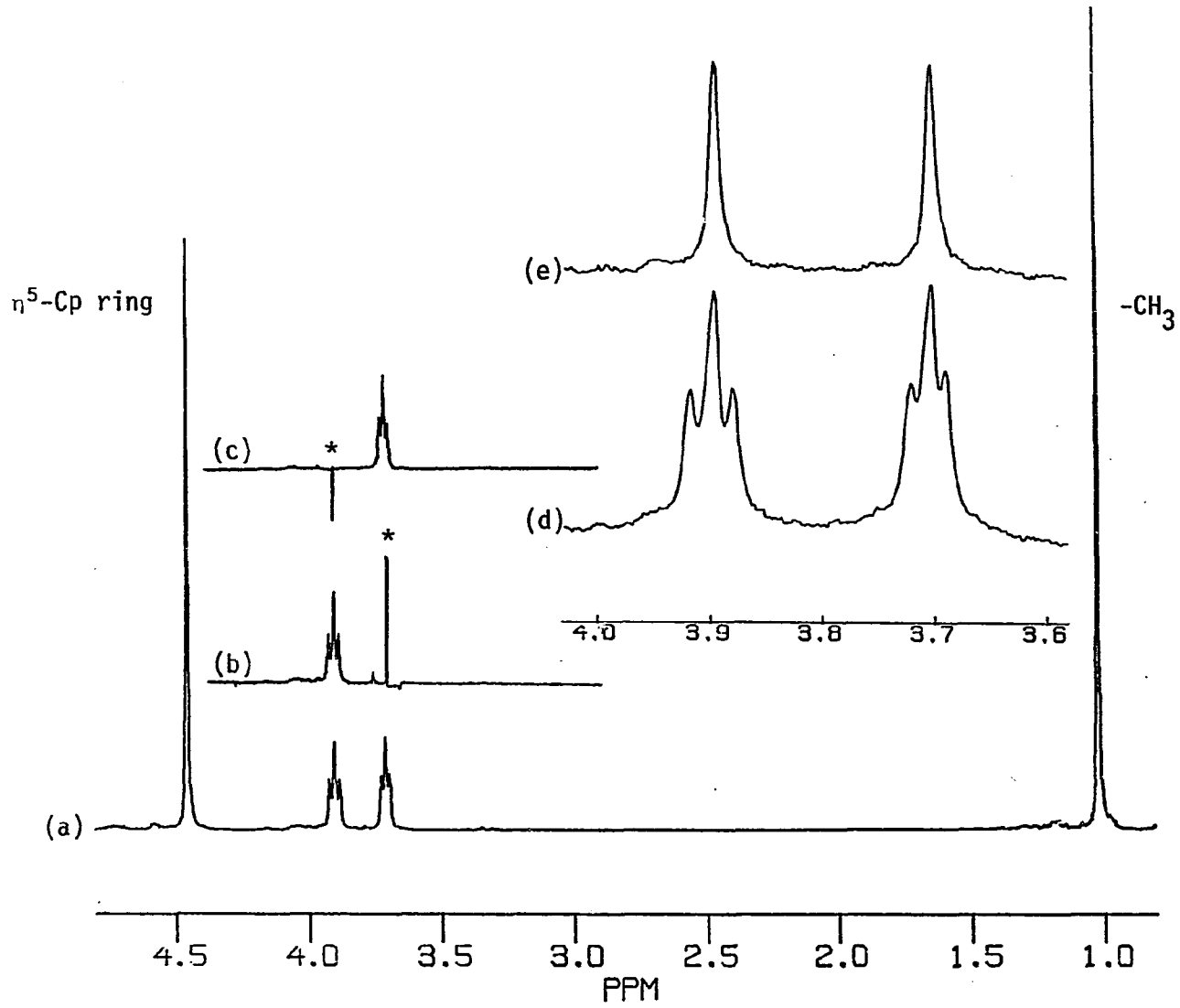


Figure 25. Computer simulated ^1H NMR spectrum in the methylene region of cis-
 $[\text{Fe}(\eta^5\text{-Cp})(\text{CO})(\mu\text{-5,5-DMP})]_2$

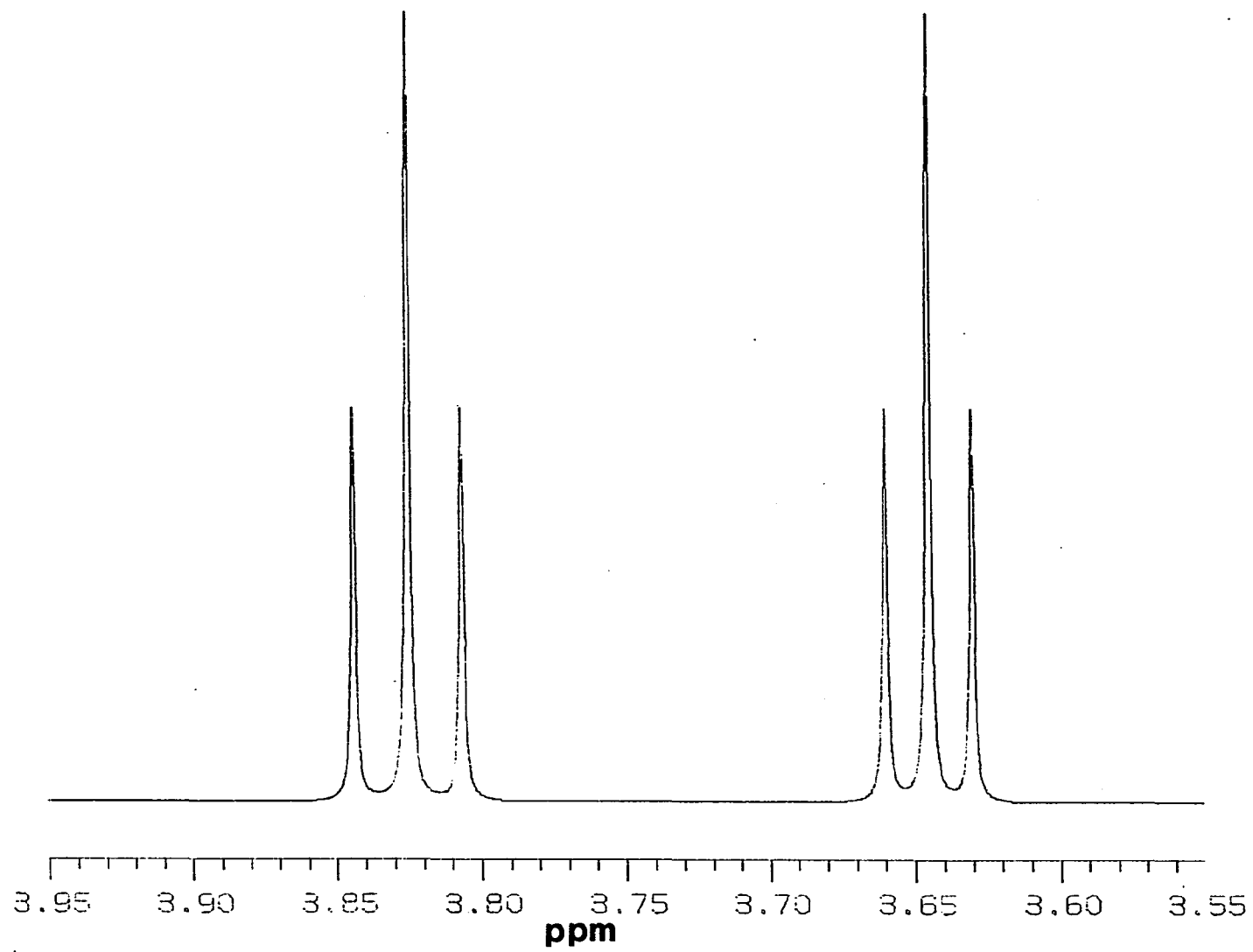
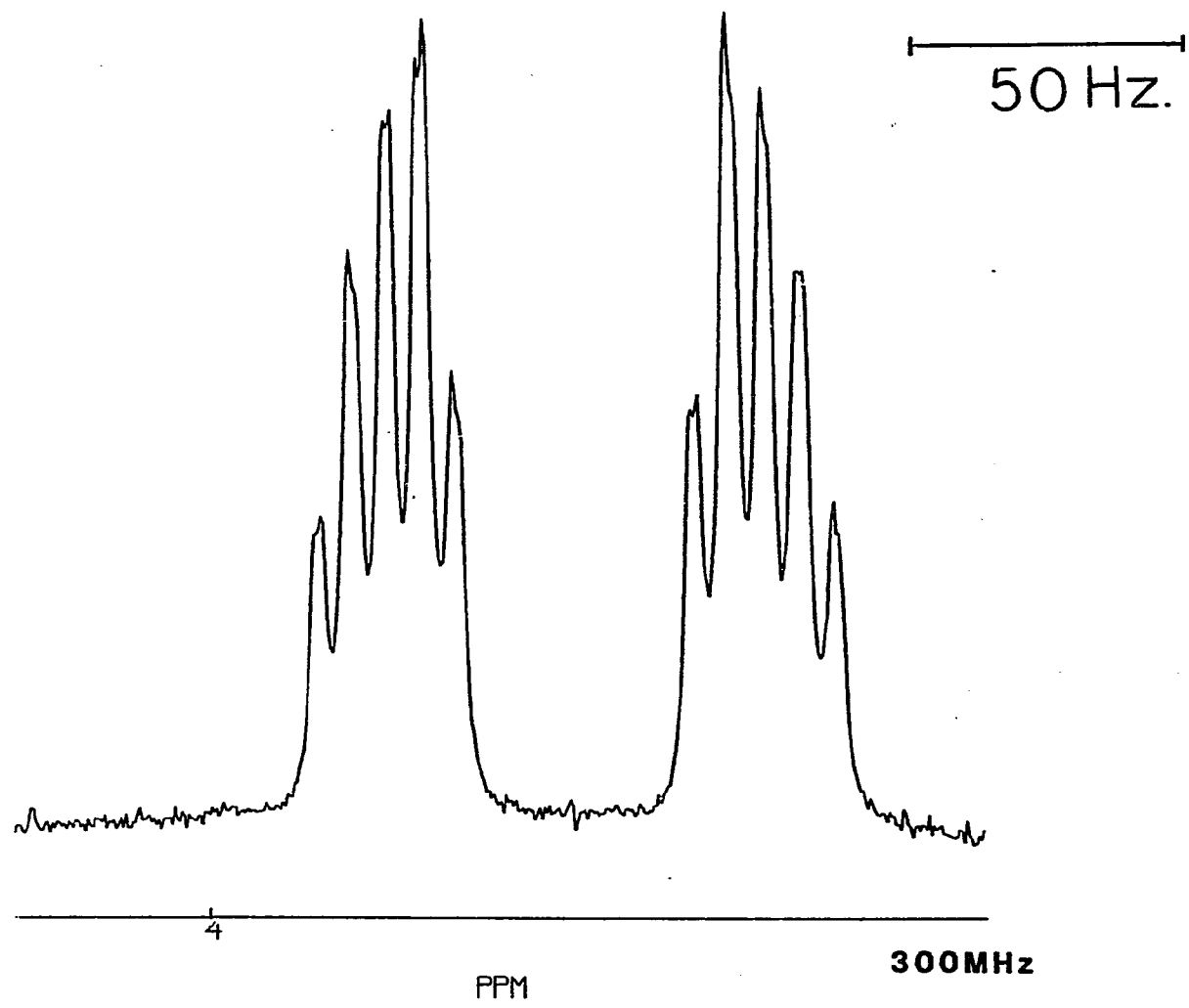


Figure 26. Proton NMR of $\text{trans-}[\text{Fe}(\eta^5\text{-Cp})(\text{CO})(\mu\text{-5,5-DMP})]_2$ in the methylene region



more complicated. These protons are observed as two sets of pentets with each member of the pentet further split into doublets. In Figure 27 are shown the equivalent protons giving rise to this pattern, as viewed down the C5-P axis. In the trans complex, the two protons on the same methylene unit are inequivalent. The reason for this can be best seen in the conformational transition state shown in the diagram where the A and A' protons are closest to the carbonyl groups and are equivalent, and the B and B' protons are closest to the cyclopentadienyl rings and are likewise equivalent. With these considerations, the spin-spin splitting observed can be rationalized from the schematic diagram in Figure 28. Each proton is first split into an AB doublet by the geminal proton and then each member of this doublet is further split into a triplet from the virtually coupled phosphorus atoms, similar to that observed in the cis complex (${}^2J_{pp} > {}^3J_{POCH}$). Due to the magnitude of the J values, these two sets of triplets overlap to form an apparent pentet. Finally, each member of this pentet is split into a doublet from "W" coupling (98) across the ring. (These values of the ${}^4J_{AB}$ are equal within experimental error.) Such coupling was presumably not resolved in the cis complex. As with the cis complex, however, decoupling experiments proved quite useful in confirming this analysis as shown in Figure 29. Irradiating either of the apparent pentets caused the remaining resonance to collapse to a virtually coupled triplet as expected. In the ${}^{31}P$ decoupled 1H NMR, the methylene resonances collapsed to a single AB pattern of two proton coupled doublets (no "W" coupling was resolved in this experiment). Computer simulation of the 1H NMR spectrum (97) of this complex further

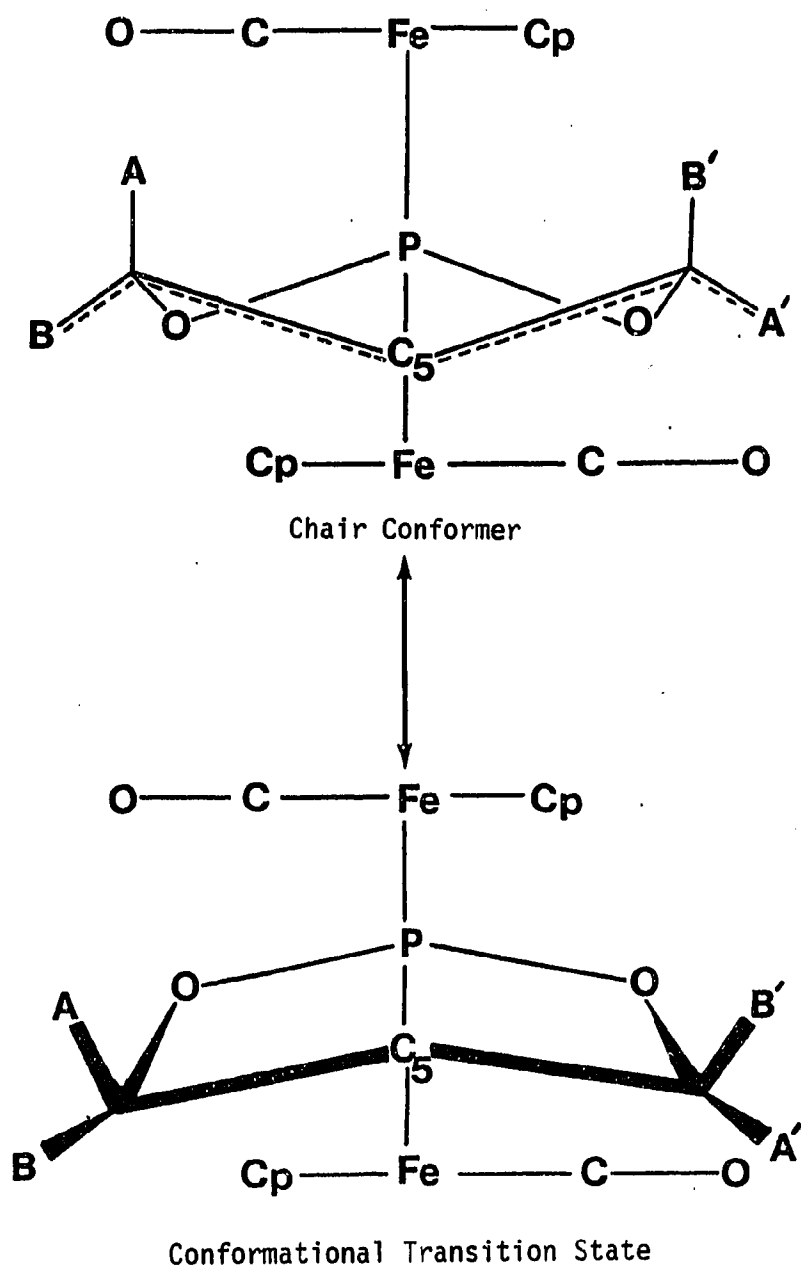


Figure 27. Diagram showing the equivalent methylene protons in $\text{trans-}[\text{Fe}(\eta^5\text{-Cp})(\text{CO})(\mu\text{-}5,5\text{-DMP})]_2$ (dashed line indicates the "W" coupling path)

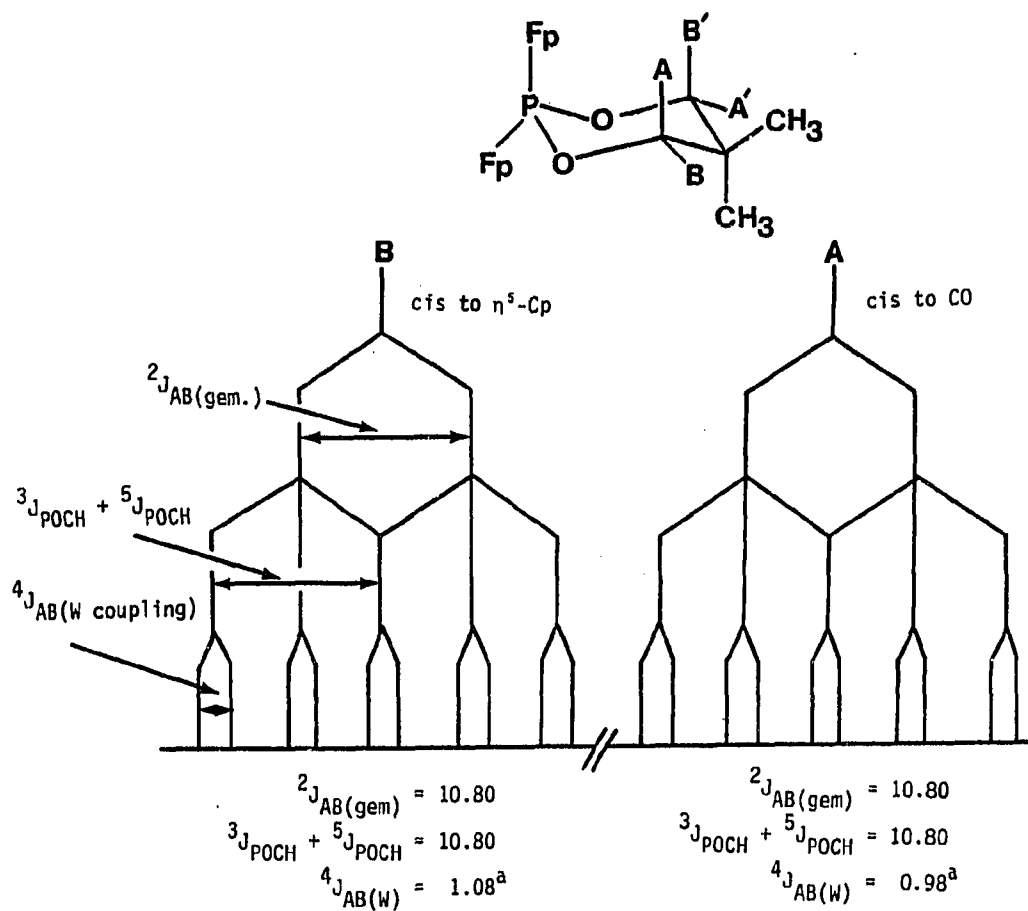
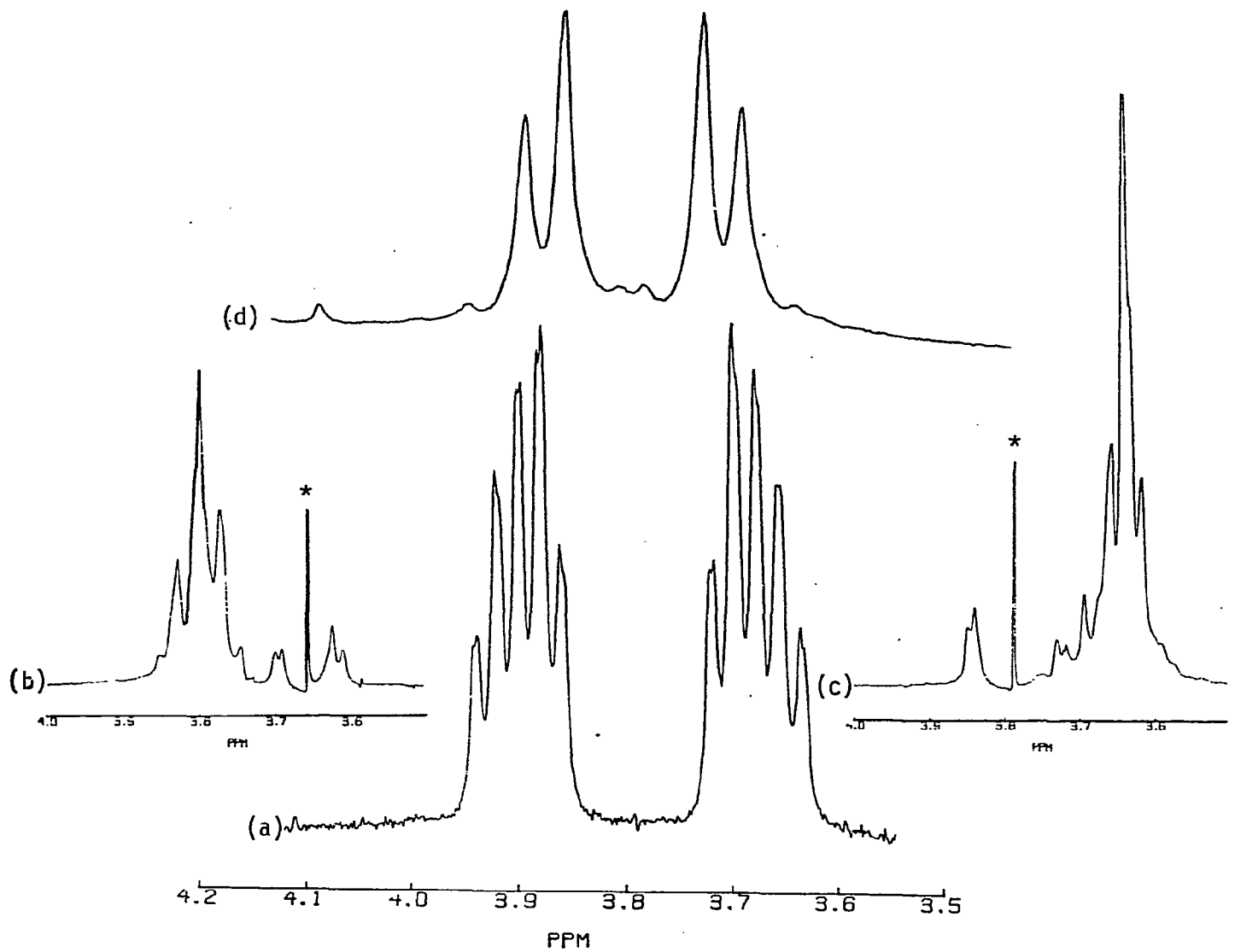


Figure 28. Schematic spin-spin splitting diagram for the ^1H NMR of $\text{trans-}[\text{Fe}(\eta^5\text{-Cp})(\text{CO})(\mu\text{-5,5-DMP})]_2$ (^aEqual values within experimental error ("W" coupling))

Figure 29. Decoupling experiments on $\text{trans-[Fe}(\eta^5\text{-Cp})(\text{CO})(\mu\text{-5,5-DMP})_2]$; a. ^1H NMR of the methylene region in CDCl_3 , b. irradiation at the upfield methylene resonance, c. irradiation at the downfield methylene resonance, and d. ^{31}P decoupled ^1H spectrum of the methylene region (asterisk indicates irradiation frequency)



supported this analysis and is shown in Figure 30. Variable temperature ^1H NMR studies over the range of +216 to +343°K revealed no changes in the spectra.

An example of a more complicated spectrum is that of trans- $[\text{Fe}(\eta^5\text{-Cp})(\text{CO})(\mu\text{-P}(\text{OEt})_2)]_2$, shown in Figure 31. The same types of interactions as those earlier discussed for cis and trans- $[\text{Fe}(\eta^5\text{-Cp})(\text{CO})(\mu\text{-5,5-DMP})]_2$ must be in effect here, however, the observed pattern is more complicated. Decoupling $^1\text{H}\{^{31}\text{P}\}$ and $^1\text{H}\{^1\text{H}\}$ experiments did not simplify the spectrum enough to allow identification of the various coupling constants.

The ^1H NMR spectra of these complexes are quite sensitive to impurities in the sample. After remaining only a short period of time in solution (~30 minutes), an unidentified paramagnetic decomposition product is probably produced. In the case of trans- $[\text{Fe}(\eta^5\text{-Cp})(\text{CO})(\mu\text{-P}(\text{OEt})_2)]_2$, this results in the total loss of the fine structure in the methylene region and the observation of only two broad nondescript signals. Column chromatography immediately prior to the measurement of the spectra was found to eliminate this problem.

The ^{13}C NMR data for the precursor Cl-ligand compounds and for the diiron complexes are shown in Tables 18 and 19, respectively. Characteristic in all the spectra of the complexes are the cyclopentadienyl resonance in the region of 81.03 to 81.76 ppm. In most cases, the signal for the carbonyl carbons were not detected due to the long T_1 relaxation times for carbonyl resonances (99). Attempts to overcome these difficulties by utilizing long pulse delay times, or by

Figure 30. Computer simulated ^1H NMR spectrum in the methylene region of trans-
 $[\text{Fe}(\eta^5\text{-Cp})(\text{CO})(\mu\text{-5,5-DMP})]_2$

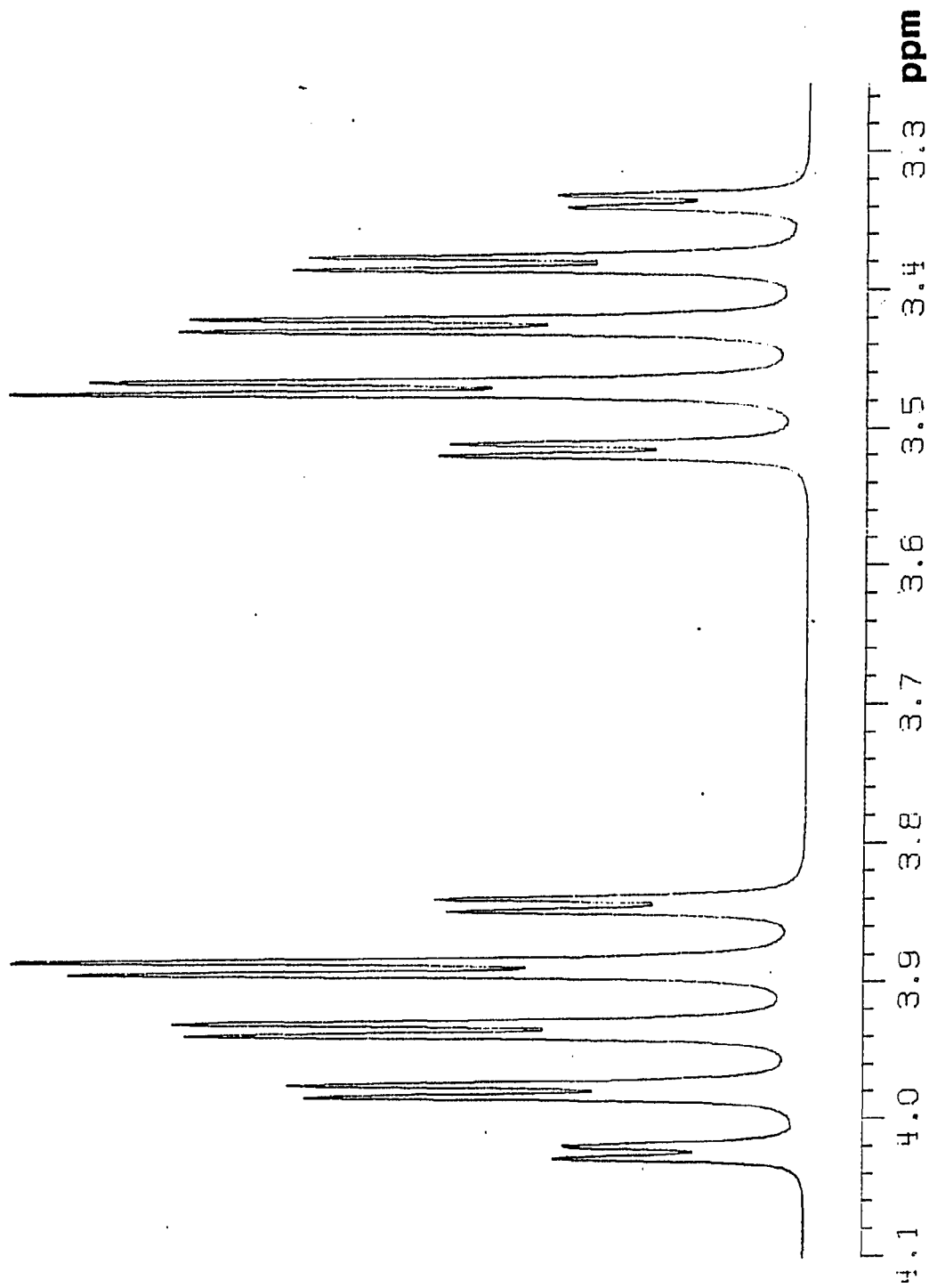


Figure 31. ^1H NMR spectrum of $\text{trans-}[\text{Fe}(\eta^5\text{-Cp})(\text{CO})(\mu\text{-P}(\text{OEt})_2)]_2$

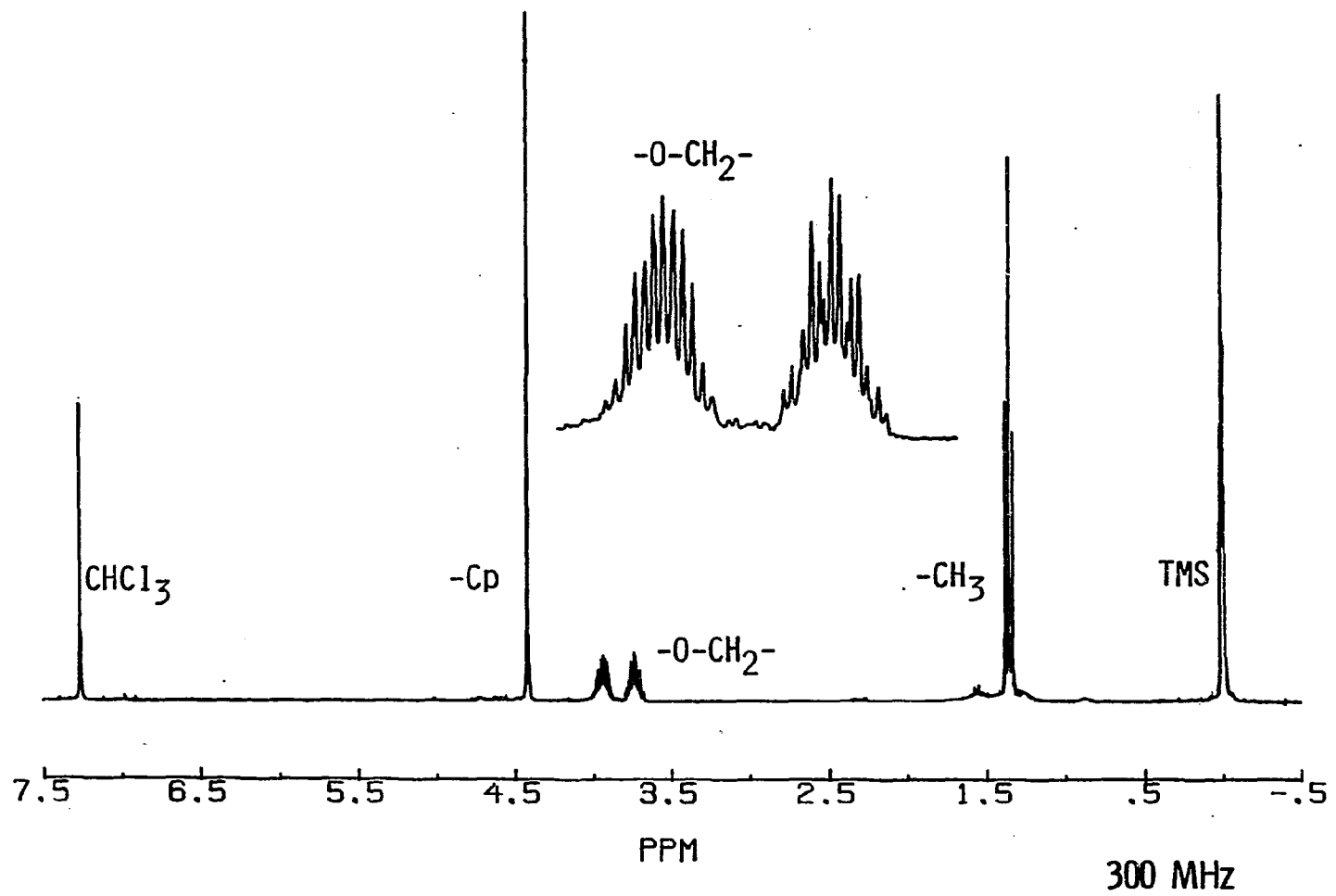
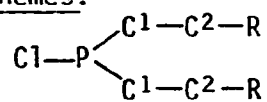
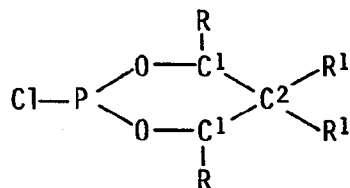


Table 18. ^{13}C NMR data for precursor chlorophosphorus(III) compounds^a

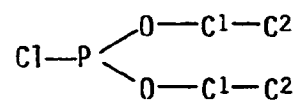
labeling schemes:



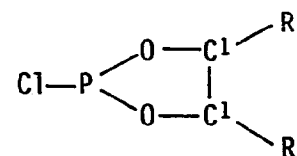
chloro phosphines



chloro-1,3,2-phosphorinanes

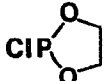


chloro phosphites



chloro-1,3,2-phospholanes

$\text{ClP} <$	C^1	J^b	C^2	J^c	R	J^d	R^1	J^e
ClPMe_2	22.51(d)	29.06	---	---	---	---	---	---
ClPPh_2^f	131.85(d)	21.87	130.18(s)	n.o. ^g	128.43(s)	n.o.	127.79(s)	n.o.
ClP(OEt)_2	61.05(d)	3.66	16.17(s)	4.88	---	---	---	---

ClP(OPh)_2^f	129.66(s)	n.o.	125.11(s)	n.o.	121.10(s)	n.o.	120.83(s)	n.o.
$\text{ClP}(\text{-O-} \begin{array}{c} \text{X} \\ \\ \text{C}_6\text{H}_2 \\ \\ \text{X} \end{array} \text{)}_2$	146.17(s) 145.34(s) 141.93(s) 123.56(s)	n.o.	35.71(s) 34.27(s) 32.53(s) 31.24(s)	n.o.	---	---	---	---
	65.17(d)	8.55	---	---	---	---	---	---

^aIn ppm relative to TMS (in CDCl_3).

d = doublet
s = singlet

^b $^2J_{\text{PC}}$ or $^3J_{\text{POC}}$ (depending on compound).

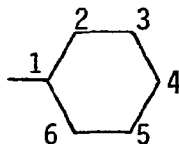
^c $^3J_{\text{POC}}$.

^d $^3J_{\text{POC}}$.

^e $^4J_{\text{PC}}$, $^4J_{\text{POC}}$, or $^5J_{\text{POC}}$.

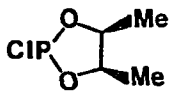
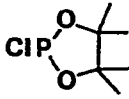
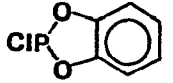
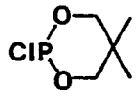
^fLabeling scheme for aromatic containing systems;

1 = C¹
2,6 = C²
3,5 = R
6 = R



^gn.o. = not observed.

Table 18 (continued)

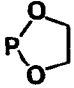
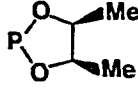
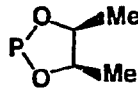
$CIP <$	C^1	J^b	C^2	J^c	R	J^d	R^1	J^e
	79.11(s)	n.o.	---	---	15.92(s)	n.o.	---	---
	88.64(d)	8.80	---	---	14.96(s)	n.o.	---	---
	144.40(s) 124.30(s) 114.06(s)	n.o.	---	---	---	---	---	---
	70.70(s)	n.o.	32.34(d)	5.86	---	---	21.80(d)	5.86

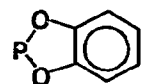
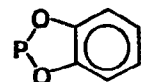
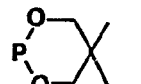
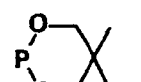
^hIn C_6D_6 .

ⁱ C^1 values are for the aromatic carbons (unassigned).

^j C^2 values are for the t-butyl carbons (unassigned).

Table 19. ^{13}C NMR data for $[\text{Fe}(\eta^5\text{-Cp})(\text{CO})(\text{L})]_2$ systems^a

Ligand	Isomer	$\eta^5\text{-Cp}$	CO	$^2J_{\text{CFeP}}$	C ¹	R	C ²	R ¹	Solvent
---	Fp ₂	88.43(s)	242.6(s)	n.o. ^b	---	---	---	---	C ₆ D ₆
PPh ₂ ^c	trans	81.76(s)	n.o.	n.o.	128.35(s) 127.97(s) 127.44(s) 127.06(s)	---	---	---	CDCl ₃
P(OEt) ₂	cis	80.40(s)	n.o.	n.o.	63.78(t) ^d (J=5.13) 61.78(t) ^d (J=5.99)	---	16.71(d) ^e (J=8.55)	---	CDCl ₃
P(OEt) ₂	trans	81.46(s)	n.o.	n.o.	61.78(t) ^d (J=5.49)	---	16.49 ^d (t) (J=3.67)	---	CDCl ₃
	trans	81.46(s)	n.o.	n.o.	67.65(s)	---	---	---	CDCl ₃
	cis	81.23(t) ^f (J=9.4)	n.o.	n.o.	75.69(s)	15.84(s)	---	---	CDCl ₃
	trans	81.23(s)	n.o.	n.o.	80.85(s)	15.92(s)	---	---	CDCl ₃

	cis	81.03(s)	n.o.	n.o.	128.43(s) 121.93(s) 113.09(s)	---	---	---	C ₆ D ₆
	trans	81.22(s)	n.o.	n.o.	128.43(s) 121.93(s) 112.50(s)	---	---	---	C ₆ D ₆
	cis	81.10(s)	n.o.	n.o.	76.04(s) 74.80(s)	---	32.59(s)	22.32(s)	C ₆ D ₆
	trans	81.43(s)	221.42(t)	24.41	76.23(s)	---	33.21(s)	22.71(s)	C ₆ D ₆

^a Labeling scheme used here is the same as that presented in Table 18.

d = doublet

s = singlet

t = triplet

^b n.o. = not observed.

^c Aromatic carbons presented under C¹ heading (unassigned).

^d Presumably coincidentally overlapping doublets (³J_{P_{OC}} and ⁵J_{P_{POC}}) to form the observed triplet.

^e Presumably coincidental overlap of doublets to form the observed doublet (see footnote d).

^f ²J_{PFeC}.

the addition of paramagnetic compounds such as $\text{Cr}(\text{acac})_3$, were unsuccessful except in the case of $\text{trans}-[\text{Fe}(\eta^5\text{-Cp})(\text{CO})(\mu\text{-}5,5\text{-DMP})]$.

As discussed in the previous sections, ^{31}P NMR spectroscopy was the most important tool for following the course of these reactions and for the identification of the products. The ^{31}P NMR data for the free chlorophosphorus(III) ligands and each of the *cis* and *trans* isomers of the $[\text{Fe}(\eta^5\text{-Cp})(\text{CO})(\text{P}\langle \rangle)]_2$ complexes are given in Table 20. The large downfield chemical shifts from the $\text{ClP}(\text{OR})(\text{ER})$ systems ($\text{E} = \text{NR}, \text{O}, \text{or S}$) to the complexes are particularly important. The pronounced deshielding may be attributable to at least partial localization of a positive charge on phosphorus. This charge localization can be reduced by π -conjugation with the substituents on the phosphorus as described before. It appears that the magnitudes of the downfield shifts (Δ) are quite sensitive to both steric and electronic factors within the complexes. The relative ordering of the magnitudes of Δ among the various ligands is shown below:

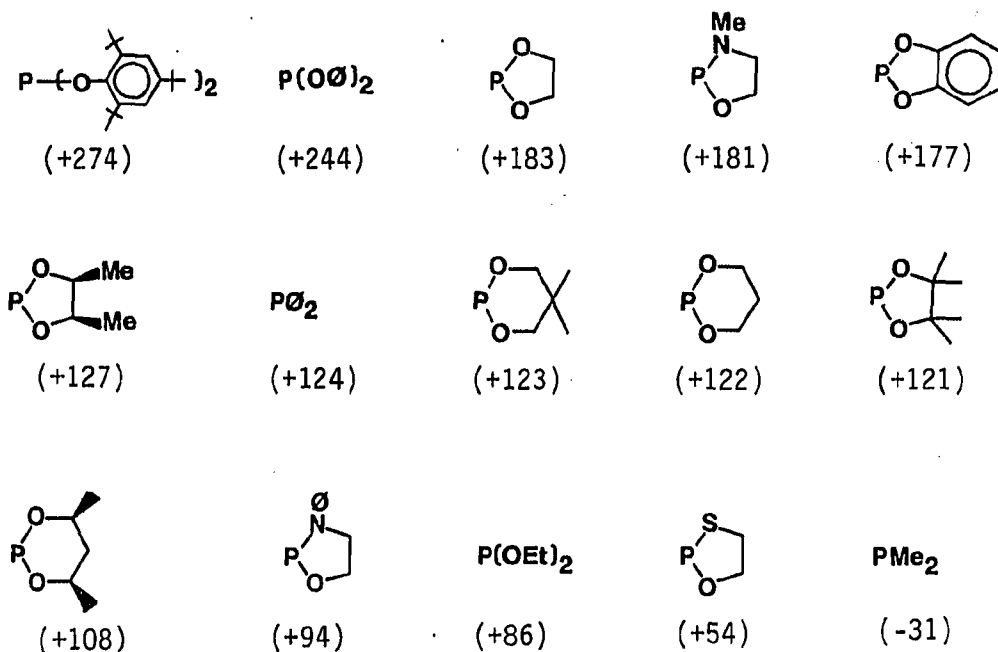
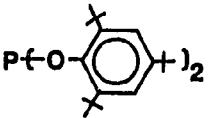
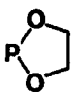
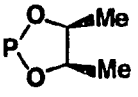
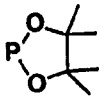


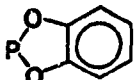
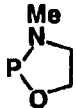
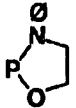
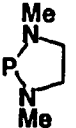
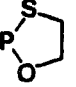
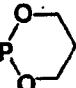
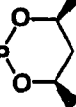
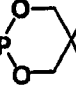
Table 20. ^{31}P NMR data for $[\text{Fe}(\eta^5\text{-Cp})(\text{CO})(\text{L})]_2$ systems

P \leq Bridging unit	^{31}P chemical shift (ppm)				
	Free ligand	Cis isomer	Δ^a	Trans isomer	Δ^a
PMe_2	94.57	63.28	-31.29	178.82	+84.25
PPh_2	81.82	206.57	+124.75	211.96	+130.14
$\text{P}(\text{OEt})_2$	164.97	250.70	+85.73	244.08	+79.11
$\text{P}(\text{OPh})_2$	156.38	400.17	+243.79	379.50	+223.12
	178.70	451.19	+272.49	415.08	+236.38
$\text{P}(\text{NMe}_2)_2$	158.71	N.R. ^b	---	N.R. ^b	---
	165.92	349.15	+183.23	342.88	+176.96
	165.89	292.55	+126.66	291.93	+126.04
		292.19	+126.30	291.76	+125.87
	173.60	294.91	+121.31	280.97	+107.37

$^a\Delta = [(\text{chem. shift of complex}) - (\text{chemical shift of free ligand})]$.

b No reaction observed (only starting material observed in the ^{31}P NMR).

Table 20 (continued)

P < Bridging unit	³¹ P chemical shift (ppm)				
	Free ligand	Cis isomer	Δ^a	Trans isomer	Δ^a
	172.08	349.21	+177.13	343.02	+170.94
	168.01	355.04	+187.03	310.56	+142.55
		355.53	+187.52	309.95	+141.94
		349.28	+181.27	309.10	+141.09
	156.58	250.29	+93.71	243.50	+86.92
		248.93	+92.35	242.45	+85.87
		247.24	+90.66	242.09	+85.51
	164.78	N.R. ^b	---	N.R. ^b	---
	202.79	256.60	+53.81	243.44	+40.65
		255.13	+52.34		
	153.91	275.81	+121.90	272.32	+118.41
	146.64	254.85	+108.21	253.13	+106.49
	146.87	270.08	+123.21	265.49	+118.62

It is interesting that the Δ value for the dimethylphosphino group is a negative value (an upfield shift relative to the chloro-ligand) while all others are positive values, indicating an increase in deshielding.

The ^1H uncoupled ^{31}P NMR spectrum of $\text{trans-}[\text{Fe}(\eta^5\text{-Cp})(\text{CO})(\mu\text{-5,5-DMP})]_2$ is shown in Figure 32. Using the $^3\text{J}_{\text{POCH}}$ values observed in the ^1H NMR spectrum of this complex, the observed splitting in Figure 32 can be rationalized as a set of overlapping triplet of triplets since $^3\text{J}_{\text{POCH(ax.)}} = ^3\text{J}_{\text{POCH(eq.)}}$. This is shown schematically in the figure.

Solid state ^{31}P spectra were also obtained on the cis and trans complexes of $[\text{Fe}(\eta^5\text{-Cp})(\text{CO})(\mu\text{-5,5-DMP})]_2$ and are shown in Figures 33 and 34, respectively. The ^{31}P chemical shifts in the solid state spectra were found to be located at the same values as were found in the solution spectra. The solid state spectra were obtained using "magic angle spinning" techniques (MAS), where the spinning frequency is large compared with the broadening, which sharpens the NMR spectra of solids (99). Spinning at frequencies smaller than one half the shielding anisotropy results in a series of "rotational echos" separated by the inverse of the spinning frequency (100). This is what is observed in the two spectra presented here. The spectra are ^1H decoupled. The splitting pattern of the trans isomer indicates two types of coupling. First, coupling to two inequivalent iron atoms within the molecule (^{57}Fe ; $I = 1/2$) and second, phosphorus-phosphorus coupling. This results in the eight line pattern observed. In the cis isomer, it appears that the iron atoms are equivalent, which leads to a simpler spectrum. These analyses

Figure 32. ^1H uncoupled ^{31}P NMR spectrum and schematic splitting diagram for trans-
 $[\text{Fe}(\eta^5\text{-Cp})(\text{CO})(\mu\text{-5,5-DMP})]_2$

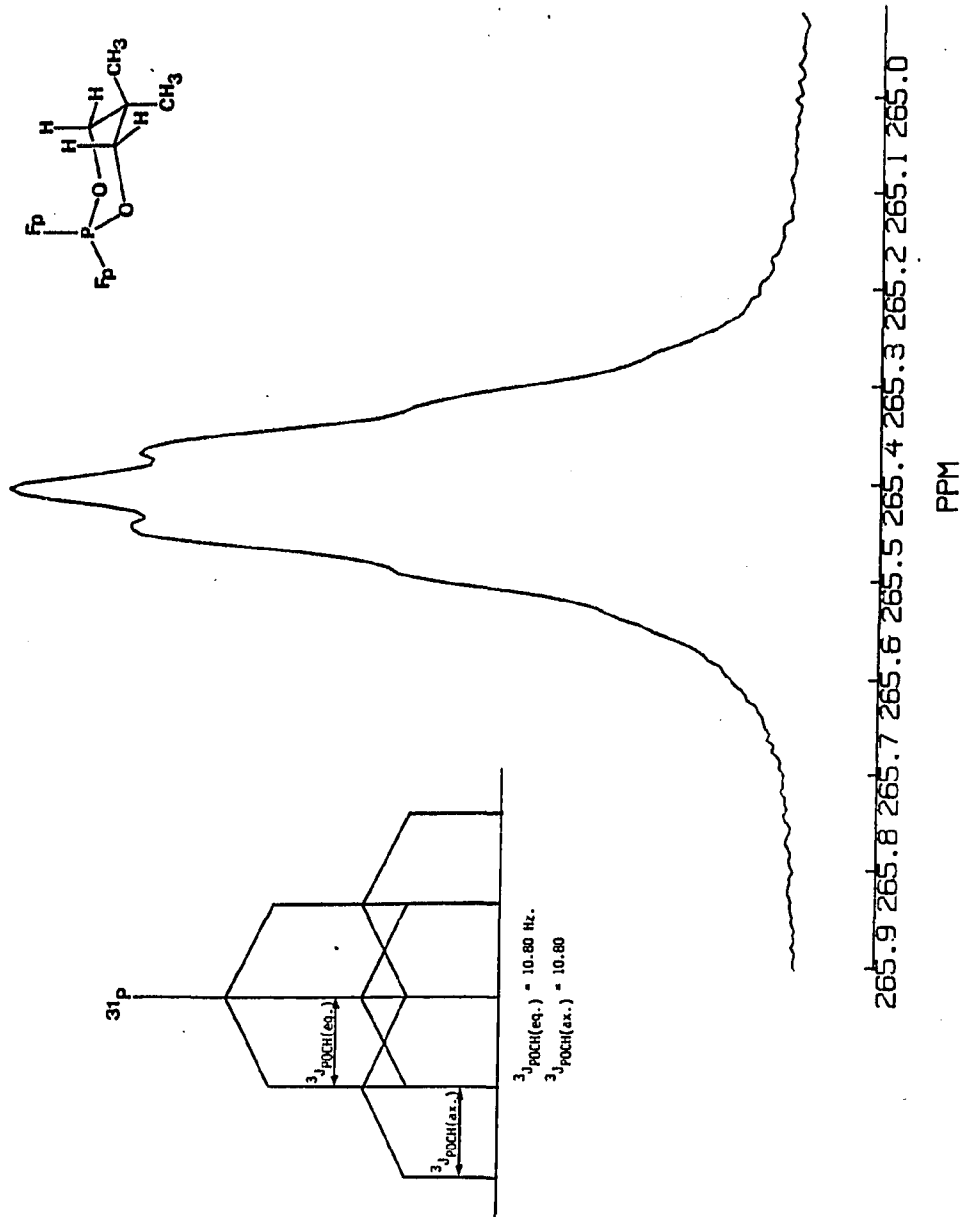


Figure 33. Solid state ^{31}P NMR of $\text{cis-}[\text{Fe}(\eta^5\text{-Cp})(\text{CO})(\mu\text{-5,5-DMP})]_2$

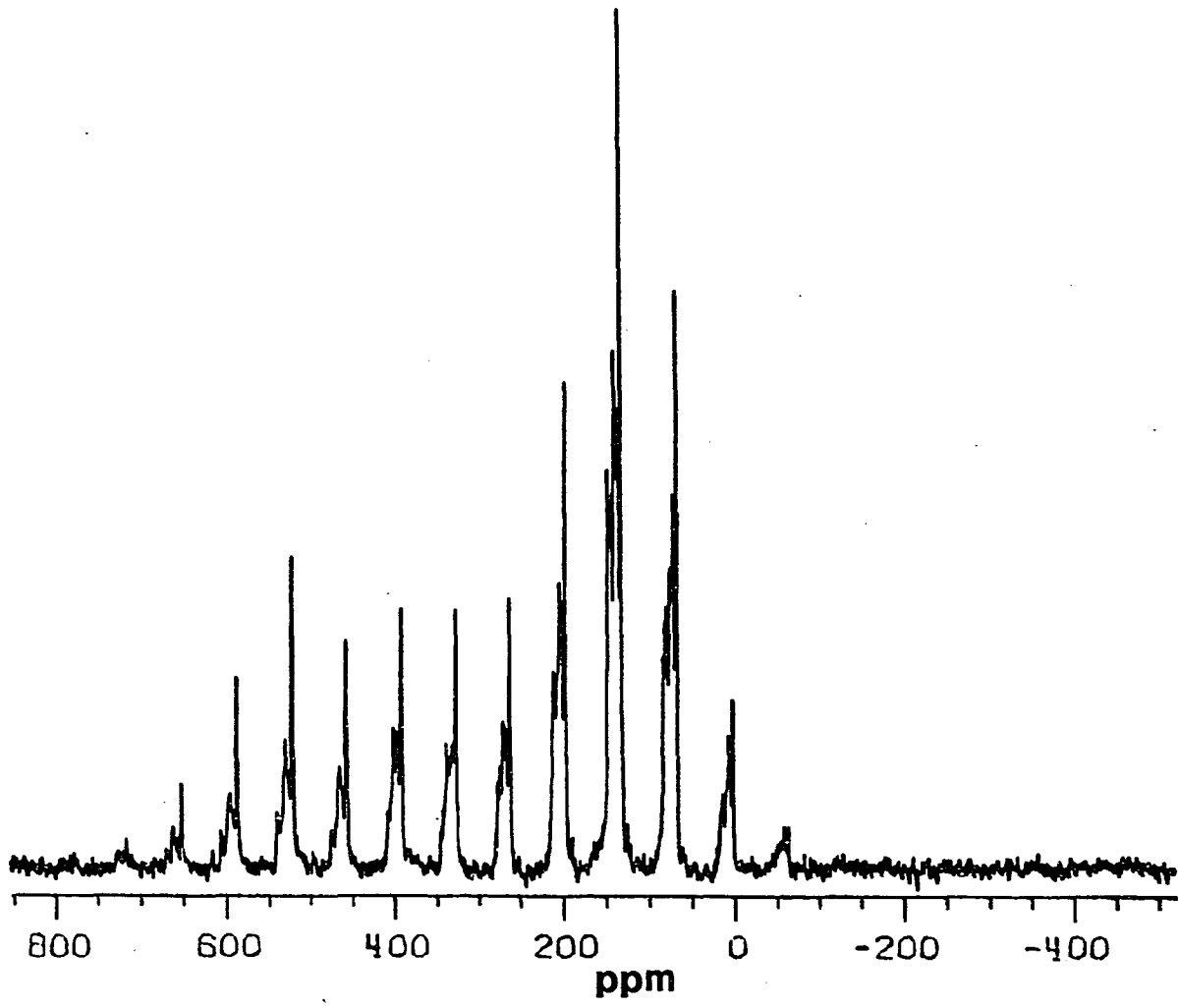
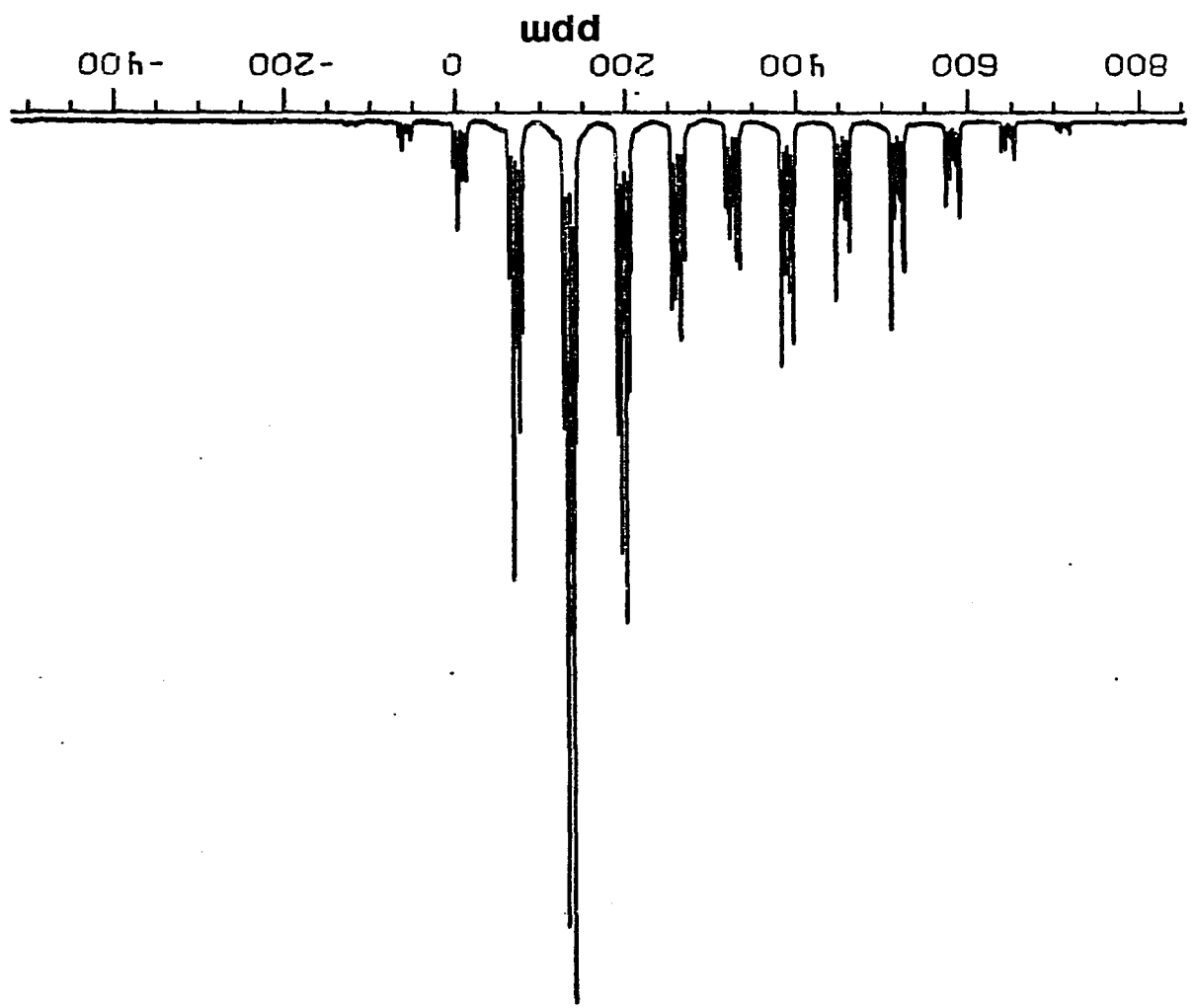


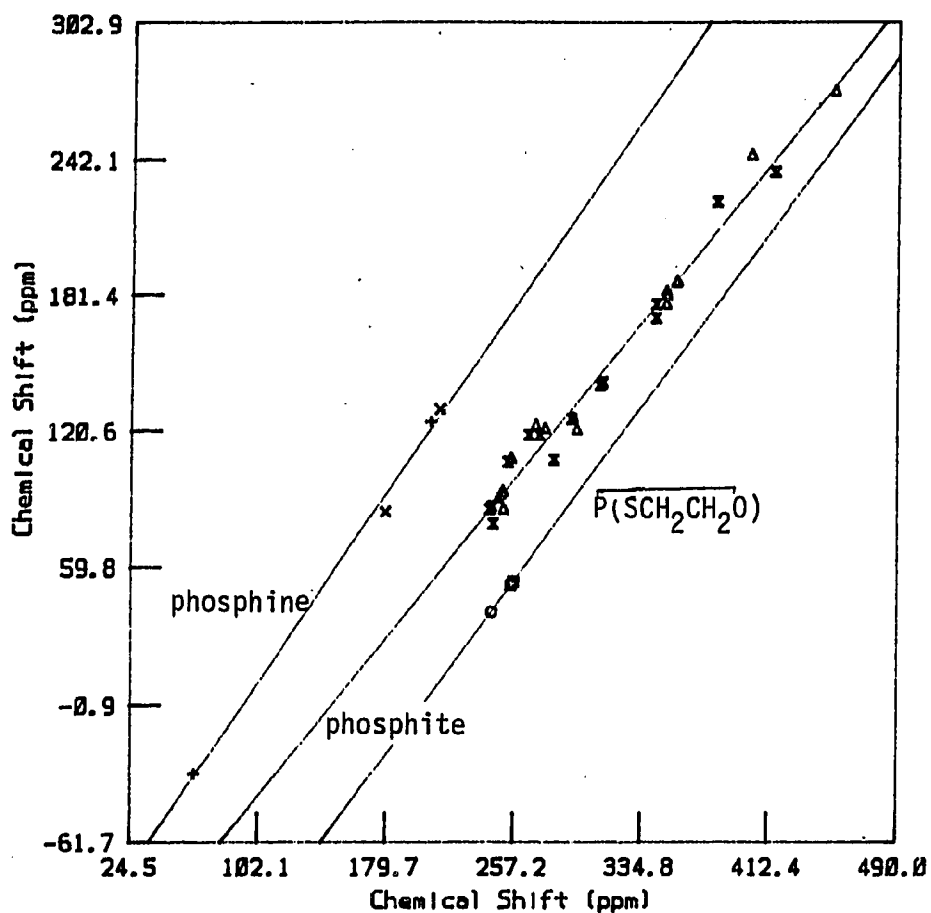
Figure 34. Solid state ^{31}P NMR of $\text{trans-}[\text{Fe}(\eta^5\text{-Cp})(\text{CO})(\mu\text{-5,5-DMP})]_2$



are based upon inequivalent or equivalent iron atoms in the solid state and were confirmed by the crystallographic studies which will be presented in Part II of this thesis.

An interesting correlation was found between the Δ ^{31}P chemical shift and the δ ^{31}P of the diiron complexes. The plot of this relationship is shown in Figure 35. As seen in this plot, three separate lines are obtained for the phosphines, the dioxo- and oxoaza- systems, and the thiooxo- systems. No anomolous deviation from the lines are observed for the cis and trans complexes of each type.

Infrared spectroscopy has proven to be a quite valuable technique in the study of these diiron complexes (101 and this work). The infrared data for these complexes are given in Table 21. A relationship was found to exist between the infrared carbonyl stretching frequencies and the ^{31}P chemical shifts as shown in Figure 36. The fit of the data points to the calculated lines is given by the R values (agreement factor) given in the figures. As can be seen, when the ^{31}P chemical shift of the complex moves to lower applied fields, the ν_{CO} stretching frequency moves to higher values. This can be rationalized in terms of the π -back bonding scheme previously mentioned (see Figure 6). As the positive charge localized on the phosphorus is increased, the phosphorus ligand will become a better π -acid with respect to the metal moiety and, therefore, it will compete more strongly with the carbonyl group for the electron density on the metal. As this electron density is less available at the metal center for π -back donation into the π^* orbitals of the carbonyl group, the effective bond order of the carbon-oxygen bond will increase,



phosphine line (4 points)

slope = 1.078; y intercept = -101.03; R = 0.998

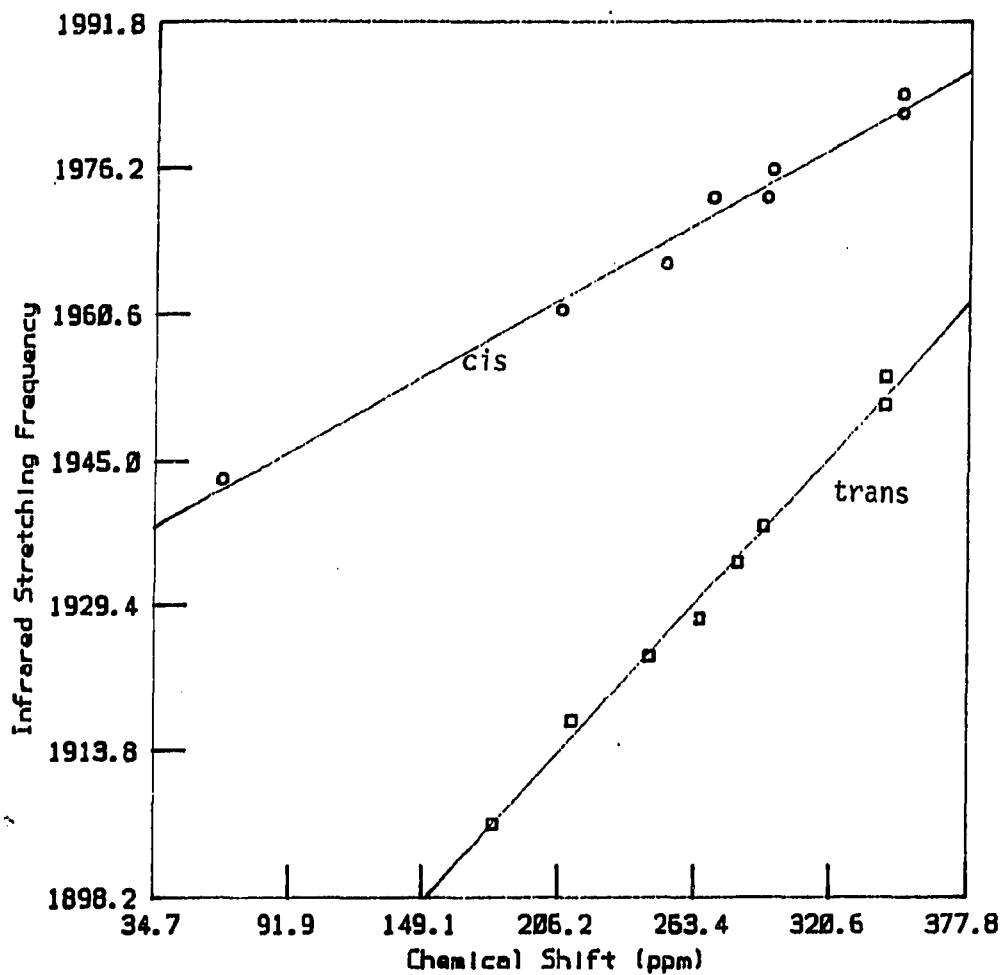
phosphite line (34 points)

slope = 0.904; y intercept = -133.61; R = 0.0990

P(SCH₂CH₂O) line (3 points)

slope = 1.000; y intercept = -202.79; R = 1.000

Figure 35. Plot of ^{31}P chemical shifts of cis and trans- $[\text{Fe}(\eta^5\text{-Cp})\text{-(CO)(L)}]_2$ complexes versus the Δ ^{31}P chemical shifts



cis line (8 points)

slope = 0.142; y intercept = 1933.00; R = 0.993

trans line (8 points)

slope = 0.280; y intercept = 1855.96; R = 0.996

Figure 36. Plot of the ³¹P chemical shifts of cis and trans-[Fe(η⁵-Cp)-(CO)(L)]₂ complexes versus the infrared carbonyl stretching frequencies

thereby raising its stretching force constant and hence the ν_{CO} stretching frequency. The phosphorus will in turn be less shielded and the observed chemical shift value will be observed further downfield. Therefore, the cationic nature of the bridging phosphorus ligand is manifested in both its NMR and infrared parameters. It would be expected, based upon literature reports of iron-phosphonium systems (30), that for these diiron systems the lability of the carbonyl group would be increased with increasing $\delta^{31\text{P}}$; however, isotopic ^{13}C O exchange studies were not carried out. This is the first report of a linear relationship between the infrared ν_{CO} and ^{31}P NMR spectroscopy. There have been reports in the literature of correlations between $\delta^{13\text{C}}(\text{CO})$ values and infrared $\nu_{(\text{CO})}$ parameters (102, 103). An increase in the stretching force constant appears to be reflected by a shielding of the carbonyl resonance and an observed shift to higher field strength. This is also in accord with the explanation presented above. For the diiron systems, two separate lines are obtained which correspond to the cis and trans complex isomers. This separation is probably due to subtle stereoelectronic effects to which the trans isomer is apparently somewhat more sensitive.

A second correlation was observed between the infrared ν_{CO} and the $\Delta^{31\text{P}}$ as shown in Figure 37. Again two lines (though with decidedly poorer correlation coefficients) are observed for the cis and trans isomers. This relationship can be rationalized in the same manner as

Table 21. Infrared data for $[\text{Fe}(\eta^5\text{-Cp})(\text{CO})\text{L}]_2$ systems

Ligand	Complex isomer	Solvent	ν_{CO} absorptions ^a	Ref.
$[\text{Fe}(\eta^5\text{-Cp})(\text{CO})_2]_2$	(trans)	CS_2	2054(w), 2005(vs) 1958(vs), 1786(vs)	101
		solid ^b	2000(sh,w), 1965(vs) 1950(vs), 1782(vs) 1770(vs)	101
PMe_2	cis	CS_2	1943 ^c	37
		— ^d	1932(vs), 1894(sh), 1888(sh), 1856(sh)	37
PMe_2	trans	CS_2	1906 ^c	37
		— ^d	1900(sh), 1888(vs), 1852(w)	37
PPh_2	cis	CS_2	1961 ^c	37
		— ^d	1953(vs), 1903(s) 1880(w), 1872(w)	37
PPh_2	trans	CS_2	1917 ^c	37
		— ^d	1912(vs), 1900(vs) 1865(w), 1856(w)	37

^a ν_{CO} given in cm^{-1} .

m moderate
sh shoulder
s sharp
vs very sharp
w weak

^bPotassium iodide pellet.

^cPeak used in Figures 36 and 37.

^dHalocarbon mull ($1300\text{--}4000 \text{ cm}^{-1}$).

Table 21 (continued)

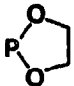
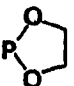
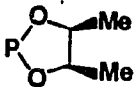
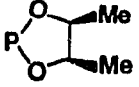
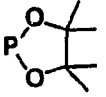
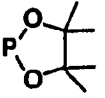
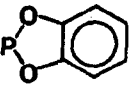
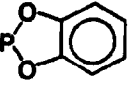
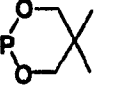
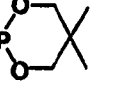
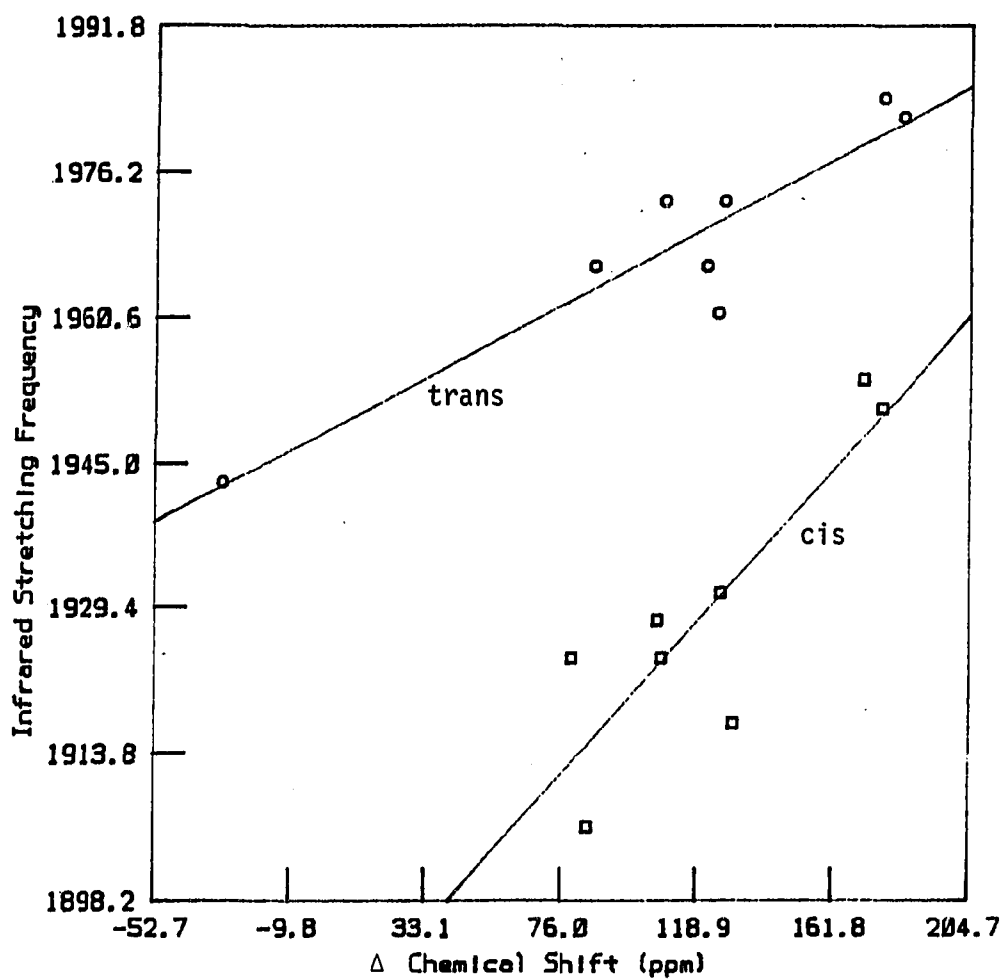
Ligand	Complex isomer	Solvent	ν_{CO} absorptions	Ref.
$\text{P}(\text{OEt})_2$	cis	CHCl_3	1966(vs) ^c , 1999(w) 1928(w)	this work
$\text{P}(\text{OEt})_2$	trans	CHCl_3	1924 ^c	this work
	cis	CHCl_3	1982(vs) ^c , 1999(sh) 1955(sh,w)	this work
	trans	CHCl_3	1951 ^c	this work
	cis	CHCl_3	1973(vs) ^b , 1937(s)	this work
	trans	CHCl_3	1938(vs) ^c	this work
	cis	CHCl_3	1976(vs) ^c , 1926(w)	this work
	trans	CHCl_3	1934(vs) ^c	this work

Table 21 (continued)

Ligand	Complex isomer	Solvent	ν_{CO} absorptions	Ref.
	cis	CHCl_3	1984(vs) ^c , 1992(sh, m) 1947(sh, m)	this work
	trans	CHCl_3	1954 ^c	this work
	cis	hexane	1973(vs) ^c , 1981(sh) 1950(m)	this work
	trans	hexane CHCl_3	1928 ^c 1928	this work

that presented for the ν_{CO} vs. $\delta^{31\text{P}}$ relationship. As the positive charge on the phosphorus increases, there is a corresponding increase in the $\Delta^{31\text{P}}$ value, and, for reasons outlined before, a shift to higher frequencies in the ν_{CO} . Again, this is the first known report of a relationship of this nature.

In the original reaction mixture of 26 with the $[\text{Fe}(\eta^5\text{-Cp})(\text{CO})_2]^-$ anion, two major products with $^{31\text{P}}$ NMR resonances at 370.19 and 220.20 ppm were observed besides the cis and trans- $[\text{Fe}(\eta^5\text{-Cp})(\text{CO})(\mu\text{-5,5-DMP})]_2$ systems. Numerous attempts to isolate these two products by a variety of techniques were performed without success, however. From $^{31\text{P}}$ NMR



cis line (8 points)

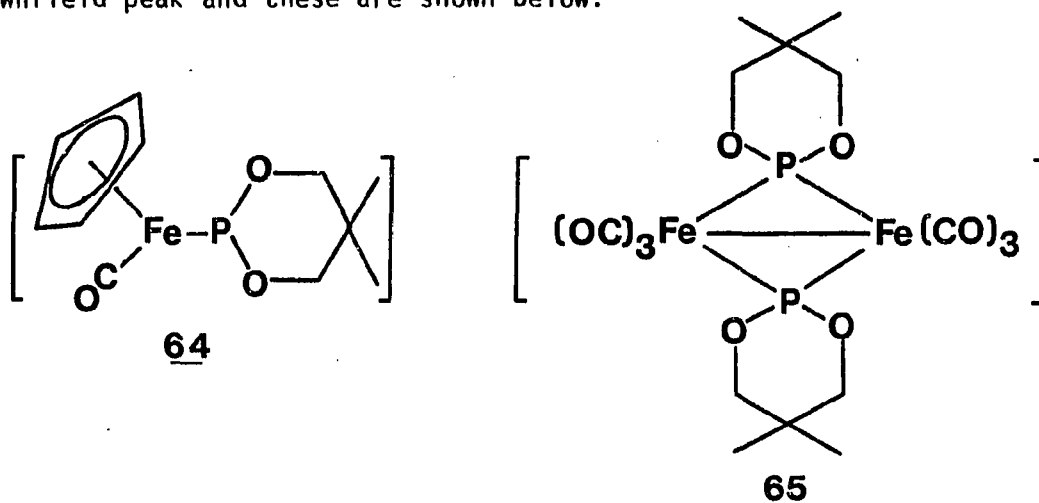
slope = 0.381; y intercept = 1882.65; R = 0.854

trans lines (8 points)

slope = 0.181; y intercept = 1942.22; R = 0.928

Figure 37. Plot of Δ ^{31}P chemical shifts of cis and trans- $[\text{Fe}(\eta^5\text{-Cp})(\text{CO})(\text{L})]_2$ complexes versus infrared stretching frequencies

experiments in which small amounts of phosphorus trichloride were added to the reaction mixture, the upfield of these two peaks was assigned to phosphorus trichloride. Two reasonable possibilities exist for the downfield peak and these are shown below:



Both are eighteen electron systems and are neutral complexes. Purification by column chromatography was not possible because this product had an R_f value indistinguishable from that of several impurities and reaction side products such as Fp_2 . In 64, the phosphorus ligand is again acting as a three electron donor, however, only to a single metal center rather than bridging two centers. This could possibly be an intermediate to the dimeric isomers. The possibility that the product is 65 is based upon a product isolated and identified from the reaction of 18 with the $[\text{Fe}(\eta^5\text{-Cp})(\text{CO})_2]^-$ anion. In this reaction, besides the cis and trans- $[\text{Fe}(\eta^5\text{-Cp})(\text{CO})(\mu\text{-}\overline{\text{P}}(\text{OC}(\text{Me})_2\text{C}(\text{Me})_2\text{O}))_2]$ isomers expected a third product was isolated. It has been shown from crystallographic studies (presented in Part III of this thesis) that in this product one

cyclopentadienyl groups has been replaced by two carbonyl ligands and the other modified to an η^4 system to yield $[\text{Fe}(\eta^4\text{-C}_5\text{H}_6)(\text{CO})-(\mu\text{-}\overline{\text{P}(\text{OC}(\text{Me})_2\text{C}(\text{Me})_2\text{O})_2}(\text{CO})_3\text{Fe})]$. The ^{31}P NMR of this compound is shown in Figure 38. Based upon this work, it appears reasonable that similar replacements might occur in the system with 26 as the reactant. The proposed structure of 65 can be eliminated, however, based upon ^{31}P chemical shift data. The synthesis of 65 from $\text{Fe}_3(\text{CO})_{12}$ and 26 has been reported previously (79) and in our work the $\delta^{31}\text{P}$ value was determined to be 305.7 ppm. Therefore, the NMR evidence points to the structure 64 as a reasonable possibility.

An interesting reaction of these cis and trans complexes was observed by ^{31}P NMR. When reacted with either water or a water-hydrochloric acid mixture (100:1 conc. $\text{HCl}:\text{H}_2\text{O}$), the proton-decoupled resonance of the original complex gradually disappeared with the appearance of an upfield and a downfield set of doublets (relative to the chemical shift of the starting complex). A stack plot of the ^{31}P spectra of the reaction of cis- $[\text{Fe}(\eta^5\text{-Cp})(\text{CO})(\mu\text{-}5,5\text{-DMP})]_2$ with water over eighteen hours is shown in Figure 39. Again numerous attempts were made to isolate these products without success. Trans isomers were found to be more stable and required a trace of acid before similar results were observed.

Figure 38. ^{31}P NMR of $[\text{Fe}(\eta^4\text{-C}_5\text{H}_6)(\text{CO})(\mu\text{-P}(\text{OC}(\text{Me})_2\text{C}(\text{Me})_2\text{O})_2(\text{OC})_3\text{Fe})]$

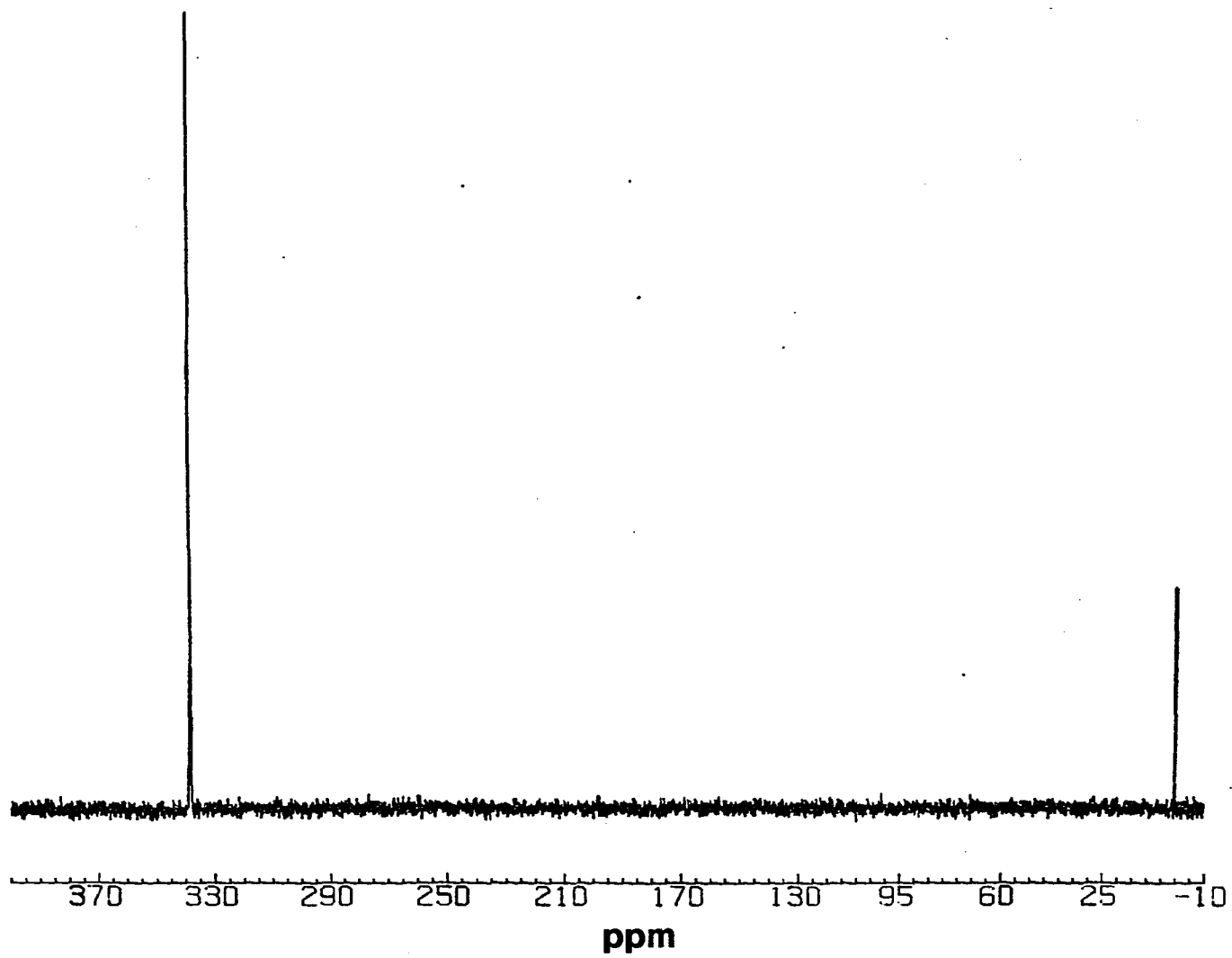
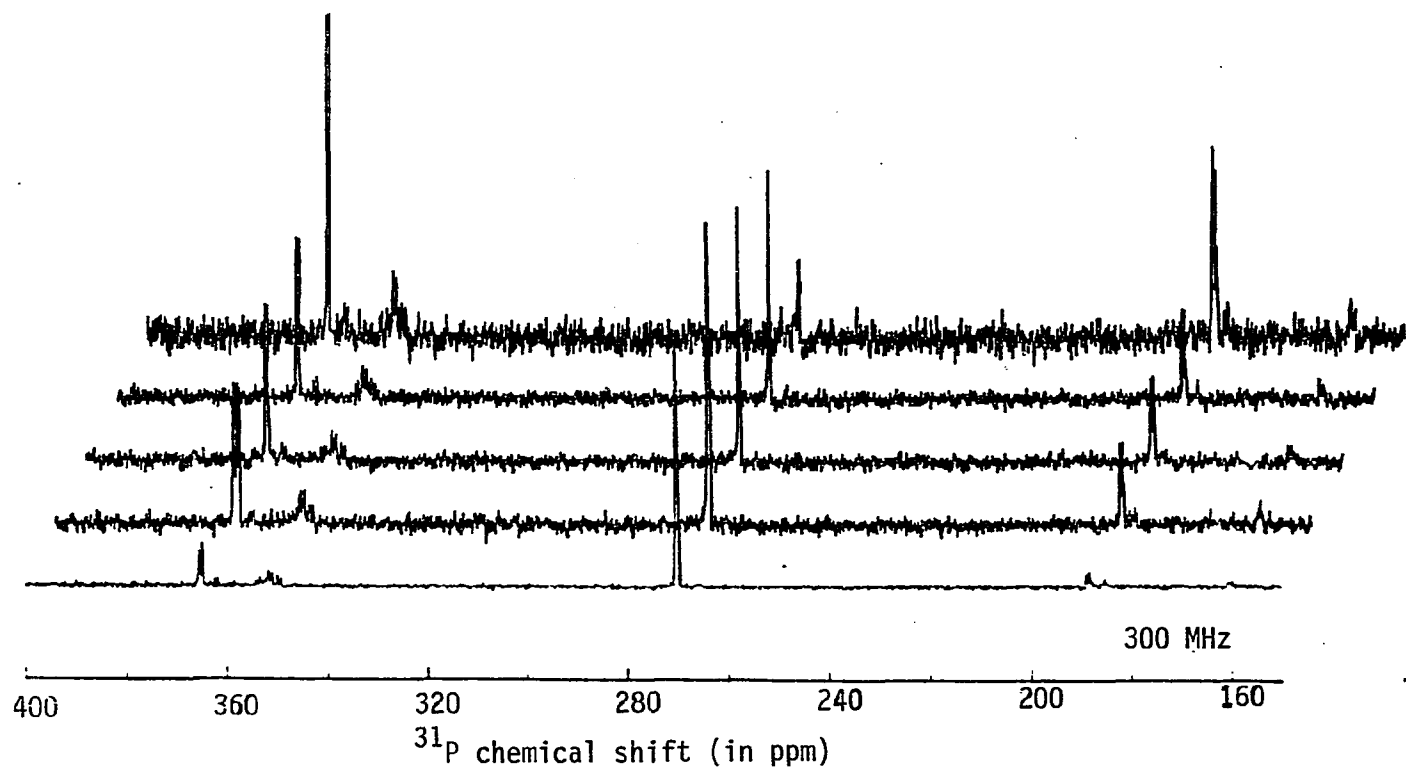


Figure 39. ^{31}P NMR stack plot of $\text{cis-}[\text{Fe}(\eta^5\text{-Cp})(\text{CO})(\mu\text{-5,5-DMP})]_2$ reacted with water over 18 hours



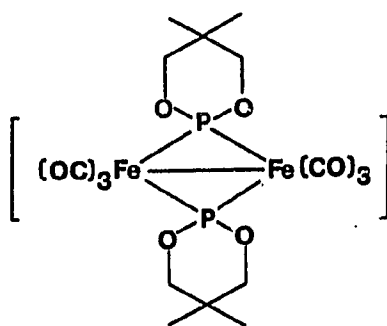
PART II.

CRYSTALLOGRAPHIC STUDIES OF THE CIS AND TRANS COMPLEXES OF
[Fe(η^5 -Cp)(CO)(μ -5,5-Dimethyl-1,3,2-dioxaphosphorinane)]₂

INTRODUCTION

In recent years there has been much interest in the chemistry of phosphorus heterocycles, especially in the phosphorinanes (92, 104). The preferred conformation of the phosphorinane ring in most of these compounds has been found to be a rigid chair on the NMR time scale. This configuration was found to persist even when the system was bonded to transition metal-carbonyl fragments, either axially (79, 105, 106) or equatorially (107). In contrast, when two identical substituents are attached to the phosphorus, such as in the case of $[\text{Me}_2\overline{\text{P}(\text{OCH}_2\text{C}(\text{Me})_2\text{CH}_2\text{O})}]^+$, the ring becomes non-rigid on the solution NMR time scale (108). In the complexes with the bridging 5,5-dimethyl-1,3,2-dioxaphosphorano group discussed in the previous chapter, the ^1H NMR spectra show these systems to be non-rigid.

A crystallographic study of the structures of the two isomeric complexes *cis* and *trans*- $[\text{Fe}(\eta^5\text{-Cp})(\text{CO})(\mu\text{-5,5-DMP})]_2$ was undertaken. First, confirmation was sought for the dimeric structure proposed on the basis of spectroscopic information presented in the previous section. Secondly, confirmation of the isomeric assignments was needed. Third, solid state ^{31}P NMR studies of these complexes had indicated important differences in the proposed Fe_2P_2 ring systems which might be elucidated by structural characterizations. Fourth, the synthesis and structural characterization of only one other example of a bridging phosphorinano moiety has been reported, namely complex 65 shown below (82, 109):



65

Furthermore, the two structures under consideration here are the first to be reported having such bridging phosphorus moieties but which do not involve a metal-metal bond. Fifth, in light of the renewed interest recently shown in dimeric complexes with bridging phosphorus units as potentially catalytically active systems (110, 111) these crystal structures are of added interest. Finally, several structural relationships based upon molecular orbital (112) and electronegativity (113) arguments have been presented for several metal-metal bonded complexes of the type $[\text{Fe}(\text{CO})_3(\mu\text{-PR}_2)]_2$. Thus, it appears that the electron withdrawing ability of substituents bonded to the phosphorus plays a very vital role in the determination of the bridging geometry exhibited by the complex. It is, therefore, of interest to discover if similar observations can be used for dioxaphosphorinano bridged systems wherein metal-metal bonding is absent.

EXPERIMENTAL

Structural Determination of $\text{cis-}[\text{Fe}(\eta^5\text{-Cp})(\text{CO})(\mu\text{-5,5-DMP})]_2$ (56)Collection and reduction of X-ray data

Single crystals of $\text{cis-}[\text{Fe}(\eta^5\text{-Cp})(\text{CO})(\mu\text{-5,5-DMP})]_2$ were recrystallized from a saturated acetone-methylene chloride solution (1:1) of the chromatographically pure cis isomer by cooling the solution to 0°C.

A rhombohedral crystal was selected for data collection (approximate dimensions 0.18 x 0.14 x 0.15 mm), sealed in a thin-walled Lindemann capillary, and mounted on a four-circle diffractometer using a standard goniometer. After centering, twelve reflections were selected from four ω -oscillation photographs, taken from various ϕ -settings, and their approximate positions were input into an automatic indexing program (114). The reduced cell and cell scalars indicated monoclinic symmetry, and subsequent ω -oscillation polaroid photographs taken around the three cell axes confirmed the 2/m Laue symmetry and the reciprocal lattice spacings predicted by the program.

A least-squares fit to the $\pm 2\theta$ values of 14 reflections, obtained immediately following data collection, provided accurate unit cell parameters and their standard deviations (Table 22). Four octants of data (hkl , $\bar{h}\bar{k}l$, $\bar{h}k\bar{l}$, $h\bar{k}\bar{l}$) were collected at room temperature on a four-circle diffractometer designed and built in the Ames Laboratory (115) using $\text{MoK}\alpha$ radiation ($\lambda = 0.70964\text{\AA}$). A total of 3745 reflections were

Table 22. Experimental crystallographic data for *cis*-[Fe(η^5 -Cp)(CO)-(μ -5,5-DMP)]₂

Molecular formula	C ₂₂ H ₃₀ Fe ₂ O ₆ P ₂
Molecular weight	564
Color	dark orange
Crystal dimensions (mm)	0.18 x 0.14 x 0.15
Crystal system	Monoclinic
Space group	C2/c
Cell dimensions	
a (Å)	15.638(4)
b (Å)	12.316(2)
c (Å)	15.407(3)
α (deg.)	90.000(0)
β (deg.)	108.51(3)
γ (deg.)	90.000(0)
Cell volume (Å ³)	2813.7(7)
Z	4
Radiation	MoK α
Wavelength (Å)	0.70964
2 θ range (degrees)	0-50°
No. unique reflections	2065
Agreement factors;	
R _F	5.8
R _{wF}	7.6

recorded and the space group C2/c was uniquely implied by the extinctions: $hk1, h + k = 2n$; $h0l, l = 2n$ ($h = 2n$); $0k0, (k = 2n)$. During data collection, the intensities of three standard reflections were remeasured every 75 reflections to monitor crystal and electronic stability and were not observed to vary significantly. Data were corrected for Lorentz-polarization effects and an absorption correction (116) applied.

The estimated variance of each intensity was calculated by Equation 10, where C_T and C_B represent the total and background counts,

$$\sigma_I = C_T + 2 C_B + (0.03 C_T)^2 + (0.03 C_B)^2 \quad (10)$$

respectively, and the factor 0.03 represents an estimate of non-statistical errors. Data reduction and averaging yielded 2065 independently observed ($I > 3 \sigma_I$) reflections with a resultant estimated R_{ave} of 0.031642.

Solution and refinement

The position of the independent iron atom was obtained from an analysis of the Patterson map. The positions of the remaining non-hydrogen atoms were determined by successive structure factor and electron density calculations. The positional and anisotropic thermal parameters for all non-hydrogen atoms were refined using a block-matrix/full-matrix least-squares procedure (117). Significant residual electron density indicated the presence of a solvent molecule in a highly

disordered state. Inclusion of a solvent molecule with partial occupancy resulted in a final $R_F = 0.058$ and weighted $R_{wF} = 0.076$. Hydrogen positions were calculated and included but not refined. The fractional atom coordinates, hydrogen fractional coordinates, anisotropic thermal parameters, and structure factors for this structure are given in Tables 23, 24, 25, and 26, respectively.

Structure Determination of $\text{trans-}[\text{Fe}(\eta^5\text{-Cp})(\text{CO})\text{-}(\mu\text{-5,5-DMP})]_2$ (56)

Collection and reduction of X-ray data

Single crystals of $\text{trans-}[\text{Fe}(\eta^5\text{-Cp})(\text{CO})(\mu\text{-5,5-DMP})]_2$ were grown from a saturated dry methylene chloride-acetone (1:2) solution of the purified trans isomer by slow evaporation of the solvent under an inert atmosphere. A suitable crystal for data collection (an irregular polyhedron, approximate dimensions 0.18 x 0.18 x 0.20 mm) was obtained by cutting a larger crystal. The crystal was sealed in a thin-walled Lindemann capillary to protect it from moisture and mounted on a four-circle diffractometer.

After centering, twelve reflections were selected from four ω -oscillation photographs taken at various ϕ -settings, and their approximate positions were input into an automatic indexing program (114). The resulting reduced cell and cell scalars indicated monoclinic symmetry. Subsequent ω -oscillation photographs, taken around the three cell axes, verified the 2/m Laue symmetry, as well as the reciprocal lattice spacings predicted by the program. Accurate unit cell parameters

Table 23. Fractional atom coordinates for $\text{cis-}[\text{Fe}(\eta^5\text{-Cp})(\text{CO})(\mu\text{-5,5-DMP})_2]$ with estimated standard deviations^a

Atom	x/a	y/b	z/c
Fe(1)	0.05579(4)	0.12239(5)	0.17081(5)
P(1)	0.07877(8)	0.09998(9)	0.31875(8)
O(1)	0.08714(32)	0.89535(34)	0.14683(31)
O(2)	0.15448(20)	0.18097(26)	0.38628(22)
O(3)	0.12051(21)	0.98263(25)	0.36130(23)
C(1)	0.07301(34)	0.98538(46)	0.15708(34)
C(2)	0.24733(32)	0.15753(42)	0.39657(36)
C(3)	0.21377(33)	0.96132(42)	0.37238(40)
C(4)	0.27591(33)	0.04604(44)	0.43750(39)
C(5)	0.37231(38)	0.02353(53)	0.43859(50)
C(6)	0.26623(42)	0.03992(49)	0.53347(41)
C(7)	0.09251(41)	0.17258(52)	0.05479(40)
C(8)	0.16246(38)	0.20026(50)	0.13751(43)
C(9)	0.12498(43)	0.27154(47)	0.18600(41)
C(10)	0.03270(41)	0.28757(42)	0.13723(41)
C(11)	0.01293(40)	0.22415(46)	0.05459(39)
C(A1) ^b	0.50000(0)	0.1322(13)	0.25000(0)
C(A2) ^b	0.56529(91)	0.1970(11)	0.32167(93)
O(A1) ^b	0.50000(0)	0.0336(18)	0.25000(0)

^aThe estimated standard deviations are given by the numbers in parenthesis, whose digits correspond to the digits of the adjacent values. This convention for specifying esd's is used throughout the tables.

^bAcetone molecule residing on a special position (C_2 axis) with an occupancy of 0.25 for the C(A1) and 0.5 for C(A2) and O(A1).

Table 24. Hydrogen fractional coordinates for $\text{cis-}[\text{Fe}(\eta^5\text{-Cp})(\text{CO})(\mu\text{-5,5-DMP})_2]$

Atom	Occupancy	x/a	y/b	z/c
H(2A)	1.0	0.2881	0.2163	0.4368
H(2B)	1.0	0.2552	0.1607	0.3292
H(3A)	1.0	0.2294	0.0342	0.4271
H(3B)	1.0	0.2055	0.0237	0.3108
H(5A)	0.5	0.4046	0.0971	0.4374
H(5B)	0.5	0.4058	-0.0211	0.4966
H(5C)	0.5	0.3707	-0.0222	0.3793
H(5D)	0.5	0.3840	-0.0612	0.4421
H(5E)	0.5	0.4166	0.0619	0.4942
H(5F)	0.5	0.3804	0.0528	0.3770
H(6A)	0.5	0.2070	0.0850	0.5333
H(6B)	0.5	0.3214	0.0713	0.5820
H(6C)	0.5	0.2548	-0.0417	0.5499
H(6D)	0.5	0.3152	-0.0085	0.5768
H(6E)	0.5	0.2672	0.1182	0.5602
H(6F)	0.5	0.2008	0.0049	0.5282
H(7)	1.0	0.0992	0.1223	0.0009
H(8)	1.0	0.2302	0.1708	0.1560
H(9)	1.0	0.1592	0.3101	0.2504
H(10)	1.0	-0.0142	0.3365	0.1592
H(11)	1.0	-0.0489	0.2181	0.0019
H(A1)	0.25	0.5407	0.2767	0.3211
H(A2)	0.25	0.5759	0.1619	0.3855
H(A3)	0.25	0.6272	0.2005	0.3071
H(A4)	0.25	0.6219	0.1494	0.3546
H(A5)	0.25	0.5354	0.2255	0.3687
H(A6)	0.25	0.5866	0.2643	0.2903

Table 25. Anisotropic thermal parameters for $\text{cis-}[\text{Fe}(\eta^5\text{-Cp})(\text{CO})(\mu\text{-5,5-DMP})]_2$

Atom	$B_{(1,1)}$	$B_{(2,2)}$	$B_{(3,3)}$	$B_{(1,2)}$	$B_{(1,3)}$	$B_{(2,3)}$
Fe(1)	2.493(33)	2.809(34)	2.890(33)	-0.257(22)	0.927(22)	0.011(23)
P(1)	2.325(50)	2.385(49)	2.775(52)	0.109(37)	0.621(39)	-0.103(37)
O(1)	6.32(25)	3.61(19)	5.66(24)	0.11(17)	1.78(19)	-1.20(16)
O(2)	2.38(13)	2.61(14)	3.62(15)	-0.01(11)	0.44(11)	-0.54(11)
O(3)	2.60(14)	2.54(13)	3.62(16)	0.12(11)	0.76(12)	0.04(12)
C(1)	3.09(21)	3.77(26)	3.05(22)	-0.33(18)	1.01(17)	-0.51(18)
C(2)	2.47(19)	3.07(21)	3.99(23)	-0.16(16)	0.67(17)	-0.96(18)
C(3)	2.33(20)	3.13(22)	4.88(27)	0.32(17)	0.25(18)	-0.82(19)
C(4)	2.29(20)	3.57(24)	4.75(28)	0.24(17)	0.37(19)	-1.00(20)
C(5)	2.72(23)	4.89(31)	7.02(37)	0.28(21)	0.43(23)	-1.76(27)
C(6)	4.61(29)	4.43(29)	4.01(27)	0.78(23)	0.48(22)	0.11(22)
C(7)	5.04(30)	4.87(28)	4.12(27)	-0.04(24)	2.63(23)	0.77(22)
C(8)	3.52(25)	5.08(30)	4.99(30)	-1.23(22)	1.68(22)	1.28(24)
C(9)	5.14(30)	3.58(25)	4.21(26)	-2.14(22)	1.08(23)	0.46(21)
C(10)	4.81(27)	2.77(21)	4.49(27)	-0.25(20)	1.83(22)	0.86(19)

C(6)	5.58(87)	6.23(96)	8.27(106)	1.91(74)	0.12(80)	0.84(82)
C(7)	9.59(118)	2.97(70)	7.72(100)	-0.47(74)	4.79(94)	-1.57(70)
C(8)	5.72(85)	4.33(81)	5.67(73)	-0.86(69)	0.37(65)	2.30(66)
C(9)	5.83(81)	4.49(66)	2.93(59)	0.99(63)	1.09(57)	0.55(55)
C(10)	4.48(76)	3.79(68)	3.89(69)	0.74(63)	1.52(61)	0.15(60)
C(11)	7.40(102)	5.70(90)	5.17(77)	1.58(78)	1.32(74)	2.26(69)
C(12)	5.61(80)	4.24(70)	6.41(88)	0.03(63)	2.48(71)	-0.19(64)
C(13)	4.65(67)	3.89(80)	7.13(91)	-1.77(63)	2.84(67)	-0.84(74)
C(14)	3.92(76)	8.56(111)	5.65(92)	-1.50(75)	1.86(70)	1.81(86)
C(15)	4.25(67)	6.18(96)	5.98(87)	-1.30(66)	2.11(64)	-1.37(74)
C(16)	2.38(57)	4.72(88)	10.05(123)	-1.16(62)	1.10(70)	2.57(91)
C(17)	3.94(69)	6.65(93)	5.11(84)	-0.18(70)	-0.03(62)	0.98(77)
C(18)	3.98(80)	4.05(98)	9.56(134)	-0.59(68)	-0.23(87)	-0.36(97)
C(19)	4.67(97)	12.3(19)	8.2(15)	-2.7(12)	2.4(10)	-4.4(15)
C(20)	5.8(11)	12.4(20)	8.8(15)	-5.6(13)	-2.63(10)	6.7(16)
C(21)	6.7(11)	3.6(10)	17.7(21)	-0.5(8)	-0.2(14)	-4.6(13)
C(22)	7.9(11)	15.5(19)	2.8(08)	-3.9(08)	0.2(8)	-2.6(12)

Table 26. Structure factor tables for $\text{cis-}[\text{Fe}(\eta^5\text{-Cp})(\text{CO})(\mu\text{-5,5-DMP})]_2$

K = -14				-6	3	128	161	-5	5	89	-78
H	L	FO	FC	-4	3	313	-307	-3	5	353	-347
-4	0	133	141	-2	3	242	-233	-1	5	210	-223
-4	1	182	197	-10	4	266	-264	-11	6	335	312
-2	2	277	257	-8	4	150	-168	-9	6	371	343
-4	3	359	-343	-6	4	274	294	-5	6	506	-500
-2	3	310	-322	-4	4	551	578	-3	6	230	-194
0	4	110	118	-2	4	525	529	-1	6	115	-75
-4	4	191	-186	0	5	92	-122	-11	7	126	-142
-2	4	140	-128	-4	5	91	96	-9	7	379	-392
-2	5	429	431	-10	6	389	366	-7	7	428	-447
K = -13				-8	6	441	414	-5	7	135	-159
H	L	FO	FC	-4	6	126	-160	-1	7	300	275
-5	1	133	121	-2	6	274	-270	-9	8	253	-249
-3	1	149	146	-8	7	150	-143	-7	8	149	186
-7	2	263	-254	-6	7	414	-424	-7	9	541	573
-5	2	315	-304	-8	8	213	-235	-5	9	435	437
-3	2	163	-168	-6	8	382	-362	-3	9	159	153
-1	2	203	194	-4	8	257	-260	-1	9	260	-251
-7	3	122	-125	-8	9	212	172	-9	10	313	-300
-5	3	366	-365	-6	9	177	148	-7	10	233	246
-3	3	558	-548	-2	9	152	-185	-5	10	379	362
-1	3	345	-357	-6	10	310	314	-3	10	380	358
-5	4	232	216	-4	10	425	429	-1	10	152	147
-3	4	251	249	-2	10	275	245	-5	11	245	-231
-1	4	320	314	K = -11				-5	12	187	-194
-7	5	94	-108	H	L	FO	FC	-3	12	198	-205
-5	5	259	241	11	-8	105	-67	K = -10			
-3	5	387	373	1	-4	117	94	H	L	FO	FC
-1	5	293	290	9	-2	82	-79	6-13	130	154	
-7	6	215	200	-9	1	608	-574	0-10	97	-73	
-5	6	153	137	-7	1	527	-537	4	-8	72	45
-3	6	107	-112	-5	1	264	-220	10	-3	106	62
-1	6	406	-402	-3	1	288	273	-12	1	128	106
-5	8	297	-319	-1	1	291	316	-10	1	418	-405
-3	8	99	-85	-7	2	268	-260	-8	1	623	-622
K = -12				-3	2	445	-428	-6	1	330	-316
H	L	FO	FC	-1	2	188	-163	-4	1	228	199
2	-7	113	-134	-9	3	230	226	-2	1	203	156
10	-2	89	-60	-7	3	374	353	-12	2	147	-131
-10	1	234	-227	-5	3	494	470	-8	2	349	312
-8	1	258	-280	-3	3	269	266	-6	2	585	598
-2	1	244	216	-1	3	91	67	-2	2	192	-196
-8	2	389	-398	-11	4	332	-343	-12	3	393	-406
-6	2	317	-323	-9	4	222	-210	-8	3	224	244
-4	2	459	-453	-7	4	118	-116	-6	3	483	470
-2	2	110	-139	-5	4	621	595	-4	3	488	527
-10	3	231	239	-3	4	578	548	-2	3	468	485
-8	3	143	167	-11	5	119	119	-12	4	125	-114
				-9	5	339	349	-10	4	131	-139

Table 26 (continued)

-8	-3	90	-103	K = 11				8	1	136	172
-4	-2	124	100	H	L	FD	FC	0	2	189	183
0	0	652	668	-5	-3	130	-95	2	2	642	624
2	0	657	692	-5	-1	87	115	4	2	391	394
4	0	526	-540	1	0	205	204	6	2	247	215
6	0	330	-307	3	0	379	-377	0	3	154	140
8	0	432	-443	5	0	314	-311	4	3	148	-148
12	0	263	262	9	0	188	177	6	3	206	-213
0	1	214	-188	11	0	197	196	8	3	163	190
2	1	873	-835	1	1	508	-523	0	4	130	135
4	1	377	-384	3	1	300	-317	2	4	181	-165
8	1	307	303	7	1	176	180	4	4	418	-435
10	1	185	206	9	1	254	241	6	4	291	-272
12	1	306	329	3	2	380	389	8	4	216	-222
0	2	510	-518	5	2	285	297	2	5	190	198
6	2	235	231	1	3	376	363	4	5	261	299
10	2	93	-84	7	3	122	151	6	5	83	30
12	2	133	-181	9	3	296	288	0	6	383	-381
0	3	305	286	1	4	271	-291	2	6	246	-248
2	3	394	374	3	4	254	-248	6	6	186	202
4	3	379	402	5	4	280	-285	0	7	278	-280
6	3	306	303	7	4	173	-198	0	8	177	184
10	3	161	-214	9	4	244	237	2	8	246	234
0	4	384	-349	1	5	462	457	4	8	301	308
2	4	365	-406	7	5	356	-372	0	9	267	276
8	4	238	242	9	5	285	-300	0	10	202	195
10	4	194	203	5	6	103	108	K = 13			
2	5	252	252	1	7	510	-547	H	L	FD	FC
4	5	259	-246	3	7	311	-328	1	0	425	-426
6	5	531	-579	7	7	237	233	5	0	169	167
8	5	452	-446	1	8	139	158	7	0	247	245
10	5	109	-132	3	8	243	232	1	1	245	239
0	6	660	665	5	8	318	316	3	1	362	348
2	6	434	442	1	9	116	119	5	1	194	196
6	6	245	-247	3	9	122	118	7	1	130	162
8	6	321	-331	3	10	267	-275	1	2	321	348
0	7	575	-570	K = 12				3	2	281	274
2	7	449	-457	H	L	FD	FC	5	2	168	191
4	7	168	-173	-4	-7	94	-99	7	2	98	-88
8	7	225	270	-2	-7	149	135	1	3	111	-135
0	8	172	-177	-2	-3	100	118	3	3	390	-392
2	8	219	-236	0	0	568	-532	5	3	478	-478
6	8	218	215	2	0	313	-296	3	4	248	-279
0	9	230	261	4	0	307	-301	5	4	103	-116
2	9	209	200	8	0	300	296	3	5	237	218
4	9	360	360	10	0	235	240	5	5	245	244
6	9	241	227	0	1	265	-284	1	6	345	-321
2	10	159	-191	2	1	108	-109				
0	11	357	354	4	1	206	223				
0	12	116	116	6	1	190	214				

Table 26 (continued)

K = 14			
H	L	FO	FC
-4	-2	80	-33
-4	-1	89	-111
0	0	413	-389
0	1	291	286
2	1	306	307
0	2	108	100
0	3	87	-20
2	3	310	-322
0	5	320	-327

and their standard deviations were obtained by a least-squares fit to the $\pm 2\theta$ values of 28 reflections obtained on a previously aligned diffractometer. Crystal data are given in Table 27.

Data were collected at $298 \text{ K} \pm 3$ using a computer-controlled Datex four-circle diffractometer equipped with a scintillation counter. Within a sphere of $2\theta \leq 50^\circ$ ($\sin \theta/\lambda = 0.595 \text{ \AA}^{-1}$), all data in the hkl , $\bar{h}\bar{k}l$, $h\bar{k}\bar{l}$, and $\bar{h}k\bar{l}$ octants were measured with $\text{MoK}\alpha$ radiation ($\lambda = .71069 \text{ \AA}$) using a 2θ - ω stepscan technique. A zirconium β -filter was used if a β -reflection could occur with $1.5^\circ\theta$ of the particular k reflection; the remaining reflections (91%) were measured without any filter.

The intensities of three standard reflections were measured every 75 reflections to monitor crystal and electronic stability and were not observed to vary significantly throughout data collection. A total of 9845 reflections were recorded and the observed extinctions $0k0$, $k = 2n + 1$ and $h0l$, $h + 1 = 2n + 1$, uniquely implied the space group $P2_1/n$.

Prior to data reduction, data collected with the β -filter were scaled to the unfiltered data using the ratio of the averaged intensities of the standard reflections, taken with and without the filter, as the scale factor. Data were corrected for Lorentz-polarization effects. No absorption correction was applied. The estimated variance of each intensity was calculated by Equation 10. Data reduction and averaging yielded 2186 independent observed ($I > 3\sigma_I$) reflections with $R_{\text{ave}} = 0.067905$.

Table 27. Experimental crystallographic data for trans-[Fe(η^5 -Cp)(CO)-
(μ -5,5-DMP)]₂

Molecular formula	C ₂₂ H ₃₀ Fe ₂ O ₆ P ₂
Molecular weight	564
Color	deep red
Crystal dimensions	0.18 x 0.18 x 0.20
Crystal system	monoclinic
Space group	P2 ₁ /n
Cell dimensions	
a (Å°)	12.497(4)
b (Å°)	13.676(2)
c (Å°)	15.093(3)
α (deg.)	90.000(0)
β (deg.)	108.59(2)
γ (deg.)	90.000(0)
Cell volume (Å ³)	2445.8(8)
Z	4
Radiation	MoK _α
Wavelength (Å)	0.71069
2θ range (degrees)	4-50
No. unique reflections	2186
Agreement factors	
R _F	8.4
R _w F	9.6

Solution and refinement

The positions of two symmetry-independent iron atoms were obtained from an analysis of a three-dimensional Patterson function. The positions of the remaining non-hydrogen atoms were determined by successive structure factor and electron density calculations. The positional and anisotropic thermal parameters for the non-hydrogen atoms were refined initially by a block-matrix and finally by a full-matrix least-squares procedure (117) yielding a final $R_F = 0.084$ and weighted $R_W F = 0.096$. Hydrogen positions were calculated and included but not refined. The fractional atom coordinates, hydrogen fractional coordinates, anisotropic thermal parameters, and structure factors for this structure are given in Tables 28, 29, 30, and 31, respectively.

Table 28. Fractional atom coordinates for trans-[Fe(η^5 -Cp)(CO)(μ -5,5-DMP)]₂ with estimated standard deviations^a

Atom	x/a	y/b	z/c	Ave. R.M.S.D. ^b
Fe(1)	0.2366(2)	0.1664(1)	0.4000(1)	0.0085
Fe(2)	0.0158(2)	0.0646(1)	0.2242(1)	0.0085
P(1)	0.0710(2)	0.2028(3)	0.2966(2)	0.0079
P(2)	0.1466(3)	0.0264(3)	0.3538(2)	0.0080
O(1)	0.1493(9)	0.1847(6)	0.5555(7)	0.0102
O(2)	0.1724(10)	0.0796(9)	0.1209(8)	0.0120
O(3)	0.9776(7)	0.2416(6)	0.3441(6)	0.0088
O(4)	0.0676(7)	0.2936(6)	0.2251(6)	0.0085
O(5)	0.2218(8)	0.9336(6)	0.3435(6)	0.0089
O(6)	0.0828(7)	0.9822(6)	0.4260(6)	0.0088
C(1)	0.1814(12)	0.1760(9)	0.4925(1)	0.0085
C(2)	0.1110(4)	0.0742(1)	0.1655(10)	0.0098
C(3)	0.9899(12)	0.3425(9)	0.3792(10)	0.0089
C(4)	0.0871(4)	0.3931(9)	0.2629(10)	0.0095
C(5)	0.9878(13)	0.4179(10)	0.3035(10)	0.0096
C(6)	0.8743(4)	0.4136(12)	0.2282(3)	0.0113
C(7)	0.0118(6)	0.5189(10)	0.3506(12)	0.0110

^aThe estimated standard deviations are given by the numbers in parenthesis, whose digits correspond to the digits of the adjacent values. This convention for specifying esds is used throughout the tables.

^bAve R.M.S.D. = Average Root Mean Square Displacement in Angstroms.

Table 28. (continued)

Atom	x/a	y/b	z/c	Ave. R.M.S.D.
C(8)	0.2884(4)	0.8826(11)	0.4278(10)	0.0102
C(9)	0.1486(12)	0.9288(10)	0.5065(9)	0.0093
C(10)	0.2097(12)	0.8432(10)	0.4813(9)	0.0086
C(11)	0.2876(14)	0.7978(12)	0.5737(10)	0.0109
C(12)	0.1254(12)	0.7687(10)	0.4242(1)	0.0098
C(13)	0.3576(12)	0.2813(1)	0.4141(12)	0.0095
C(14)	0.3301(12)	0.2388(14)	0.3240(12)	0.0103
C(15)	0.3573(12)	0.1438(12)	0.3340(11)	0.0098
C(16)	0.4040(11)	0.1215(12)	0.4315(14)	0.0100
C(17)	0.4031(12)	0.2097(13)	0.47756(11)	0.0100
C(18)	0.8518(14)	0.0910(13)	0.1512(20)	0.0106
C(19)	0.8606(17)	0.0583(24)	0.2353(20)	0.0120
C(20)	0.8959(20)	0.9691(26)	0.2454(20)	0.0134
C(21)	0.9184(17)	0.9428(15)	0.1690(28)	0.0134
C(22)	0.8832(18)	0.0234(26)	0.1075(12)	0.0130

Table 29. Hydrogen fractional coordinates for trans-[Fe(η^5 -Cp)(CO)-(μ -5,5-DMP)]₂

Atom	Occupancy	x/a	y/b	x/c	RMSD (A°)
H(3A)	1.0	0.0707	0.3495	0.4344	0.1125
H(3B)	1.0	0.9272	0.3599	0.4084	0.1125
H(4A)	1.0	0.0402	0.3759	0.3188	0.1125
H(4B)	1.0	0.0026	0.4422	0.2075	0.1125
H(6A)	0.5	0.8297	0.4801	0.2247	0.1125
H(6B)	0.5	0.8237	0.3557	0.2368	0.1125
H(6C)	0.5	0.8846	0.4043	0.1597	0.1125
H(6D)	0.5	0.8624	0.3467	0.1893	0.1125
H(6E)	0.5	0.8074	0.4223	0.2545	0.1125
H(6F)	0.5	0.8683	0.4711	0.1774	0.1125
H(7A)	0.5	0.9356	0.5511	0.3506	0.1125
H(7B)	0.5	0.0652	0.5108	0.4197	0.1125
H(7C)	0.5	0.0511	0.5637	0.3136	0.1125
H(7D)	0.5	0.0990	0.5327	0.3718	0.1125
H(7E)	0.5	0.9837	0.5200	0.4091	0.1125
H(7F)	0.5	0.9692	0.5729	0.3029	0.1125
H(8A)	1.0	0.3522	0.9293	0.4725	0.1125
H(8B)	1.0	0.3351	0.8222	0.4103	0.1125
H(9A)	1.0	0.1024	0.9144	0.5576	0.1125
H(9B)	1.0	0.1978	0.9621	0.5359	0.1125
H(11A)	0.5	0.3749	0.7998	0.5760	0.1125

Table 29 (continued)

Atom	Occupancy	x/a	y/b	z/c	RMSD (A°)
H(11B)	0.5	0.2832	0.8365	0.6331	0.1125
H(11C)	0.5	0.2682	0.7236	0.5812	0.1125
H(11D)	0.5	0.2426	0.7736	0.6176	0.1125
H(11E)	0.5	0.3494	0.8496	0.6122	0.1125
H(11F)	0.5	0.3342	0.7366	0.5604	0.1125
H(12A)	0.5	0.0409	0.7885	0.4230	0.1125
H(12B)	0.5	0.1415	0.6985	0.4529	0.1125
H(12C)	0.5	0.1240	0.7668	0.3540	0.1125
H(12D)	0.5	0.1634	0.7140	0.3968	0.1125
H(12E)	0.5	0.0804	0.7356	0.4660	0.1125
H(12F)	0.5	0.0626	0.8040	0.3671	0.1125
H(13)	1.0	0.3507	0.3440	0.4089	0.1125
H(14)	1.0	0.2751	0.2676	0.2614	0.1125
H(15)	1.0	0.3478	0.0952	0.2798	0.1125
H(16)	1.0	0.4284	0.0521	0.4727	0.1125
H(17)	1.0	0.4289	0.2187	0.5489	0.1125
H(18)	1.0	0.8227	0.1586	0.1246	0.1125
H(19)	1.0	0.8400	0.0994	0.2847	0.1125
H(20)	1.0	0.9052	0.9287	0.3020	0.1125
H(21)	1.0	0.9532	0.8793	0.1567	0.1125
H(22)	1.0	0.8846	0.0244	0.0406	0.1125

Table 30. Anisotropic thermal parameters for trans-[Fe(η^5 -Cp)(CO)(μ -5,5-DMP)]₂

	B _(1,1)	B _(2,2)	B _(3,3)	B _(1,2)	B _(1,3)	B _(2,3)
Fe(1)	3.374(87)	3.570(89)	3.446(85)	-0.168(76)	0.737(69)	-0.220(75)
Fe(2)	4.159(98)	3.779(95)	3.280(86)	-0.387(83)	0.683(75)	-0.090(77)
P(1)	3.23(16)	3.42(16)	3.41(15)	0.13(13)	0.69(13)	0.08(13)
P(2)	3.65(17)	3.20(16)	3.36(15)	-0.14(13)	0.94(13)	0.07(13)
O(1)	6.14(58)	6.52(63)	3.99(46)	1.61(49)	1.73(45)	0.31(45)
O(2)	8.95(80)	9.44(81)	6.06(67)	-1.56(67)	4.41(64)	-2.11(61)
O(3)	3.98(45)	4.01(47)	4.78(46)	-0.52(38)	1.41(39)	0.38(38)
O(4)	4.06(45)	3.52(42)	4.00(40)	0.86(37)	1.11(35)	0.55(35)
O(5)	5.09(50)	3.44(42)	4.45(46)	0.68(39)	2.10(41)	0.52(38)
O(6)	4.50(46)	4.58(47)	3.49(42)	-0.34(38)	1.49(37)	0.08(37)
C(1)	3.92(68)	2.66(61)	5.26(81)	0.61(53)	1.24(63)	0.67(59)
C(2)	6.48(87)	3.87(71)	3.54(68)	-0.92(66)	0.13(64)	-1.18(59)
C(3)	4.66(78)	3.74(58)	5.23(74)	-0.48(56)	2.58(65)	-0.71(56)
C(4)	6.21(91)	2.42(58)	6.15(85)	0.09(59)	2.49(73)	-0.01(56)
C(5)	5.48(86)	4.32(72)	5.59(80)	1.84(63)	2.14(71)	0.70(60)

C(11)	4.50(28)	3.97(25)	3.73(25)	-0.03(21)	1.47(21)	1.12(20)
C(A1)	8.73(80)	3.99(00)	5.62(69)	0.00(00)	4.42(57)	0.00(00)
C(A2)	5.74(66)	5.33(00)	5.69(66)	0.00(00)	0.15(54)	0.00(00)
O(A1)	15.55(125)	10.05(125)	10.42(125)	0.00(00)	6.99(104)	0.00(00)

Table 31. Structure factor tables for trans-[Fe(η^5 -Cp)(CO)(μ -5,5-DMP)]₂

H = -14				-5	3	280	271	-5	4	474	-453
K	L	FO	FC	-5	11	267	286	-5	12	165	-165
-1	7	217	-189	-4	4	320	-308	-4	5	223	244
0	2	204	-201	-4	5	191	184	-4	9	265	-271
0	6	231	254	-4	12	143	-132	-4	11	173	200
H = -13				-3	6	375	-366	-4	12	126	122
K	L	FO	FC	-3	8	210	205	-4	15	229	193
-6	9	137	-154	-3	10	235	245	-3	2	224	252
-4	2	328	354	-3	11	205	246	-3	3	344	-341
-1	4	279	-294	-3	13	165	-111	-3	4	245	-254
0	5	377	340	-2	1	248	266	-3	6	203	215
0	7	155	-149	-2	2	442	393	-3	7	554	532
H = -12				-2	3	322	-324	-3	11	110	-157
K	L	FO	FC	-2	4	124	90	-2	4	218	251
-8	5	155	138	-2	8	332	-346	-2	5	301	-308
-7	4	146	-177	-2	9	132	-125	-2	7	184	185
-7	7	183	177	-2	10	183	205	-2	8	490	-438
-6	6	135	-252	-1	1	253	-301	-2	10	193	189
-6	12	156	178	-1	2	155	166	-2	13	305	-272
-5	1	330	-347	-1	7	312	267	-1	8	226	-233
-5	6	276	272	-1	8	254	-255	-1	9	230	197
-4	13	192	-210	-1	12	267	-215	-1	11	114	-98
-3	11	233	227	-1	14	178	139	-1	14	310	252
-2	3	217	237	0	3	352	-325	0	0	93	-151
-2	9	268	-248	0	9	300	263	0	2	172	-150
-2	12	233	-200	0	11	117	-135	0	8	144	-149
-1	12	188	-201	9	-2	118	103	0	12	303	-255
0	2	347	367	H = -10				0	16	133	138
0	4	239	-226	K	L	FO	FC	5	-2	150	-114
0	10	322	321	-11	2	149	-176	6	-3	126	-135
8	0	128	-114	-11	6	155	-202	7	0	159	156
H = -11				-10	9	153	-136	H = -9			
K	L	FO	FC	-9	1	410	-408	K	L	FO	FC
-10	8	149	144	-9	2	132	194	-12	4	147	118
-9	7	176	-212	-9	7	190	216	-12	5	167	173
-9	8	178	171	-9	8	196	198	-11	1	248	-292
-8	1	118	-112	-8	3	330	-359	-11	7	145	166
-8	2	187	200	-8	6	321	-341	-10	1	133	-169
-8	9	192	-212	-7	2	186	242	-10	4	170	203
-7	1	181	-227	-7	7	122	188	-10	5	164	-163
-7	4	260	233	-7	11	212	236	-10	6	389	-364
-7	7	195	196	-6	6	157	140	-10	10	150	134
-7	10	185	-182	-6	7	224	200	-9	2	191	216
-7	12	153	155	-6	8	213	221	-9	4	180	236
-6	4	145	-190	-6	9	219	-206	-9	10	187	-191
-6	5	256	-249	-6	10	127	-138	-8	2	181	-200
-6	7	173	149	-6	11	132	134	-8	4	309	310
				-5	2	176	144	-8	5	426	-395
								-8	7	288	277

Table 31 (continued)

-6	3	490	-508	-1	3	304	281	-9	3	451	474
-6	4	398	-403	-1	4	1146	1084	-9	6	241	-230
-6	5	480	-481	-1	5	1053	1068	-9	7	339	362
-6	6	308	-297	-1	6	828	-821	-9	8	135	-122
-6	7	923	917	-1	7	285	319	-9	9	614	-593
-6	9	107	-133	-1	8	503	-485	-8	1	161	-168
-6	10	240	243	-1	9	497	-500	-8	2	768	740
-6	13	345	-349	-1	10	273	259	-8	3	583	-560
-5	2	231	-270	-1	11	300	-278	-8	4	941	-882
-5	3	738	-713	-1	13	163	-188	-8	6	145	160
-5	4	194	342	-1	14	223	214	-8	7	713	645
-5	5	150	-169	-1	15	318	333	-8	9	167	177
-5	6	177	-236	-1	16	219	-231	-8	11	167	-162
-5	11	260	272	0	1	104	118	-8	12	324	294
-5	12	192	223	0	5	1279	1261	-8	14	223	-163
-4	1	381	456	0	7	288	268	-7	2	959	883
-4	2	368	474	0	9	387	415	-7	3	134	98
-4	3	429	422	0	11	597	-585	-7	4	313	364
-4	4	136	133	0-15	129	-188		-7	5	489	-471
-4	6	1432	1358	4	-7	128	147	-7	6	376	-376
-4	8	612	-564	6	-7	117	-136	-7	7	284	304
-4	9	338	-335	11	-2	122	-142	-7	8	326	-316
-4	10	298	285	12	-6	144	-190	-7	9	208	226
-4	12	643	-609	13	-4	129	109	-7	11	249	237
-4	14	207	215					-7	13	144	-161
-4	15	179	189					-6	2	186	-207
-4	16	203	229					-6	3	968	-883
-3	1	321	-284	-15	3	137	-148	-6	4	141	-145
-3	2	248	-289	-15	5	196	184	-6	5	128	92
-3	3	1227	-1199	-14	1	206	-215	-6	7	153	-96
-3	4	480	-524	-14	6	198	-176	-6	8	170	-184
-3	5	136	199	-14	7	258	294	-5	1	560	571
-3	6	157	146	-13	4	264	217	-5	2	185	188
-3	8	322	311	-13	5	183	216	-5	3	584	610
-3	9	242	-276	-13	6	233	-260	-5	4	127	-138
-3	10	459	446	-13	7	198	-178	-5	5	1029	-985
-3	11	116	118	-13	9	197	174	-5	8	216	-227
-3	12	304	-322	-12	4	126	-139	-5	9	275	-296
-3	14	255	-264	-12	7	194	221	-5	10	559	561
-2	1	196	-226	-12	10	192	-200	-5	11	185	181
-2	2	265	332	-11	1	157	149	-5	12	212	-285
-2	4	529	-541	-11	5	127	-149	-5	13	234	-209
-2	5	298	259	-11	6	400	-396	-4	1	227	242
-2	7	201	-228	-11	8	466	451	-4	2	422	-423
-2	8	212	-205	-11	11	130	138	-4	3	375	388
-2	11	442	-415	-10	3	230	223	-4	4	686	-601
-2	13	483	444	-10	6	120	-99	-4	6	93	46
-2	17	136	-134	-10	9	172	-167	-4	7	170	-204
-1	1	877	907	-10	10	176	196	-4	9	382	-384
-1	2	696	-703	-10	13	249	243	-4	10	315	321
				-9	1	736	-705				

Table 31 (continued)

7	2	377	356	6	0	250	-258	7	4	162	-172	
7	3	274	-261	6	2	290	258					
7	4	221	-204	6	5	283	-270		H = 12			
7	5	248	-239	6	7	165	168	K	L	FO	FC	
7	7	142	185	7	1	159	177	-9	-8	122	-93	
8	0	414	-415	7	2	193	-221	-9	-5	153	-183	
8	1	162	166	7	6	158	177	-9	-3	145	160	
8	4	240	222	8	1	378	304	-7	-1	174	-162	
9	0	169	-269	8	4	260	-215	-6	-11	184	-176	
9	6	203	197	11	0	139	153	-6	-5	203	184	
10	1	410	371					-6	-2	196	155	
11	1	286	254		H = 11			-5	-8	172	172	
12	1	186	-165		K	L	FO	FC	-5	-7	174	145
					-10	-3	241	224	-4	-8	123	118
					-10	-1	205	-183	-3	-7	273	-237
					-9	-4	227	-216	-3	-5	205	194
					-9	-1	143	128	-3	-4	280	265
					-8	-6	139	173	-3	-2	271	-252
					-8	-3	141	169	-3	-1	133	145
					-7	-9	124	135	-2	-14	151	155
					-6	-1	178	-165	-2	-7	214	-218
					-5	-8	184	-141	-2	-5	206	-121
					-5	-7	165	132	-1	-6	129	110
					-5	-2	202	195	-1	-4	187	167
					-4	-9	130	-138	-1	-2	164	165
					-4	-1	225	-201	0	-12	140	-123
					-3	-12	197	-193	0	-8	155	-175
					-2	-5	201	179	1	0	259	235
					-2	-4	175	98	1	2	136	166
					-1	-10	200	164	1	3	188	172
					0	1	437	421	2	1	318	-295
					0	5	245	-231	3	0	296	-259
					0	-7	130	121	3	2	190	195
					1	0	135	-159	5	0	187	-185
					1	1	236	-217	6	3	253	225
					1	1	236	-217				
					1	2	305	-285				
					1	3	405	363				
					1	4	335	337				
					2	1	299	-288		H = 13		
					2	4	257	-259	K	L	FO	FC
					3	0	140	165	-6	-3	300	250
					3	2	155	173	-6	-1	173	-204
					3	3	149	156	-5	-7	227	-196
					3	6	200	-192	-5	-4	206	-174
					4	0	482	-405	-5	-1	155	141
					4	2	246	240	-4	-8	278	219
					5	0	160	-122	-4	-4	185	146
					5	5	236	-218	-3	-10	214	-164
					6	1	344	312	-2	-7	257	-211
					7	3	169	164	-2	-6	259	-186
									-2	-3	151	-136
									-2	-2	145	134

Table 31 (continued)

-1-12	168	-137
-1-11	232	-258
-1-10	166	139
-1 -7	131	111
-1 -3	137	-162
-1 -1	322	-259
0 1	248	-234
0 -3	124	137
0 -1	168	-127
1 0	216	212
1 1	121	-94
2 0	212	-230

H = 14			
K	L	FO	FC
-5	-4	176	193
-4	-3	127	-131
-3	-8	251	172
-3	-5	274	204
-2	-5	198	210
0	0	154	180

RESULTS AND DISCUSSION

The bond distances, selected non-bonding distances, bond angles, least-squares planes and the dihedral angles between these planes for the cis and trans isomers are given in Tables 32, 33, 34, 35, and 36, respectively, for the cis complex, and Tables 37, 38, 39, 40, and 41, respectively, for the trans complex. In Figures 40 and 41 are shown the computer ORTEP drawings for the cis isomer from two perspectives. Similar drawings for the trans isomer are shown in Figures 42 and 43.

The crystal structures clearly show the assignment based upon the previously presented spectroscopic data of the cis and trans dimeric isomers to be correct.

In both complexes, the iron-carbon and carbon-oxygen bond lengths and the angles of the carbonyl groups are typical of those observed for other iron-carbonyl complexes, with the Fe-C-O angles approximately linear. Also the iron-carbon distances and angles to the cyclopentadienyl groups exhibit typical values. A comparison of the known diiron complexes that have bridging phosphorus groups and have been crystallographically characterized is presented in Table 42.

In both structures, the phosphorinane ring system adopts the chair conformation. In the cis isomer, the molecule has an approximate C_2 symmetry with the axis passing through the center of the Fe_2P_2 ring system. The bridging units are tilted away from the cyclopentadienyl rings, partially in response to steric interactions between these two bulky groups. The two iron atoms are, therefore, symmetry equivalent

Table 32. Bond distances (Å°) in $\text{cis-}[\text{Fe}(\eta^5\text{-Cp})(\text{CO})(\mu\text{-5,5-DMP})]_2$ with estimated standard deviations

Fe(1)-P(1)	2.209(2)	Fe(1)'-P(1)	2.178(2)
Fe(1)-P(1)'	2.178(2)	Fe(1)''-P(1)''	2.209(2)
Fe(1)-C(1)	1.732(6)	Fe(1)-Cp(C7-C11) ^a	2.116(6)
C(1)-O(1)	1.151(7)		
5,5-dimethyl-1,3,2-dioxaphosphorinane ring system			
P(1)-O(2)	1.642(3)	C(2)-C(4)	1.518(8)
P(1)-O(3)	1.635(3)	C(3)-C(4)	1.556(8)
O(2)-C(2)	1.439(6)	C(4)-C(5)	1.528(8)
O(3)-C(3)	1.438(6)	C(4)-C(6)	1.535(8)
cyclopentadienyl ring system			
C(7)-C(8)	1.432(9)	C(10)-C(11)	1.441(8)
C(8)-C(9)	1.397(9)	C(11)-C(7)	1.396(9)
C(9)-C(10)	1.413(9)	C-C(Cp) ^a	1.416(9)

^aAverage value.

Table 33. Selected non-bonded distances (\AA) in $\text{cis-}[\text{Fe}(\eta^5\text{-Cp})(\text{CO})-(\mu\text{-5,5-DMP})]_2$

Fe(1)-Fe(1)'	3.421(2)	P(1)-P(1)'	2.691(3)
P(1)-C(1)	2.839(5)	P(1)'-C(1)	2.885(5)

Within the 5,5-dimethyl-1,3,2-dioxaphosphorinane ring system

O(2)-O(3)	2.503(4)	C(5)-C(6)	2.543(9)
C(2)-C(3)	2.476(7)	C(5)-C(2)	2.482(8)
C(2)-P(1)	2.623(5)	C(5)-C(3)	2.484(8)
C(3)-P(1)	2.636(5)	C(6)-C(2)	2.498(8)
C(2)-O(3)	2.861(6)	C(6)-C(3)	2.545(8)
C(3)-O(2)	2.890(6)	C(5)-O(2)	3.778(7)
C(4)-O(2)	2.457(6)	C(5)-O(3)	3.768(7)
C(4)-O(3)	2.466(6)	C(6)-O(2)	2.949(7)
C(4)-P(1)	3.116(5)	C(6)-O(3)	2.981(7)

Between the 5,5-dimethyl-1,3,2-dioxaphosphorinane ring system and other atoms.

C(1)-O(3)	2.949(6)	C(1)-O(3)'	2.995(6)
Fe(1)-O(2)	3.205(3)	Fe(1)''-O(2)'	3.266(3)
Fe(1)-O(3)	2.1532(3)	Fe(1)''-O(3)'	3.273(3)

Between the cyclopentadienyl ring system and other atoms ($<3.40 \text{\AA}$)

C(1)-C(7)	2.863(8)	O(2)-C(9)	3.174(7)
C(1)-C(8)	3.053(8)	O(2)-C(10)	3.122(7)
C(1)-C(11)	3.329(8)	O(2)-C(11)	3.079(7)
P(1)-C(9)	3.179(6)	P(1)-C(11)	3.159(6)
P(1)-C(10)			

Table 34. Bond angles (degrees) in *cis*-[Fe(η^5 -Cp)(CO)(μ -5,5-DMP)]₂

P(1)-Fe(1)-P(1)'	75.67(6)	Fe(1)-P(1)-Fe(1)'	102.46(6)
P(1)'-Fe(1)-C(1)	91.36(17)	P(1)-Fe(1)-C(1)'	94.41(17)
Fe(1)-C(1)-O(1)'	177.43(48)		
5,5-dimethyl-1,3,2-dioxaphosphorinane ring system			
Fe(1)-P(1)-O(2)	115.23(13)	Fe(1)-P(1)-O(3)	115.95(13)
Fe(1)'-P(1)-O(2)	113.28(13)	Fe(1)'-P(1)-O(3)	110.76(13)
P(1)-O(2)-C(2)	116.57(29)	P(1)-O(3)-C(3)	118.02(29)
O(2)-C(2)-C(4)	112.40(39)	O(3)-C(3)-C(4)	110.89(40)
C(2)-C(4)-C(3)	107.31(42)	C(5)-C(4)-C(6)	112.28(49)
C(2)-C(4)-C(5)	109.16(45)	C(3)-C(4)-C(5)	107.31(45)
C(2)-C(4)-C(6)	109.78(45)	C(3)-C(4)-C(6)	110.84(44)
O(2)-P(1)-O(3)	99.62(22)		
Cyclopentadienyl ring system			
C(1)-Fe(1)-C(7)	94.94(24)	P(1)-Fe(1)-C(7)	154.29(17)
C(1)-Fe(1)-C(8)	104.23(24)	P(1)-Fe(1)-C(8)	115.01(17)
C(1)-Fe(1)-C(9)	140.22(24)	P(1)-Fe(1)-C(9)	94.86(17)
C(1)-Fe(1)-C(10)	159.06(23)	P(1)-Fe(1)-C(10)	109.50(17)
C(1)-Fe(1)-C(11)	119.61(23)	P(1)-Fe(1)-C(11)	148.47(16)
Avg C-C-C (C7-C11)	107.99(51)		

Table 35. Least-squares planes in $\text{cis-}[\text{Fe}(\eta^5\text{-Cp})(\text{CO})(\mu\text{-5,5-DMP})]_2^a$

I.	Plane through Fe(1), Fe(1)', P(1)	$0.1359x + 0.9796y + 0.1480z = 1.851$
II.	Plane through Fe(1), Fe(1)', P(1)'	$-0.1359x + 0.9796y - 0.1480z = 1.102$
III.	Plane through Fe(1), P(1), P(1)'	$-0.1189x + 0.9872y + 0.1060z = 1.748$
IV.	Plane through Fe(1)', P(1), P(1)'	$0.1189x + 0.9873y - 0.1060z = 0.6830$
V.	Plane through P(1), O(2), O(3)	$-0.7729x + 0.0348y + 0.6336z = 3.246$
VI.	Plane through P(1)', O(2)', O(3)'	$-0.7729x - 0.0348y + 0.6336z = 3.246$
VII.	Plane through O(2), O(3), C(2), C(3)	$-0.1336x - 0.1230y + 0.9834z = 5.203$
VIII.	Plane through O(2)', O(3)', C(2)', C(3)'	$-0.1336x + 0.1230y + 0.9834z = 2.307$
IX.	Plane through P(1), P(1)', O(2), O(3), O(2)', O(3)'	$-0.7575x + 0.0000y + 0.6528z = 3.311$
X.	Plane through C(7), C(8), C(9), C(10), C(11)	$0.4112x + 0.7814y - 0.4695z = 1.761$
XI.	Plane through C(7)', C(8)', C(9)', C(10)', C(11)'	$-0.4112x + 0.7814y + 0.4695z = 6.196$

^aThe variables x, y, and z here are fractional coordinates.

Table 36. Dihedral angles between planes (degrees) in $\text{cis-}[\text{Fe}(\eta^5\text{-Cp})\text{-}(\text{CO})(\mu\text{-5,5-DMP})]_2$

I-II	23.18
III-IV	55.14
V-VI	3.98
V-VIII	43.07
VI-VII	43.07
VII-VIII	14.13
X-XI	77.23

with one iron in an axial position with respect to one of the bridging ring systems and equatorial with respect to the other. The situation in the trans isomer is quite different. There is no symmetry element located within the molecule itself, requiring each atom to be positionally unique. In this isomer, one iron is equatorial with respect to both rings, while the other iron is axial with respect to the two ring systems. This situation is represented schematically in Figure 44. This type of inequivalence of the two iron atoms in the trans complex has not been observed previously and can account for the differences observed between the two isomers in their solid state ^{31}P NMR spectra. Since the cis isomer has two equivalent irons (^{57}Fe ; $I = 1/2$), the Fe-P spin-spin splitting results in a triplet. In the trans isomer, however, the two inequivalent iron atoms lead to a substantially more complicated splitting pattern. In solution NMR studies, there must be rapid interconversion occurring within the molecule such that the irons become equivalent for both structures.

Table 37. Bond distances(A°) in trans-[Fe(η^5 -Cp)(CO)(μ -5,5-DMP)]₂ with estimated standard deviations

Fe(1)-P(1)	2.215(4)	Fe(2)-P(1)	2.183(4)
Fe(1)-P(2)	2.217(4)	Fe(2)-P(2)	2.177(4)
Fe(1)-C(1)	1.748(15)	Fe(2)-C(2)	1.699(15)
Fe(1)-Cp(C13-C17) ^a	2.111(15)	Fe(2)-Cp(C18-C22) ^a	2.053(27)
C(1)-O(1)	1.150(18)	C(2)-O(2)	1.173(19)
5,5-Dimethyl-1,3,2-dioxaphosphorinane Ring Systems			
P(1)-O(3)	1.640(9)	P(2)-O(6)	1.656(9)
P(1)-O(4)	1.640(9)	P(2)-O(5)	1.616(9)
O(3)-C(3)	1.469(15)	O(6)-C(9)	1.431(16)
O(4)-C(4)	1.465(15)	O(5)-C(8)	1.457(17)
C(3)-C(5)	1.534(20)	C(9)-C(10)	1.511(19)
C(4)-C(5)	1.586(22)	C(8)-C(10)	1.555(21)
C(5)-C(6)	1.510(23)	C(10)-C(12)	1.520(20)
C(5)-C(7)	1.538(20)	C(10)-C(11)	1.554(21)
Cyclopentadienyl Ring Systems			
C(13)-C(14)	1.417(24)	C(18)-C(19)	1.318(40)
C(14)-C(15)	1.340(26)	C(19)-C(20)	1.289(47)
C(15)-C(16)	1.433(26)	C(20)-C(21)	1.322(47)
C(16)-C(17)	1.393(25)	C(21)-C(22)	1.417(42)
C(17)-C(13)	1.361(23)	C(22)-C(18)	1.268(36)
C-C ^a (Cp)	1.389(25)	C-C ^a (Cp)	1.323(43)

^aAverage value.

Table 38. Selected non-bonded distances (Å) in trans-[Fe(η^5 -Cp)(CO)(μ -5,5-DMP)]₂

Fe(1)-Fe(2)	3.454(3)	P(1)-P(2)	2.634(5)
P(1)-C(1)	2.860(6)	P(2)-C(1)	2.859(14)
P(1)-C(2)	2.810(5)	P(2)-C(2)	2.810(14)

within the 5,5-dimethyl-1,3,2-dioxophosphorinane ring systems

O(3)-O(4)	2.506(12)	O(5)-O(6)	2.527(12)
C(3)-C(4)	2.529(21)	C(8)-C(9)	2.488(21)
C(3)-P(1)	2.653(4)	C(9)-P(2)	2.657(13)
C(4)-P(1)	2.671(13)	C(8)-P(2)	2.645(16)
C(3)-O(4)	2.870(16)	C(9)-O(5)	2.886(15)
C(4)-O(3)	2.956(17)	C(8)-O(6)	2.901(18)
C(5)-O(3)	2.502(17)	C(10)-O(6)	2.446(16)
C(5)-O(4)	2.457(17)	C(10)-O(5)	2.466(16)
C(5)-P(1)	3.133(15)	C(10)-P(2)	3.104(14)
C(6)-C(7)	2.532(24)	C(12)-C(11)	2.539(22)
C(6)-C(3)	2.475(22)	C(12)-C(9)	2.488(20)
C(6)-C(4)	2.558(23)	C(12)-C(8)	2.552(21)
C(7)-C(3)	2.481(19)	C(11)-C(9)	2.477(22)
C(7)-C(4)	2.528(21)	C(11)-C(8)	2.492(21)
C(6)-O(3)	2.970(19)	C(12)-O(6)	2.970(16)
C(6)-O(4)	2.934(19)	C(12)-O(5)	2.994(17)
C(7)-O(3)	3.814(17)	C(11)-O(6)	3.774(18)
C(7)-O(4)	3.795(17)	C(11)-O(5)	3.792(17)

Table 38 (continued)

between the 5,5-dimethyl-1,3,2-dioxaphosphorinane ring systems and other atoms

O(3)-O(6), (endo)	3.848(12)	O(4)-O(5), (exo)	3.661(12)
C(1)-O(3)	2.945(17)	C(1)-O(6)	2.961(16)
C(2)-O(4)	3.228(17)	C(2)-O(5)	3.234(17)
Fe(1)-O(3)	3.241(9)	Fe(1)-O(6)	3.267(9)
Fe(2)-O(3)	3.149(9)	Fe(2)-O(6)	3.103(9)
Fe(1)-O(4)	3.301(9)	Fe(1)-O(5)	3.285(9)
Fe(2)-O(4)	3.197(9)	Fe(2)-O(5)	3.182(9)

between the cyclopentadienyl ring systems and other atoms (< 3.40 Å°)

C(1)-C(17)	2.887(20)	C(2)-C(22)	2.787(28)
C(1)-C(13)	3.159(20)	C(2)-C(21)	3.018(27)
C(1)-C(16)	3.282(21)	C(2)-C(18)	3.185(23)
C(14)-O(4)	3.230(17)	C(19)-O(3)	3.097(37)
C(15)-O(5)	3.361(19)	C(20)-O(6)	2.977(28)
C(14)-P(1)	3.170(15)	C(19)-P(1)	3.183(26)
C(15)-P(2)	3.178(16)	C(20)-P(2)	3.138(25)

Table 39. Bond angles (degrees) in $\text{trans-[Fe}(\eta^5\text{-Cp})(\text{CO})(\mu\text{-5,5-DMP})_2]$

P(1)-Fe(1)-P(2)	72.94(14)	P(1)-Fe(2)-P(2)	74.34(14)
Fe(1)-P(1)-Fe(2)	103.49(16)	Fe(1)-P(2)-Fe(2)	103.65(16)
Fe(1)-C(1)-O(1)	177.0(13)	Fe(2)-C(2)-O(2)	176.6(14)
P(1)-Fe(1)-C(1)	91.59(48)	P(1)-Fe(2)-C(2)	91.85(50)
P(2)-Fe(1)-C(1)	91.52(44)	P(2)-Fe(2)-C(2)	92.11(52)

5,5-dimethyl-1,3,2-dioxaphosphorinane ring system

Fe(1)-P(1)-O(3)	113.60(35)	Fe(1)-P(2)-O(6)	114.28(35)
Fe(1)-P(1)-O(4)	117.20(35)	Fe(1)-P(2)-O(5)	117.15(37)
Fe(2)-P(1)-O(3)	110.10(36)	Fe(2)-P(2)-O(6)	107.33(34)
Fe(2)-P(1)-O(4)	112.87(34)	Fe(2)-P(2)-O(5)	113.25(36)
O(3)-P(1)-O(4)	99.81(47)	O(6)-P(2)-O(5)	101.13(47)
P(1)-O(3)-C(3)	117.01(79)	P(2)-O(6)-C(9)	118.55(80)
P(1)-O(4)-C(4)	118.80(78)	P(2)-O(5)-C(8)	118.70(82)
O(3)-C(3)-C(5)	112.8(11)	O(6)-C(9)-C(10)	112.4(10)
O(4)-C(4)-C(5)	107.2(11)	O(5)-C(8)-C(10)	109.8(12)
C(3)-C(5)-C(4)	108.3(11)	C(9)-C(10)-C(8)	108.4(11)
C(6)-C(5)-C(7)	112.4(13)	C(11)-C(10)-C(12)	111.3(12)

cyclopentadienyl ring systems

C(1)-Fe(1)-C(13)	108.08(62)	C(2)-Fe(2)-C(18)	117.26(92)
C(1)-Fe(1)-C(14)	145.13(66)	C(2)-Fe(2)-C(19)	154.87(96)

Table 39 (continued)

cyclopentadienyl ring systems			
C(1)-Fe(1)-C(15)	157.69(65)	C(2)-Fe(2)-C(20)	141.7(10)
C(1)-Fe(1)-C(16)	117.54(73)	C(2)-Fe(2)-C(21)	105.8(11)
C(1)-Fe(1)-C(17)	96.03(63)	C(2)-Fe(2)-C(22)	94.69(74)
P(1)-Fe(1)-C(13)	112.11(43)	P(1)-Fe(2)-C(18)	102.79(56)
P(1)-Fe(1)-C(14)	93.80(44)	P(1)-Fe(2)-C(19)	98.93(92)
P(1)-Fe(1)-C(15)	110.71(45)	P(1)-Fe(2)-C(20)	126.30(87)
P(1)-Fe(1)-C(16)	150.62(58)	P(1)-Fe(2)-C(21)	161.41(78)
P(1)-Fe(1)-C(17)	149.10(50)	P(1)-Fe(2)-C(22)	134.43(96)
P(2)-Fe(1)-C(3)	159.26(44)	P(2)-Fe(2)-C(18)	150.63(78)
P(2)-Fe(1)-C(14)	122.95(51)	P(2)-Fe(2)-C(19)	112.61(83)
P(2)-Fe(1)-C(15)	95.37(47)	P(2)-Fe(2)-C(20)	94.70(77)
P(2)-Fe(1)-C(16)	100.91(47)	P(2)-Fe(2)-C(21)	110.17(88)
P(2)-Fe(1)-C(17)	136.43(50)	P(2)-Fe(2)-C(22)	150.00(96)
Avg C-C-C (C13-C17)	108.00(147)	Avg C-C-C (C18-C22)	107.9(24)

Table 40. Least-Squares Planes in $\text{trans-}[\text{Fe}(\eta^5\text{-Cp})(\text{CO})(\mu\text{-5,5-DMP})]_2^a$

I.	Plane through Fe1, Fe2, P1	$-0.7043x - 0.2395y + 0.6683z = 2.552$
II.	Plane through Fe1, Fe2, P2	$-0.8310x + 0.2147y + 0.5132z = 2.567$
III.	Plane through Fe1, P1, P2	$-0.6730x + 0.06311y + 0.7370z = 3.666$
IV.	Plane through Fe2, P1, P2	$-0.8850x - 0.09083y + 0.4567z = 2.164$
V.	Plane through P1, O3, O4	$-0.07729x + 0.6452y + 0.7601z = 5.057$
VI.	Plane through P2, O5, O6	$0.4772x - 0.02760y + 0.8784z = 4.499$
VII.	Plane through O5, O6, C8, C9	$0.4385x + 0.8307y + 0.3429z = 12.79$
VIII.	Plane through O3, O4, C3, C4	$-0.1670x - 0.3479y + 0.9225z = 1.621$
IX.	Plane through P1, P2, O3, O4, O5, O6	$-0.04360x - 0.09722y + 0.9943z = 4.049$
X.	Plane through C13, C14, C15, C16, C17	$0.9756x + 0.2168y - 0.03626z = 3.041$
XI.	Plane through C18, C19, C20, C21, C22	$0.8672x + 0.3529y + 0.3515z = 14.62$

^aThe variables x, y, and z here are fractional coordinates.

Table 41. Dihedral angles between planes (degrees in $\text{trans-}[\text{Fe}(\eta^5\text{-Cp})(\text{CO})(\mu\text{-5,5-DMP})]_2$)

I-II	28.74
III-IV	22.12
V-VI	52.20
V-VIII	110.20
VI-VII	60.82
VII-VIII	85.31
X-XI	24.54

Figure 40. ORTEP drawing of $\text{cis-}[\text{Fe}(\eta^5\text{-Cp})(\text{CO})(\mu\text{-5,5-DMP})]_2$

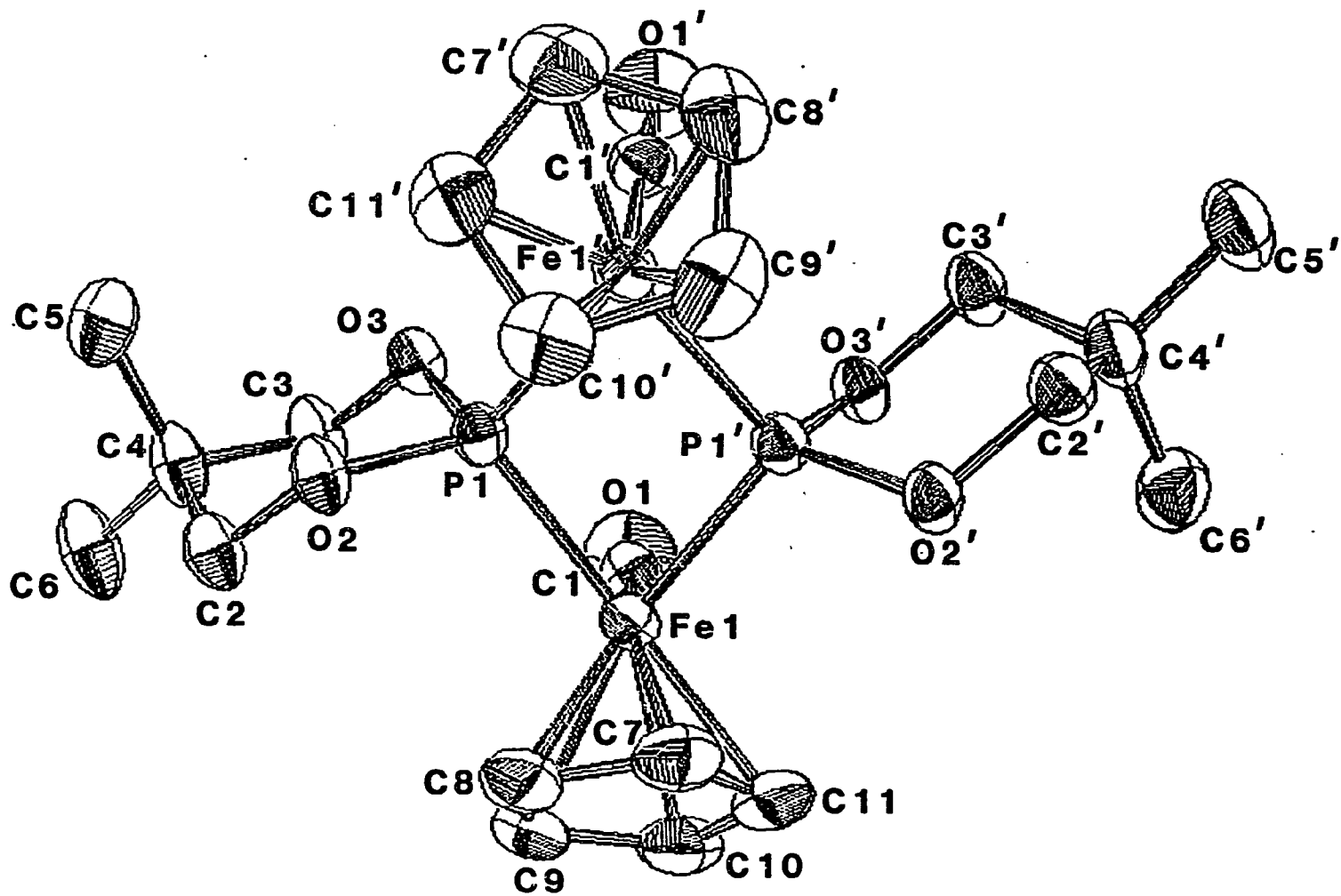


Figure 41. ORTEP drawing of $\text{cis-}[\text{Fe}(\eta^5\text{-Cp})(\text{CO})(\mu\text{-5,5-DMP})]_2$

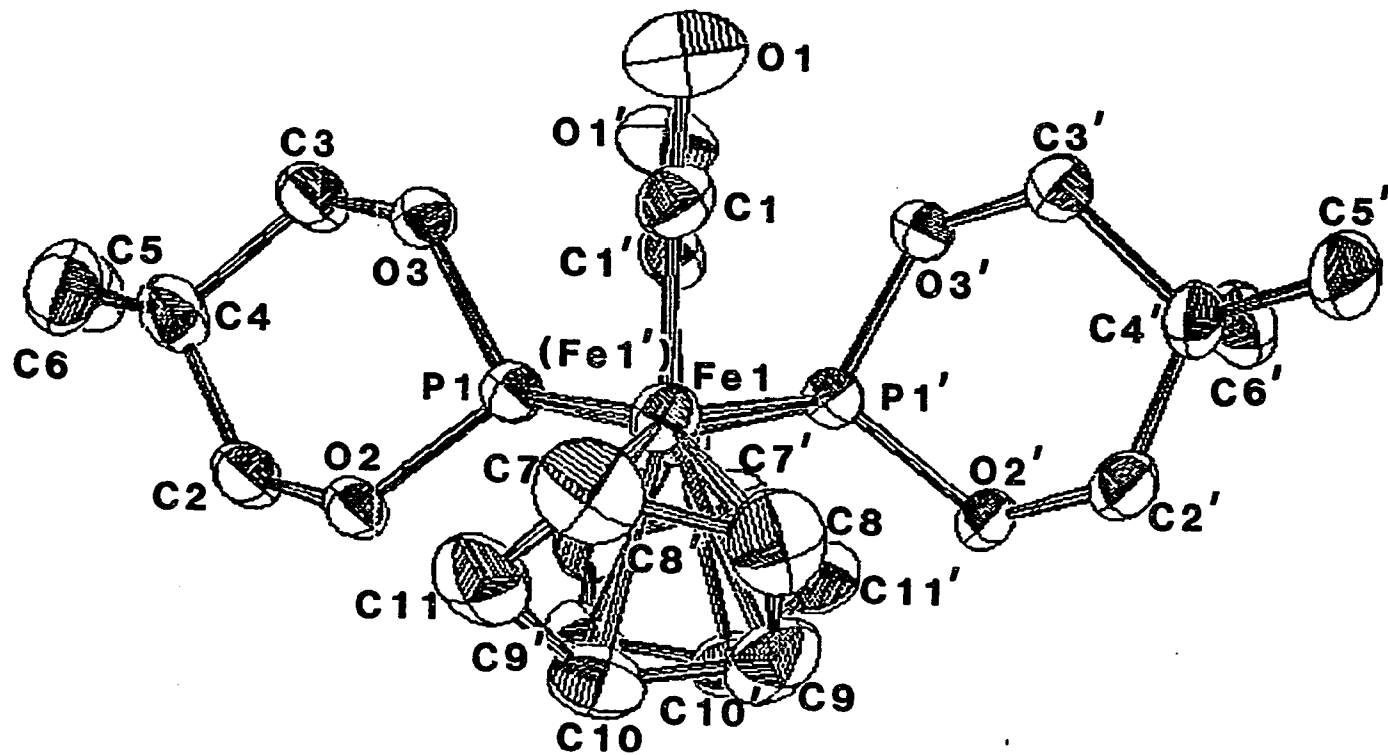


Figure 42. ORTEP drawing of trans-[Fe(η^5 -Cp)(CO)(μ -5,5-DMP)]₂

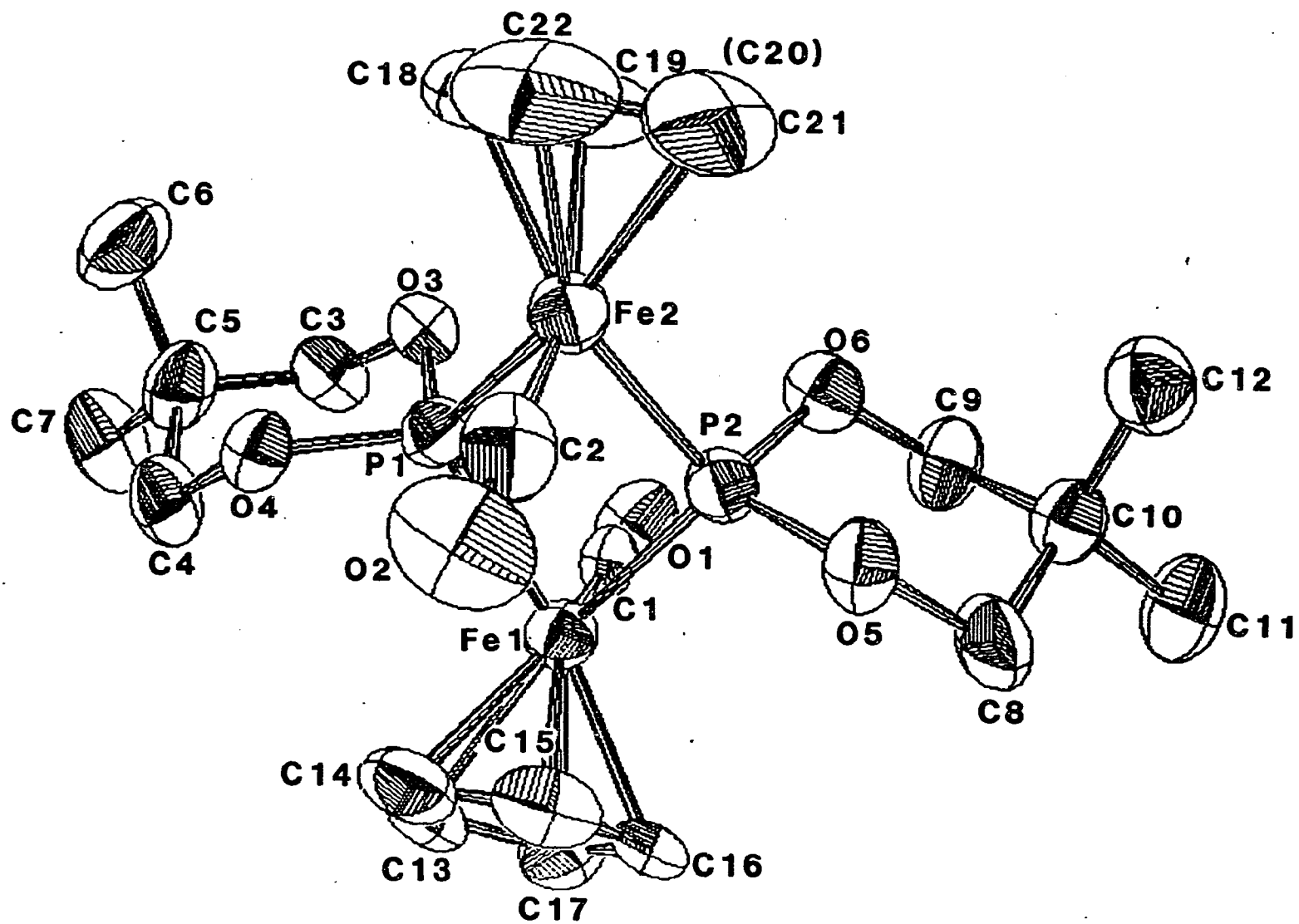


Figure 43. ORTEP drawing of $\text{trans-}[\text{Fe}(\eta^5\text{-Cp})(\text{CO})(\mu\text{-5,5-DMP})]_2$
viewing down the iron-iron axis.

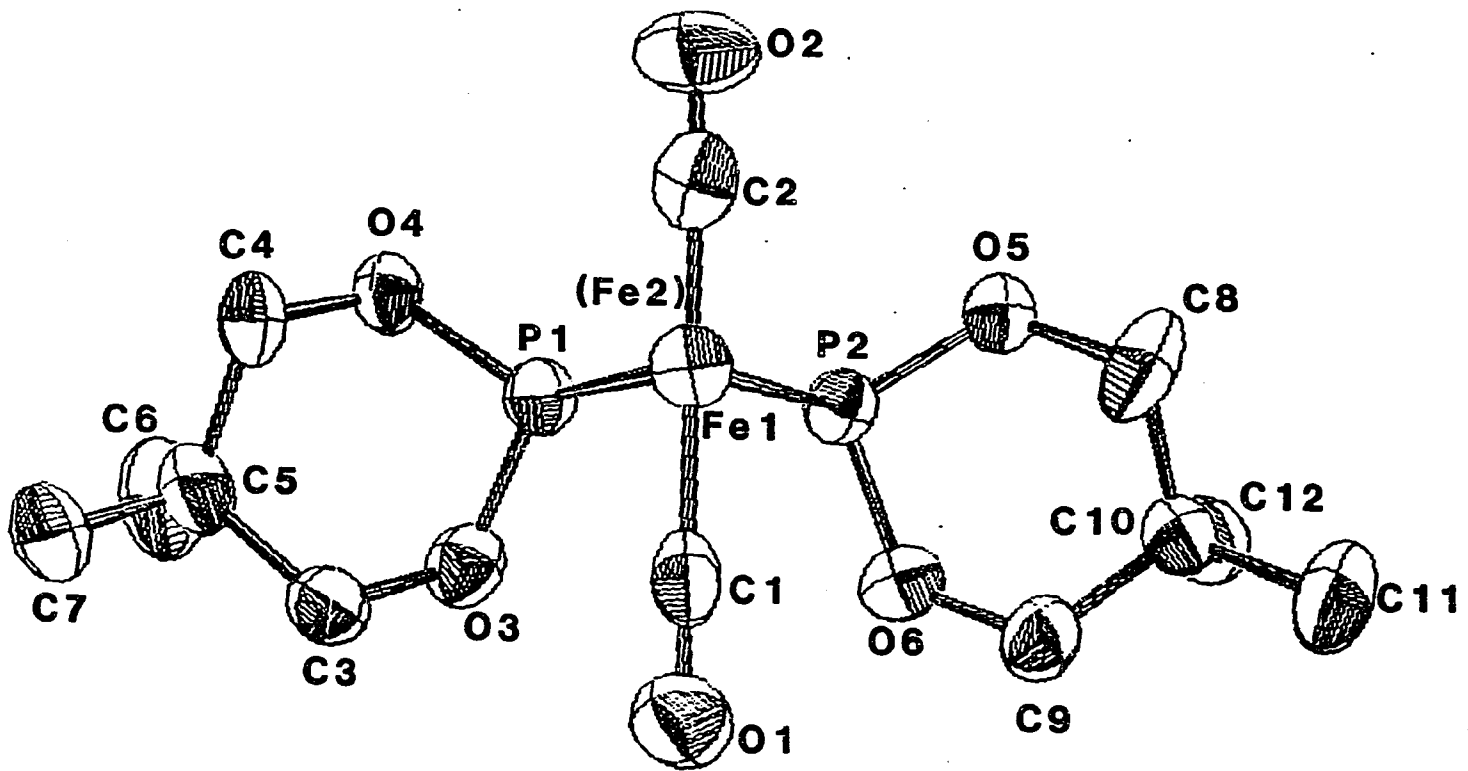


Table 42. Crystallographic and $\delta^{31}\text{P}$ data for diiron- μ -phosphorus systems

Complex	Distances			Angles			$\delta^{31}\text{P}$	B.O. ^a (M-M)	Ref.
	Fe-Fe	Fe-P	P-P	P-Fe-P	Fe-P-Fe	Flap			
$[(\text{OC})_3\text{Fe}(\text{P}(\text{CF}_3)_2)]_2$	2.819	2.193	2.921	83.5	80.0	118.9	---	1	113
$[(\text{CO})_3\text{Fe}(\text{PRR}')]_2$									
R = R' = Ph	2.623	2.233	2.866	79.9	72.0	100.0	---	1	113
R = Ph, R' = Me	2.619	2.217	2.864	80.5	72.0	101.4	---	1	113
R = Ph, R' = H	2.662	2.212	2.790	78.2	74.0	101.7	---	1	113
R = Me, R' = H	2.661	2.203	2.725	76.4	74.3	100.5	---	1	113
R = R' = Me	2.665	2.209	2.925	82.9	74.2	107.3	---	1	113
$[(\text{OC})_6\text{Fe}_2(\text{P}(\text{p-tol})_2)\text{OH}]$	2.511	2.239	2.670 (P-O)	78.4 (P-Fe-O)	68.3	75.8	---	1	113
$[(\text{OC})_3\text{Fe}(\mu\text{-5,5-DMP})]_2$	2.680	2.170	2.773	79.4	76.2	108.5	305.7	1	108, ³¹ P, this work
$\text{trans-}[\text{FeCp}(\text{CO})(\mu\text{-5,5-DMP})]_2$	3.454	2.216	2.634	73.64	103.57	151.26	265.1	0	this work
$\text{cis-}[\text{FeCp}(\text{CO})(\mu\text{-5,5-DMP})]_2$	3.421	2.194	2.691	75.67	102.5	156.85	270.1	0	this work
$[(\text{OC})_6\text{Fe}_2(\text{PPh}_2)_2]^{-2}$	3.630	2.279	2.759	74.5	105.5	180.0	---	0	117

$[\text{FeCp}(\text{CO})(\text{PPh}_2)]_2$	3.498	2.261	2.839	77.8	101.4	168.0	---	0	118-120
$[\text{FeCp}(\text{CO})(\text{PPh}_2)]_2^{+2}$	2.764	2.236	3.510	103.4	76.3	176.0(?)	---	1	120

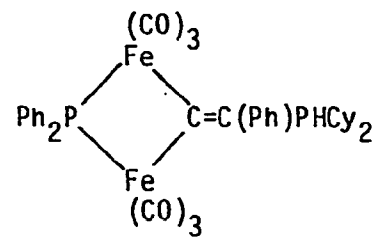
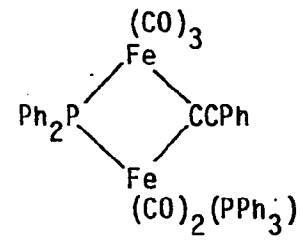
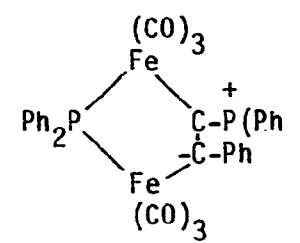
	2.576	2.249 2.216	---	77.5 (P-Fe-P)	70.5	---	154.0	1	121
--	-------	----------------	-----	------------------	------	-----	-------	---	-----

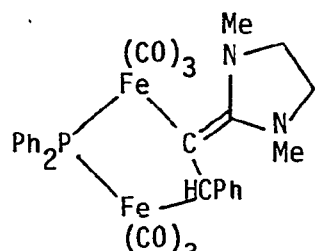
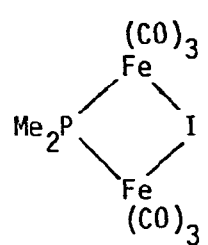
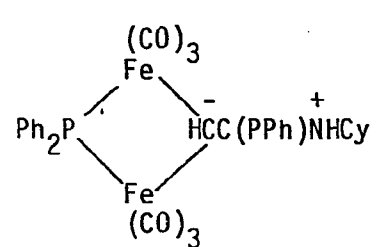
	2.628	2.233 2.214	---	82.3 89.6	72.5	---	187.9	1	121,122
--	-------	----------------	-----	--------------	------	-----	-------	---	---------

	2.548	2.211 2.224	---	---	70.1	----	153.9	1	123,124
--	-------	----------------	-----	-----	------	------	-------	---	---------

^aMetal-metal bond order.

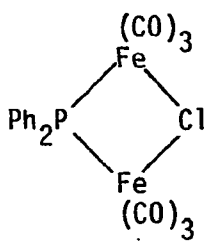
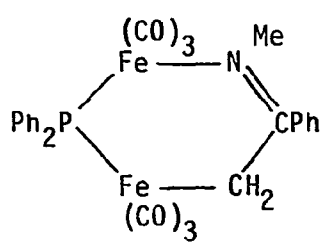
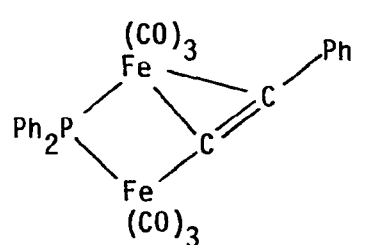
Table 42 (continued)

Complex	Distances				Angles			$\delta^{31}\text{P}$	B.O. ^a (M-M)	Ref.
	Fe-Fe	Fe-P	P-P	P-Fe-P	Fe-P-Fe	Flap				
	2.550	2.214	---	75.3	70.7	---	123.0	1	124,125	
	2.648	2.121 2.233	---	77.2 72.5	73.1	---	148.4	1	126	
	---	---	---	---	---	---	---	1	127 ^b	

	2.644	---	---	---	73.4	---	190.3	1	124
	2.588	2.216	---	83.6 83.4	71.5	105	---	1	124
	2.576	---	---	---	70.5	---	158.3	1.	122,124

^bThe communication reporting this structure did not include any of the data reported in this table.

Table 42 (continued)

Complex	Distances			Angles			$\delta^{31}\text{P}$	B.O. ^a (M-M)	Ref.
	Fe-Fe	Fe-P	P-P	P-Fe-P	Fe-P-Fe	Flap			
	2.561	2.238	---	79.4 (P-Fe-Cl)	69.8	---	142.0	1	122,124
	2.707	---	---	---	75.6	---	198.5	1	122,124
	2.597	2.213 2.224	---	---	71.64	---	---	1	128

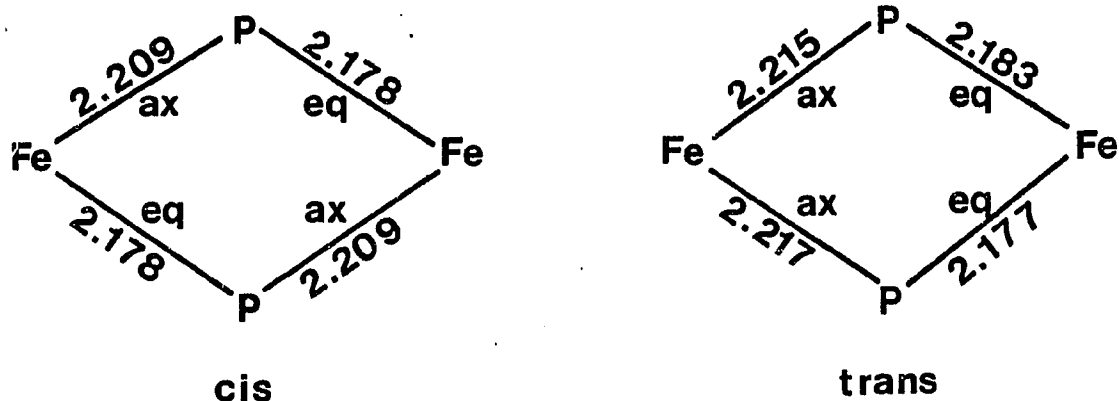


Figure 44. Iron orientations with respect to the bridging dioxaphosphorinane ring systems (eq = equatorial, ax = axial)

In metal-metal bonded diiron systems of the type $[\text{Fe}(\text{CO})_3(\mu\text{-PR}_2)]_2$, the Fe_2P_2 ring is substantially puckered compared to the coplanar configuration. This observation has been rationalized by Burdett using molecular orbital calculations (112). It was found that the observed geometry depends upon several factors, including the presence and strength of the metal-metal interaction, the type of bridging atom (phosphorus, arsenic, nitrogen, or sulfur), the electronegativity of the bridging atom substituents, and the geometry around the bridging atom. In the cis and trans complexes of 56, it appears that the most important of these factors governing the Fe_2P_2 geometry should be the electronegativity of the substituents attached to the phosphorus. This is primarily due to the very weak (formally non-bonding) interaction between the two metals. It was found that within the PX_2 unit, the more electronegative substituent has a higher "demand" for the phosphorus 3p character in the P-X bonding. This, in turn, leaves more phosphorus 3s

character for bonding to the iron atoms. This results in a smaller ϕ_1 angle and a larger ϕ_2 angle shown in Figure 45.

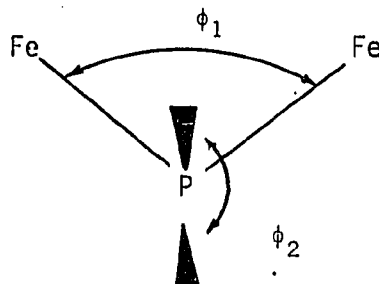


Figure 45. Angles within the Fe₂P₂ subunit

This argument also supports a shorter Fe-P distance as the electronegativity increases. In the metal-metal nonbonded system, [Fe(CO)₃(μ-PPh₂)₂]⁻², the flap angle observed was 180° (i.e., coplanarity of the four Fe₂P₂ ring atoms). It might be expected that other metal-metal nonbonded systems would have similar flap angles. In the case of the cis and trans isomers of 56, however, the flap angles are unexpectedly low (156.85° and 151.26°, respectively). This could be explained using Burdett's model with the increase in the electronegativities of the substituents on the phosphorus (relative to [Fe(η⁵-Cp)(CO)(PPh₂)₂]₂, for example (120)), resulting in the lower flap angles and smaller X-P-X angles observed for the ligand ([Ni((sec-butyl-0)P(OCH₂CMe₂CH₂O)₄)] with O-P-O angles of 101.38 and 102.55 (75), compared with cis-56 99.62, trans-56 99.81). This extension to systems containing the M(CO)_x(η⁵-Cp)⁻ fragment is quite valid since the valence orbitals of the M(CO)₃ fragment are isolobal with the orbitals on the M(CO)(η⁵-Cp)⁻

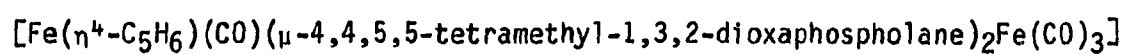
fragment. It appears that steric factors are relatively unimportant in determining the observed geometries and bond distances in these complexes. In the trans isomer of 56, which shows the greatest variation from 180°, the steric interactions of the dioxaphosphorinane ring within the complex are actually smaller than those of the cis isomer. This conclusion is further supported by the molecular orbital work of Teo et al. (129), who determined that the energy levels and orbital characteristics were relatively insensitive to the steric requirements of the substituents on the phosphorus in complexes of the type $[\text{Fe}(\text{CO})_3(\text{PX}_2)]_2$. No unusual intermolecular interactions were observed within the crystal packing of the unit cell and all intermolecular distances were greater than 4.0 Å. The unit cell drawings for these two structures are given in the appendices.

Carty has recently published several correlations between ^{31}P NMR spectral data and some structural parameters for complexes of the type $[\text{Fe}(\text{CO})_3(\text{PR}_2)]_2$ (130). In this type of complex, PR_2 units bridging nonbonding metals have ^{31}P values at a very high applied field. This can be seen in the comparison between $\text{Ru}_3(\text{CO})_9(\text{C}\equiv\text{CPr})(\text{PPh}_2)$ (metal-metal nonbonded; $\delta^{31}\text{P} = -65.4$) and $\text{Ru}_3(\text{CO})_8(\text{C}\equiv\text{CPr})(\text{PPh}_2)$ (metal-metal bonded; $\delta^{31}\text{P} = +113.0$) which shows a difference of 178.4 ppm between the $\delta^{31}\text{P}$ values. A similar trend can also be seen in the dioxaphosphorinane bridged systems between $[\text{Fe}(\eta^5\text{-Cp})(\text{CO})_{\mu-5,5}\text{-DMP}]$ (metal-metal nonbonded; $\delta^{31}\text{P} = 270.1$) and $[\text{Fe}(\text{CO})_3(\mu-5,5\text{-DMP})]_2$ (metal-metal bonded; $\delta^{31}\text{P} = 305.7$). However, the magnitude of the downfield shift (35.6 ppm) is significantly smaller. An important difference between the phosphido,

(PR₂), bridged systems and the dioxaphosphorinano-bridged systems also observed in the ³¹P NMR is that the latter usually occur greater than 200 ppm further downfield than the former. This points out that there are significant differences between the electronic environments of the phosphorus in the two types of complexes. It appears further that for PR₂ groups bridging metal-metal nonbonded systems that the δ³¹P value shifts to higher applied fields (upfield) as the M-P-M angle increases. This observation could partially explain the very large Δ values for the [Fe(η⁵-Cp)(CO)-P(O-1,3,5-tri(tert-butyl)phenyl)₂]₂ complexes compared with 56 (see Table 20 of Part I). The very bulky substituent in the case of the former complex would tend to increase the O-P-O angle which would in turn cause a concomitant decrease in the M-P-M angle (112) and result in the large downfield Δ shift. These observations show clearly that there are definite relationships between structural parameters and spectroscopic data observed for these complexes.

PART III.

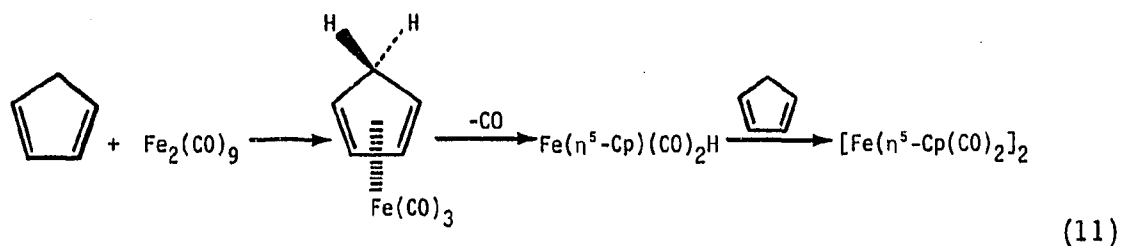
CRYSTALLOGRAPHIC STUDY OF



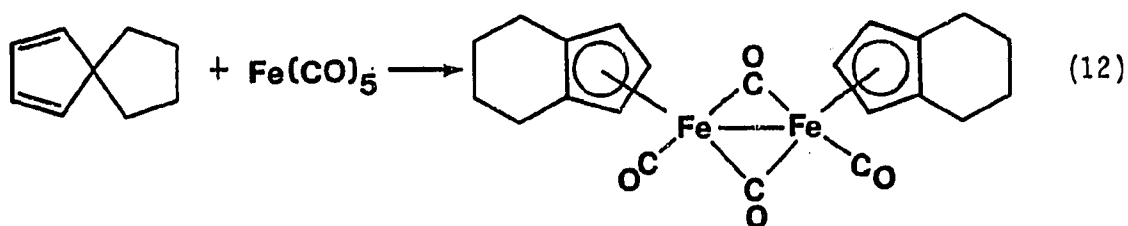
INTRODUCTION

The first organometallic compound, discovered in 1827 by the Dutch pharmacist Zeiss (131), was not understood for over a century, when it was finally identified as an olefin-transition metal complex. In the last 25 years, however, an enormous amount of work has been done with olefin-metal complexes (132). Many of these complexes have been either postulated or proven to be very important in a wide variety of catalytic and synthetic processes.

The η^5 -cyclopentadienyl ligand is one of the most common unsaturated hydrocarbon ligands encountered in organometallic chemistry. By contrast, the η^4 -cyclopentadiene ligand has received less attention, primarily due to synthetic difficulties in preparing these complexes. The iron tricarbonyl complexes of the η^4 -systems of cycloheptadiene, cyclohexadiene, and cyclobutadiene have been well characterized as thermally stable compounds; however, the corresponding η^4 -cyclopentadiene complex could not be synthesized by analogous techniques, yielding the η^5 -cyclopentadienyl dimeric complex instead (133). This reaction sequence is shown in Equation 11. This reaction

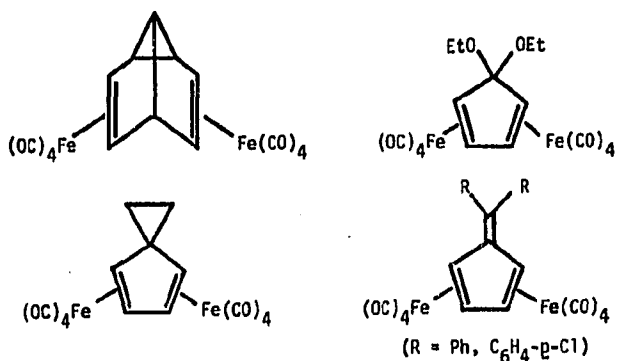


was recently shown to proceed by way of the $\eta^4\text{-C}_5\text{H}_6$ complex which quickly rearranges with loss of carbon monoxide and hydrogen to yield the $\eta^5\text{-Cp}$ dimeric system (134). The strong tendency of cyclopentadiene derivatives to produce $\eta^5\text{-Cp}$ systems when reacted with iron carbonyl compounds is illustrated in Equation 12, in which a carbon skeleton rearrangement must have occurred (135). The synthesis of $\text{Fe}(\eta^4\text{-C}_5\text{H}_6)(\text{CO})_3$ was finally



reported as having been accomplished by either the reduction of the $[\text{Fe}(\eta^5\text{-Cp})(\text{CO})_3]^+$ complex with sodium cyanoborohydride (133) or by the reaction of cyclopentadiene with $\text{Fe}_2(\text{CO})_9$ (134). It is interesting to note that the reduction of the cationic complex with sodium borohydride gives none of the $\eta^4\text{-C}_5\text{H}_6$ complex but is reported to lead only to mixtures of the hydride and the dimeric complexes (see Equation 11). A variety of other $\eta^4\text{-C}_5\text{H}_6$ complexes have been previously reported and are given in Table 43 along with representative examples of the analogous fulvine, cyclopentadienone, and butadiene complexes. There are two types of structures most commonly encountered with the $\eta^4\text{-C}_5\text{H}_6$ systems. First, the ligand can serve as a bridge between two metal centers by two

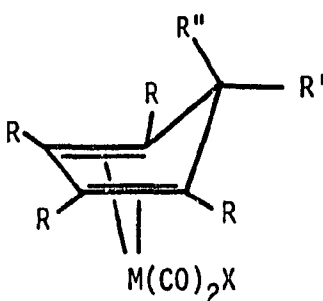
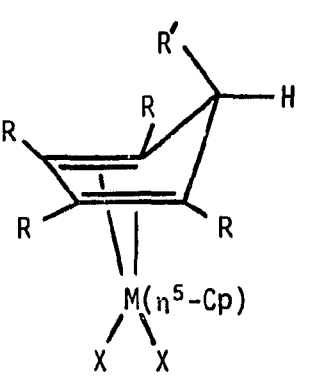
electron donation to each metal. This is directly analogous to a variety of bridging butadiene complexes (136, 137). Examples of this type of cyclopentadiene bonding are illustrated below (138-141). The second mode



of bonding, in which the cyclopentadiene ligand is bound to only one metal as a four electron donor, is by far more common. Examples of this type of complex are given in detail in Table 43.

As discussed in Part I of this thesis, the reaction of chloro-phosphorus(III) compounds with the Fp^- anion yields the cis and trans- $[Fe(\eta^5-Cp)(CO)(P \quad)]_2$ isomers as the major products. An interesting and unique third product was isolated from the reaction of 18 with the Fp^- anion and is the subject of this chapter. An X-ray crystallographic study of this complex was undertaken for several important reasons, first of all to confirm the composition of the product as an $\eta^4-C_5H_6$ system of the type $[Fe(\eta^4-C_5H_6)(CO)(P(OC(Me)_2C(Me)_2O))_2Fe(CO)_3]$, proposed on the basis of spectroscopic information. Secondly, there appears to be no structural data for unsubstituted $\eta^4-C_5H_6$ complexes. Finally, it should be informative to compare this structure with those reported in Part II of this thesis which also contain bridging $P(OR)_2$ units but in systems

Table 43a. η^4 -complexes

Compound	Substituents	Ref.
a. Cyclopentadiene complexes		
	X=CO; R=H; R'=R''=H; M=Fe	133,134,142
	X=CO; R=H; R'=H, R''=CH ₂ Ph; M=Fe ^a	143
	X=CO; R=H; R'=CH ₃ , CH ₂ OH	
	R''=CH ₃ , CH ₂ OH, CO ₂ Et, CH ₂ OCH ₃ ; M=Fe	144
	X=CO; R=Ph; R'=R''=H; M=Fe	145
	X=PPh ₃ ; R=R'=R''=H; M=Fe	133
	X=CO; R=H; R'=H; R''=H, Me, Pr,	
	Ph, <i>t</i> -Bu, C ₆ H ₄ - <i>p</i> -Et; M=Ru, Os	146
	X=CO; R=R'=R''=H; M=Ru	147
	X=CO; R=H; R'=Ph; M=V (unstable)	148
	X=CH ₃ ; R=H; R'=CH ₃ ; M=Re ^a	149,150,151
	X= --; R=H; R'=H; M=Co	152,153
	X= --; R=H; R'=Me; M=Co	150
	X= --; R=H; R'=CF ₃ ; M=Co	150
	X= --; R=H; R'=CCl ₃ ; M=Co	154
	X= --; R=H; R'=CH ₂ Y; M=Co	155
	X= --; R=H; R'=Ph; M=Co ^a	156,157
	X= --; R=H; R'=CO ₂ Me; M=Co ^a	158
	X= --; R=H; R'=CY ₂ COZ; Y=H,Cl	
	Z=OMe, Ph; M=Co (unstable)	159
X= --; R=H; R'=COPh; M=Co ^a	160,161	

^aStudied crystallographically.

Table 43a (continued)

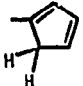
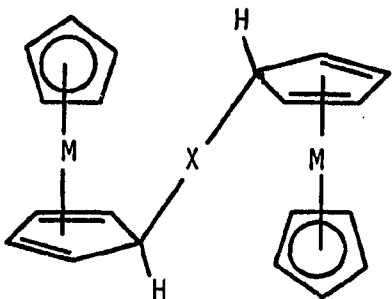
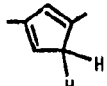
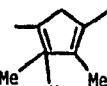
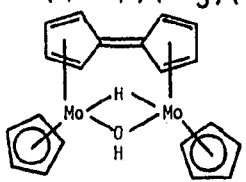
Compound	Substituents	Ref.
	X= --; R=H; R'=H; Rh	154,152,153,162
	X= --; R=Me; R'=Me (endo & exo); M=Rh, Ir	162
	X= --; R=H; R'=H; M=Ir	153
	X= --; R=H; R' =  ; M=Rh	163
	X=CF ₂ CF ₂ ; M=Co	164
	X =  ; M=Co	165,145
	X =  ; M=Co	165
	X= --; M=Rh	166
Fe(PF ₃) ₃ (η ⁴ -C ₅ H ₆)	---	167
PtCl ₂ (η ⁴ -Me ₅ C ₅ H)	---	168
Mo(η ⁵ -Cp)(CF ₃)(η ⁴ -(CF ₃) ₄ C ₅ NBu)	--- ^a	169
	--- ^a	170

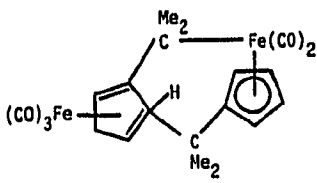
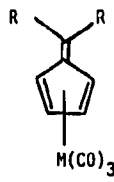
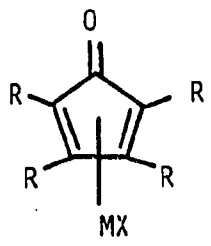
Table 43a(continued)

Compound	Substituents	Ref.
	---a	171
b. Selected butadiene complexes		
	---a	172
	---a	173
	---a	174
	---a	175

Table 43a (continued)

Compound	Substituents				Ref.
	R ₁	R ₂	R ₃	R ₄	
	H	H	H	H	154
	CH ₃	H	H	H	176
	H	CH ₃	H	H	176
	C ₆ H ₅	H	H	H	177
	C ₆ H ₅	H	H	C ₆ H ₅	177,178
	CH ₃	H	H	CO ₂ C ₂ H ₅	176
	CH ₃	H	H	CO ₂ H	179
	CH ₃	H	H	CONH ₂	180
	CH ₃	H	H	COCH ₃	176
	CH ₃	H	H	CN	176
	CH ₃	H	H	CHO	176
	CH ₃	H	H	CH ₂ OH	181
	H	H	H	CH ₂ OH	181
	C ₆ H ₅	H	H	C ₆ H ₅ -Cr(CO) ₃	177,178
	H	H	H	C ₆ H ₅ -Cr(CO) ₃	177
	C ₆ H ₅ -Cr(CO) ₃	H	H	C ₆ H ₅ -Cr(CO) ₃	177
	H	C ₅ H ₄ Mn(CO) ₂	C ₅ H ₄ Mn(CO) ₃	H	177
	C ₆ H ₅	C ₆ H ₅	C ₆ H ₅	C ₆ H ₅	154

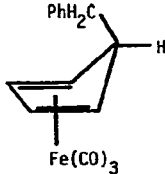
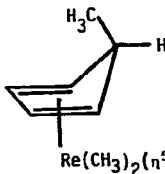
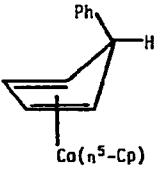
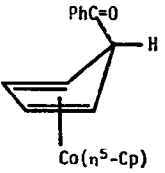
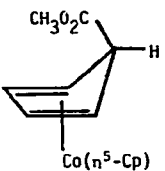
Table 43a (continued)

Compound	Substituents	Ref.
	<p>-----a</p>	182
c. η^4-Fulvene complexes		
	<p>R=Ph; M=Cr R=Ph; M=Fe R=C₆H₄-p-Cl; M=Fe R=C₆H₁₀; M=Fe</p>	<p>145 183,141 183,141 183,141</p>
d. Iron and selected cobalt η^4-cyclopentadienone complexes^b		
	<p>X=(CO)₃; R=H; M=Fe X=(CO)₃; R=CH₃; M=Fe X=(CO)₃; R=CF₃; M=Fe^a X=(CO)₂(PPh₃); R=H; M=Fe X=(CO)₃; R=C₆H₄-p-Y; M=Fe X=η^5-Cp; R=H; M=Co X=η^5-Cp; R=CH₃; M=Co^a X=η^5-Cp; R=CF₃; M=Co^a</p>	<p>184 185 186,142 145 185 154 187 188</p>

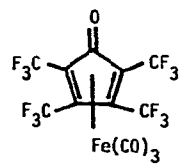
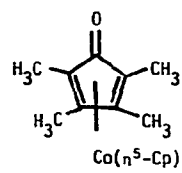
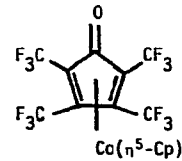
^bFor complexes of other metals in this class, see references 145, 191, and 192.

Table 43b. Selected crystallographic parameters of η^4 -complexes

II. Selected crystallographic parameters of η^4 -complexes

Complex	Ring system dihedral angle	Ring system					Ref.
		1	2	3	4	5	
 $\text{Fe}(\text{CO})_3$	34.7 ^a	1.425(7)	1.414(8)	1.427(7)	1.513(8)	1.527(7)	143
 $\text{Re}(\text{CH}_3)_2(\eta^5\text{-Cp})$	40.7	1.419(8)	1.417(9)	1.412(8)	1.516(8)	1.526(7)	
 $\text{Co}(\eta^5\text{-Cp})$	36.5	1.538(30)	1.359(30)	1.491(29)	1.532(26)	1.506(26)	157
 $\text{Co}(\eta^5\text{-Cp})$	37	---	---	---	---	---	161
 $\text{Co}(\eta^5\text{-Cp})$	32	1.468(26)	1.412(33)	1.453(29)	1.457(23)	1.537(18)	158

b. Iron and selected cobalt η^4 -cyclopentadiene complexes

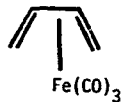
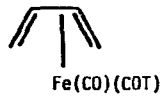
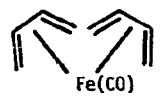
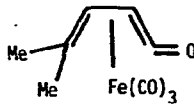
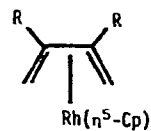
	16.2	1.416(33)	1.395(24)	1.365(24)	1.460(40)	1.504(30)	189,186
	9	--- ^d	---	---	---	---	187
	21.3	1.403(27)	1.439(27)	1.494(27)	1.500(28)	1.494(28)	189,188

^aTwo crystallographically independent molecules.

^bNo data given.

Table 43b (continued)

c. Selected butadiene complexes

	---	1.46(5)	1.45(6)	1.446(5)	---	---	172
	---	1.397(7)	1.429(14)	1.397(7)	---	---	173
	---	1.43(2)	1.46(1)	1.43(2)	---	---	174
	---	1.416(8)	1.407(8)	1.442(9)	---	---	175
							
R=Cl	---	1.43(2)	1.44(2)	1.41(2)	---	---	190
R=Me	---	1.45(2)	1.45(2)	1.42(2)	---	---	190

without metal-metal bonding. Based upon the 18 electron rule, the proposed structure for $[\text{Fe}(\eta^4\text{-C}_5\text{H}_6)(\text{CO})(\overline{\text{P}(\text{OC}(\text{Me})_2\text{C}(\text{Me})_2\text{O}))}_2\text{Fe}(\text{CO})_3]$ is expected to contain a metal-metal bond which should significantly affect the observed geometry of the complex.

This is the first report of the synthesis and structural characterization of a dimeric $\eta^4\text{-C}_5\text{H}_6$ complex in which the $\eta^4\text{-C}_5\text{H}_6$ moiety is in a terminal position. Finally, it is only the second structure reported of a diiron complex containing both bridging $\text{P}(\text{OR})_2$ groups and a metal-metal bond and it is the first such system involving the 1,3,2-dioxaphospholane ring (109).

EXPERIMENTAL

Synthesis of $[\text{Fe}(\eta^4\text{-C}_5\text{H}_6)(\text{CO})(\mu\text{-P}(\text{OC}(\text{Me})_2\text{C}(\text{Me})_2\text{O}))_2\text{Fe}(\text{CO})_3]$

This complex was prepared as a by-product from the reaction of the Fp^- anion with the chlorophosphorane 18 to form the cis and trans 49 isomers. The procedure used for its preparation, isolation, and purification is described in detail below.

In a flame-dried 250 mL round bottom flask and under an inert nitrogen atmosphere, 5.000 grams (14.12 mmol) of the dimeric Fp complex was converted to the Fp^- anion (28.25 mmol) by reaction with 1.05 grams of sodium and 15 mL of triply distilled mercury in 100 mL of dry THF. After one hour at room temperature with constant stirring, the reaction mixture was cooled to 0°C and 5.159 grams (28.25 mmol) of 18 added rapidly with a syringe. Carbon monoxide evolution was observed immediately upon the addition. The reaction was then allowed to warm slowly to room temperature and to stir for an additional 12 hours. The THF was removed in vacuo and the residue redissolved in 50 mL of chloroform and chromatographed on a 2.5 x 25 cm alumina column utilizing a nitrogen pressure to facilitate flow through the column. All the mobile components were collected as a single fraction. The methylene chloride was then removed in vacuo and the material redissolved in a minimum of benzene. This was chromatographed on a 2.5 x 50 cm. alumina column and eluted with benzene. The $[\text{Fe}(\eta^4\text{-C}_5\text{H}_6)(\text{CO})(\text{L})_2\text{Fe}(\text{CO})_3]$ complex traveled very close to the solvent front as a yellowish-orange band. R_f values for the reaction products are given in Table 44. The complex was

Table 44. R_f values for the reaction products of the Fp^- anion with 18

Complex	R_f^a (benzene)
$[Fe(\eta^4-C_5H_6)(CO)(\overline{P(OC(Me)_2C(Me)_2O)})_2Fe(CO)_3]$	0.99
trans- <u>49</u>	0.94
cis- <u>49</u>	0.87

^a R_f measured on TLC strips.

obtained as a yellowish-orange microcrystalline, air stable solid in approximately 5% overall yield upon removal of the solvent. Final purification was accomplished by recrystallization from a 1:1 mixture of benzene/methylene chloride (CIMS; 584 (M^+ , rel. int. = 0.01%), 583 (M^+-H , rel. int. = 0.27%), 582 (M^+-2H , rel. int. = 0.16%), 147 ($+\overline{P(OC(Me)_2C(Me)_2O)}$), rel. int. = 14.62), 79 (base peak): ir ν_{CO} (± 2 cm^{-1} , $CDCl_3$); 2022(s)₂, 1994(s), 1963(m), 1952(m) cm^{-1} : 1H NMR ($CDCl_3$); 1.28 (t, 24H, $^4J_{POCH} + ^6J_{POCH} = 3.4$, methyls on the phospholane rings), 1.15 (m, 2H, H1 α and H1 β on the η^4 -Cp ring), 1.40 (m, 2H, H2 and H5 on the η^4 -Cp ring), 5.15 (m, 2H, H3 and H4 on the η^4 -Cp ring): ^{31}P ($CDCl_3$); 337.9 (s)).

Structural Determination

Collection and reduction of X-ray data

Yellow-orange single crystals of $[Fe(\eta^4-C_5H_6)(CO)-(\mu-\overline{P(OC(Me)_2C(Me)_2O)})_2Fe(CO)_3]$ were recrystallized from a saturated dry

benzene/methylene chloride solution of the chromatographically pure complex by slow evaporation under an inert atmosphere. A suitable crystal for data collection (approximate dimensions 0.1 x 0.2 x 0.4 mm) was mounted on a glass fiber and subsequently placed on a goniometer head which was in turn mounted on a four-circle Syntex P2₁ automated diffractometer.

After centering, fifteen reflections were selected from a rotation photograph and their approximate positions input into an automatic indexing program (BLIND) (114). The resulting reduced cell and cell scalars indicated triclinic symmetry and the ω -oscillation photographs, taken about the three cell axes, indicated $\bar{1}$ Laue symmetry. Accurate unit cell parameters and their standard deviations were obtained by a least-squares fit to the $\pm 2\theta$ values of the reflections obtained. The experimental crystallographic data are given in Table 45.

Data were collected at 298°K ($\pm 3^\circ$ K) using the computer-controlled Syntex diffractometer. Within a 2θ sphere of 40°, 3453 independent reflections were collected utilizing an ω -stepscan technique and corrected for both Lorentz polarization and absorption effects ($0.846 < 0.999$). Very little data with measurable intensities above $2\theta = 40^\circ$ were observed. An empirical absorption correction ($\mu = 11.96 \text{ cm}^{-1}$) was made using the method previously described (116). A total of 1473 of these reflections with $I > 3\sigma(I)$ were retained for use in subsequent calculations. The estimated variance of each intensity was calculated by Equation 13, where C_T and C_B represent the total and background counts,

Table 45. Experimental crystallographic data for $[\text{Fe}(\eta^4\text{-C}_5\text{H}_6)(\text{CO})\text{-}(\mu\text{-P}(\text{OC}(\text{Me})_2\text{C}(\text{Me})_2\text{O}))_2\text{Fe}(\text{CO})_3]$

Molecular formula	$\text{C}_{21}\text{H}_{30}\text{Fe}_2\text{O}_8\text{P}_2$
Molecular weight	584
Color	yellow-orange
Crystal dimensions (mm)	0.1 x 0.2 x 0.4
Crystal system	triclinic
Space group	$\text{P}\bar{1}$
Cell dimensions	
a (Å)	11.558(6)
b (Å)	15.962(9)
c (Å)	9.687(5)
α (deg.)	105.11(4)
β (deg.)	106.04(4)
γ (deg.)	101.17(4)
Cell volume (Å ³)	1588.8(15)
Z	2
Radiation	$\text{MoK}\alpha$
Wavelength (Å)	0.71069
2 θ range (deg.)	0-40
No. of unique reflections	1473
Agreement factors	
R_F	9.5
R_{WF}	11.6

$$\sigma(I)^2 = C_T + C_B + (0.03C_T)^2 + (0.03C_B)^2 + (0.03I)^2 \quad (13)$$

respectively, and the factor 0.03 is an estimate of non-statistical errors.

Solution and refinement

The positions of the two symmetry independent iron atoms were obtained from an analysis of a three-dimensional Patterson function. The positions of the remaining non-hydrogen atoms were determined by successive structure factor and electron density map calculations. The positional and anisotropic thermal parameters for these atoms were refined initially by a block-matrix and finally by a full-matrix least squares procedure (117). Significant residual electron density indicated the presence of a methylene chloride solvent molecule with unit occupancy. This solvent molecule was included in refinements using the procedure described above. The positional parameters for the hydrogen atoms were calculated and included at fixed positions in the final full matrix calculation with fixed isotropic temperature factors. The final conventional residual index ($R_F = \sum ||F_O| - k|F_C|| / \sum |F_O|$) was 0.095 with a corresponding weighted index ($R_{WF} = [\sum w(|F_O| - |F_C|)^2 / \sum w F_O^2]^{1/2}$) of 0.116, and the function minimized in the least squares refinement was $\sum w(|F_O| - |F_C|)^2$, where w is $1/\sigma(F)^2$. The atomic scattering factors were those from the International Tables for X-ray Crystallography (193), modified for the real and imaginary parts of anomalous dispersion. The final atom positional coordinates, hydrogen positional coordinates, anisotropic

thermal parameters, and structure factors are given in Tables 46, 47, 48, and 49, respectively.

Table 46. Atom Coordinates [$\times 10^4$] and average temperature factor [$\text{\AA}^3 \times 10^3$] for $[\text{Fe}(\eta^4\text{-C}_5\text{H}_6)(\text{CO})(\mu\text{-P}(\text{OC}(\text{Me})_2\text{C}(\text{Me})_2\text{O}))_2\text{Fe}(\text{CO})_3]$

Atom	x^a	y	z	$U(\text{ave})^b$
Fe(1)	5392(3)	2413(2)	6678(4)	51
Fe(2)	3739(3)	1656(2)	3761(4)	46
P(1)	3372(6)	2151(5)	5790(8)	51
P(2)	5382(6)	2764(4)	4655(8)	47
O(1)	5020(17)	1290(12)	8500(19)	93
O(2)	6057(19)	4237(12)	8756(21)	88
O(3)	7755(17)	1999(15)	6770(24)	107
O(4)	2215(21)	2656(16)	2189(25)	142
O(7)	5292(14)	3722(9)	4507(18)	54
O(8)	6619(14)	2779(11)	4140(19)	80
O(9)	2464(14)	1482(11)	6324(18)	62
O(10)	2694(13)	2954(10)	6105(17)	58
C(1)	5142(23)	1711(17)	7774(27)	63
C(2)	5799(22)	3503(17)	7950(30)	65
C(3)	6818(20)	2171(18)	6719(30)	61
C(4)	2809(20)	2286(15)	2774(23)	107
C(7)	6335(23)	4198(18)	4168(30)	67

^aCoordinates are given in terms of fractions of the unit cell and numbers in parentheses represent the standard deviations corresponding to the least significant figures.

^b $U(\text{ave})$ is the average of U_{11} , U_{22} , and U_{33} .

Table 46 (continued)

Atom	x ^a	y	z	U(ave) ^b
C(8)	6919(23)	3467(18)	3502(36)	93
C(9)	1613(25)	1902(19)	6823(37)	108
C(10)	1674(38)	2747(23)	6606(52)	217
C(11)	7254(34)	4869(28)	5766(44)	134
C(12)	6080(47)	4810(27)	3406(58)	231
C(13)	8222(38)	3744(25)	3849(55)	198
C(14)	6142(39)	3033(26)	1720(34)	126
C(15)	1155(32)	3417(20)	6961(44)	136
C(16)	461(44)	2005(75)	4878(47)	393
C(17)	824(44)	1356(30)	7199(64)	256
C(18)	2718(40)	2749(63)	8824(39)	360
C(19)	2518(19)	340(15)	1068(24)	33
C(20)	3882(25)	813(16)	1651(28)	63
C(21)	4536(27)	618(16)	3053(31)	74
C(22)	3479(25)	343(16)	3640(28)	58
C(23)	2312(21)	353(16)	2599(27)	46
C(1S)	7738(22)	663(16)	-54(27)	54
C1(1)	9389(7)	1199(5)	528(9)	80
C1(2)	7386(8)	610(6)	1610(9)	100

Table 47. Atom coordinates [$\times 10^4$] and temperature factor [\AA^3 , $\times 10^3$] for hydrogen atoms in $[\text{Fe}(\eta^4\text{-C}_5\text{H}_6)(\text{CO})-(\mu\text{-P}(\text{OC}(\text{Me})_2\text{C}(\text{Me})_2\text{O}))_2\text{Fe}(\text{CO})_3]$ with estimated standard deviations

Atom ^a	x	y	z	U
H(11A)	7407.5(0)	5587.3(0)	5869.1(0)	50.7(0)
H(11B)	6815.1(0)	4835.4(0)	6657.0(0)	50.7(0)
H(11C)	8122.9(0)	4773.3(0)	6173.6(0)	50.7(0)
H(11D)	7489.5(0)	4543.4(0)	6597.4(0)	50.7(0)
H(11E)	6774.1(0)	5357.4(0)	6292.9(0)	50.7(0)
H(11F)	8081.9(0)	5295.3(0)	5809.5(9)	50.7(0)
H(12A)	6726.4(0)	5212.5(0)	3234.4(0)	50.7(0)
H(12B)	5364.6(0)	5092.2(0)	3643.6(0)	50.7(0)
H(12C)	5446.7(0)	4299.4(0)	2119.9(0)	50.7(0)
H(12D)	4965.3(0)	4524.3(0)	2765.8(0)	50.7(0)
H(12E)	6246.5(0)	5436.8(0)	3878.2(0)	50.7(0)
H(12F)	6325.8(0)	4642.9(0)	2353.8(0)	50.7(0)
H(13A)	8509.9(0)	4430.7(0)	3883.9(0)	50.7(0)
H(13B)	8648.5(0)	3744.9(0)	4983.2(0)	50.7(0)
H(13C)	8544.4(0)	3342.6(0)	3117.4(0)	50.7(0)
H(13D)	8625.3(0)	3248.0(0)	4105.8(0)	50.7(0)
H(13E)	8590.8(0)	4336.2(0)	4872.3(0)	50.7(0)

^aMethyl hydrogens attached to carbons C14 and C18 could not be calculated.

Table 47 (continued)

Atom	x	y	z	U
H(13F)	8486.7(0)	3933.9(0)	3006.5(0)	50.7(0)
H(15A)	1618.6(0)	4054.6(0)	6978.8(0)	50.7(0)
H(15B)	1003.0(0)	3499.0(0)	8023.8(0)	50.7(0)
H(15C)	273.0(0)	3166.4(0)	6089.7(0)	50.7(0)
H(15D)	309.9(0)	3091.5(0)	7079.5(0)	50.7(0)
H(15E)	1655.7(0)	3979.3(0)	7973.6(0)	50.7(0)
H(15F)	929.0(0)	3649.1(0)	6039.2(0)	50.7(0)
H(16A)	-396.3(0)	2128.9(0)	4883.6(0)	50.7(0)
H(16B)	408.3(0)	1331.2(0)	4838.6(0)	50.7(0)
H(16C)	651.7(0)	2103.4(0)	3930.6(0)	50.7(0)
H(16D)	839.0(0)	1581.0(0)	4217.2(0)	50.7(0)
H(16E)	-208.4(0)	1604.7(0)	5171.2(0)	50.7(0)
H(16F)	33.0(0)	2377.8(0)	4264.3(0)	50.7(0)
H(17A)	-85.2(0)	1557.3(0)	7136.4(0)	50.7(0)
H(17B)	1109.2(0)	1258.4(0)	8212.1(0)	50.7(0)
H(17C)	385.9(0)	659.6(0)	6306.2(0)	50.7(0)
H(17D)	1025.8(0)	760.1(0)	7301.3(0)	50.7(0)
H(17E)	553.0(0)	1657.5(0)	8129.3(0)	50.7(0)
H(17F)	-168.9(0)	1057.7(0)	6223.6(0)	50.7(0)

Table 48. Anisotropic thermal parameters for $[\text{Fe}(\eta^4\text{-C}_5\text{H}_6)(\text{CO})-(\mu\text{-P}(\text{OC}(\text{Me})_2\text{C}(\text{Me})_2\text{O}))_2\text{Fe}(\text{CO})_3]$ with estimated standard deviations

Atom	U_{11}	U_{22}	U_{33}	U_{12}	U_{13}	U_{23}
Fe(1)	49(3)	56(3)	48(2)	21(2)	16(2)	21(2)
Fe(2)	48(2)	45(2)	44(2)	16(2)	17(2)	17(2)
P(1)	54(5)	56(5)	43(5)	16(4)	15(4)	22(4)
P(2)	56(5)	37(5)	49(5)	17(4)	22(4)	16(4)
O(1)	107(16)	100(15)	70(13)	60(13)	42(12)	65(12)
O(2)	113(17)	68(14)	84(15)	31(13)	15(13)	13(12)
O(3)	68(14)	138(2)	115(18)	30(14)	11(13)	54(16)
O(4)	132(19)	157(22)	136(20)	101(17)	40(16)	105(18)
O(7)	61(12)	27(10)	75(13)	6(9)	30(10)	20(9)
O(8)	60(12)	85(14)	94(14)	42(11)	60(11)	62(12)
O(9)	49(11)	69(12)	68(12)	12(10)	29(10)	43(10)
O(10)	50(11)	55(11)	70(12)	33(9)	29(10)	43(10)
C(1)	67(19)	73(20)	51(18)	31(16)	28(15)	39(16)
C(2)	49(17)	68(20)	77(21)	27(15)	16(15)	41(17)
C(3)	13(15)	89(22)	80(21)	-16(15)	-27(14)	42(18)
C(4)	109(17)	120(19)	91(17)	-26(15)	51(14)	-25(14)
C(7)	57(18)	68(18)	77(20)	2(15)	19(15)	39(16)
C(8)	56(18)	60(19)	163(29)	18(15)	83(20)	49(19)
C(9)	71(20)	85(21)	169(29)	30(17)	106(21)	64(21)
C(10)	223(40)	119(28)	309(49)	117(28)	249(40)	158(33)

Table 48 (continued)

Atom	U ₁₁	U ₂₂	U ₃₃	U ₁₂	U ₁₃	U ₂₃
C(11)	100(27)	157(35)	145(33)	-1(25)	28(25)	8(28)
C(12)	278(50)	124(31)	289(50)	108(33)	208(44)	138(34)
C(13)	172(36)	117(29)	306(52)	80(27)	165(37)	145(34)
C(14)	194(38)	142(32)	43(21)	-14(28)	1(23)	8(21)
C(15)	140(30)	66(21)	202(37)	46(21)	130(29)	26(23)
C(16)	121(38)	124(36)	50(27)	114(65)	-21.26	192(40)
C(17)	215(43)	169(38)	383(65)	136(34)	227(46)	181(43)
C(18)	119(35)	68(21)	29(23)	181(61)	26(23)	16(47)
C(19)	29(15)	34(15)	36(15)	-15(12)	-3(12)	-7(12)
C(20)	93(22)	45(18)	52(18)	34(16)	24(2)	7(6)
C(21)	109(25)	34(17)	79(22)	27(17)	37(19)	14(16)
C(22)	88(22)	32(17)	54(19)	13(16)	12(17)	-2(14)
C(23)	34(16)	41(17)	64(19)	2(13)	5(14)	-8(14)
C(1S)	58(18)	51(18)	54(18)	3(15)	30(15)	1(15)
Cl(1)	79(6)	78(6)	82(6)	-8(5)	15(5)	-4(5)
Cl(2)	106(7)	121(8)	73(6)	14(6)	46(5)	1(5)

Table 49 (continued)

10	-3	176	204	6	0	254	205	3	-7	299	305	0	-6	325	-315
10	-2	145	-114	6	2	221	221	3	-6	589	-590	0	-5	227	239
				6	3	203	226	3	-5	424	369	0	-4	734	-730
				6	-8	189	-197	3	-4	171	183	0	-2	554	572
				6	-3	362	330	3	-3	173	-146	0	-1	264	-259
				6	-2	93	44	3	-2	578	558	1	1	749	-769
				7	1	137	66	3	-1	683	-653	1	2	561	532
				7	2	138	130	4	0	462	511	1	3	279	-300
				7	-8	223	244	4	1	313	-327	1	4	380	-366
				7	-7	137	-134	4	2	295	-282	1	5	317	381
				8	0	171	142	4	4	192	-126	1	-6	471	531
				8	-8	263	-243	4	-9	229	234	1	-5	529	-569
				8	-5	323	-299	4	-8	145	-98	1	-4	250	332
				9	-6	209	-166	4	-5	118	-102	1	-2	763	-717
				9	-4	204	189	4	-3	305	285	1	-1	563	493
				10	-4	278	-235	4	-2	170	-189	2	0	606	-583
				10	-3	159	199	4	-1	152	157	2	1	649	651
				10	-2	153	-86	5	0	302	-351	2	2	280	-288
								5	2	126	97	2	3	184	-197
								5	3	291	-266	2	4	315	315
								5	-7	140	119	2	5	214	-222
								5	-6	192	203	2	-6	209	-203
								5	-5	225	-266	2	-5	639	619
								5	-4	739	757	2	-3	457	-401
								5	-3	411	-394	2	-1	414	-437
								5	-1	800	770	3	0	355	366
								6	0	211	242	3	1	455	-474
								6	1	138	95	3	3	158	139
								6	3	210	193	3	4	336	-292
								6	-7	173	-196	3	-9	141	46
								6	-5	703	724	3	-7	193	165
								6	-4	433	-469	3	-6	165	-80
								6	-3	525	492	3	-5	178	-143
								6	-2	226	183	3	-3	315	317
								6	-1	371	-381	3	-2	163	-151
								7	0	131	134	3	-1	570	-631
								7	1	148	-119	4	0	477	-499
								7	2	255	267	4	2	357	-327
								7	-7	223	178	4	3	293	-291
								7	-5	314	-522	4	4	134	89
								7	-4	368	327	4	-7	190	-200
								7	-3	124	47	4	-6	184	170
								8	1	349	355	4	-5	178	-175
								8	-6	139	-107	4	-4	233	240
								8	-2	206	184	4	-3	159	-111
								9	0	349	274	4	-2	170	-180
								9	-3	166	157	4	-1	585	609
								9	-2	142	-149	5	0	150	151
								10	-4	133	88	5	1	232	-238
												5	-8	155	-101
												5	-7	205	217
												5	-6	213	187
												5	-4	170	-126
												5	-3	138	142
												6	0	144	137
												6	-8	193	208
												6	-6	152	-111
												6	-5	444	439
												6	-3	205	185

Table 49 (continued)

2 -6 231 259	4 -4 295 278	K = 13
2 -4 300 -479	4 -1 241 199	H L FO FC
2 -3 347 341	5 -4 230 -200	0 -7 259 -251
2 -1 134 152	5 -3 190 203	0 -6 205 229
3 0 344 305	6 -3 323 -309	0 -4 257 -228
3 -8 383 -351		0 -3 243 299
3 -6 177 -104	K = 11	0 -2 182 -168
3 -5 212 -204	H L FO FC	1 -6 279 -239
3 -4 338 325	0 1 131 -124	1 -4 199 231
3 -3 113 -82	0 -6 158 -155	1 -3 250 -266
4 2 153 -111	0 -5 161 183	2 -4 151 -104
4 -8 307 299	0 -4 343 330	2 -1 190 -230
4 -7 275 -285	0 -3 266 -284	3 -5 162 -140
4 -5 253 289	0 -2 284 298	3 -3 186 199
4 -4 368 -318	0 -1 168 -178	3 -2 321 -381
4 -2 245 237	1 0 142 -104	3 -1 290 290
5 1 132 -168	1 -7 305 -299	
5 -8 235 -191	1 -6 367 361	K = 14
5 -5 208 -248	1 -4 384 -375	H L FO FC
5 -2 219 -218	1 -3 476 463	0 -3 165 -127
5 -1 150 155	2 2 150 124	1 -4 175 174
6 -3 293 -313	2 -7 357 311	
7 -2 206 -226	2 -6 257 -241	K = 15
	2 -4 255 266	H L FO FC
	2 -3 187 -185	0 -4 242 214
	2 -1 155 126	0 -3 196 -171
	3 1 240 226	
	3 -5 188 176	
	3 -2 339 317	
	4 -4 188 196	
	4 -3 249 220	
	4 -2 218 -218	
	4 -1 226 238	
	5 -5 151 -76	
	5 -3 174 -139	
	5 -2 298 248	
	6 -4 167 -225	
	6 -3 217 217	
	K = 12	
	H L FO FC	
	0 1 151 -108	
	0 -7 176 -160	
	0 -5 137 123	
	0 -4 219 -220	
	0 -3 427 423	
	0 -2 400 -426	
	1 1 148 -165	
	1 -3 145 -180	
	1 -2 158 201	
	2 1 191 133	
	2 -7 150 122	
	2 -1 136 -123	
	3 -6 154 58	
	4 -3 183 235	
	5 -5 120 98	
K = 10		
H L FO FC		
0 0 337 -342		
0 1 314 343		
0 2 142 -109		
0 -6 191 -140		
0 -5 190 178		
0 -4 386 418		
0 -3 562 -570		
0 -2 595 657		
0 -1 260 -266		
1 0 141 215		
1 1 179 -219		
1 -4 214 -227		
1 -3 701 636		
1 -2 267 -294		
1 -1 149 129		
2 1 137 106		
2 2 143 228		
2 3 227 -222		
2 -4 156 178		
2 -3 239 -209		
2 -2 129 135		
2 -1 232 246		
3 0 367 352		
3 1 242 247		
3 2 161 -173		
3 -6 233 -228		
3 -5 321 315		
3 -4 249 -234		
3 -2 196 156		
3 -1 139 -114		
4 1 140 -151		
4 -7 217 -223		
4 -6 139 80		

RESULTS AND DISCUSSION

The bond distances, bond angles, least squares planes, and the dihedral angles between these planes for this complex are given in Tables 50, 51, 52, and 53, respectively. In Figures 46 and 47 are shown the computer ORTEP drawings. The unit cell and stereopair ORTEP drawings for this complex are located in Appendix III.

A good rationalization for the observed synthesis of this complex is not readily apparent at this point. One potential explanation involves the initial formation of either the cis or trans- 49 complexes, followed by either sequential or simultaneous one electron reductions of the η^5 -cyclopentadienyl groups to η^4 -cyclopentadiene substituted intermediates. The proton source is also unclear, possibly being supplied from the tetrahydrofuran solvent. One of these η^4 -C₅H₆ ligands could potentially be replaced by carbon monoxide ligands, which are in excess during the progress of the reaction, to yield the observed complex. This is based upon the premise that an η^4 -C₅H₆ group could be more easily supplanted by carbon monoxide than the η^5 -Cp ligands. The method of the apparent reduction, the nature of the reducing agent, or the nature of the complex intermediates are not known.

The molecule was found to have a crystallographic P₁ symmetry and an approximate C_s molecular symmetry. It appears that a substantial amount of thermal motion is associated with the outer atoms of the dioxaphosphorane rings, especially the 4 and 5 methyl groups. This thermal motion resulted in slightly inflated R_F and R_{WF} values and few

Table 50. Bond distances (Å) in $[\text{Fe}(\eta^4\text{-C}_5\text{H}_6)(\text{CO})(\mu\text{-P}(\text{OC}(\text{Me})_2\text{C}(\text{Me})_2\text{O}))_2\text{-Fe}(\text{CO})_3]$ with estimated standard deviations

Fe(1)-P(1)	2.167(8)	Fe(2)-P(1)	2.109(8)
Fe(1)-P(2)	2.173(8)	Fe(2)-P(2)	2.114(8)
Fe(1)-Fe(2)	2.727(5)	P(1)-P(2)	2.942(10)
Fe(1)-C(1)	1.772(25)	Fe(2)-C(4)	1.855(21)
Fe(1)-C(2)	1.732(26)	C(4)-O(4)	1.121(31)
Fe(1)-C(3)	1.752(22)	Fe(2)-C(19)	2.673(22)
C(1)-O(1)	1.110(30)	Fe(2)-C(20)	2.202(25)
C(2)-O(2)	1.156(32)	Fe(2)-C(21)	2.105(26)
C(3)-O(3)	1.167(29)	Fe(2)-C(22)	2.028(23)
C(1S)-C1(1)	1.792(25)	Fe(2)-C(23)	2.176(23)
		C(1S)-C1(2)	1.788(25)
Within the phosphorane ring system			
P(1)-O(9)	1.630(17)	P(2)-O(7)	1.594(15)
P(1)-O(10)	1.636(16)	P(2)-O(8)	1.639(17)
O(9)-C(9)	1.418(32)	O(7)-C(7)	1.454(29)
O(10)-C(10)	1.409(44)	O(8)-C(8)	1.423(33)
C(9)-C(10)	1.410(32)	C(7)-C(8)	1.541(37)
C(9,10)-C(15,18) ^a	1.599(58)	C(7,8)-C(11-14) ^a	1.493(47)
Within the ($\eta^4\text{-C}_5\text{H}_6$) ring system			
C(19)-C(20)	1.483(34)	C(22)-C(23)	1.451(35)
C(20)-C(21)	1.503(37)	C(23)-C(19)	1.558(32)
C(21)-C(22)			

^aAverage value.

Table 51. Bond angles (degrees) in $[\text{Fe}(\eta^4\text{-C}_5\text{H}_6)(\text{CO})\text{-}(\mu\text{-P}(\text{OC}(\text{Me})_2\text{C}(\text{Me})_2\text{O}))_2\text{Fe}(\text{CO})_3]$ with estimated standard deviations

P(1)-Fe(1)-P(2)	85.39(29)	P(1)-Fe(2)-P(2)	88.31(30)
Fe(1)-P(1)-Fe(2)	79.26(27)	Fe(1)-P(2)-Fe(2)	79.02(26)
Fe(1)-C(1)-O(1)	177.7(22)	Fe(2)-C(4)-O(4)	177.5(20)
Fe(1)-C(2)-O(2)	177.8(23)	P(1)-Fe(2)-C(4)	93.44(68)
Fe(1)-C(3)-O(3)	178.4(24)	P(2)-Fe(2)-C(4)	91.70(68)
P(1)-Fe(1)-C(1)	87.38(83)	C(4)-Fe(2)-C(19)	81.37(80)
P(1)-Fe(1)-C(2)	99.50(83)	C(4)-Fe(2)-C(20)	93.50(92)
P(1)-Fe(1)-C(3)	154.31(90)	C(4)-Fe(2)-C(21)	134.25(99)
P(2)-Fe(1)-C(1)	157.69(83)	C(4)-Fe(2)-C(22)	135.15(101)
P(2)-Fe(1)-C(2)	98.05(89)	C(4)-Fe(2)-C(23)	95.02(91)
P(2)-Fe(1)-C(3)	87.20(89)	P(1)-Fe(2)-C(20)	165.75(69)
Cl(1)-C(1S)-Cl(2)	107.78(127)	P(1)-Fe(2)-C(23)	102.72(66)
		P(2)-Fe(2)-C(20)	103.40(72)
		P(2)-Fe(2)-C(23)	166.68(65)
Within the phosphorane ring system			
Fe(1)-P(1)-O(9)	120.30(64)	Fe(1)-P(2)-O(7)	123.28(67)
Fe(1)-P(1)-O(10)	122.08(64)	Fe(1)-P(2)-O(8)	118.13(69)
Fe(2)-P(1)-O(9)	120.81(67)	Fe(2)-P(2)-O(7)	119.93(66)
Fe(2)-P(1)-O(10)	123.74(65)	Fe(2)-P(2)-O(8)	124.65(68)
O(9)-P(1)-O(10)	93.83(82)	O(7)-P(2)-O(8)	94.82(86)
P(1)-O(9)-C(9)	111.1(15)	P(2)-O(7)-C(7)	113.65(139)

Table 51 (continued)

P(1)-O(10)-C(10)	114.6(17)	P(2)-O(8)-C(8)	114.4(14)
O(9)-C(9)-C(10)	112.8(27)	O(7)-C(7)-C(8)	106.3(19)
C(17)-C(9)-C(18)	101.6(35)	C(13)-C(8)-C(14)	113.4(31)
C(15)-C(10)-C(16)	98.5(41)	C(11)-C(7)-C(12)	99.5(29)

Within the ($\eta^4\text{-C}_5\text{H}_6$) ring system

C(19)-C(20)-C(21)	110.5(21)	C(22)-C(23)-C(19)	107.6(19)
C(20)-C(21)-C(22)	102.8(22)	C(23)-C(19)-C(20)	99.9(17)
C(21)-C(22)-C(23)	108.7(21)		

Table 52. Least squares planes in $[\text{Fe}(\eta^4\text{-C}_5\text{H}_6)(\text{CO})_2(\mu\text{-P}(\text{OC}(\text{Me})_2\text{C}(\text{Me})_2\text{O}))_2\text{Fe}(\text{CO})_3]^a$

I.	Plane through Fe(1), Fe(2), P(1)	$-0.0288x + 0.9947y - 0.0983z = 1.013$
II.	Plane through Fe(1), Fe(2), P(2)	$0.7787x - 0.5919y - 0.2079z = 0.6522$
III.	Plane through Fe(1), P(1), P(2)	$-0.2471x + 0.8337y + 0.4939z = 3.404$
IV.	Plane through Fe(2), P(1), P(2)	$0.5566x - 0.72346y + 0.4086z = 1.878$
V.	Plane through P(1), O(9), O(10)	$0.3310x + 0.0942y + 0.9389z = 5.478$
VI.	Plane through P(2), O(7), O(8)	$0.2606x + 0.1399y + 0.9553z = 5.381$
VII.	Plane through O(7), O(8), C(7), C(8)	$0.3490x + 0.1363y + 0.9272z = 5.678$
VIII.	Plane through O(9), O(10), C(9), C(10)	$0.3303x + 0.1110y + 0.9373z = 5.495$
IX.	Plane through P(1), P(2), O(7), O(8), O(9), O(10)	$0.3079x + 0.1312y + 0.9423z = 5.523$
X.	Plane through C(20), C(21), C(22), C(23)	$0.1874x + 0.8175y + 0.5446z = 0.693$
XI.	Plane through C(19), C(20), C(23)	$0.4326x - 0.8968y - 0.0926z = 0.825$

^aThe variables x, y, and z here are fractional coordinates.

Table 53. Dihedral angles (degrees) between planes in $[\text{Fe}(\eta^4\text{-C}_5\text{H}_6)(\text{CO})-(\mu\text{-P}(\text{OC}(\text{Me})_2\text{C}(\text{Me})_2\text{O}))_2\text{Fe}(\text{CO})_3]$

I-II	126.21
III-IV	124.24
V-VI	4.90
V-VIII	0.97
VI-VII	5.32
VII-VIII	1.89
X-XI	149.84

observed reflections at 2θ values greater than 40° , as would be expected with this type of thermal disorder. It is noteworthy, however, that the $[\text{Fe}_2(\text{CO})_4(\eta^4\text{-C}_5\text{H}_6)(\mu\text{-PO}_2)_2]$ framework refined very well with little anisotropic thermal motion and relatively small standard deviations. The crystal packing, shown in the unit cell ORTEP drawing in Appendix III, exhibits no unusual intermolecular interactions, with all the intermolecular distances greater than 4.0 Å. The physical and spectroscopic data for this complex are given in the Experimental Section.

The structure, as seen in Figure 46, clearly confirms the postulated structure containing two bridging dioxaphospholane rings and an $\eta^4\text{-C}_5\text{H}_6$ ligand on one of the two dissimilar iron atoms. There are a number of very interesting structural features in this system, which are seen most clearly in Figure 47 (wherein the phospholane ring atoms have been

Figure 46. ORTEP computer drawing of $[\text{Fe}(\eta^4\text{-C}_5\text{H}_6)(\text{CO})(\mu\text{-P}(\text{OC}(\text{Me})_2\text{C}(\text{Me})_2\text{O}))_2\text{Fe}(\text{CO})_3]$ showing atom labeling scheme

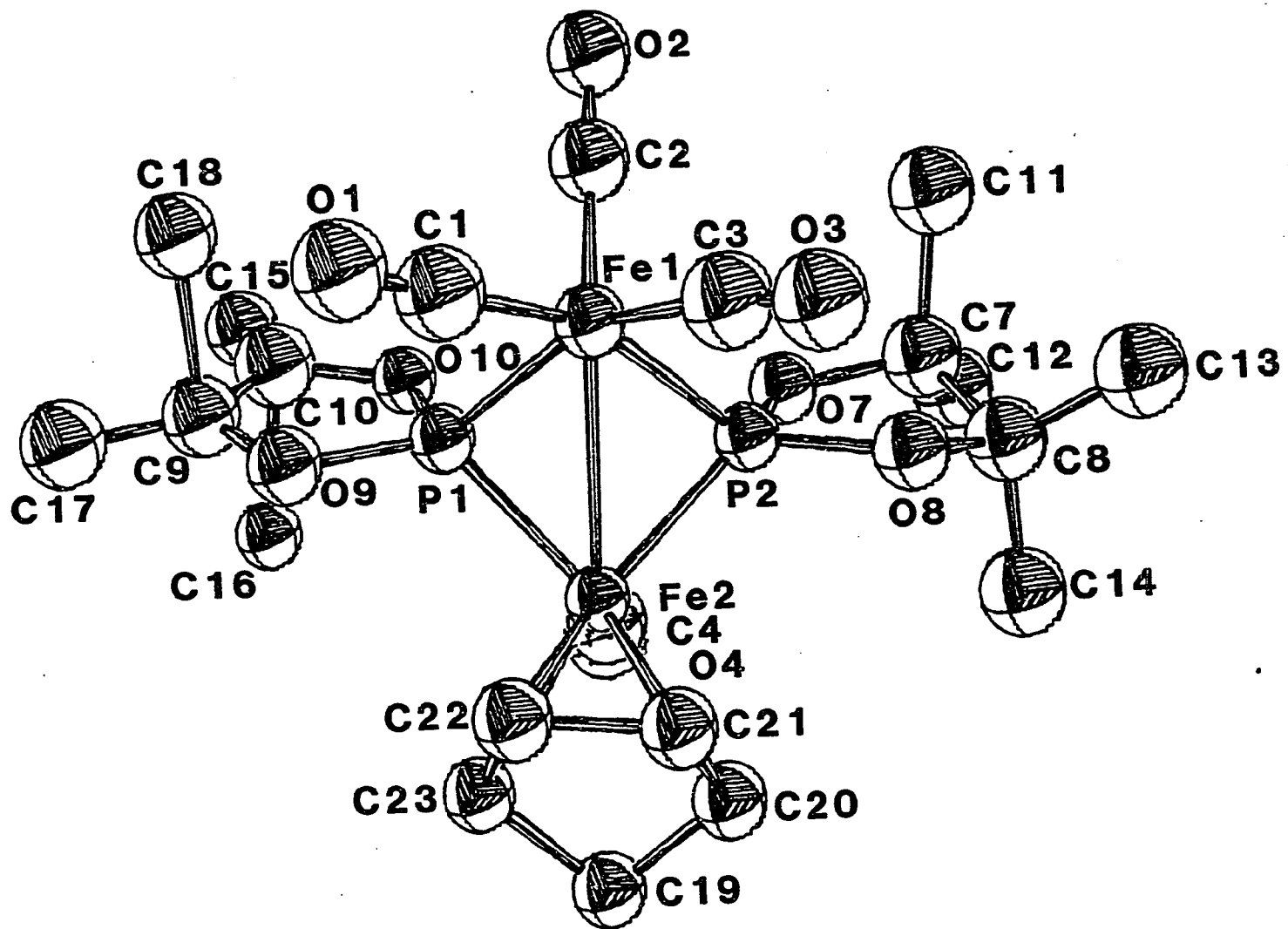
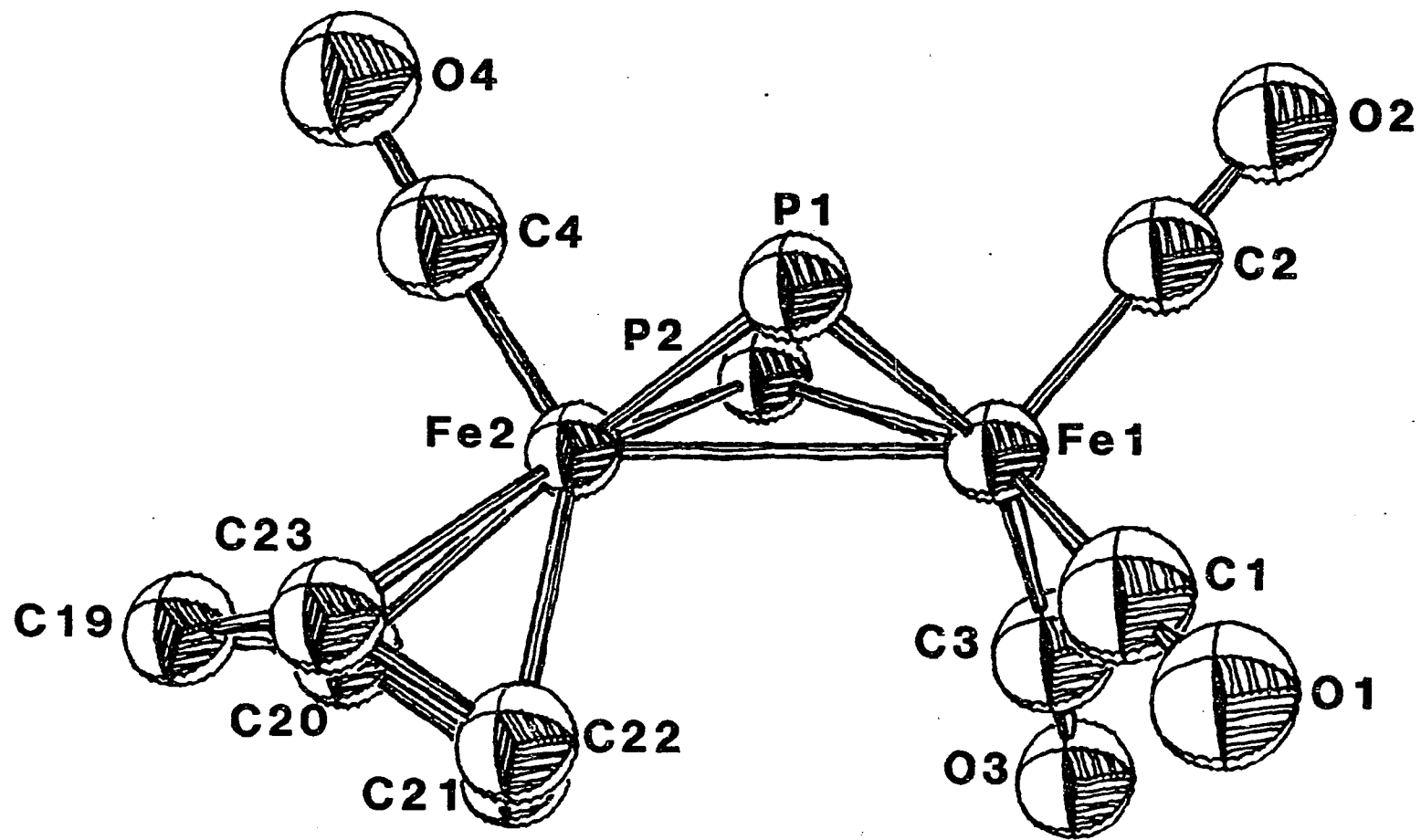


Figure 47. ORTEP computer drawing of $[\text{Fe}(\eta^4\text{-C}_5\text{H}_6)(\text{CO})(\mu\text{-P}(\text{OC}(\text{Me})_2\text{C}(\text{Me})_2\text{O}))_2\text{Fe}(\text{CO})_3]$ showing the orientation of the $\eta^4\text{-C}_5\text{H}_6$ ring and carbonyls (phospholane ring atoms omitted for clarity)



omitted). All the iron-carbon and carbon-oxygen bond lengths and angles are typical of those observed for other iron-carbonyl complexes with the Fe-C-O angles approximately linear. The geometry of the $\eta^4\text{-C}_5\text{H}_6$ ring system shows a very pronounced distortion from the planar configuration observed for $\eta^5\text{-Cp}$ systems. Four of the ring carbons (C(20)-C(23)) are bonded to the iron atom and these iron-carbon bond lengths, ranging from 2.028 Å to 2.202 Å, are quite typical for this type of bonded system (average values of Fe-C distances in cis and trans-56 are 2.116 and 2.053 Å, respectively). The fifth ring carbon (C(19)) is bent out of the plane formed by the other four ring carbons and away from the iron center at a distance of 2.673 Å. This distance is significantly longer than the sum of the covalent radii for iron and carbon (covalent radii for Fe and C are 1.23 Å and 0.77 Å, respectively (194)). The dihedral angle formed between the two planes formed by C(20)-C(23) and C(19), C(20) and C(23) is 30.16 degrees, which compares favorably with those in the known ring-substituted $\eta^4\text{-C}_5$ complexes reported in Table 43 and with the $\eta^5\text{-cyclohexadienyl}$ chromium complex (195-197) shown in Figure 48. As can be

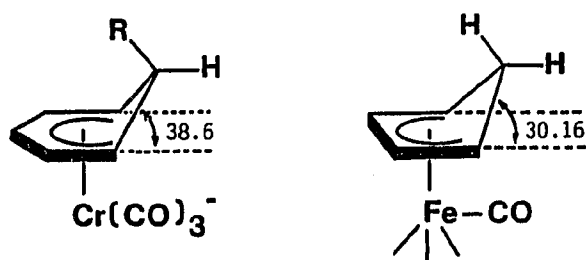


Figure 48. Dihedral angles in the $\eta^5\text{-cyclohexadienyl}$ and the $\eta^4\text{-cyclopentadiene}$ ligand systems

seen in Figure 46, C(19) of the $\eta^4\text{-C}_5\text{H}_6$ ring is under the CO ligand. This configuration may be due to steric interactions between the C_5 ring and the CO with the least crowded orientation being the one observed in the solid state structure. Olefins are well-known to be good π -acid ligands. In the case of the $\eta^4\text{-C}_5\text{H}_6$ ligand in this complex, it appears to compete favorably with the adjacent carbonyl group for the electron density available at the iron atom through a backbonding scheme as proposed by Dewar and Ford (198) and shown in Figure 49. The π -acid

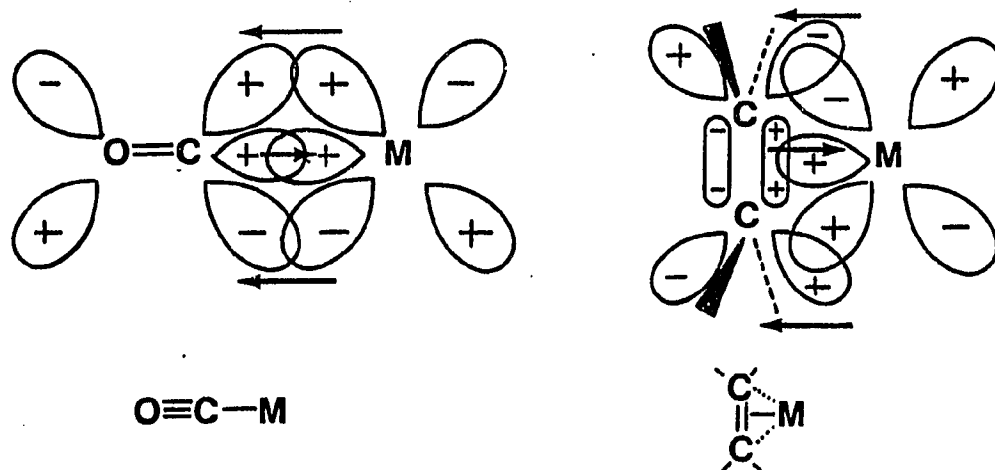


Figure 49. σ -donation and π -backbonding schemes for metal-olefin and metal-carbonyl systems

capacity of the $\eta^4\text{-C}_5\text{H}_6$ ligand, therefore, results in less π -backdonation from the metal to the adjacent carbonyl. This phenomenon is clearly seen from the structure. The Fe(1)-C(1,2,3) carbonyl bond distances range from

1.732 Å to 1.772 Å, which correspond well to the iron-carbon distances reported in Part II of 1.732 Å (*cis*-56) and 1.725 Å (average values for *trans*-56). The bond distance observed for the Fe(2)-C(4) interaction of 1.855 Å is significantly larger than the other iron-carbon carbonyl distances indicating an attenuation in the Fe \rightarrow CO π -backdonation, presumably due to the competition for electron density with the η^4 -C₅H₆ ligand. This results in a lower iron-carbon carbonyl bond order. This trend can also be seen, although less strikingly, in the variations in the carbon-oxygen bond distances in which the C(4)-O(4) distance of 1.121 Å is shorter than the average C(1,2,3)-O(1,2,3) bond distance of 1.144 Å.

The carbon-carbon distances within the η^4 -cyclopentadiene ring are quite typical and compare well with those reported for analogous systems as shown in Table 43.

The basic geometry of the Fe₂P₂ ring system appears to be typical of bridged diiron compounds of the type [Fe₂(CO)₆(μ -PR₂)₂] (see Table 42 of Part II). As can be clearly seen in Figure 47, this four membered ring is folded about the iron-iron axis with a flap angle of 126.21 degrees. Upon comparison of several important structural features of this complex with those presented in Table 42, some significant differences stand out between them. First, the iron-iron bond is much longer in the present compound than in any other reported system possessing a metal-metal bond (2.727(2) Å versus the average of 2.614 Å for other complexes). Second, the iron-phosphorus distances are the shortest reported (2.143(1) average versus the average of 2.212 Å for other complexes). Third, the

Fe-P-Fe angles are larger than in all the others except one (79.14° (average) versus the average of 72.7° for the other complexes). Fourth, the phosphorus-phosphorus distance is the largest for a metal-metal bonded complex ($2.942(1)$ Å versus the average of 2.801 Å for the other complexes). Finally, the flap angle is the largest known for the M-M bonded systems in general (112). For the structural features just mentioned, most of the diiron complexes containing a M-M bond have very similar values (with the exception of $[\text{Fe}_2(\text{CO})_6(\mu\text{-P}(\text{CF}_3)_2)_2]$ (113)). The present complex, however, differs significantly from these typical values. These structural features are all directly interrelated and are discussed below.

From previous work (113), it appears unlikely that these observed differences arise primarily from steric or crystal packing considerations since it was shown that the size and shape of the phosphorus substituents are relatively unimportant in influencing these parameters. Based upon Bent's isovalent hybridization arguments (199), a relatively simple rationalization of these observed features can be found. As the electronegativities of the substituents on the phosphorus increase, the orbitals on phosphorus used in bonding to these groups will have progressively greater p character, thereby producing a smaller X-P-X angle (16° less than tetrahedral in the present complex). As a result of this, more phosphorus s character is left for bonding to the iron atoms, which directly results in a larger Fe-P-Fe angle and shorter iron-phosphorus bond distances. As a result of the increase in the Fe-P-Fe bond angle, a concomitant increase in the flap angle also occurs. These

arguments have been recently supported by molecular orbital calculations on systems of the type $[\text{Fe}_2(\text{CO})_6(\mu\text{-PR}_2)_2]$ (112) as presented previously in Part II of this thesis. In summary, it was found that the iron-phosphorus bonding interactions were substantially more important than the iron-iron bonding by several orders of magnitude. Also, it was found that the energy of the HOMO varied markedly with respect to the other molecular orbitals with changes in the flap angle, so it is this orbital which primarily determines the observed configurations. The a_1 HOMO arises from the combination of the d_{z^2} and the d_{yz} orbitals on the iron atoms and the p_z orbitals on the phosphorus and is iron-iron bonding and iron-phosphorus antibonding as shown in Figure 50. If it is assumed that the P-Fe-P bond angles remain approximately constant, an increase in the flap angle weakens the iron-iron bonding interaction but also decreases the iron phosphorus repulsions. The HOMO is also antibonding with respect to the substituents on the phosphorus (112) and, therefore, increasing the electronegativities of these substituents increases the p character of the P-X bond and hence augments the contribution of the phosphorus p_z orbital to the HOMO. This, in turn, leads to greater iron-phosphorus antibonding interactions and a larger flap angle. The relatively high electronegativities of the oxygen substituents in the present complex, therefore, causes a large enough shift in the relative orbital contributions and the resultant molecular orbital energies to produce very long iron-iron and phosphorus-phosphorus distances, very short iron-phosphorus distances, and very large Fe-P-Fe and flap angles by the rationalizations presented above.

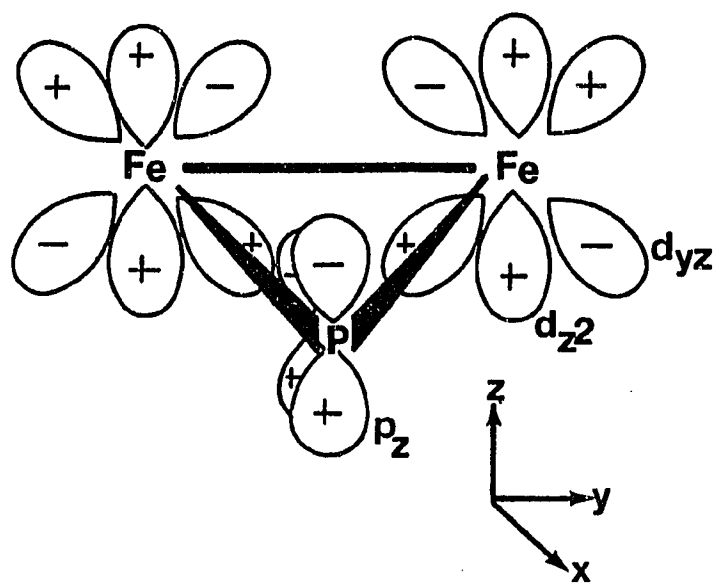


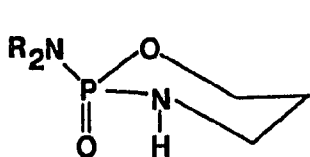
Figure 50. Highest occupied molecular orbital (HOMO) for $[\text{Fe}_2(\text{CO})_6[\mu\text{-PR}_2)_2]$ systems

PART IV.
STEREOCHEMICAL STUDIES OF ORGANOPHOSPHORUS TRIESTERS
WITH PHOSPHORUS AS THE PRIMARY CHIRAL SITE

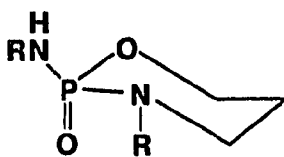
INTRODUCTION

The study of the stereochemistries of compounds with phosphorus as the primary chiral site has long been an important area of organophosphorus chemistry (200-202). Knowledge of such stereochemistries is particularly important in view of the wide variety of potential applications of optically pure phosphorus compounds to areas such as medicine, catalysis, synthesis, and mechanistic studies; especially with phosphorus in the trivalent form.

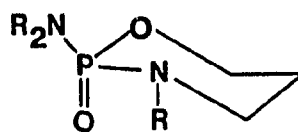
It is well-known that the stereochemistries of compounds greatly affects their biological behavior and with the increased usage of organophosphorus drugs with the chiral center at phosphorus, enhanced activity could result from the use of optically pure material. Recently, the potent antitumor agents 66, 67, and 68 were prepared in optically pure form by a variety of methods (203-209). Biological studies have shown that the (+) enantiomer of 66 is more readily metabolized by humans (210) while the (-) enantiomer is more potent against PC6 mouse tumors (211).



Cyclophosphamide

66R = CH₂CH₂Cl

Isophosphamide

67

Triphosphamide

68

In the areas of synthesis and catalysis, chiral phosphines have recently been employed as effective ligands in transition metal catalysts used for asymmetric hydrogenation (212,213). The yields (% ee) in these asymmetric syntheses have been found to be very much dependent upon the nature of the coordinated chiral phosphorus(III) ligand.

For these reasons, it is of interest to develop a method for the optical resolution of phosphorus(III) compounds other than phosphines. The literature dealing with the optical resolution of phosphorus(III) compounds with phosphorus at the primary chiral center is focused mainly on phosphines (i.e., PRR'R") (214-227), although other classes have received some attention. Previous attempts by others to resolve a variety of esters have been restricted to a small number of structurally related systems, generally with low optical purity. There are several reports on the resolution of esters of the types R(Ph)PER (E = S, O) (228-231), PhP(OEt)(OZMe₃)₂ (Z = Si, Sn) (232), and MeP(OMe)(O-i-Pr) (233), but none could be found which described the optical resolutions of a P(OR)(OR')(OR") system.

Two procedures for the resolution of phosphinites, PR₂(OR), have been reported. Each of these methods have intrinsic difficulties and are not readily extendable to systems other than the phosphinites. In the first of these methods (228), tert-butylphenylmethylphosphinite is stereospecifically synthesized from the resolved form of tert-butylphenylphosphinoselenic acid (229) by the procedure shown in Figure 51.

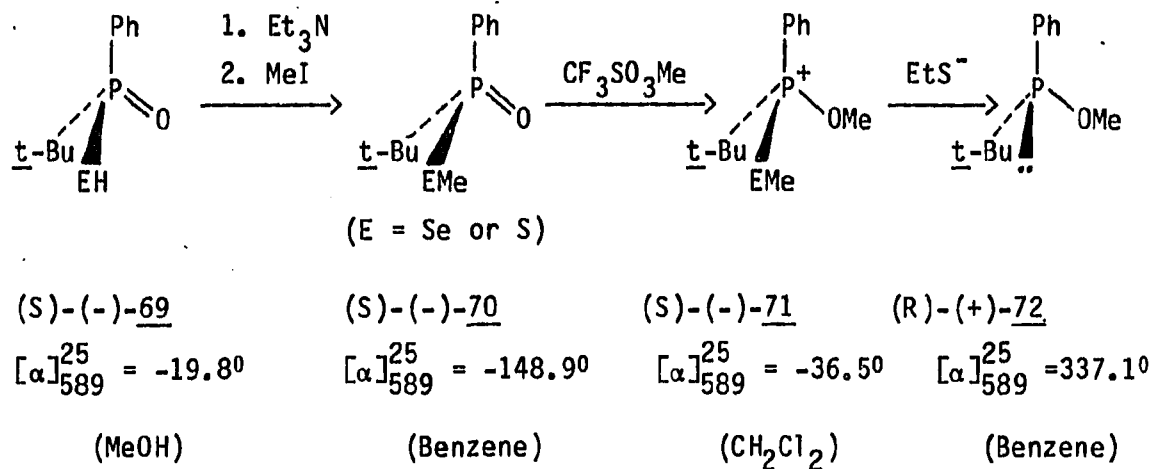
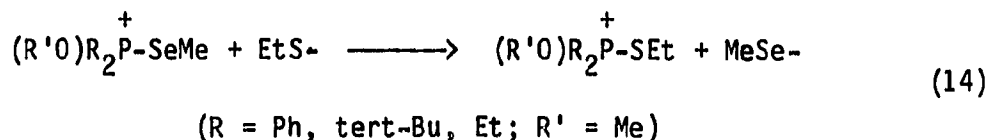


Figure 51. Stereospecific Synthesis of 72

The conversion of 71 to the final chiral product involves a nucleophilic reaction and phosphonium salts such as compound 71 are generally susceptible to nucleophilic attack at the phosphorus, carbon, or chalcogen centers. The first two of these pathways is well documented in the literature (234,235). In the case of the last step of the reaction sequence in Figure 51, however, the ethylmercapto anion was shown to exhibit a high degree of "thiophilicity", preferentially attacking at the sulfur or selenium center to produce the free trivalent phosphinite and a mixture of disulfides and/or diselenides. An important problem with this approach is that undesired nucleophilic substitution at phosphorus rather than at sulfur or selenium can occur. This results in rapid alkylseleno-alkylthio (or seleno) exchange at the chiral phosphorus resulting in racemization by inversion of configuration at the phosphorus as shown in Equation 14. The presence of a tert-butyl group directly



attached to phosphorus strongly decreases the rate of nucleophilic substitution at the phosphorus and leads to the desired trivalent compound in up to 85% optically pure form (236,237). From this study, it appears that the tert-butyl group is necessary for the stereospecific synthesis to occur without rapid racemization. This procedure further requires the optically active form of a precursor compound which is exceedingly difficult to prepare in optically pure form. Both of these factors greatly limit any possible extensions of this method to other systems.

In the second procedure, optically active phosphinites are prepared by the asymmetric reaction between racemic phosphorus(III) chlorides and achiral alcohols or thiols in the presence of optically active tertiary amines (230,231) as shown in Figure 52. The chirality of these phosphinites were determined by reacting the product from the reaction in Figure 52 with either elemental sulfur or methyl iodide. Since the stereochemical courses of both of these derivatization reactions are well known and the stereochemistries of these derivatives are also independently known, it was possible to determine the extent of asymmetric induction in the original reaction. Although this route appears to be quite general and simple for phosphinites, it leads to chiral esters of very low optical purity (30 % ee maximum, but usually only about 10% ee). This method also is probably limited to monoesters

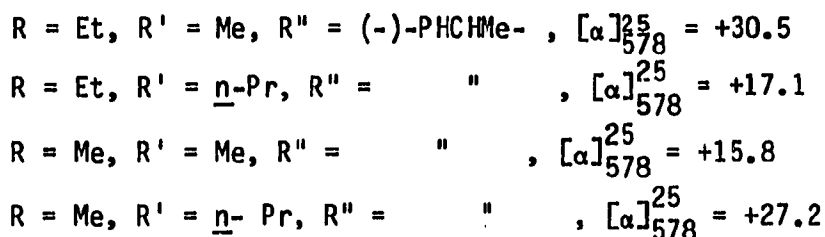
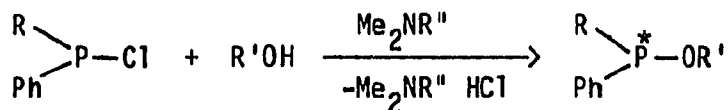


Figure 52. Synthesis of chiral phosphinites in the presence of a chiral amine (230,231)

because of the extreme difficulty in preparing chlorides of other classes of organophosphorus compounds such as $(\text{RO})(\text{R}'\text{O})\text{PCl}$ in pure form.

Two procedures have been reported for the isolation of optically active phosphonites, $\text{PR}(\text{OR})(\text{OR}')$. Both require the use of optically active phosphonates as starting materials. In the first method (232), the precursor phosphonate is reacted with either ClSiMe_3 or $\text{Me}_3\text{SnNEt}_2$ as shown in Figure 53. The reactions of ethylphenylphosphinate with

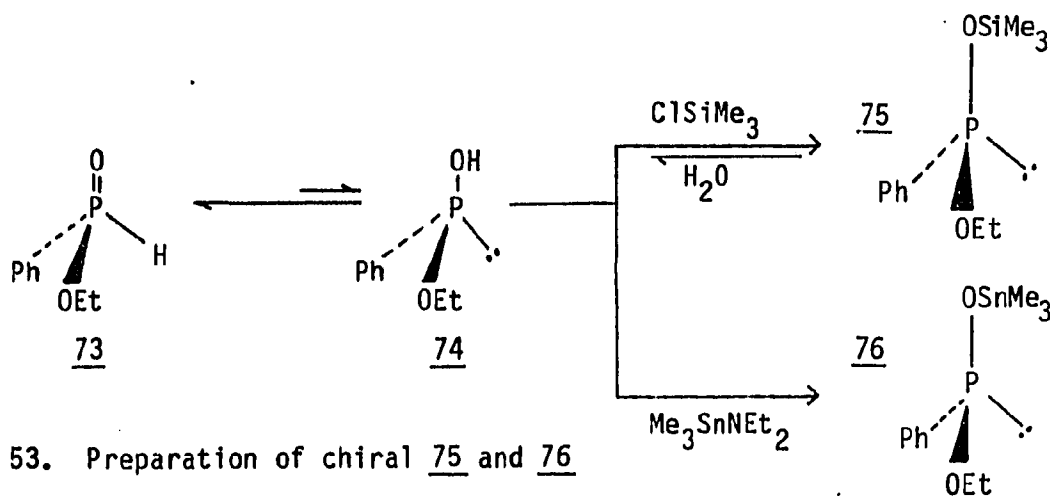


Figure 53. Preparation of chiral 75 and 76

these reagents were shown to proceed with complete or almost complete retention of configuration. There appear to be at least three major limitations to the usefulness of this method. First, both of the final products have been found to be very moisture and oxygen sensitive, thus rendering their handling difficult. Secondly, the precursor ethylphenylphosphinate is very difficult to obtain with any significant optical purity (> 5% ee), thus limiting the degree of optical purity of the formed phosphonite. Finally, the presence of either the trimethylsilyl or the trimethylstannyl group poses a very serious limitation to the application of these compounds for studies of organophosphorus mechanistic investigations because nucleophilic reagents preferentially attack at the silyl or stannyl groups rather than at the phosphorus center.

The second method (233) involves the reaction of methyltrifluoromethanesulfonate with the chiral resolved organophosphinate ester as shown in Figure 54. The stereochemical

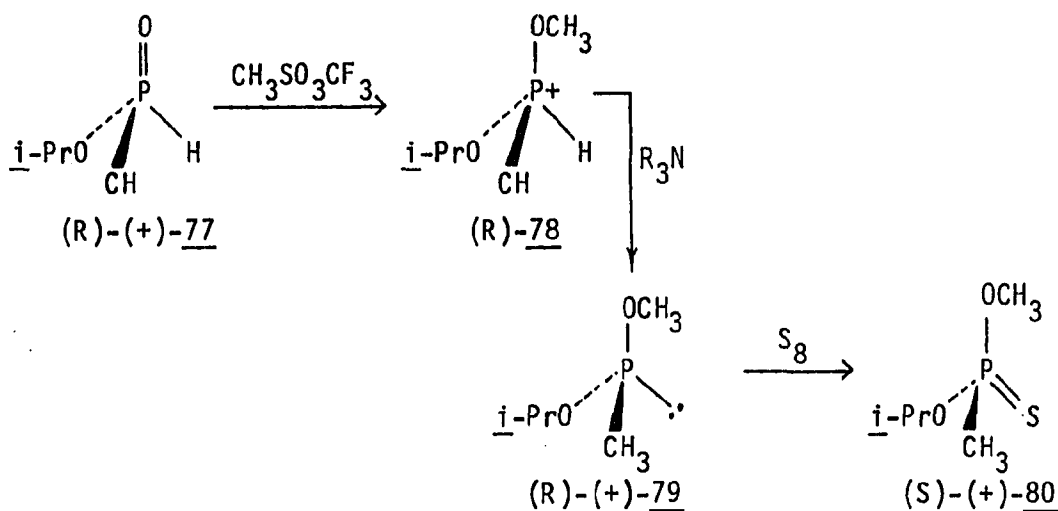


Figure 54. Preparation of chiral 79

assignments were made by reacting the product with elemental sulfur, a reaction known to proceed with retention of configuration, and comparing properties of the resulting sulfide 80 with the known compound whose stereochemical properties have been reported. This reaction appears to be very sensitive to reaction conditions and substituents on the phosphorus, which potentially limit its applicability to phosphinites and phosphonites. Most importantly, both methods involve the use of the resolved forms of organophosphonate compounds which are very difficult to obtain in optically pure form (238).

Tertiary phosphines have received the most attention in resolution techniques. Optically active phosphines have been prepared by a variety of methods (214-224) including silane reduction of the phosphine oxide (214) and cathodic reduction of phosphonium salts (215). None of these methods, however, is readily applicable to other trivalent phosphorus compounds.

In attempts to circumvent many of these problems described above, direct methods using transition metals in diastereomeric complexes have been utilized with good success. The first application of this method to trivalent phosphorus systems was reported by Chan (223) and involved the preparation of asymmetric platinum(II) phosphine complexes. This procedure, summarized in Figure 55, involves the preparation of diastereomeric platinum(II) complexes containing the phosphine to be resolved and a chiral resolved amine ligand. The two diastereomers were separated by fractional recrystallization and the free resolved phosphine obtained by destruction of the complex with cyanide. Similar procedures

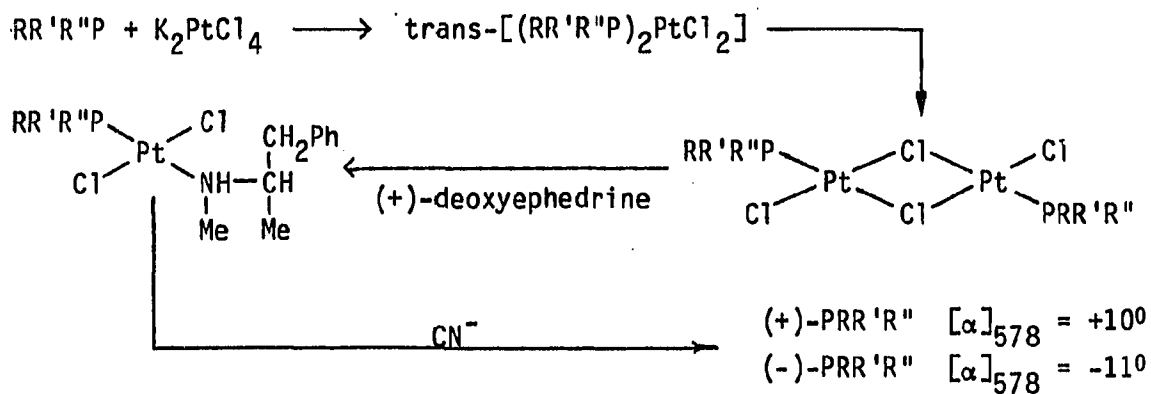


Figure 55. Optical resolution of phosphines by asymmetric platinum(II) complexes

were developed using palladium(II) diastereomeric complexes to resolve other tertiary phosphines (224,225). This method has also been used for arsines with the final separation of the diastereomeric complexes accomplished either by chromatography or fractional crystallization (239). Recently, this method has been shown to be effective using other metal systems (particularly ruthenium) and the stereochemistries of these arsine and phosphine systems have been studied in detail (226,227). The resolutions involving diastereomeric transition metal complexes were restricted to tertiary phosphines and arsines until it was successfully employed to resolve cyclophosphamide 66, isophosphamide 67, and triphosphamide 68. The resolution of triphosphamide 68 by this technique is shown in Figure 56 (209).

This transition metal approach has a number of advantages over the previously mentioned resolution methods. First, both optical isomers should be obtainable in pure form from the initial racemic material. Furthermore, this method usually produces significantly better optical

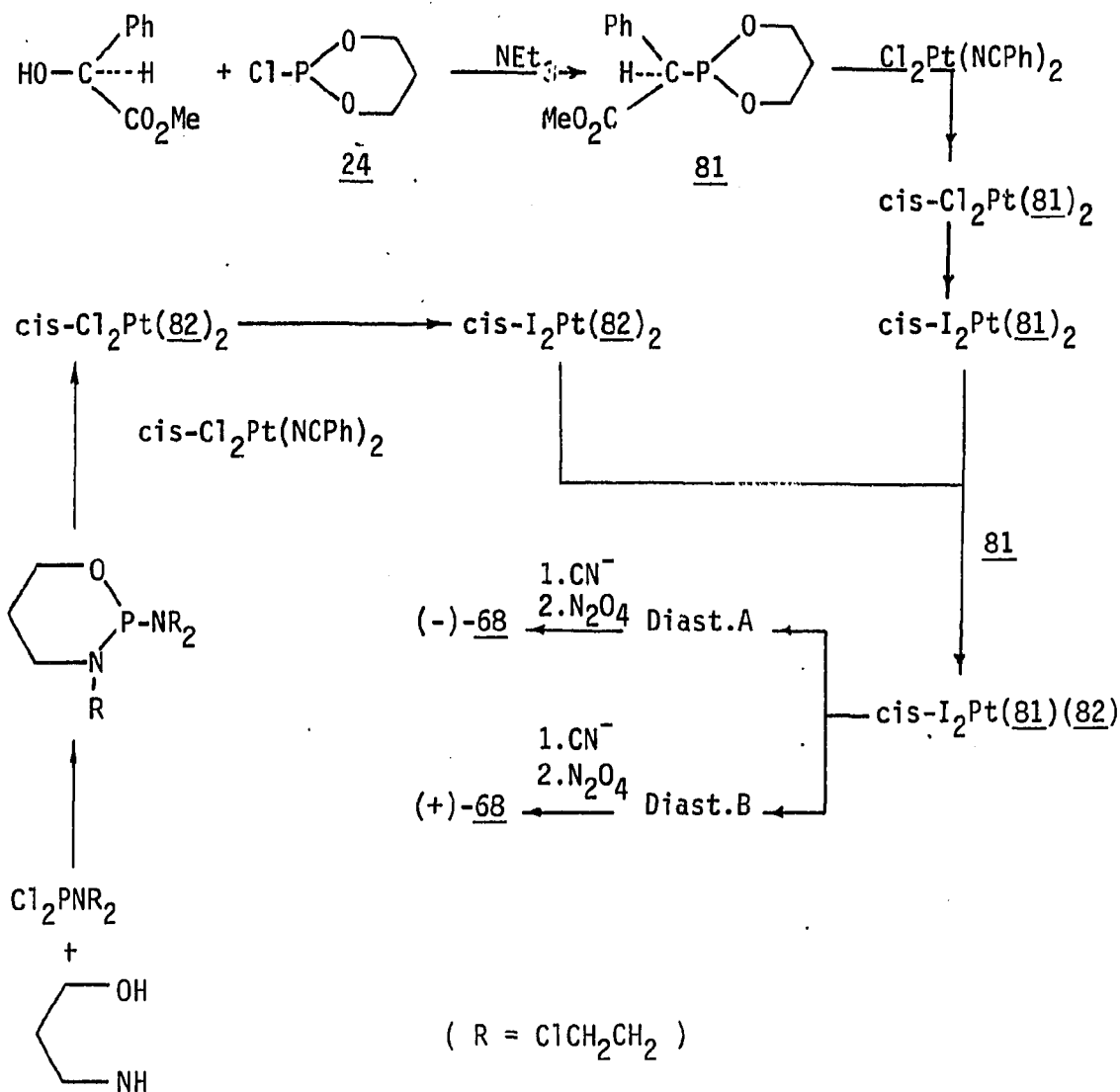


Figure 56. Resolution of triphosphamide 68 via platinum diastereomers

yields which do not rely on an initial difficult resolution of a precursor phosphorus compound. The resolving reagents used in the transition metal diastereomeric complexes (+)-deoxyephedrine and 81 are readily available and easily synthesized in optically pure form, respectively. Finally, as presented here in the following section, the

method appears to be extendable to other phosphorus(III) compounds, particularly phosphites, which is not the case for the other resolution techniques previously discussed.

EXPERIMENTAL

Materials

All solvents used were reagent grade or better and dried according to standard procedures (240). Prior to use, the dry solvents were stored over 4A molecular sieves.

Borane-tetrahydrofuran complex, L-(-)-proline, (S)-(+)-mandelic acid, trifluoroacetic acid, tris[3-((heptafluoropropyl)hydroxymethylene)-d-camphorato]-europium(III)[Eu(hfc)₃], and tris-(6,6,7,7,8,8,8-heptafluoro-2,2-dimethyl-3,5-octa-dionato)europium(III) [Eu(Fod)₃] were used as supplied by the Aldrich Chemical Company. Para-cresol, para-chlorophenol, 1,3-propanediol, and thionylchloride were purchased from the Aldrich Chemical Company and vacuum distilled prior to use. Tris[((trifluoromethyl)hydroxymethylene)-d-camphorato]europium(III) [Eu(Tfc)₃] was used as supplied by Willow Brook Laboratories.

Techniques

NMR spectroscopy

All spectra were obtained in either d₆-benzene or d₁-chloroform solutions at 30°C unless otherwise indicated.

Proton NMR spectra were obtained on a Varian Associates A-60 spectrometer in 5mm (o.d.) tubes. Chemical shifts (ppm) are given relative to tetramethylsilane (TMS) as the internal standard with a positive shift indicating a resonance at a lower applied field than that of the standard. In most of the following experimental procedures,

proton NMR spectroscopy was not found to be a generally useful tool owing to the complexity of the spectra and the similarity of the spectra of many compounds. Thus, proton NMR spectra are not usually reported.

^{31}P NMR spectra were obtained on solution in 10 mm (o.d.) tubes on a Bruker HX-90 spectrometer operating at 36.434 MHz while in the FT mode and locked on the deuterium resonance of the solvent. The spectrometer was interfaced with a Nicolet Instruments 1080 minicomputer system. Eighty-five percent phosphoric acid was used as the external standard in a 1 mm capillary tube held coaxially in the sample tube by a Teflon vortex plug. Chemical shifts at lower applied fields are reported as positive values.

Mass spectrometry

High resolution mass spectra were obtained on an AEI-MS-902 high resolution mass spectrometer and exact masses were obtained by peak matching. Low resolution nominal scan mass spectra were obtained on a Finnigan 4000 mass spectrometer interfaced with a gas chromatograph. All spectral data are reported at 70 eV unless otherwise noted and are rounded to the nearest integral mass unit.

Chromatography

Thin-layer chromatography (TLC) was carried out using Baker-flex (silica gel IB-F and aluminum oxide IB-F) precoated plates. The spots were visualized either by exposure to iodine vapors or UV light.

Column chromatography was performed either with Baker 60-200 mesh silica gel or aluminum oxide which had been dried in an oven at 120°C for 2-3 days. Fractions were collected with an automatic fractionator and the locations of the components were identified by TLC. The columns used were 2.5 x 20 cm and eluted at a rate of 1.0 to 2.0 mL/min. unless otherwise noted.

Melting points

Melting points were measured on a Thomas-Hoover capillary melting point apparatus and are uncorrected.

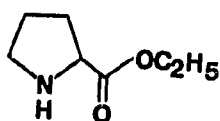
Optical rotations

Optical rotations were measured with a Perkin-Elmer 141 Polarimeter at 25°C. Specific rotations were calculated using equation 15.

$$[\alpha]_{\lambda} = \text{specific rotation} = \frac{\alpha}{lc} \quad (15)$$

λ = wavelength
 α = observed rotation (degrees)
 l = path length (dm)
 c = concentration (gm/mL)

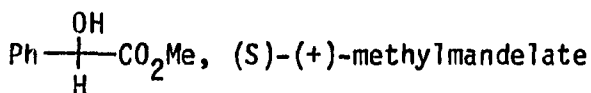
Specific rotations are reported at the specified wavelengths a 1.0 decimeter constant temperature cell.



Preparations

, L-(-)-ethylprolinate

This compound was prepared according to the procedure of Shibaski et al. (241) and purified by vacuum distillation (bp₍₃₎ = 65°C) prior to use.



, (S)-(+)-methylmandelate

This compound was prepared by the method reported previously by Bear and Kates (242) and purified by recrystallization from a benzene/hexane solution.

Cl₂P(OPh), dichlorophenylphosphite, 83

This chlorophosphite was prepared by the reaction of phosphorus trichloride and phenol by the procedure of Schwartz and Geulen (243) and vacuum distilled (bp₍₁₀₎ = 90-92°C) prior to use.

ClP(OCH₂CH₂O), 2-chloro-1,3,2-dioxaphosphorinane, 24

The preparation and purification of this phosphorochloridite was described in Part I of this thesis.

Pt(PhCN)₂Cl₂, bis(benzonitrile)dichloroplatinum(II)

This complex was prepared and purified by the synthetic procedure of Church and Mayo (244).

Pt(COD)Cl₂, (cyclooctadienyl)dichloroplatinum(II)

This complex was prepared as previously reported by Drew and Doyle (245).

para-tolyltrifluoroacetate

This compound was prepared according to the previously reported procedure of Kochi et al. (246) and Belous et al. (247).

Preparation of chiral organophosphorus triesters

Two methods were developed for the preparation of the chiral triester P(OC₆H₅)(OC₆H₄-p-Cl)(OC₆H₄-p-Me), 84, and are described in detail below. Once the purified triester is obtained, it is remarkably stable. After standing at room temperature for three days, only the chiral triester was present (by monitoring with ³¹P NMR spectroscopy). Upon heating a purified sample for 1.5 hours at 100°C, only a small amount of byproducts were obtained (δ³¹P NMR products in (CD₃)₂CO (percentages from integration); 128.4 ppm, P(OC₆H₅)(OC₆H₄-p-Me)₂, 6.0%; 127.8 ppm, 84, 88.1%; 127.3 ppm, P(OC₆H₅)(OC₆H₄-p-Cl)₂, 1.0%). However, the product is not stable in warm solutions containing either triethylamine or triethylamine hydrochloride. Only about 75% and 45% of

the chiral triester remained from the pure sample after 1.5 hours at 100°C in dry ether solutions containing either triethylamine or the hydrochloride, respectively.

Preparation of racemic (para-methylphenoxy)(para-chlorophenoxy)(phenoxy)phosphite (84)

In method A, a solution of 13.96 grams (71.63 mmol) of dichlorophenylphosphite in 500 mL of dry diethyl ether was cooled to 0°C under a dry nitrogen atmosphere in a three liter flask which was equipped with a mechanical stirring apparatus. To this was added slowly over a period of one hour a solution of 7.736 grams (71.63 mmol) of para-cresol and 7.248 grams (71.63 mmol) of freshly distilled triethylamine in 500 mL of dry ether. After the addition was complete, the reaction was stirred for an additional hour at 0°C. To this was then added over one hour a second solution containing 9.201 grams (71.63 mmol) of para-chlorophenol and 7.248 grams (71.63 mmol) of triethylamine in 500 mL of dry ether. When the addition was complete, the reaction was allowed to warm slowly to room temperature while stirring for an additional half hour (note: increased reaction time only increases the amount of side products). The triethylamine hydrochloride was filtered off and washed with 100 mL of cold diethyl ether. The filtered amine hydrochloride was dried and a 99.6% (19.65 grams) yield was recovered. The ether was removed by a water aspirator evaporator from the product leaving a yellowish oil which was purified first by a rapid flame distillation (b.p.(0.5) = 150°C)

followed by column chromatography on 60 grams of silica gel per gram of sample dissolved in eluate solvent mixture and eluted with 4 hexane:1 chloroform (see Table 54 for product data). The chromatography was continuously monitored by TLC and ^{31}P NMR. The desired pure product was obtained as a clear, colorless oil in 41.4% yield (based on the amount of 84 in the material chromatographed, as estimated by ^{31}P NMR) and was stored under dry nitrogen at 0°C until used. (^1H NMR (CDCl_3) 6.61-7.42 (complex multiplet centered at 7.06 (13H), 2.28 (s, 3H); other data in Table 55).

In method B, a solution of 3.30 grams (25.7 mmol) of para-chlorophenol, 2.77 grams (25.7 mmol) of para-cresol, and 5.19 grams (51.3 mmol) of triethylamine in 200 mL of dry ether was added dropwise over a period of two hours to a solution of 5.00 grams (25.7 mmol) of dichlorophenylphosphite in 500 mL of dry ether at 0°C under a nitrogen

Table 54. Chromatographic and spectroscopic data of product from method A for $\text{P}(\text{OC}_6\text{H}_5)(\text{OC}_6\text{H}_4\text{-p-Cl})(\text{OC}_6\text{H}_4\text{-p-Me})$ 84

Compound	R_f	% of product ^a	δ ^{31}P	P^+ (%) ^b
$(\text{ClPhO})_2\text{POPh}$	0.22	16.3	128.35	379.(7.1)
<u>84</u>	0.18	48.6	127.83	358.(11.9)
$(\text{MePhO})_2\text{POPh}$	0.12	35.1	127.31	338.(2.3)

^aPercentages after distillation but prior to chromatography.

^bMass spectral parent ion (m/e) in given % of base peak.

Table 55. Chromatographic retention times (R_f)^a of some diastereomeric organophosphorus compounds on silica gel

Compound	Solvent	R_f
<u>86</u> P(OPh)(O-C ₆ H ₄ -p-Cl)(L-EtProl) ^b	4PhH/1 CHCl ₃	0.35 ^c 0.29 ^c
<u>87</u> P(OPh)(OEt)(L-EtProl)	8PhH/1 CHCl ₃	0.83 ^{c,d} 0.78 ^{c,d}
<u>88</u> P(OPh)(OCH ₂ CH ₂ φ)(L-EtProl)	10PhH/1 CHCl ₃	0.50 ^{c,d} 0.48 ^{c,d}
<u>89</u> P(OPh)(OEt)(D-Methamphet.) ^e	6PhH/1 CHCl ₃	0.6 ^{c,d} 0.6 ^{c,d}
<u>90</u> P(OPh)(OEt)(L-EtProl)-BH ₃	9PhH/1 CHCl ₃	0.45 ^c 0.41 ^c

$${}^a R_f = \frac{\text{distance from origin to spot}}{\text{distance from origin to solvent front}}$$

^bL-EtProl refers to the group $-\overline{N(CH_2CH_2CH_2CH(CO_2Et))}$.

^cDiastereomers.

^dA great deal of "smearing" of the spots occurs making actual spot location difficult.

^eD-methamphet refers to the group $-N(Ph)CH(Me)(CH_2Me)$.

atmosphere. After the addition was complete, the reaction was allowed to stir for an additional hour at 0°C followed by filtration of the precipitated amine hydrochloride which, after washing with 50 mL of cold ether and drying, gave a 99.0% yield (6.99 grams). The ether was removed via a water aspirator evaporator to yield a colorless oil. Purification of the chiral triester from the other reaction products was accomplished via column chromatography, as in method A, to obtain a 50.9% yield.

Preparation of racemic trialkyl-phosphites

The method used to prepare 84 also works well for the preparation of the chiral trialkylphosphite 85, beginning, however, with phosphorus trichloride and sequentially adding various alcohols.

Preparation of racemic (tert-butoxy)(ethoxy)(methoxy) phosphite (85)

A solution containing 13.40 grams (97.56 mmol) of phosphorus trichloride in one liter of dry diethyl ether was placed in a two liter flask equipped with a dry nitrogen flush, mechanical stirring apparatus, and an ice bath. To this was added dropwise over one hour a solution of 7.231 grams (97.56 mmol) of tert-butyl alcohol freshly distilled from calcium hydride and 9.872 grams (97.56 mmol) of triethylamine in 100 mL of ether. After the addition was complete, a second solution containing 4.495 grams (97.56 mmol) of dry ethanol and 9.872 grams (97.56 mmol) of triethyl amine in 100 mL of ether was added dropwise over one hour. This was followed by a solution containing 3.126 grams (97.56 mmol) of dry methanol and 9.872 grams (97.56 mmol) of triethylamine in 100 mL of ether. Ice temperature and rapid stirring was maintained throughout each of these additions. The reaction mixture was filtered and the precipitate washed with 200 mL of cold, dry ether which, upon drying, gave a 98.70% yield (39.76 grams) of triethylamine hydrochloride. The solvent was removed in vacuo to yield a colorless oil. Further purification was accomplished by column chromatography on 60 grams of silica gel per 1.0 gram of sample with 4 hexanes:1 chloroform used as

eluates. (^{31}P NMR (CDCl_3) single peak at 135.70; m/e of P^+ = 180.1, 0.01 rel. int.).

This compound appears to be somewhat less stable toward redistribution reactions at room temperature than the triarylphosphite as shown by monitoring with ^{31}P NMR spectroscopy. It also appears that the order of the alcohol addition is important with the bulkiest alcohol being reacted first and the least bulky last.

(S)-(+)-((carbomethoxy)phenyl)methoxy)-1,3,2-dioxaphosphorinane (81)

The reaction of 2-chloro-1,3,2-dioxaphosphorinane with optically pure (S)-(+)-methyl mandelate yielded the (S)-(+)-2-((carbomethoxy)phenyl)methoxy)-1,3,2-dioxaphosphorinane by a modified procedure similar to that of Wroblewski et al. (209) but sufficiently modified so that a complete description of the procedure is given here. In a typical experiment, a solution containing 2.76 (16.6 mmol) of (S)-(+)-methyl mandelate and 1.68 grams (11.6 mmol) of triethylamine in 75 mL of ether was added dropwise over two hours to a mechanically stirred solution of 2.33 grams (16.6 mmol) of 2-chloro-1,3,2-dioxaphosphorinane 24 in 200 mL of dry ether cooled to 0°C and under a nitrogen atmosphere. The reaction mixture was allowed to slowly warm to room temperature over two hours and the amine hydrochloride filtered off and washed with two 50 mL portions of ether. The amine hydrochloride was dried and yielded 97.7% of the expected amount (2.24 grams). The ether was removed with a water aspirator evaporator and the product was flame distilled ($\text{bp}(0.025) =$

135°C) to obtain a 75.1% yield (3.02 grams) of the pure material ($[\alpha]_{589}^{25} = 45.1$ (CHCl_3) (lit. value = 44.9 (209)); ^1H and ^{31}P NMR spectra corresponded to that previously reported (209).

Preparation of (p-methylphenyl)(p-chlorophenyl)phenylphosphate (91)

Under an atmosphere of dry nitrogen, 1.00 gram (26.7 mmol) of the pure triester 84 was dissolved in 50 mL of dry methylene chloride and cooled to -30°C . Gaseous N_2O_4 was bubbled through the solution through an 18 gauge needle until the solution became greenish in color. The reaction mixture was allowed to stir for 0.5 hours at -30°C and then warmed slowly to room temperature. This solution was first washed with 75 mL of a 5% aqueous sodium bicarbonate solution followed by washing with 150 mL of distilled water. The organic layer was then separated and dried over sodium sulfate and the solvent removed in vacuo to obtain a slightly yellowish oil in 88.2% yield ($\delta^{31}\text{P}$ NMR (CDCl_3) -17.20).

Diastereomeric organophosphorus esters

Several diastereomeric phosphorus triesters and their derivatives have been synthesized herein using an optically active amine. These chiral amino groups can then be quantitatively removed by reaction with para-tolyltrifluoroacetate to generate the racemic free enantiomeric para-tolyl triester with the chiral site at phosphorus. These diastereomeric compounds were synthesized in attempts to resolve the

triesters directly using classical resolution techniques followed by amine removal to obtain the enantiomeric triester.

Chromatographic retention times (R_f) for these compounds which were purified by chromatography are given in Table 55.

(phenoxy)(chloro)(L-ethylprolinato)phosphite (92)

Under a dry nitrogen atmosphere, 4.209 grams (20.41 mmol) of dichlorophenylphosphite 83 was dissolved in one liter of dry diethyl ether in a flask equipped with a mechanical stirring apparatus and ice bath. To this solution was added dropwise a solution of 3.088 grams (21.60 mmol) of L-ethylprolinate and 2.185 grams (21.60 mmol) of triethylamine in 100 mL of dry ether. After the addition was complete, the amine hydrochloride was filtered off and washed with 100 mL of cold ether which, after drying, gave a 97.51% yield (2.899 grams). The solvent was removed in vacuo to obtain a clear, colorless oil (δ^{31P} NMR ($CDCl_3$) 166.6 and 166.1 for the two diastereomers).

(phenoxy)(para-chlorophenoxy)(L-ethylprolinato)phosphite 86

In 125 mL of dry diethyl ether was dissolved 4.220 grams (21.65 mmol) of dichlorophenylphosphite 83 in a 500 mL flask equipped with a nitrogen inlet and mechanical stirring apparatus. To this solution, cooled to 0°C, was added dropwise over two hours a solution containing 3.099 grams (21.65 mmol) of L-ethylprolinate and 2.191 grams (21.65 mmol) of triethylamine in 75 mL of ether. After this addition was complete, a

solution containing 2.781 grams (21.65 mmol) of para-chlorophenol and 2.191 grams (21.65 mmol) of triethylamine in 75 mL of ether was added dropwise over two hours while maintaining the 0°C temperature. After this last addition was complete, the reaction mixture was allowed to stir for an additional fifteen minutes and the amine hydrochloride filtered off and washed with 50 mL of cold ether which, after drying, gave a 98.50% yield (5.870 grams). The ether was removed in vacuo yielding a colorless oil. The product was purified by a rapid, short path, vacuum distillation (b.p.(0.1) = 165-170°C; $\delta^{31}\text{P}$ NMR (d_6 -acetone) 136.9 and 137.4; m/e P^+ 394.(12.36%), (base) at 77. (+Ph)).

(phenoxy)(ethoxy)(L-ethylprolinato)phosphite 87

In a manner analogous to that used in the preparation of 86, 3.979 grams (20.41 mmol) of dichlorophenylphosphite 83 was dissolved in one liter of dry diethyl ether followed by a solution of 2.923 grams (20.41 mmol) of L-ethylprolinate and 2.065 grams (20.41 mmol) of triethylamine in 75 mL of ether and a solution of 0.9390 grams (20.41 mmol) of dry ethanol and 2.065 grams (20.41 mmol) of triethylamine in 100 mL of dry ether. The amine hydrochloride, after filtration, washing, and drying, yielded 97.4% (5.473 grams) of the expected amount. The solvent was removed in vacuo to yield a colorless oil. The product was further purified by column chromatography on silica gel using benzene/1 chloroform as eluant ($\delta^{31}\text{P}$ NMR (CDCl_3) at 141.2 and 139.9 for the two diastereomers; m/e P^+ at 311. (base) at 77. (+Ph)).

(phenoxy)(phenethoxy)(L-ethylprolinato)phosphite 88

To a solution of 5.079 grams (26.06 mmol) of dichlorophenylphosphite 83 in one liter of dry diethyl ether in a flask equipped with a mechanical stirring apparatus, ice bath, and dry nitrogen purge was added dropwise a solution containing 3.730 grams (26.06 mmol) of L-ethylprolinate and 2.637 grams (26.06 mmol) of triethylamine in 100 mL of dry ether. When this addition was complete, a second solution containing 3.184 grams (26.06 mmol) of phenethyl alcohol and 2.637 grams (26.06 mmol) of triethylamine in 100 mL of ether. After the reaction mixture had warmed to room temperature, the amine hydrochloride was filtered off, washed with 250 mL of cold ether, and dried to give a 95.11% (6.823 grams) yield. The product was purified by column chromatography using silica gel and eluting with a 3 benzene/1 chloroform solution ($\delta^{31}\text{P}$ NMR (CDCl_3) 141.1 and 139.7 for the two diastereomers).

(phenoxy)(ethoxy)(D-methamphetamino)phosphite 89

In a manner analogous to that used for 87, 3.942 grams (20.22 mmol) of dichlorophenylphosphite 83 was dissolved in one liter of dry diethyl ether in a flask equipped with a mechanical stirring apparatus and cooled to 0°C while under a dry nitrogen atmosphere. To this was added in a dropwise manner a solution of 2.277 grams (20.22 mmol) of D-methamphetamine and 2.046 grams (20.22 mmol) of triethylamine in 100 mL of dry ether followed by a solution of 0.9301 grams (20.22 mmol) of dry ethanol and 2.046 grams (20.22 mmol) of triethylamine in 100 mL of dry

ether. After the additions were complete, the reaction mixture was warmed to room temperature and the amine hydrochloride filtered off to give (after washing with 250 mL of cold ether and drying) a 91.6% (5.099 grams) yield. The ether was then removed in vacuo to give a slightly yellowish oil. This material was purified by column chromatography using silica gel (2.5 x 20 cm) and eluted with a solution mixture of 1 chloroform/3 benzene. The final product was obtained as a clear, colorless oil ($\delta^{31}\text{P}$ NMR (CDCl_3) 144.6 and 143.6 for the two diastereomers; m/e P+ at 317. m/e , (base) at 77).

(phenoxy)(ethoxy)L-ethylprolinato)phosphite-borane adduct 90

Under a dry nitrogen atmosphere, 1.774 grams (5.705 mmol) of the trivalent phosphite 87 was dissolved in 175 mL of dry diethyl ether and cooled to 0°C. To this was then added dropwise a 1.0 M solution containing 6.846 mMol (20% stoichiometric excess) of a borane-tetrahydrofuran complex solution over ten minutes. The reaction was allowed to warm slowly to room temperature followed by removal of the solvent in vacuo. The crude product was obtained as a very viscous, clear, colorless oil. This material was purified by column chromatography on silica gel eluting with 9 benzene/1 chloroform. Upon removal of the solvent in vacuo, a viscous, clear, colorless oil was obtained as the final product ($\delta^{31}\text{P}$ NMR (CHCl_3) 73.3 and 70.2 for the two diastereomers).

Reaction of 86 with para-tolyltrifluoroacetate

At room temperature and under a dry nitrogen atmosphere, 1.0 gram (2.5 mmol) of 86 was treated with 0.52 grams (2.5 mmol) of para-tolyltrifluoroacetate. A summary of the reaction conditions and times of reactions is shown in Table 56. The best results are obtained using no solvent and allowing the two reactants to mix for two days at room temperature. Compound 84 is obtained pure via column chromatography using silica gel and eluting with 4 benzene/1 chloroform. Under these chromatographic conditions, 84 has an R_f of 0.73 while all impurities either stay near the origin (para-chlorophenol, L-ethylproline, and para-tolyltrifluoroacetate) or at R_f 's of 0.35 and 0.29 (for the two diastereomeric 86 reactants). Other properties of 84 correspond well with those already presented for this compound.

Table 56. Product dependence on the reaction conditions of 86 with paratolyltrifluoroacetate

Solvent	Temp.	Reaction time	Percentage of component		
			<u>84</u>	<u>86</u>	Other
Ether	R.T.	1.5 hr.	0.0	100.0	0.0
CH ₂ Cl ₂	R.T.	2.0 da.	4.1	95.8	0.1
None	100°	1.0 hr.	16.2	78.2	5.6
None	100°	4.0 hr.	27.0	70.9	2.1
None	R.T.	2.0 da.	62.8	37.1	0.1
None	R.T.	4.0 da.	27.0	70.9	2.1

Chiral stationary phase and normal phase liquid chromatography

Two 3,5-dinitrobenzoyl derivatized porasil (highly purified 10 micron silica gel) chiral stationary phase (CSP) column packings were prepared ("CSP IV" and "CSP XIII", using Pirkle and Finn's nomenclature (248)). Chiral stationary phase IV was prepared as described in the literature (249). Chiral stationary phase XIII was prepared from the aminofunctionalized porasil using 3,5-dinitrobenzoylphenylglycine, in the presence of N-ethoxycarbonyl-2-ethoxy-1,2-dihydroquinoline (EEDQ) by the procedure previously published (250). The HPLC columns were prepared by standard slurry packing procedures in stainless steel liquid chromatography (LC) tubes (30 cm x 4.1 mm i.d.). All experiments were conducted using HPLC grade solvents at 25°C on a Varian Associates Model 5000 Liquid Chromatograph operating at pressures ranging from 10 to 100 atm. The elution of compounds was monitored by observed optical absorptions at 256 nm. The sample solutions were injected into the stream via syringe in 1-10 μ L quantities.

Normal phase LC was carried out as above using a standard 10 μ porasil LC column (30 cm x 4.1 mm i.d.). The operation of this system was checked each time prior to use to injection of a solution containing dinonyl, dibutyl, diethyl, and dimethyl phthalates and eluting with 15% tetrahydrofuran-85% hexane. The elution was monitored at 256 nm and the separation evaluated by comparison with reported separations.

Purification of 84 was accomplished on the porasil column eluting with a 4:1 benzene/chloroform mixture at a flow rate of 1.2 mL/min and a

pressure of 24 psi. The elution of the product was monitored by observed optical absorptions at 256 nm.

Resolution of a triaryl phosphite via diastereomeric platinum complexes
cis-dichloro-bis(phosphito)platinum(II) complexes

Two methods have been developed for the preparation of the cis-dichloroplatinum(II) complexes of the chiral phosphite 84. Method A involves the direct interaction of the trivalent chiral phosphite with a platinum(II) precursor complex. This procedure requires the preparation and purification of the chiral phosphite previous to coordination. Because of the mobility of the phenoxy groups in aromatic triesters, it is difficult to prepare these triesters easily in high purity (see previous procedure for 84). For these reasons, method B was developed which involved the initial coordination of a readily available and easily purified dichloro-phosphorus(III) precursor compound to the platinum, followed by the generation of the chiral triester complex in situ by subsequent reaction of the dichloro-phosphorus complex with alcohols. Method B, therefore, has some advantages over method A to prepare the desired complex and is readily extendable to other phosphite systems (vide infra).

cis-[Cl₂Pt(84)₂] 93

In method A, a solution of 0.5437 grams (15.17 mmol) of pure 84 in 25 mL of methylene chloride was added dropwise to a solution of 0.7160

grams (15.17 mmol) of cis-dichloro-bis(benzonitrile)platinum(II) in 50 mL of dry methylene chloride at 0°C under nitrogen. The colorless reaction mixture was allowed to slowly warm to room temperature and stir overnight. To this solution was added 25 mL of dry ethanol and the methylene chloride removed by a water aspirator evaporator until the colorless complex crystallized. The solution was then stored at 0°C for 24 hours and the white crystals collected, washed with cold ether, and dried under vacuum (yield = 58.97%, 0.8796 grams; mp = 134–136°C; $\delta^{31\text{P}}$ NMR (CHCl_3) 60.39, $^1J_{\text{PtP}} = 5784$ Hz).

In method B, a solution of 0.826 grams (4.24 mmol) of dichloro-phenylphosphite 83 in 10 mL of chloroform was added to a solution of 1.00 grams (2.12 mmol) of cis-dichloro-bis(benzonitrile)platinum(II) in 25 mL of dry chloroform. The reaction mixture was refluxed for 1.5 hours under a dry nitrogen atmosphere. The mixture was then cooled to 0°C and a solution of 0.458 grams (4.24 mmol) of para-cresol and 0.429 grams (4.24 mmol) of triethylamine in 50 mL of chloroform was added dropwise. After the addition was complete, the reaction was allowed to stir for 0.5 hours while maintaining the temperature at 0°C. To this mixture was then added dropwise a solution of 0.545 grams (4.24 mmol) of para-chlorophenol and 0.429 grams (4.24 mmol) of triethylamine in 50 mL of chloroform. The solution was allowed to warm to room temperature and stir for one hour. The chloroform was removed by a water aspirator evaporator and to the residue was added 75 mL of dry acetone. The triethylamine hydrochloride was then filtered off and washed twice with 25 mL of ethanol giving a 91.3% yield (after drying). The acetone was evaporated and the complex

recrystallized from methylene chloride/ethanol to obtain a 51.3% yield based upon the amount of cis-dichloro-bis(benzonitrile)platinum(II) used as reactant.

As shown in Table 57, the main product is the desired chiral triester complex but the disubstituted triesters are also formed as impurities. There appears to be a slight temperature dependence on the ratios of products formed. The complex containing the chiral trivalent ligand can be obtained in a pure form by column chromatography using silica gel and eluting with chloroform (2.5 x 50 cm.; see Table 57 and method A for R_f values and characterization data, respectively).

Table 57. Spectroscopic and yield data for cis-[Cl₂PtL₂] complexes from method B

Ligand	δ ³¹ P	R_f	M.p.	Reaction Temperature		
				-25 %	0 %	+25 %
PhOP(OPhMe) ₂	59.6	0.82	154°	17.9	50.0	33.3
PhOP(OPhCl) ₂	61.0	0.65	159°	30.8	15.0	25.0
<u>84</u>	60.39	0.34	134-136°	51.3	35.0	41.7

Using this procedure, other cis-dihaloplatinum-bis(phosphite) complexes can easily be prepared in an analogous manner. Data for these complexes are shown in Table 58.

Table 58. Spectroscopic and physical data for cis-platinum-phosphite complexes, cis-[X₂PtL₂]

X	Ligand	% Yield	M.p.	δ ³¹ P	¹ J _{PtP} (Hz)	δ ³¹ P free ligand
Cl	PhOPCl ₂	----	oil	98.2	5619	176.8
Cl	PhOP(OPhMe) ₂	91.6	154	59.7	5797	127.4
Cl	PhOP(OPhCl) ₂	92.5	159	61.0	5761	128.4
Cl	MePhOP(OPhCl) ₂	77.3	173	60.9	5766	127.3
Cl	ClPhOP(OPhMe) ₂	81.7	165	60.2	5784	127.7
Cl	<u>84</u>	51.3	135	60.4	5784	127.8
I	PhOP(OPhMe) ₂	86.4	164	59.6	5517	127.4
I	ClPhOP(OPhMe) ₂	81.3	130	60.1	5493	127.7
I	<u>84</u>	88.2	130	59.6	5496	127.8

cis-[Cl₂Pt(81)₂](94)

This complex was prepared by the reaction of 0.9743 grams (2.064 mmol) of cis-dichlorobis-(benzonitrile)platinum(II) with 0.5576 grams (2.064 mmol) of 81 by the method of Wroblewski et al. (209). A 53.0% yield of product was obtained after column chromatography on 50 grams of silica gel eluted first with methylene chloride (to elute the liberated benzonitrile), then methylene chloride/acetone (40:1, to remove the starting dichloro-bis(benzonitrile)platinum(II) complex), and finally methylene chloride/acetone (10:1, to obtain the desired product).

Optical rotations and NMR data corresponded well with those previously reported (209) ($\delta^{31\text{P}}$ NMR (C_6D_6) 69.1, $^1J_{\text{PtP}} = 5742$ Hz).

cis-[I₂Pt(84)₂](95)

This complex was prepared from the corresponding dichloride by halogen methasis (251) using a large excess of sodium iodide. To a stirred solution of 0.8792 grams (0.8946 mmol) of the cis-dichloro-bis(84)platinum(II) complex in 50 mL of dry acetone under nitrogen was added 0.3401 grams (2.267 mmol) of vacuum dried sodium iodide. The reaction was allowed to stir for four hours, filtered, and the acetone removed in vacuo. The product was extracted from the resulting residue with two 100 mL portions of methylene chloride and filtered. The solvent was then removed and the remaining yellow powder redissolved in a minimum of methylene chloride and chromatographed with methylene chloride on 50 grams of silica gel to give the yellow crystalline product (88.18% yield; m.p. = 130°C; $\delta^{31\text{P}}$ NMR (d^6 -acetone) 59.6, $^1J_{\text{PtP}} = 5496$ Hz).

cis-[I₂Pt(81)₂](96)

Halogen methasis (251) of the corresponding dichloroplatinum(II) precursor complex yielded, after column chromatography on silica gel and eluted with methylene chloride, the diiodoplatinum complex. Optical rotations and NMR data corresponded well with those previously reported (206) ($\delta^{31\text{P}}$ NMR (C_6D_6) 75.1, $^1J_{\text{PtP}} = 5525$ Hz).

Preparation and resolution of diastereomeric cis-[I₂Pt(84)(81)] complexes

(97 A and B)

In 150 mL of dry benzene, 0.2000 grams (0.2021 mmol) of cis-[I₂Pt(81)₂], 0.2357 grams (0.2021 mmol) of cis-[I₂Pt(84)₂] and 0.002 grams of free 81 were dissolved. The reaction mixture was refluxed for 10 hours under a dry nitrogen atmosphere. The solution was then filtered, followed by evaporation of the solvent to yield a yellow powder as product. This material was then dissolved in a minimum of dry methylene chloride and chromatographed on 70 grams of silica gel at a flow rate of 1.0 mL per minute. Five mL fractions were collected and monitored by TLC. Four distinct bands were observed and collected and the identity of each band was determined by R_f values and NMR spectroscopic data (Table 59).

Liberation and purification of resolved chiral 84

From the separated diastereomeric complexes described in the previous section, the optically pure phosphite enantiomers were obtained by reaction of the complex with cyanide ion. Compound 84 was separated from 81 by column chromatography. The procedure described below was the same for both of the diastereomeric complexes.

Table 59. Chromatographic separation and NMR data for diastereomeric cis-[I₂Pt (84)(81) complexes

Compound	Band	Fraction	R _f	δ ³¹ P	¹ J _{PtP}
unreacted cis-[I ₂ Pt(<u>84</u>) ₂]	1	8-11	0.72	59.6	5496
<u>97</u> , diastereomer A	2	15-18	0.41	64.8	5869
				63.6	5481
<u>97</u> , diastereomer B	3	28-32	0.31	66.6	5852
				64.5	5487
unreacted cis-[I ₂ Pt(<u>81</u>) ₂]	4	60-70	0.14	75.1	5525

To a solution of 0.1020 grams (0.08718 mmol) of the resolved diastereomeric complex dissolved in 75 mL of dry methylene chloride was added 0.0340 grams (0.8718 mmol) of dry sodium cyanide. The solution turned colorless immediately and was allowed to stir overnight under a dry nitrogen atmosphere. The colorless precipitate was filtered off and the solvent removed in vacuo to yield a colorless oil. This oil was redissolved in a minimum of dry benzene and chromatographed on 20 grams of silica gel by elution with pure benzene. Five mL fractions were collected on an automatic fractionator and the location of the two components identified by TLC. The R_f values (silica gel/benzene) were; 84 = 0.76, 81 = 0.09. The solvent was removed in vacuo to yield the pure enantiomer.

Optical rotations and other data for the two enantiomers are reported in Table 60.

Table 60. Spectroscopic and yield data for the resolved enantiomeric phosphite triesters 84

Enantiomer (<u>84</u>)	A	B
% Yield ^a	40.4	39.5
$\delta^{31\text{P}}$	127.8	127.8
optical rotation data ^b :		
obs. rot. (α) (degrees)	+0.124	-0.104
spec. rot. $[\alpha]_{589}^{25}$ (degrees)	+21.4	-18.6

^aBased upon the amount of complex 97 chromatographed.

^bRotations were measured at 589 nm and 25°C in CHCl_3 with a 1.00 dm cell. The concentrations used were diast. A. = 0.058 grams/10 mL, diast. B = 0.056 grams/10 mL.

RESULTS AND DISCUSSION

Chiral Triesters

The first reports of chiral phosphorous triesters of the type $P(OAr)(OAr')(OAr'')$ appeared in a U.S. patent in 1940 (252) and in a brief Russian account in 1956 (253). In the procedure described (252), the substituted phenols were sequentially added to dichlorophenylphosphite while a stream of nitrogen gas was passed through the solution to remove the hydrogen chloride produced. The reaction mixture was then refluxed and distilled under vacuum. The authors did not report, however, further details or attempts to isolate the chiral products from the reaction mixtures in a purified form. In our attempts to prepare chiral triesters by this procedure we found that, in addition to the desired chiral triester, a large number of other triesters were formed. When we performed the reaction of para-cresol and para-chlorophenol with dichlorophenylphosphite at least nine of the ten possible triesters attainable by exchange of the phosphorus substituents were obtained, as identified by ^{31}P NMR spectroscopy. This result was verified by the independent synthesis and characterization of esters of the type $P(OAr)_3$ and of $P(OAr)(OAr')_2$ and measurement of their ^{31}P NMR spectra (254). From the work of Abicht (254) and as seen in Figure 57, replacement of OPh in $P(OPh)_3$ by OC_6H_4-p-Me and OC_6H_4-p-Cl gives rise to downfield and upfield ^{31}P chemical shifts, respectively, in accord with dominance of the paramagnetic term for this nucleus. Furthermore, replacement of OC_6H_4-p-Me in $P(OC_6H_4-p-Me)_3$ by OC_6H_4-p-Cl drives the chemical shift upfield ($P(OC_6H_4-p-Me)_2(OC_6H_4-p-Cl)$, 127.8 ppm; $P(OC_6H_4-p-Cl)_2$, 127.3

Compound	δ ^{31}P
$\text{P}(\text{OC}_6\text{H}_5)_3$	127.8
$\text{P}(\text{O}-\underline{p}\text{-C}_6\text{H}_4\text{Cl})_3$	126.7
$\text{P}(\text{O}-\underline{p}\text{-C}_6\text{H}_4\text{Me})_3$	128.3
$\text{P}(\text{OC}_6\text{H}_5)_2(\text{O}-\underline{p}\text{-C}_6\text{H}_4\text{Cl})$	127.4
$\text{P}(\text{OC}_6\text{H}_5)(\text{O}-\underline{p}\text{-C}_6\text{H}_4\text{Cl})_2$	127.0
$\text{P}(\text{OC}_6\text{H}_5)_2(\text{O}-\underline{p}\text{-C}_6\text{H}_4\text{Me})$	127.9
$\text{P}(\text{OC}_6\text{H}_5)(\text{O}-\underline{p}\text{-C}_6\text{H}_4\text{Me})_2$	128.3

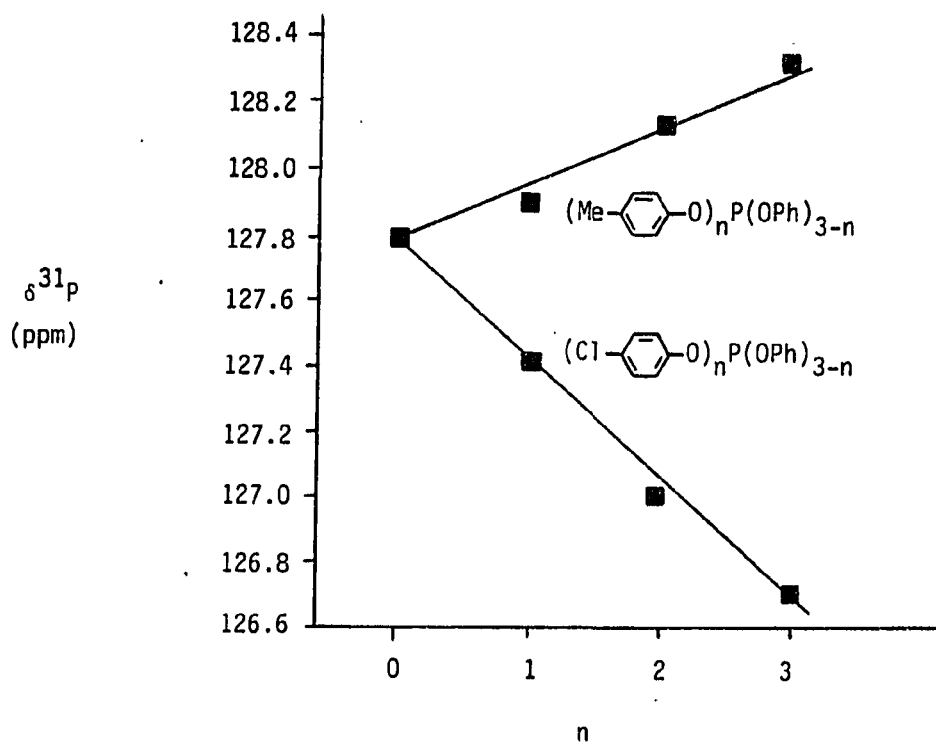


Figure 57. ^{31}P chemical shift dependence upon aromatic substitution in triesters (254)

ppm) while 84 (127.6 ppm) resonates between these values. By this synthetic method, it was also found by Abicht that only triesters of the type $P(OAr)(OAr')_2$ could be obtained in pure form. The mechanism for the exchange involved in such reactions has been postulated to involve a four-center interaction of the type shown in Figure 58 (255).

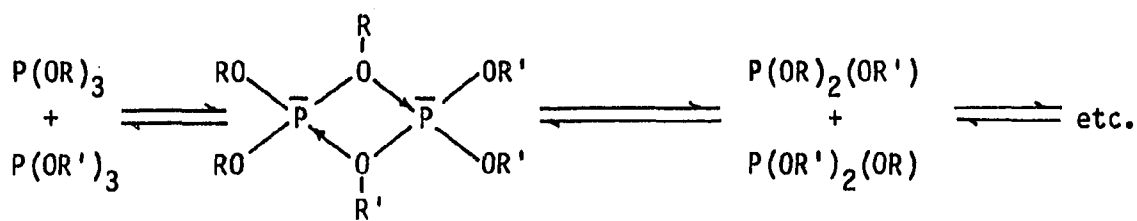
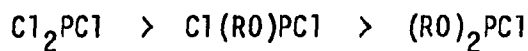


Figure 58. Proposed four-center interaction to account for the observed phosphite product distribution (255)

Very recently, the preparation of $P(O\text{Me})(O\text{-tert-Bu})(O\text{-cyclo-C}_5\text{H}_9)$ has been reported from the reaction of $P(O\text{Me})\text{Cl}_2$ with tert-butanol followed by cyclohexanol in ether (bp. (3.2) = 68-74°C; δ ^{31}P 133.9) (256).

The synthesis of the pure chiral triester in our work was attempted using the three slightly varied procedures shown in Figure 59. The order of the phosphorus-chloro group reactivity with respect to alcohols decreases in the sequence shown below;



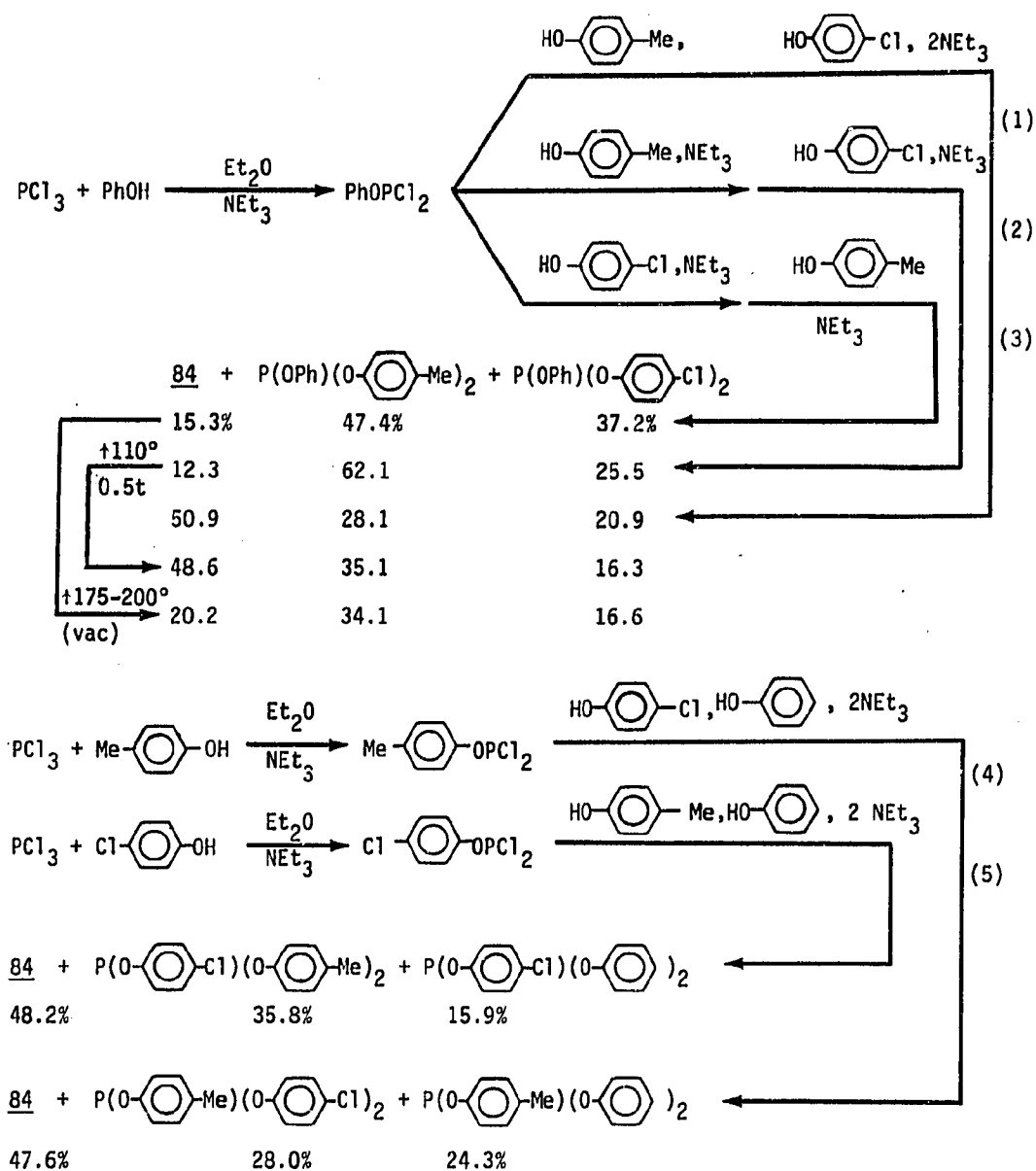


Figure 59. Preparation of chiral triaryl phosphites

From this order of reactivity, it might be expected that addition of the less nucleophilic $\text{HOC}_6\text{H}_4\text{-p-Cl}$ followed by the more nucleophilic $\text{HOC}_6\text{H}_4\text{-p-Me}$ would produce the highest yield of 84. This turns out not to be the case since the highest yield of product, as determined by ^{31}P NMR spectroscopy, is obtained by the simultaneous rather than the sequential addition of the substituted phenols to dichlorophenoxyposphite. On the other hand, rapid flame distillation of the products of reaction (2) in Figure 59 at 110°C and 0.05 torr raised the yield of 84 from 12.3 to 48.6%. Carrying out a slow distillation on the product of reaction (3) in Figure 59 between 175°C and 200°C at correspondingly higher pressures increased the yield of 84 to only 20.2% and four mixed esters in addition to those shown in Figure 59 are detected in the ^{31}P NMR spectrum in yields ranging from 6-8%. Similarly, heating an equimolar mixture of $\text{P}(\text{OC}_6\text{H}_5)(\text{OC}_6\text{H}_4\text{-p-Cl})_2$ and $\text{P}(\text{OC}_6\text{H}_5)(\text{OC}_6\text{H}_4\text{-p-Me})$ at 100°C for 1.5 h showed 19.4% 84 in the complex reaction mixture. In the simultaneous addition procedure, it was also noted that the yield of 84 is dependent upon the temperature at which the addition is done (-25°C , 38.2%; $+35^\circ\text{C}$, 41.3%).

These results suggest that addition of the first phenol derivative in the sequential additions result in considerable reaction of the last phosphorus-chlorine bond before the second phenol derivative is added, especially when the $\text{HO-C}_6\text{H}_4\text{-p-Me}$ is added first. Simultaneous addition of the two substituted phenols to the PhPCl_2 results in an approximate random distribution of the three products (considering no redistribution of groups occurs after formation of the product). Rapid vacuum distillation of the product mixture from reaction (2) greatly increases

the percentage of 84 and results in a product distribution similar to that observed for the simultaneous addition. When the product mixture from the sequential addition in reaction (3) of Figure 59 is slowly distilled, however, the amount of 84 increases only slightly while the percentages of the $\text{PhOP}(\text{OR})_2$ compounds are reduced. In this slow distillation, the percentages of the products approach the expected random distribution amounts based upon complete freedom toward the redistribution of the aryl groups. The expected random distribution values for reaction products with and without substituent redistribution after initial product formation are given in Table 61. This indicates that under prolonged heating, the product distribution is under thermodynamic control while in the rapid distillation the observed product ratio is under kinetic control. The aromatic group in the $\text{Cl}_2\text{P}(\text{OAr})$ starting material does appear to have a small effect upon the resulting product distribution as seen in Table 62.

The chiral triester 84 was isolated in pure form from the other product triesters by column chromatography utilizing a very slow flow rate (0.35 mL/min) and a large ratio of silica gel to triester (circa 60:1) to maximize separation efficiency. High performance liquid chromatography using standard techniques previously discussed and a porasil column was also successful in purifying this triester in a significantly shorter time (see Experimental Section). After purification, 84 is quite stable at room temperature. In d_6 -acetone, for example, the first evidence of scrambling in the ^{31}P NMR appears after

Table 61. Expected random distribution values for the $P(OR)_x(OR')_y(OR'')_z$ systems from the $(RO)PCl_2 + R'OH/R''OH$ reaction with and without substituent redistribution

$(RO)PCl_2 + R'OH/R''OH \longrightarrow P(OR)_x(OR')_y(OR'')_z$					
$OR = OC_6H_5$ $OR' = OC_6H_4-p-Me$ $OR'' = OC_6H_4-p-Cl$					
Expected random distribution values (product percentages)					
x	y	z	without substituent redistribution	with substituent redistribution	
3	0	0	0.0	3.7	
0	3	0	0.0	3.7	
0	0	3	0.0	3.7	
1	2	0	25.0	11.1	
1	0	2	25.0	11.1	
1	1	1	50.0	22.2	
2	1	0	0.0	11.1	
2	0	1	0.0	11.1	
0	2	1	0.0	11.1	
0	1	2	0.0	11.1	

Table 62. Preparation of 84

$$\begin{array}{c} \text{ROH} \\ \text{R}'\text{OH} \\ 2 \text{NEt}_3 \end{array} + \text{R}''\text{OPCl}_2 \xrightarrow{\text{Et}_2\text{O}} (\text{RO})(\text{R}'\text{O})(\text{R}''\text{O})\text{P} + (\text{R}''\text{O})\text{P}(\text{OR})_2 + (\text{R}''\text{O})\text{P}(\text{OR}')_2$$

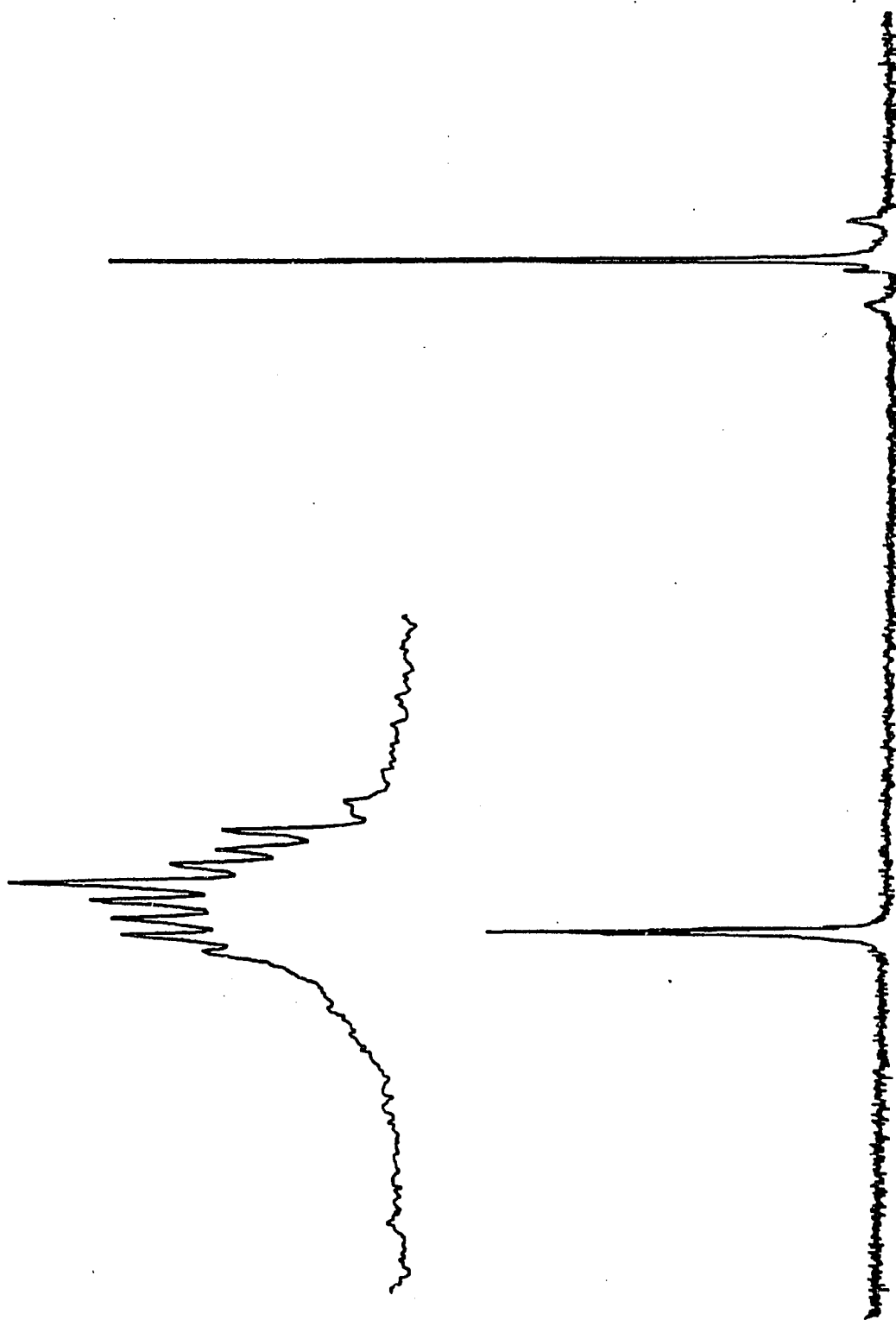
R	R'	R''	Percent Product ^a		
			(RO)(RO')(R''O)P <u>84</u>	(R''O)P(OR) ₂	(R''O)P(OR') ₂
C1Ph-	MePh	Ph-	50.9	20.9	28.1
MePh-	Ph-	C1Ph-	48.2	35.8	15.9
C1Ph-	Ph-	MePh-	47.6	28.0	24.3

^aAs monitored by ³¹P NMR.

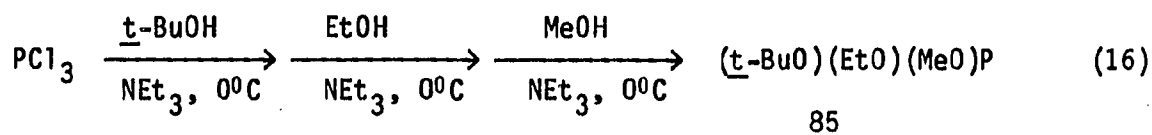
three days. A sample of 84 heated for 1.5 hours at 100°C still retains 88.1% of the starting material along with approximately equal amounts of (PhO)P(OC₆H₄-p-X)₂ (X = Me or Cl). After two months of standing at room temperature, a significant amount of redistribution of the substituents had occurred and at least nine products were observed. The ³¹P NMR spectrum of this sample is shown in Figure 60. In the presence of small amounts of amines or aminehydrochlorides, however, 84 gives rise to 75% of 84 left in the reaction mixture in the former case after 1.5 hours and only 45% of 84 along with a comparatively large number of scrambling products in the latter case after 1.5 hours.

Sequential additions of alcohols to chlorophosphorus compounds is apparently a feasible synthetic procedure for the preparation of mixed trialkyl phosphorus(III) esters. In this manner, (tert-BuO)(EtO)(MeO)P 85

Figure 60. ^{31}P NMR spectrum of 84 after two months at room temperature



was prepared in good yield according to the reaction shown in Equation 16.

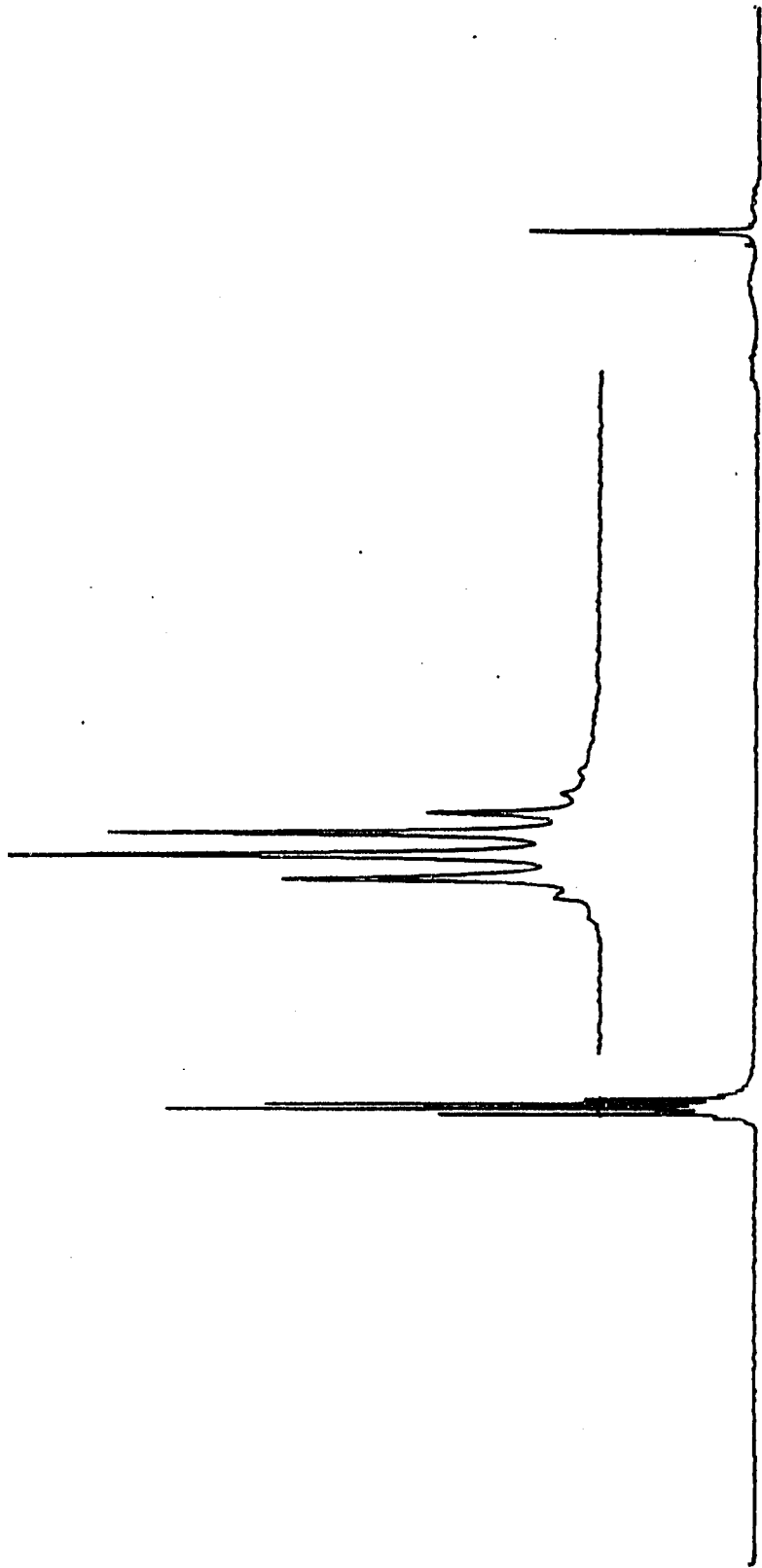


The racemic chiral product can be purified by column chromatography on silica gel. The pure product so obtained is reasonably stable toward redistribution reactions at room temperature but is significantly less stable than the triaryl systems. After four days at room temperature, a substantial amount of scrambling of the phosphorus substituents was found to have occurred as seen in the ^{31}P spectrum shown in Figure 61. As with the triaryl system, the presence of either an amine or its hydrochloride salt was found to greatly increase the rate of substituent redistribution.

Diastereomeric Organophosphorus Esters

The preparation and isolation of the chiral triesters described in the previous section involve rather lengthy and complicated experimental procedures. In an attempt to circumvent some of these synthetic difficulties and at the same time develop a method for the resolution of these compounds, the technique of diastereomer formation and separation was examined. The ease with which paracresyltrifluoroacetate replaces a diethylamino group on phosphorus(III) compounds with a paracresyloxy

Figure 61. ^{31}P NMR spectrum of 85 after four days at room temperature



group with retention of configuration as reported by Horner and Jordan (257) prompted us to investigate this reaction as a possible pathway to chiral phosphorus(III) triesters. In this scheme, the organophosphorus ester is synthesized with one substituent being a chiral amino group in the resolved form, thus forming diastereomeric compounds with chiral centers both at the phosphorus and on the amino substituent. Following the separation of these diastereomers from each other, the chiral amino group could then be replaced by a paracresyloxy group without racemization to generate the free enantiomeric chiral triester. This procedure is summarized in Figure 62.

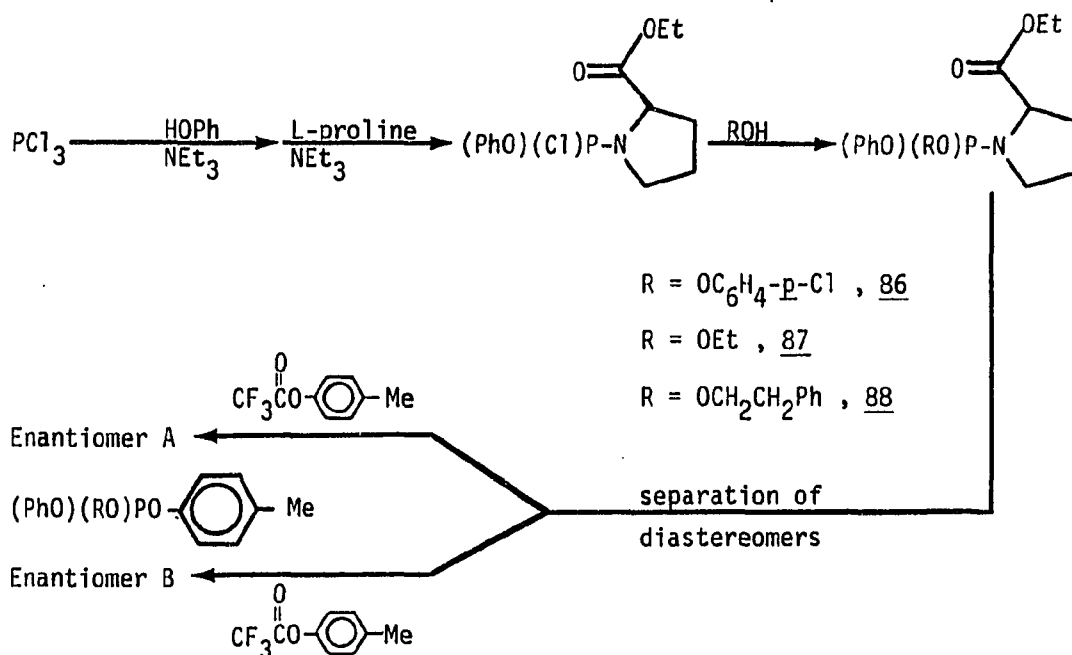
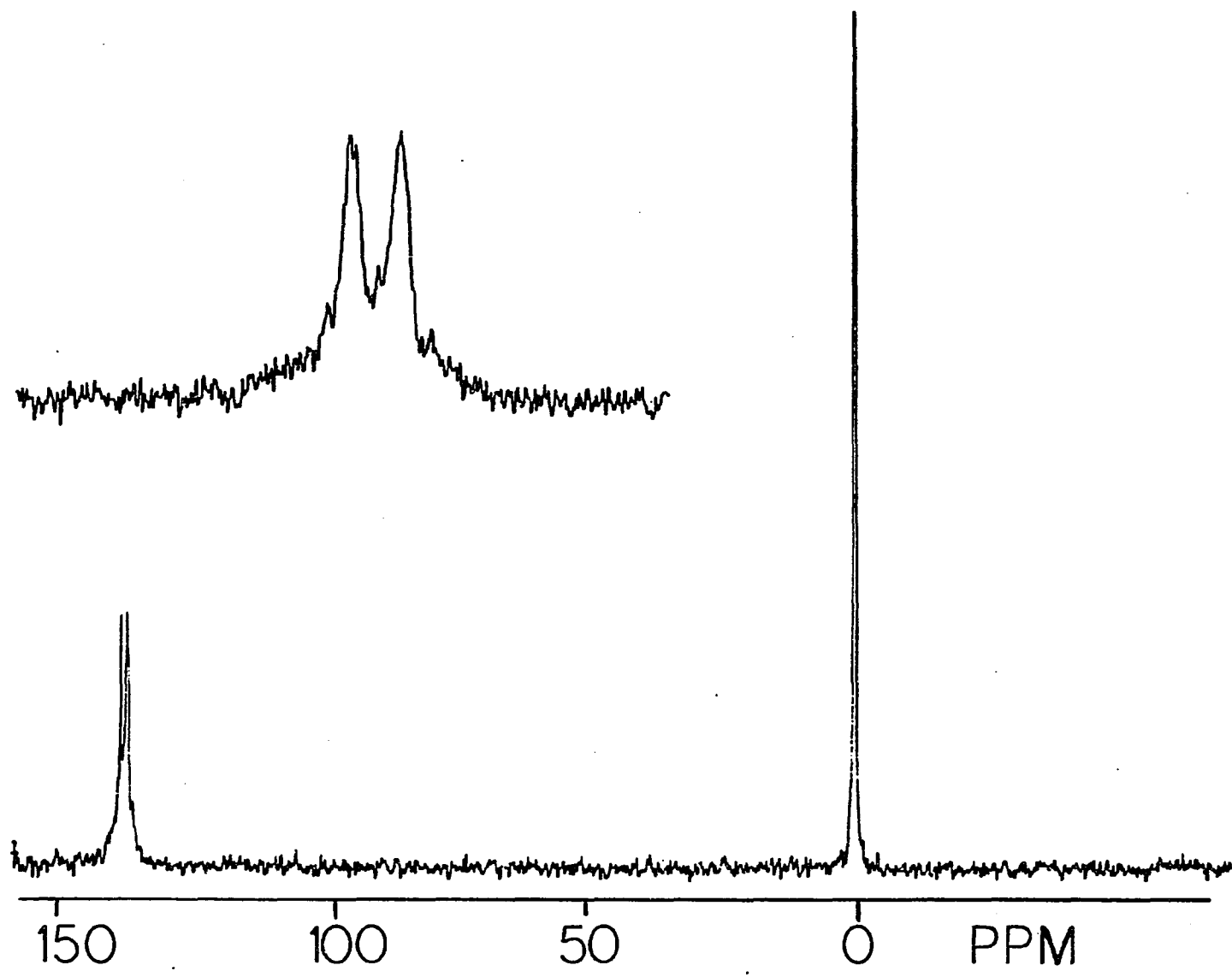


Figure 62. Resolution scheme via chiral amine substituted phosphites

This route potentially could have four important advantages over the previously discussed resolution procedures. First, it appeared to be experimentally convenient because of fewer synthetic steps and involving mainly reactions known to proceed with high yield in closely related systems. Furthermore, this approach did not require the initial preparation, purification, and resolution of precursor organophosphorus compounds which, in most cases, are quite difficult to obtain in pure form. The second potential advantage of the route was that it would use as the resolving agent chiral secondary amines which are readily and inexpensively obtained in stereochemically pure form, either from commercial sources or in the laboratory. Thirdly, the final conversion from the diastereomeric compound to the free enantiomer would be carried out under quite mild experimental conditions and would probably be stereoretentive. Finally, both enantiomers could be obtained from this method, depending, of course, upon the quality of the diastereomer separation.

A number of these diastereomeric organophosphorus compounds of the type $P(OR)(OR')(NRR)$ were prepared in high yield as shown in Figure 62. The resolved chiral secondary amino group found to give the best results (primarily based on ^{31}P NMR spectroscopy) in terms of purity and separation of the diastereomer peaks in the NMR spectrum was L-ethylprolinate, which was conveniently synthesized from the commercially available L-proline. Purification of these compounds was achieved by rapid vacuum distillation followed by column chromatography. The ^{31}P NMR spectrum of 87, shown in Figure 63, for example, showed two peaks at

Figure 63. ^{31}P NMR of 87



141.15 and 139.87 ppm arising from the chemical shifts of the two diastereomers. The last step of the reaction sequence involving the conversion of the diastereomers to the free enantiomers with para-tolyltrifluoroacetate was found to proceed as expected on the racemic mixture of 86 under mild conditions. The reaction produced a 62.8% yield of the racemic enantiomeric product which could be readily purified by column chromatography.

The separation of the diastereomers of 86 and 87 was attempted using thin-layer chromatography, classical liquid chromatography, high performance liquid chromatography, preparative thin-layer chromatography, derivatization followed by chromatography, and fractional distillation. TLC of 86 and 87 on neutral alumina and cellulose strips with a large number of solvent systems were entirely unsuccessful, resulting either in no separation or decomposition of the compounds. TLC on silica gel strips achieved only slightly better results. Most of the solvent systems and their binary combinations showed no detectable separation of the two diastereomers. However, using a solvent system of 4 benzene/1 chloroform on silica, some separation of 87 was observed. The two mobile components for the diastereomers had calculated R_f values of approximately 0.19 and 0.22. It appeared, however, that the spots were significantly overlapped. Other ratios of this binary solvent system resulted in no better separation of the spots with the maximum efficiency obtained at the four to one ratio. In attempts to improve upon this result, column chromatography using the same solvent system on 60-200 mesh silica gel was employed utilizing large compound to silica gel

ratios (>1:200) and very slow flow rates to maximize efficiency. This method proved unsuccessful since both of the diastereomers eluted simultaneously. Similar results were also obtained with alumina and cellulose columns. A great deal of work has been reported recently involving the development and successful applications of high performance liquid chromatography to separation problems which were very difficult or even impossible to accomplish using classical liquid chromatographic techniques (258). With this in mind, the separation of the diastereomers was attempted using both analytical and preparative HPLC systems on porasil (analytical) and silica gel (preparatory) using the binary benzene/chloroform systems. A wide range of proportions of the two solvents was employed (from 0% benzene/100% chloroform to 100% benzene/0% chloroform in 5% increments) with several flow rates (1.0, 1.5, 2.0, and 4.0 mL per minute). Elution of the components were conveniently monitored by UV spectroscopy. Under all experimental conditions tried, the diastereomers were eluted as a rather broad peak without any apparent resolution. This inability to observe two peaks may be related to the overlap encountered with TLC. Because of these resolution difficulties with both classical chromatography and HPLC techniques, the method of preparative TLC was investigated. Once again, using the best solvent system (4 benzene/1 chloroform) the resolution of the mobile components was not improved over TLC.

The diastereomeric mixture of 87 was then derivatized to the borane adduct since its polarity could potentially aid in separation and the borane group could later be easily removed. TLC of this compound on

silica and alumina with a variety of organic solvents (hexanes, benzene, chloroform, methylene chloride, acetonitrile, acetone, and ethyl acetate) and their binary combinations proved unsuccessful in separating the two diastereomers. Similar attempts with analogous HPLC systems also were unsuccessful.

In a final attempt, a high-resolution spinning band vacuum distillation was performed but once again the two diastereomers were recovered unchanged as a single fraction as determined by ^{31}P NMR spectroscopy.

Chiral Stationary Phase HPLC

Recently the use of chiral stationary phase (CSP) high-performance liquid chromatography has been shown to work quite successfully to resolve a variety of chiral molecules (248,250). Using a chiral recognition rationale, several chiral bonded phases have been prepared which have proven capable of separating the enantiomers of compounds including chiral sulfoxides, lactones, and derivatives of alcohols, amines, amino acids, and mercaptans. In CSP chromatography, a resolved chiral molecule is chemically bonded to a stationary support (i.e. silica gel), as shown in Figure 64 for the case of "CSP XIII" (Pirkle's nomenclature). For this technique to be successful, there must be at least three simultaneous interactions which must be stereochemically dependent between the CSP and one of the solute enantiomers. This "chiral recognition scheme" suggested by Pirkle has been used

successfully to rationally develop several chiral bonded phases for the chromatographic separation of optical isomers.

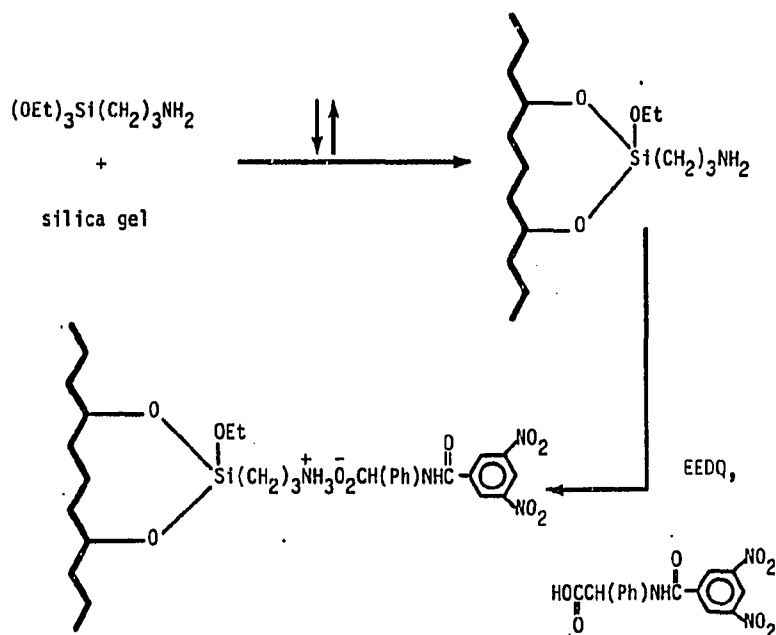


Figure 64. Preparation of "CSP XIII" (250)

In an extension of this work to our problem, several of these phases were prepared and investigated. A wide variety of pure, binary, and tertiary solvent systems were tried on the CSP columns under a variety of conditions as presented in the experimental section. Under all conditions investigated, no resolution of the organophosphorus triesters was observed and both enantiomers were eluted simultaneously.

The apparent failure of the chiral phases investigated to separate the triesters may result from two possible factors. First, because of

the rather bulky size of the substituents on both the phosphorus and surrounding the chiral center in the bonded stationary phase, the required close approach of the two groups may be significantly hindered. This would serve to attenuate any interaction of the "three points" required in Pirkle's recognition scheme to distinguish the handedness of the chiral triester. A second possible reason may be that the different groups located at the para positions of the substituent aromatic rings on the triester are located relatively far from the chiral center at the phosphorus. This spatial restriction may result in too large a separation between the groups responsible for the chirality and thereby creating too subtle an effect for the bonded chiral center to recognize effectively. A combination of these factors is, of course, also possible.

Diastereomeric Platinum(II) Complexes

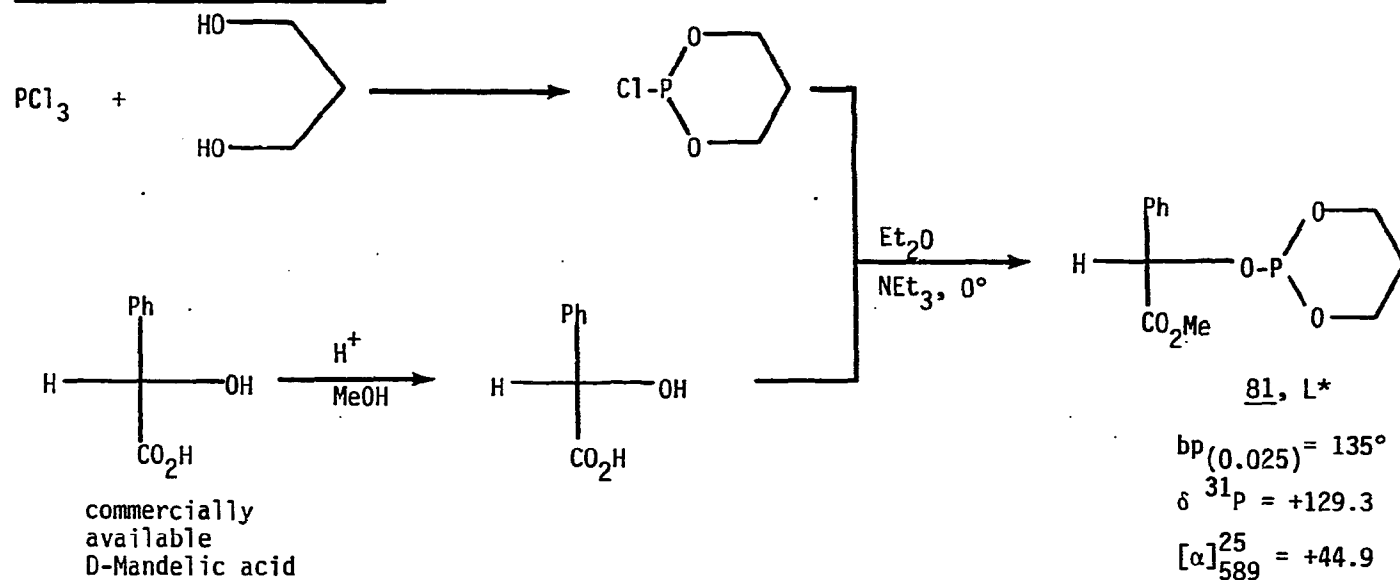
Due to the difficulties encountered with the resolution techniques described above, resolution via diastereomeric platinum(II) complexes was investigated. By preparing the platinum complexes of the chiral triester 84, the free resolved enantiomeric forms of the triester were successfully obtained.

The procedure developed involves two main experimental components; the synthesis and purification of the ligands, and the preparation, separation, and destruction of the diastereomeric platinum complexes. To accomplish the formation of the diastereomeric complexes, it is necessary to utilize two ligands; a resolving ligand 81 (L*) and the ligand to be

resolved 84 (P*). These are prepared by the reactions shown in Figure 65. The L* ligand is synthesized from the interaction of 2-chloro-1,3,2-dioxaphosphorinane 24 with D-methylmandelate and is obtained in pure form by vacuum distillation. This ligand is convenient in that the optically pure D-methylmandelate reactant is easily prepared from the commercially available and relatively inexpensive D-mandelic acid to yield the chiral ligand in pure form. Furthermore, the chlorophosphorus precursor is also readily obtained in high yield and purity. The synthesis and purification of the triester to be resolved, P* 84, has been previously discussed. The second portion of this resolution scheme is summarized in Figure 66. Complexes of organophosphorus triesters of the type $P(OR)_3$ and $P(OR)(OR')_2$ are well-known in the literature (259-261). Beginning with the readily synthesized bis(benzonitrile)dichloro platinum(II) complex, the di-substituted cis-dichloro complexes of P* and of L* were prepared and each purified by column chromatography. The cis isomers of these complexes were used preferentially over the trans complexes primarily because it has been shown that the former more readily undergo in higher yield an important equilibration step later in the resolution (Figure 66). These dichloro complexes were then converted into the corresponding diiodides in nearly quantitative yields by simple halogen methasis with sodium iodide. The reason for this conversion is that the iodides are typically highly crystalline compounds and are more easily purified than the dichlorido analogues. Stoichiometric amounts of these two ocomplexes were then mixed with a one mole percent of added L*. This addition of a catalytic amount of L* follows from the observation by

Figure 65. Preparation of ligands for the platinum phosphite resolution

RESOLVING LIGAND, 81, L* ;



LIGAND TO BE RESOLVED, 84, P* ;

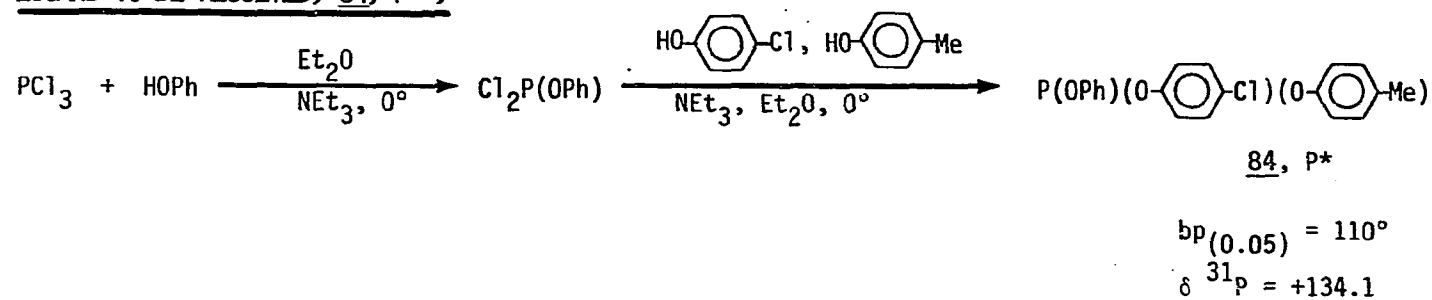
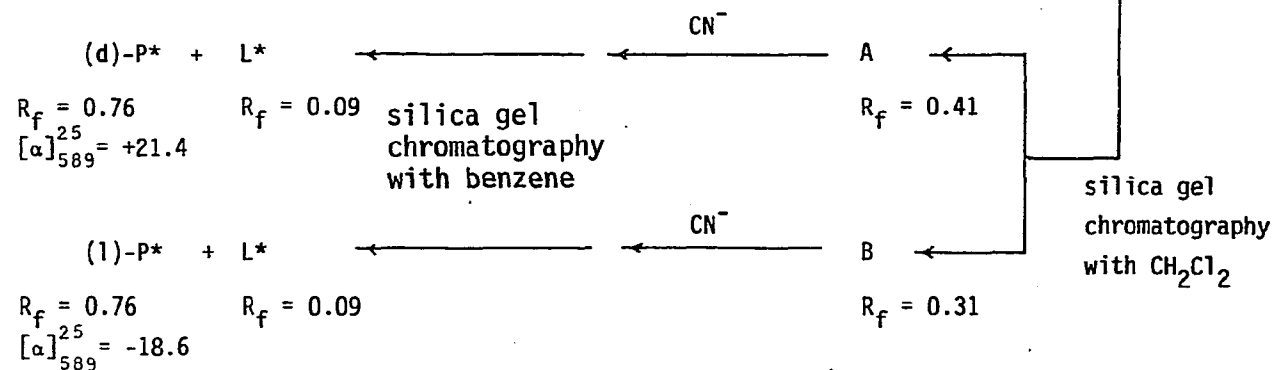
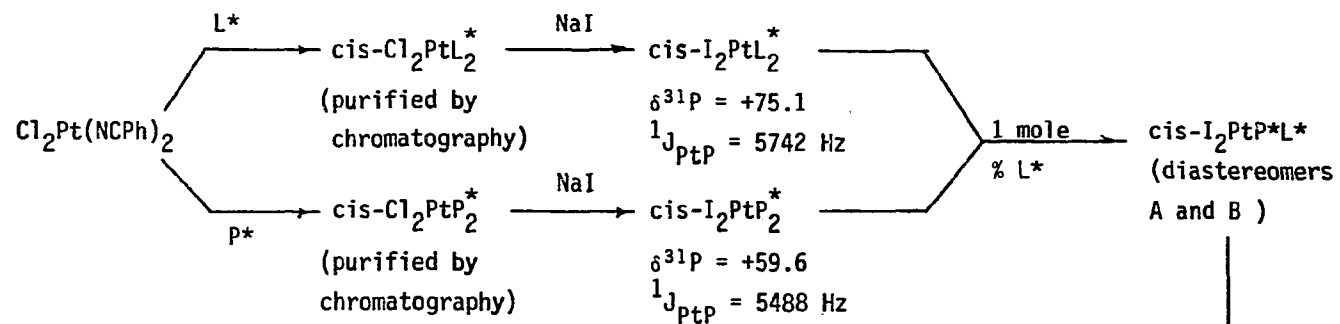


Figure 66. Resolution of 84 via platinum diastereomers



Wroblewski et al. (209) that yields of mixed-ligand diastereomeric platinum complexes can be greatly improved when a small amount of this ligand is added. This observation had no previous precedent in the literature and it was suggested that the equilibration may proceed via the formation of a reactive five-coordinate platinum(II) complex. The two diastereomeric mixed ligand complexes were successfully separated from one another using standard liquid chromatographic techniques with silica gel using methylene chloride as eluant. The R_f values of the four possible cis complexes in the reaction mixture ($I_2(P^*)_2Pt$, diastereomer A and B of $I_2(P^*)(L^*)_2Pt$, and $I_2(L^*)_2Pt$) were all significantly different to effect complete separation (Table 59 in the Experimental Section). All the platinum complexes prepared were characterized by R_f values and ^{31}P NMR spectroscopy with particular emphasis on the diagnostic ^{195}Pt - ^{31}P coupling constant values (see Experimental Section).

Difficulty was at first encountered with the cyanide destruction of the complexes to liberate the free ligands, since the conditions reported previously (209) were insufficient. When the reaction was performed in methylene chloride with an excess of sodium cyanide, however, the reaction proceeded smoothly and quantitatively. The two free ligands were then easily separated by column chromatography with the resolving ligand staying near the origin and the resolved enantiomers of 84 traveling near the solvent front on silica gel. Optical rotations were measured and found to be nearly equal and of opposite sign.

Several attempts were made to determine the quality and completeness of the resolution by examining the interaction of the racemic and resolved chiral triesters with lanthanide shift reagents. The interaction of $\text{Eu}(\text{fod})_3$, $\text{Eu}(\text{hfc})_3$, and $\text{Eu}(\text{tfc})_3$ with the triester was very weak and the ^1H and ^{31}P NMR resonances of the two enantiomers could not be resolved as observed, however. To introduce more polar groups into the triester and hence potentially strengthen the interactions, the trivalent ester was oxidized to the phosphate with N_2O_4 which is known to proceed with retention of configuration (209). ^{31}P NMR spectra of 91 with the shift reagents showed an apparently stronger interaction but the signals were so broad that adequate resolution was not achieved. Similar difficulties were encountered in the ^1H NMR spectra using these shift reagents.

The cause of the failure of these reagents to adequately resolve the NMR peaks in the racemic mixture may be related to the failure of the CSP technique to separate the enantiomers. The proposed explanation for the effect of shift reagents on NMR chemical shifts is based upon a pseudo contact mechanism (262). In triester 84, the groups inducing the chirality of the phosphorus spatially lie far apart so that the chiral shift reagent may not be able to distinguish their inequivalence because of size limitations on effective contact. It may be that the diastereomeric cis-platinum(II) complexes are more easily separated because the sources of the chirality in the para positions of 84 are sterically exposed to the chromatographic medium while the phosphorus atom is not, since it is in the sterically congested primary

coordination sphere. In contrast, the free ligand, as well as its derivatives discussed above, may tend to interact with shift reagents at the phosphorus or phosphoryl oxygen in the phosphate 91. Similar reasoning may apply to the failure of the diastereomeric phosphite ester derivatives to separate on chromatography.

The diastereomeric platinum(II) complex approach has several advantages over other procedures. First, it can provide both of the resolved enantiomers from the racemic mixture and does not rely upon the preparation of a previously resolved precursor organophosphorus compound. Secondly, in the chromatographic separation of the diastereomers, the location of the components can be easily determined by simple visual inspection since the complexes themselves are colored. This very convenient property can also be used effectively to determine qualitatively the efficiency of the chromatographic separation of the diastereomers. Thirdly, the ^{31}P NMR and especially the ^{195}Pt - ^{31}P coupling constant values allow facile characterization of the intermediate complexes and assignment of their purity. On the other hand, this procedure does have several limitations. First, it requires the use of expensive platinum reagents, although these may be recycled. Secondly, it is rather lengthy and time consuming procedure and is not easily scaled up to prepare larger amounts of optically pure material.

CONCLUSIONS

In this dissertation, the preparation of oxygen substituted phosphonium ions was investigated. ^{31}P NMR was found to be the best method for following the courses of these reactions. Most of the attempted halide abstraction procedures proved unsuccessful for the preparation of the "free" dioxaphosphonium ions. It appears that these species can, however, be formed by the reaction of aminodioxaphosphorus(III) and diaminoxaphosphorus(III) compounds with several protic acids but they are tightly ion paired with their counteranions. In an attempt to prepare metallophosphonium ion complexes, oxygen substituted compounds of the type $\text{ClP}(\text{OR})_2$ were reacted with metal nucleophiles and metal- $\text{PCl}(\text{OR})_2$ complexes were reacted with halide abstractors such as aluminum trichloride. From ^{31}P NMR data, several of the observed products can be considered to have substantial phosphonium ion character. In the reaction of $\text{ClP}(\overline{\text{OCH}_2\text{C}(\text{CH}_3)_2\text{CH}_2\text{O}})$ with the Fp^- anion, four major products were observed. These were shown to correspond to cis and trans- $[\text{Fe}(\eta^5\text{-Cp})(\text{CO})(\mu\text{-}\overline{\text{P}(\text{OCH}_2\text{C}(\text{CH}_3)_2\text{CH}_2\text{O}))_2]$, PCl_3 and possibly $[\text{Fe}(\eta^5\text{-Cp})(\text{CO})(\overline{\text{P}(\text{OCH}_2\text{C}(\text{CH}_3)_2\text{CH}_2\text{O}))]$, of which only the first two were isolated. Similar results were also obtained for a large number of other $\text{ClP}(\text{OR})_2$ systems. Proton NMR of these cis and trans complexes were quite informative and showed that in the case of the phosphorinane ring system compounds, the ring becomes non-rigid on the NMR time scale compared with the rigid precursor chlorophosphorus compounds. It appears that both steric size and the electron donating/withdrawing properties of

the substituents on phosphorus are important in determining the coordination chemical shifts in the ^{31}P NMR for these complexes. Linear correlations between ^{31}P NMR and infrared parameters were observed for the first time. Results indicate that these bridging phosphorus units act as good π -acceptors which compete quite favorably for the π -electron density at the metal with the carbonyl group.

Crystallographic studies of both *cis* and *trans*-

$[\text{Fe}(\eta^5\text{-Cp})(\text{CO})(\mu\text{-P}(\text{OCH}_2\text{C}(\text{CH}_3)\text{CH}_2\text{O}))_2]_2$ were undertaken which confirmed both the dimeric structure and isomer identification as predicted based upon spectroscopic data. These are the first reported structures of a bridging $\text{P}(\text{OR})_2$ unit in a metal-metal non-bonded system. Structural features were rationalized in terms of molecular orbital consideration.

From the reaction of the Fp^- anion with $\text{ClP}(\text{OC}(\text{CH}_3)_2\text{C}(\text{CH}_3)\text{O})$, another quite unusual product was isolated and studied crystallographically. This compound, $[\text{Fe}(\eta^4\text{-C}_5\text{H}_6)(\text{CO})(\mu\text{-P}(\text{OC}(\text{CH}_3)\text{C}(\text{CH}_3)\text{O}))_2(\text{OC})_3\text{Fe}]$, appears to be the first unsubstituted $\eta^4\text{-C}_5\text{H}_6$ diiron system structured. A number of other interesting features were observed. The very short Fe-P, long Fe-Fe and large Fe-P-Fe and flap angles were rationalized by isovalent hybridization and molecular orbital considerations. It appears that the electronegativities of the substituents on the bridging phosphorus units play a very important role in the observed geometry.

Finally, the first procedure for the optical resolution of a trivalent organophosphorus triester with phosphorus as the primary chiral site was developed. This was accomplished by the use of diastereomeric

Pt(II) complexes which were separated chromatographically. The free enantiomers were obtained by destruction of the complex with cyanide followed by a final chromatographic purification. This procedure yields both enantiomers of apparently high purity.

REFERENCES

1. Olah, G. A. J. Am. Chem. Soc. **1972**, 94, 808.
2. Gassman, P. G. Acc. Chem. Res. **1970**, 3, 26.
3. Olah, G. A.; Field, L. D. Organometallics **1982**, 1, 1485.
4. Baxter, S. G.; Collins, R. L.; Cowley, A. H.; Sena, S. F. Inorg. Chem. **1983**, 22, 3475.
5. Flemming, S.; Lupton, M. K.; Jekot, K. Inorg. Chem. **1972**, 11, 2534.
6. Maryanoff, B. E.; Hutchins, R. D. J. Org. Chem. **1972**, 37, 3475.
7. Halman, M. Top. Phosphorus Chem. **1967**, 4, 49.
8. Flemming, S.; Parry, R. W. Inorg. Chem. **1972**, 11, 1.
9. Thomas, M. G.; Schultz, C. W.; Parry, R. W. Inorg. Chem. **1977**, 16, 994.
10. Dimroth, K.; Hoffman, P. Chem. Ber. **1966**, 99, 1325.
11. Dimroth, K. Top. Curr. Chem. **1973**, 38, 1.
12. Cowley, A. H.; Kemp, R. A.; Wilburn, J. C. Inorg. Chem. **1981**, 20, 4289.
13. Cowley, A. H.; Cushner, M. C.; Lattman, M.; McKee, M. L.; Szobota, J. S.; Wilburn, J. C. Pure Appl. Chem. **1980**, 52, 789.
14. Dahl, O. Tet. Lett. **1982**, 23, 1493.
15. Cowley, A. H.; Lattman, M.; Wilburn, J. C. Inorg. Chem. **1981**, 20, 2916.
16. Baxter, S. G.; Collins, R. L.; Cowley, A. H.; Sena, A. H. J. Am. Chem. Soc. **1981**, 103, 714.
17. Cowley, A. H.; Ebsworth, A. V.; Kemp, R. A.; Rankin, D. W. H.; Stewart, C. A. Organometallics **1982**, 1, 1720.
18. Cowley, A. H.; Kilduff, J. E.; Pakulski, M.; Stewart, C. A. J. Am. Chem. Soc. **1983**, 105, 1655.
19. Issleib, K.; Seidel, W. Chem. Ber. **1959**, 92, 2681.

20. Cardin, D. J.; Cetinkaya, B.; Lapert, M. F. Chem. Rev. **1972**, 72, 545.
21. Cowley, A. H.; Cushner, M. C.; Szobota, J. S. J. Am. Chem. Soc. **1978**, 100, 7784.
22. Clardy, J. C.; Kolpa, R. L.; Verkade, J. G. Phosphorus **1974**, 4, 133.
23. Chatt, J.; Duncanson, L. A. J. Chem. Soc. **1953**, 2, 959.
24. Montemayor, R. G.; Sauer, D. T.; Flemming, S.; Bennett, D. W.; Thomas, M. G.; Parry, R. W. J. Am. Chem. Soc. **1978**, 100, 2231.
25. Light, R. W.; Paine, R. T.; Maier, D. E. Inorg. Chem. **1979**, 18, 2345.
26. Hutchins, L. D.; Light, R. W.; Paine, R. T. Inorg. Chem. **1982**, 21, 266.
27. Light, R. W.; Paine, R. T. J. Am. Chem. Soc. **1978**, 100, 2230.
28. Hutchins, L. D.; Paine, R. T.; Campana, C. F. J. Am. Chem. Soc. **1980**, 102, 4521.
29. Hutchins, L. D.; Duesler, E. N.; Paine, R. T. Organometallics **1982**, 1, 1254.
30. Bennett, D. W.; Parry, R. W. J. Am. Chem. Soc. **1979**, 101, 755.
31. Brown, I. D.; Brown, M. C.; Hawthorne, F. C. "Bond Index to the Determination of Inorganic Crystal Structures"; Institute for Materials Research, McMaster University: Canada, 1969-1977.
32. Malisch, W.; Kuhn, M. J. Organomet. Chem. **1974**, 73, C1.
33. Malisch, W.; Meyer, A. J. Organomet. Chem. **1980**, 198, C29.
34. Muetterties, E. L.; Kirner, J. F.; Evans, W. J.; Watson, P. L.; Abdel-Meguid, S.; Tavanaiepour, I.; Day, V. W. Proc. Natl. Acad. Sci. USA **1978**, 75, 1056.
35. Choi, H. W.; Gavin, R. M.; Muetterties, E. L. J. Chem. Soc., Chem. Commun. **1979**, 1085.
36. Day, V. M.; Tavanaiepour, I.; Abdel-Meguid, S. S.; Kirner, J. F.; Goh, L.-Y.; Muetterties, E. L. Inorg. Chem. **1982**, 21, 657.

37. Hayter, R. G. J. Am. Chem. Soc. **1964**, 85, 3120.
38. Jones, R. A.; Stuart, A. L.; Atwood, J. L.; Hunter, W. E.; Rogers, R. D. Organometallics **1982**, 1, 1721.
39. Carty, A. J.; Hartstock, F.; Taylor, N. J. Inorg. Chem. **1982**, 21, 1349.
40. King, R. B. "Transition-metal organometallic chemistry", Academic Press: New York, **1969**; p. 109.
41. Cook, H. G.; Ilett, J. D.; Saunders, B. C.; Stacey, G. J.; Watson, H. G.; Wilding, I. G. E.; Woodcock, S. J. J. Chem. Soc. **1949**, 2921.
42. Michalski, J.; Modro, T.; Zwierzak, A. J. Chem. Soc. **1961**, 4904.
43. Fluck, E.; Van Wazer, J. R. Z. Anorg. Chem. **1961**, 307, 113.
44. Jones, R. A. Y.; Katritzky, A. R. Angew. Chem. Internat. Ed. **1962**, 1, 32.
45. Hewertson, W.; Smith, B. C.; Shaw, R. A. Inorganic Synth. **1966**, 8, 68.
46. Connant, J. B.; Wallingford, V. H.; Gandheker, S. S. J. Am. Chem. Soc. **1923**, 45, 762.
47. Shepard, A. F.; Dannels, B. F. U. S. Pat. 3,281,506, **1966**; C. A. **1967**, 66, 10739s.
48. Kopp, R. W.; Bond, A. C. Parry, R. W. Inorg. Chem. **1976**, 15, 3042.
49. Van Wazer, J. R.; Maier, L. J. Am. Chem. Soc. **1964**, 86, 811.
50. Schmutzler, R. J. Chem. Soc. **1965**, 5630.
51. Cason, J.; Baxter, W. N.; De Acetis, W. J. Org. Chem. **1959**, 24, 247.
52. Zwierzak, A. Can. J. Chem. **1967**, 45, 2501.
53. Oswald, A. A. Can. J. Chem. **1959**, 37, 1498.
54. Bergesen, K.; Vikane, T. Acta Chem. Scand. **1972**, 26, 2153.
55. Denney, D. Z.; Chen, G. Y.; Denney, D. B. J. Am. Chem. Soc. **1969**, 91, 6838.

56. Goldwhite, H. Chem. Ind. (London) **1964**, 494.
57. Anschutz, L.; Boedeker, W.; Neher, R.; Ohnheiser, A. Chem. Ber. **1943**, 76, 218.
58. Arbuzov, A. E.; Valitova, F. G. Trudy Kazansk. Khim. Tekhnol. Inst. **1940**, 8, 12; CA **1941**, 35, 2485.
59. Fusco, R.; Bertulli, G. M. Chem. Ind. **1955**, 37, 839.
60. Ramirez, F.; Patwardhan, A. V.; Kugler, H. J.; Smith, C. P. J. Am. Chem. Soc. **1967**, 89, 6276.
61. Ramirez, F.; Patwardhan, A. V.; Kugler, H. J.; Smith, C. P. Tetrahedron Lett. **1966**, 3053.
62. Hayter, R. G. Inorg. Chem. **1963**, 2, 1031.
63. Kosolapoff, G. M.; Maier, L. "Organic Phosphorus Compounds"; Wiley-Interscience: New York, **1973**; Vol. 5, Chapter 15.
64. Bergesen, K.; Bjoroey, M.; Gramstad, T. Acta Chem. Scand. **1972**, 26, 2156.
65. Lucas, H. J.; Mitchell, F. W.; Scully, C. N. J. Am. Chem. Soc. **1950**, 72, 5491.
66. Pritchard, J. G.; Vollmer, R. L. J. Org. Chem. **1963**, 28, 1545.
67. White, D. W.; Bertrand, R. B.; McEwen, G. K.; Verkade, J. G. J. Am. Chem. Soc. **1970**, 92, 7125.
68. Edmundson, R. S. Chem. Ind. (London) **1965**, 1220.
69. Houalla, D.; Sanchez, M.; Wolf, R. Bull. Soc. Chim. France **1965**, 2368.
70. Abramov, V. S.; Druzhina, Z. S. Zh. Obshch. Khim. **1966**, 36, 923; CA **1966**, 65, 10580g.
71. Edmundson, R. S.; Lambie, A. J. J. Chem. Soc., C **1966**, 1997.
72. Sanchez, M.; Wolf, R.; Burgada, R.; Mathis, F. Bull. Soc. Chim. France **1968**, 773.
73. Arbuzov, A. E.; Zoroastrova, V. Izv. Akad. Nauk SSSR, Ser. Khim. **1952**, 770, 779; CA **1953**, 47, 9900e.

74. Grechkin, N. P.; Grishina, L. M. Izv. Akad. Nauk SSSR, Ser. Khim. **1965**, 1502; CA **1965**, 63, 16280f.
75. Schiff, D. E. Ph.D. Thesis, Iowa State University, **1983**.
76. King, R. B. Inorg. Chem. **1963**, 2, 936.
77. Butts, S. B.; Shriver, D. F. J. Organomet. Chem. **1979**, 169, 191.
78. Braterman, P. S. J. Organomet. Chem. **1968**, 11, 198.
79. Bartish, C. M.; Kraihanzel, C. S. Inorg. Chem. **1973**, 12, 391.
80. King, R. B. "Transition-metal organometallic chemistry"; Academic Press: New York, **1969**; p. 107.
81. Wilkinson, G. J. Am. Chem. Soc. **1954**, 76, 209.
82. Bartish, C. M.; Kraihanzel, C. S. Inorg. Chem. **1978**, 17, 735.
83. King, R. B.; Stone, F. G. A. Inorg. Synth. **1963**, 7, 198.
84. Akitt, J. W. Annu. Rep. NMR Spectrosc. **1972**, 5, 465.
85. Allred, A. L.; Rochow, E. G. J. Inorg. Nuclear Chem. **1958**, 5, 264.
86. Verkade, J. G. Phosphorus and Sulfur **1966**, 2, 251.
87. Dessy, R. E.; Pohl, R. L.; King, R. B. J. Am. Chem. Soc. **1966**, 88, 5121.
88. King, R. B. Trans. N. Y. Acad. Sci. **1966**, 28, 889.
89. Gagnaire, D.; Robert, J.-B.; Verrier, J. Bull. Chim. Soc. Fr. **1966**, 3719.
90. Bergesen, K.; Albriktsen, P. Acta Chem. Scand. **1971**, 25, 2257.
91. Emsley, J. W.; Feeney, J.; Sutcliffe, L. H. "High Resolution Nuclear Magnetic Resonance Spectroscopy"; Pergamon Press: New York, **1965**; Vol. 1.
92. Verkade, J. G. Phosphorus Sulfur **1976**, 2, 251.
93. Gagnaire, D.; Robert, J. B.; Verrier, J. Bull. Soc. Chim. Fr. **1968**, 2392.
94. Sternhill, S. Pure Appl. Chem. **1964**, 14, 15.

95. Harris, R. K. Can. J. Chem. **1964**, 42, 2275.
96. Bertrand, R. D.; Compton, R. D.; Verkade, J. G. J. Am. Chem. Soc. **1970**, 92, 2702.
97. NMCSIM computer program; Nicolet Magnetics Corp.: Fremont, CA, **1983**.
98. Jackman, L. M.; Sternhall, S. "Applications of NMR Spectroscopy in Organic Chemistry"; Pergamon: New York, **1969**.
99. Farrar, T. C.; Becker, E. D. "Pulse and Fourier Transform NMR"; Academic Press: New York, **1971**.
100. Gerstein, B. C. Anal. Chem. **1983**, 55, 8994.
101. Cotton, F. A.; Liehr, A. D.; Wilkinson, G. J. Inorg. Nucl. Chem. **1955**, 1, 175.
102. Gansow, D. A.; Kimura, B. Y.; Dobson, G. R.; Brown, R. A. J. Am. Chem. Soc. **1971**, 93, 5922.
103. Bodner, G. M.; May, M. P.; McKinney, L. E. Inorg. Chem. **1980**, 19, 1951.
104. Quin, L. D. "The Heterocyclic Chemistry of Phosphorus"; John Wiley and Sons: New York, **1981**.
105. Parrot, D. W.; Hendricker, D. G. J. Coord. Chem. **1973**, 2, 235.
106. Kraihanzel, C. S.; Bartish, C. M. Phosphorus **1974**, 4, 271.
107. VandeGriend, L. J.; Verkade, J. G. Inorg. Nucl. Chem. Lett. **1973**, 9, 1137.
108. White, D. W. Phosphorus **1971**, 1, 33.
109. Dean, W. K.; Heyl, B. L.; Van Dervear, D. G. Inorg. Chem. **1978**, 17, 1909.
110. Ryan, R. C.; Carty, A. J. J. Am. Chem. Soc. **1975**, 97, 6904.
111. Collman, J. P. Rothrock, R. K.; Finke, R. G.; Rose-Munch, F. J. Am. Chem. Soc. **1977**, 99, 7381.
112. Burdett, J. K. J. Chem. Soc., Dalton Trans. **1977**, 423.
113. Clegg, W. Inorg. Chem. **1976**, 15, 1609.

114. Jacobson, R. A. J. Appl. Crystallogr. **1976**, 9, 115.
115. Rohrbaugh, W. J.; Jacobson, R. A. Inorg. Chem. **1974**, 13, 2535-9.
116. An empirical absorption correction was made with use of the method described by: Karcher, B.A. Ph.D. dissertation, Iowa State University, **1981**.
117. Lapp, R. L.; Jacobson, R. A. "AUS, A Generalized Crystallographic Least-Squares Program", USDOE Report IS-4708; Ames Laboratory-DOE and Iowa State University: Ames, Iowa, **1979**. Calculations were carried out on a VAX 11/780 computer.
118. Treichel, P. M.; Dean, W. K.; Calabrese, J. C. Inorg. Chem. **1973**, 12, 2908.
119. Ginsburg, R. E.; Rothrock, R. K.; Finke, R. G.; Collman, J. P.; Dahl, L. F. J. Am. Chem. Soc. **1979**, 101, 6550.
120. Sinclair, J. D. Ph.D. Thesis, Univ. of Wis. (Madison), **1972**.
121. Carty, A. J.; Mott, G. N.; Taylor, N. J.; Yule, J. E. J. Am. Chem. Soc. **1978**, 100, 3051.
122. Mott, G. N.; Carty, A. J. Inorg. Chem. **1979**, 18, 2926.
123. Carty, A. J.; Taylor, N. J.; Smith, W. F.; Paik, H. M.; Yule, J. E. J. Chem. Soc., Chem. Commun., **1976**, 41.
124. Fischer, K.; Vahrenkamp, H. Z. Anorg. Allg. Chem. **1981**, 475, 109.
125. Carty, A. J.; Ferguson, G.; Kahn, M. A.; Mott, G. W.; Roberts, P.; Taylor, N. J. J. Organomet. Chem. **1978**, 149, 345.
126. Smith, W. F.; Yule, J.; Taylor, N. J.; Paik, H. N.; Carty, A. J. Inorg. Chem. **1977**, 16, 1593.
127. Wong, Y. S.; Paik, H. N.; Cheih, P. C.; Carty, A. J. J. Chem. Soc., Chem. Commun. **1975**, 309.
128. Patel, H. A.; Fischer, R. G.; Carty, A. J.; Naik, D. V.; Palenik, G. J. J. Organomet. Chem. **1973**, 60, C49.
129. Teo, B. K.; Hall, M. B.; Fenske, R. F.; Dahl, L. F. Inorg. Chem. **1975**, 12, 3103.
130. Carty, A. J. Adv. Chem. Series **1982**, 96, 163.
131. Zeiss, W. C. Ann. Phys. **1827**, 9, 932.

132. Collman, J. P.; Hegedus, L. S. "Principles and Applications of Organotransition Metal Chemistry", University Science Books: Mill Valley, Calif., 1980.
133. Kochhar, R. K.; Pettit, R. J. J. Organomet. Chem. 1966, 6, 272.
134. Whitesides, T. H.; Shelly, J. J. J. Organomet. Chem. 1975, 92, 215.
135. Hallam, B. F.; Pauson, P. L. J. Chem. Soc. 1958, 646.
136. Prince, S. R. Cryst. Struct. Comm. 1976, 5, 451.
137. Pierpont, C. G. Inorg. Chem. 1978, 17, 1976.
138. Ehntholt, A. R.; Rosenblum, M. J. J. Organomet. Chem. 1973, 56, 315.
139. Eisenstadt, A.; Scharf, G.; Fuchs, B. Tetrahedron Lett. 1971, 679.
140. De Puy, C. H.; Kobal, V. M.; Gibson, D. H. J. Organomet. Chem. 1968, 13, 266.
141. Weiss, E.; Hubel, W. Chem. Ber. 1962, 95, 1186.
142. Boston, J. L.; Sharp, D. W. A.; Wilkinson, G. J. Chem. Soc. 1962, 3488.
143. Sim, G. A.; Woodhouse, D. I.; Knox, G. R. J. Chem. Soc., Dalton 1979, 629.
144. Muller, H.; Herberich, G. E. Chem. Ber. 1971, 104, 2772.
145. Fischer, E. O.; Werner, H. "Metal π -Complexes", Elsevier Publishing: London, 1966.
146. Filbey, A. H. U. S. Pat. 1963, 3, 178, 463; C.A. 1963, 63, 4334b.
147. Humphries, A. P.; Knox, S. A. R. J. Chem. Soc., Chem. Commun. 1973, 326.
148. Fachinetti, G.; Floriani, C. J. Chem. Soc., Chem. Commun. 1974, 516.
149. Cooper, R. L.; Green, M. L. H.; Moelwyn-Hughes, J. T. J. Organomet. Chem. 1965, 3, 261.
150. Alcock, N. W. J. Chem. Soc., A 1967, 2001.
151. Alcock, N. W. J. Chem. Soc., Chem. Commun. 1965, 177.

152. Ariyaratne, J. P. K.; Green, M. L. H.; Nagy, P. L. I. Proc. Chem. Soc. **1963**, 107.
153. Brenner, K. S.; Fischer, E. O.; Fritz, H. P.; Kreiter, C. G. Chem. Ber. **1963**, 96, 2632.
154. Green, M. L. H.; Pratt, L.; Wilkinson, G. J. Chem. Soc. **1959**, 3753.
155. Herberich, G. E.; Muller, H. Chem. Ber. **1971**, 104, 2781.
156. Cotton, F. A.; Wilkinson, G. "Advanced Inorganic Chemistry", Interscience Publishers: New York, **1972**.
157. Churchill, M. R.; Mason, R. Proc. Roy. Soc. A, **1964**, 279, 191.
158. El Murr, N.; Sheats, J. E.; Agnew, M. J. Chem. Soc., Dalton, **1979**, 901.
159. Herberich, G. E.; Griess, G. J. Organomet. Chem. **1971**, 27, 113.
160. Fischer, E. O.; Herberich, G. E. Chem. Ber. **1961**, 94, 1517.
161. Churchill, M. R. J. Organomet. Chem. **1965**, 4, 258.
162. Moseley, K.; Kang, J. W.; Maitlis, P. M. J. Chem. Soc. A **1970**, 2875.
163. Angelici, R. J.; Fischer, E. O. J. Am. Chem. Soc. **1963**, 85, 3733.
164. Hoehn, H. H.; Pratt, L.; Watterson, K. F.; Wilkinson, G. J. Chem. Soc. **1961**, 2738.
165. Fritz, H. P.; Keller, H. J. Chem. Ber. **1962**, 95, 2259.
166. Fischer, E. O.; Wawersik, H. J. Organomet. Chem. **1966**, 5, 559.
167. Kruck, T.; Knoll, L. Chem. Ber. **1972**, 105, 3783.
168. Balakrishnan, P. V.; Maitlis, P. M. J. Chem. Soc., A **1971**, 1715.
169. Laine, R. M.; Ford, P. C. J. Organomet. Chem. **1977**, 124, 29.
170. Prout, K.; Couldwell, M. C. Acta Cryst. **1977**, B33, 2146.
171. Clemens, J.; Green, J.; Stone, F. G. A. J. Chem. Soc., Dalton **1974**, 93.
172. Mills, O. S.; Robinson, G. Acta Cryst. **1963**, 16, 758.

173. Bassi, I. W.; Scordamaglia, R. J. Organomet. Chem. **1972**, 37, 353.
174. Whiting, D. A. Cryst. Struct. Comm. **1972**, 1, 379.
175. Binger, P.; Cetinkaya, B.; Kruger, C. J. Organomet. Chem. **1978**, 159, 63.
176. King, R. B.; Manuel, T. A.; Stone, F. G. A. J. Inorg. Nucl. Chem. **1961**, 16, 233.
177. Cais, M.; Feldkimmel, M. Tetrahedron Lett. **1961**, 444.
178. Manuel, T. A.; Stafford, S. L.; Stone, F. G. A. J. Am. Chem. Soc. **1961**, 83, 3597.
179. Pettit, R.; Emerson, G. F. Adv. Organomet. Chem. **1964**, 1, 1.
180. Hubel, W.; Braye, E. H. J. Inorg. Nucl. Chem. **1959**, 10, 250.
181. Mahler, J. E.; Pettit, R. J. Am. Chem. Soc. **1962**, 84, 1511.
182. Behrens, U.; Weiss, E. J. Organomet. Chem. **1974**, 73, C64.
183. Weiss, E.; Hubel, W. Angew. Chem. **1961**, 73, 298.
184. Green, M. L. H.; Pratt, L.; Wilkinson, G. J. Chem. Soc. **1960**, 989.
185. Kruczynski, L.; Takats, J. Inorg. Chem. **1976**, 15, 3140.
186. Bailey, N. A.; Mason, R. Acta Cryst. **1966**, 21, 652.
187. Dahl, L. F.; Smith, D. L. J. Am. Chem. Soc. **1961**, 83, 752.
188. Gerloch, M.; Mason, R. Proc. Roy. Soc. **1964**, 279A, 170.
189. Bailey, N. A.; Gerloch, M.; Mason, R. Nature **1964**, 201, 72.
190. Drew, M. G. B.; Nelson, S. M.; Sloan, M. J. Organomet. Chem. **1972**, 39, C9.
191. Churchill, M. R.; Mason, R. Adv. Organomet. Chem. **1967**, 5, 93.
192. Coates, G. E.; Green, M. L. H.; Wade, K. "Organometallic Compounds", Methuen: London, **1967**.
193. Cromer, D. T.; Waber, J. T. "International Tables for X-ray Crystallography", Kynoch Press: Birmingham, England, **1974**; Vol. IV, Table 2.2A, pp. 71-79. Templeton, D. H., "International Tables for

- X-ray Crystallography", Kynoch Press: Birmingham, England, 1962; Vol. III, Table 3.3.2.c, pp. 215-216.
194. Pauling, L. "The Nature of the Chemical Bond", Cornell University Press: New York, 1960.
 195. Semmelhack, M. F.; Hall, H. T.; Farina, R.; Yoshifuji, M.; Clark, G.; Bargar, T.; Hirotsu, K.; Clardy, J. J. Am. Chem. Soc. 1979, 101, 3535.
 196. Semmelhack, M. F.; Hall, H. T.; Yoshifuji, M.; Clark, G. J. Am. Chem. Soc. 1975, 97, 1247.
 197. Jones, D.; Wilkinson, G. Chem. and Ind. 1961, 1408.
 198. Dewar, M. J. S.; Ford, G. P. J. Am. Chem. Soc. 1979, 101, 783, and references therein.
 199. Bent, H. A. J. Chem. Phys., 1960, 33, 1259.
 200. McEwen, W. Top. Phosphorus Chem. 1965, 2, 1.
 201. Gallagher, M. J.; Jenkins, D. Top. Stereochem. 1969, 3, 2.
 202. Criste, H.; Cristau, H. J. Ann. Chim. 1971, 6, 179.
 203. Kinas, R.; Pankiewicz, K.; Stec, W. J. Bull. Acad. Pol. Sci., Ser. Sci. Chim. 1975, 23, 981.
 204. Pankiewicz, K.; Kinas, R.; Stec, W. J.; Foster, A. B.; Jarman, M.; Van Maanen, J. M. S. J. Am. Chem. Soc. 1979, 101, 7712.
 205. Kawashima, T.; Kroshefsky, R. D.; Kok, R. A.; Verkade, J. G. J. Org. Chem. 1978, 43, 1111.
 206. Kinas, R.; Pankiewicz, K.; Stec, W. J.; Farmer, P. B.; Foster, A. B.; Jarman, M. Bull. Acad. Pol. Sci., Ser. Sci. Chim. 1978, 26, 39.
 207. Ludeman, S. M.; Bartlett, D. L.; Zon, G. J. J. Org. Chem., 1979, 44, 1163.
 208. Wroblewski, A. E.; Verkade, J. G. J. Am. Chem. Soc. 1979, 101, 7719.
 209. Wroblewski, A. E.; Socol, S. M.; Okruszek, A.; Verkade, J. G. Inorg. Chem. 1980, 19, 3713.

210. Cox, P. J.; Farmer, P. B.; Foster, A. G.; Gilby, E. D.; Jarman, M. Cancer Treat. Rep. **1976**, 60, 483.
211. Cox, P. J.; Farmer, P. B.; Jarman, M.; Jones, M.; Stec, W. J.; Kinas, R. P. Biochem. Pharmacol. **1976**, 25, 993.
212. Morrison, J. D.; Masler, W. F.; Neuberg, M. K. Adv. Catal. **1976**, 25, 81.
213. Amma, J. P.; Stille, J. K. J. Org. Chem. **1982**, 47, 468.
214. Horner, L.; Balzer, W. D. Tetrahedron Lett. **1965**, 1157.
215. Horner, L. Pure Appl. Chem. **1964**, 9, 225.
216. Horner, L.; Winkler, H.; Rapp, A.; Mentup, A.; Hoffman, H.; Beck, P. Tetrahedron Lett. **1961**, 161.
217. Korpium, O.; Lewis, R. A.; Chickos, J.; Mislou, K. J. Am. Chem. Soc. **1968**, 90, 4842.
218. Chodkiewicz, W.; Jore, D.; Pierrat, A. J. Organomet. Chem. **1979**, 174, C21.
219. Chodkiewicz, W.; Jore, D.; Wodzki, W. Tetrahedron Lett. **1979**, 1069.
220. Mathey, F.; Mercier, F. Tetrahedron Lett. **1979**, 3081.
221. Omelanczuk, J.; Perlikowska, W.; Micolajczuk, M. J. Chem. Soc., Chem. Commun. **1980**, 24.
222. Micolajczyk, M.; Omelanczuk, J.; Perlikoska, W. Tetrahedron Lett. **1979**, 35, 1531.
223. Chan, T. H. J. Chem. Soc., Chem. Commun. **1968**, 895.
224. Tani, K.; Brown, L. D.; Ahmed, J.; Ibers, J. A.; Yokota, M.; Nakamura, A.; Otsuka, S. J. Am. Chem. Soc. **1977**, 99, 7876.
225. Otsuka, S.; Nakamura, A.; Kano, T. J. Am. Chem. Soc. **1971**, 93, 4301.
226. Grocott, S. C.; Wild, S. B. Inorg. Chem. **1982**, 21, 3526.
227. Grocott, S. C.; Wild, S. B. Inorg. Chem. **1982**, 21, 3535.
228. Omelanczuk, J.; Micolajczuk, M. J. Am. Chem. Soc. **1979**, 101, 7292.

229. Krawiecka, B.; Skrzypczynski, Z.; Michalski, J. Phosphorus **1973**, 3, 177.
230. Mikolajczyk, M.; Drabowicz, J.; Omelanczuk, J.; Fluck, E. J. Chem. Soc., Chem. Commun. **1975**, 382.
231. Lakshmikantham, M. V.; Cava, M. P.; Garito, A. F. J. Chem. Soc., Chem. Commun., **1975**, 383.
232. Vandenberg, G. R.; Platenburg, D. H. J. M.; Benschop, H. P. J. Chem. Soc., Chem. Commun. **1971**, 606.
233. Szafraniec, L. J.; Szafraniec, L. L.; Aaron, H. S. J. Org. Chem. **1982**, 47, 1936.
234. De'ath, N. J.; Ellis, K.; Smith, D. J. H.; Trippett, S. J. Chem. Soc., Chem. Commun. **1971**, 714.
235. Omelanczuk, J.; Mikolajczuk, M. J. Chem. Soc., Chem. Commun. **1976**, 1025.
236. Crofts, P. C.; Kosolapoff, G. M. J. Am. Chem. Soc., **1953**, 75, 3379.
237. Mislow, K. Acc. Chem. Res. **1970**, 3, 321.
238. Benschop, H. P.; VanDenBerg, G. R. J. Chem. Soc., Chem. Commun., **1970**, 1431.
239. Bunich, B.; Wild, S. B. J. Am. Chem. Soc. **1970**, 92, 459.
240. Gordon, A. J.; Ford, R. A. "The Chemists Companion", John Wiley and Sons: New York, **1972**, 445.
241. Shibaski, M.; Terashimai, S.; Yamadai, S. Chem. Pharm. Bull. **1975**, 23, 279.
242. Bear, E.; Kates, M. J. J. Am. Chem. Soc. **1945**, 67, 1483.
243. Schwartz, R.; Geulen, H. Chem. Ber. **1957**, 90, 954.
244. Church, M. J.; Mays, M. J. Inorg. Nucl. Chem. **1971**, 33, 253.
245. Drew, D.; Doyle, J. R. Inorg. Synth. **1972**, 13, 48.
246. Kochi, I. K.; Tang, R. T.; Bernath, T. J. Am. Chem. Soc. **1973**, 95, 7114.
247. Belous, V. M.; Heksëeva, L. A.; Yagupolskii, L. M. Zh. Org. Khim. **1975**, 11, 1679.

248. Pirkle, W. H.; Finn, J. M. J. Org. Chem. **1981**, 46, 2935.
249. Pirkle, W. H.; House, D. W. J. Org. Chem. **1979**, 44, 1957.
250. Pirkle, W. H.; House, D. W.; Finn, J. M. J. Chromatogr. **1980**, 192, 143.
251. Jenkins, J. M.; Verkade, J. G. Inorg. Chem. **1967**, 6, 2250.
252. Clarence, L. M. U. S. Pat. Off. **1940**, 2,220,845.
253. Kirsanov, A. V.; Sherchenko, V. I. Z. Obsch. Chem. **1956**, 26, 74.
254. Abicht, H. P., Postdoctoral Research Associate, **1980-1981**, Iowa State University, unpublished results.
255. Mikołajczyk, M. Pure. Appl. Chem. **1980**, 52, 959.
256. Cooper, D.; Trippett, S.; White, C. J. J. Chem. Research (S), **1983**, 234.
257. Horner, L.; Jordon, M. Phos. Sulfur **1980**, 8, 235.
258. Snyder, L. R.; Kirkland, J. J. "Introduction to Modern Liquid Chromatography", John Wiley and Sons: New York, **1974**.
259. Tolman, C. A. J. Am. Chem. Soc. **1970**, 92, 2953.
260. Verkade, J. G.; Coskran, K. J. "Organic Phosphorus Compounds" (Kosolapoff, G. M.; Maier, L., Editors), Wiley-Interscience: New York, **1972**, 2.
261. Suzuki, K.; Jindo, A. Inorg. Chim. Acta **1980**, 44, 237.
262. Silverstein, R. M.; Bassler, G. C.; Morrill, T. C. "Spectrometric Identification of Organic Compounds", 3rd ed., John Wiley and Sons: New York, **1974**.

ACKNOWLEDGMENTS

I would like to express my sincere gratitude to Dr. John Verkade whose direction, guidance, enthusiasm, and support made this work possible. I would also like to thank Dr. Espenson, Dr. McCarley, Dr. Barton, and Dr. Swift for their assistance over the years, their service on the committee, and their review of this thesis.

I wish to acknowledge the assistance of Dr. Robert Jacobson and Dr. Jim Richardson in the crystallographic studies in this thesis.

I would like to thank the past and present members of Dr. Verkade's research group for their assistance and lively discussions.

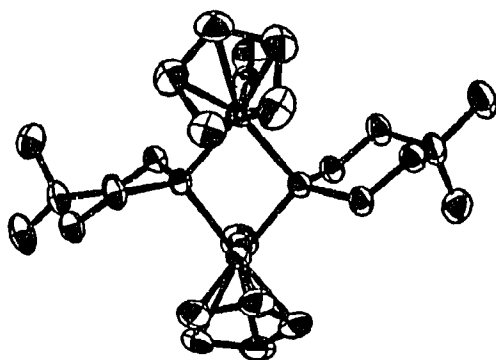
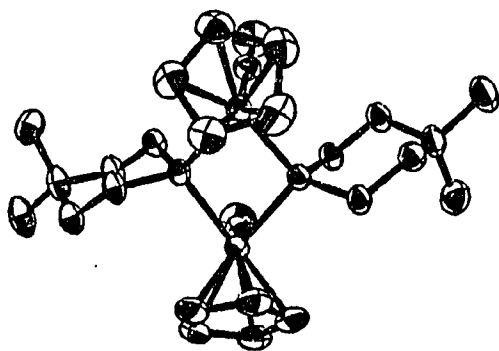
I wish to thank Dr. Dennis Johnson and Rev. Mark Sullivan, whose friendship and support have meant and continues to mean a great deal to me. A note of special thanks goes to the members of the "Tarnished Brass", Dr. Dave Stephenson, Dr. George Kizer, Mr. Roger Andersen, and Dr. John Verkade, of which I have been honored to be a charter member, for providing a lively and enjoyable diversion to my studies in chemistry. I also wish to express my appreciation to Ms. Elaine Wedeking for typing this thesis and for assistance and advice for staying within the required guidelines.

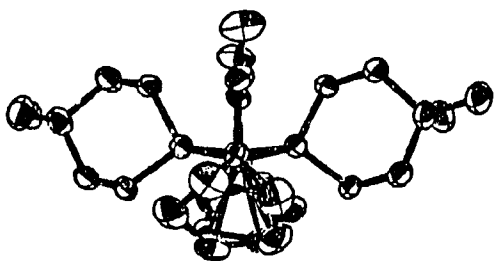
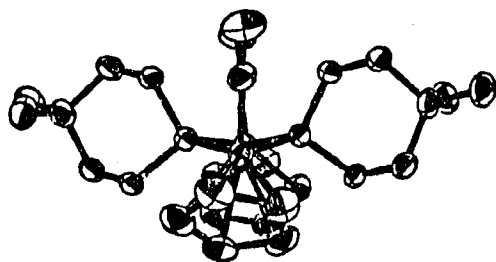
I wish to also acknowledge all the love and support shown to me by my parents, friends and family, both in Iowa and the great state of New York.

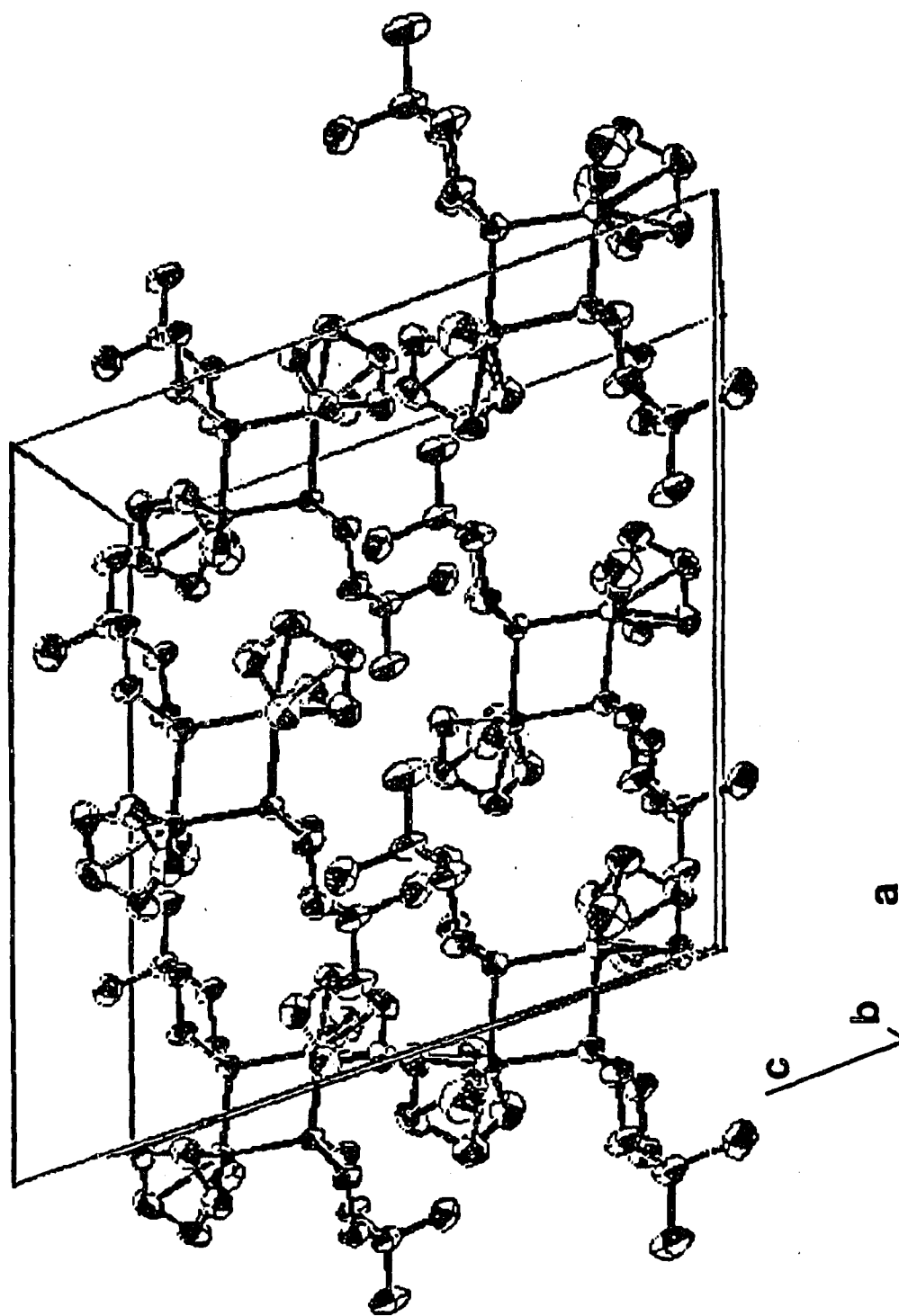
Finally, I wish to especially acknowledge the love, patience, and encouragement given to me by my wife Judy, without whom this work could

APPENDIX I

Stereopair Drawings and Unit Cell Drawing of
 $\text{cis-}[\text{Fe}(\eta^5\text{-Cp})(\text{CO})(\mu\text{-5,5-dimethyl-1,3,2-dioxaphosphorinane})]_2$

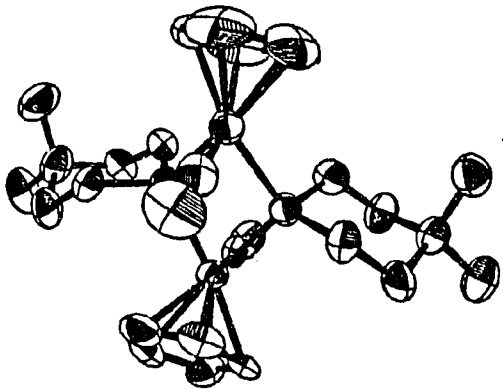
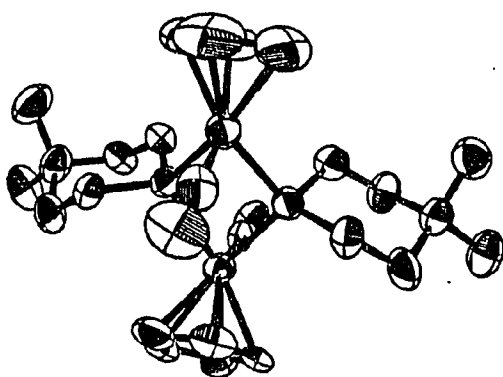


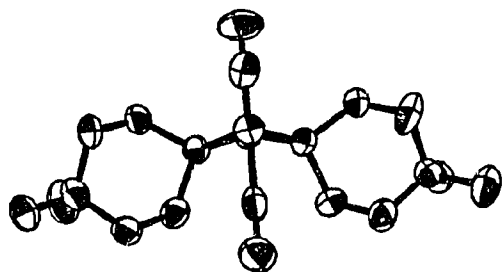
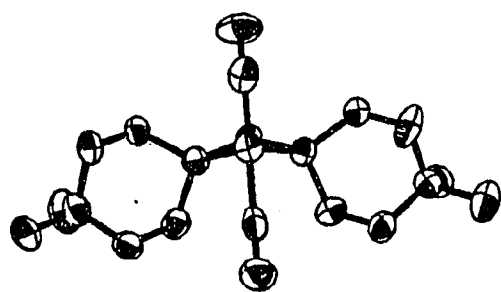


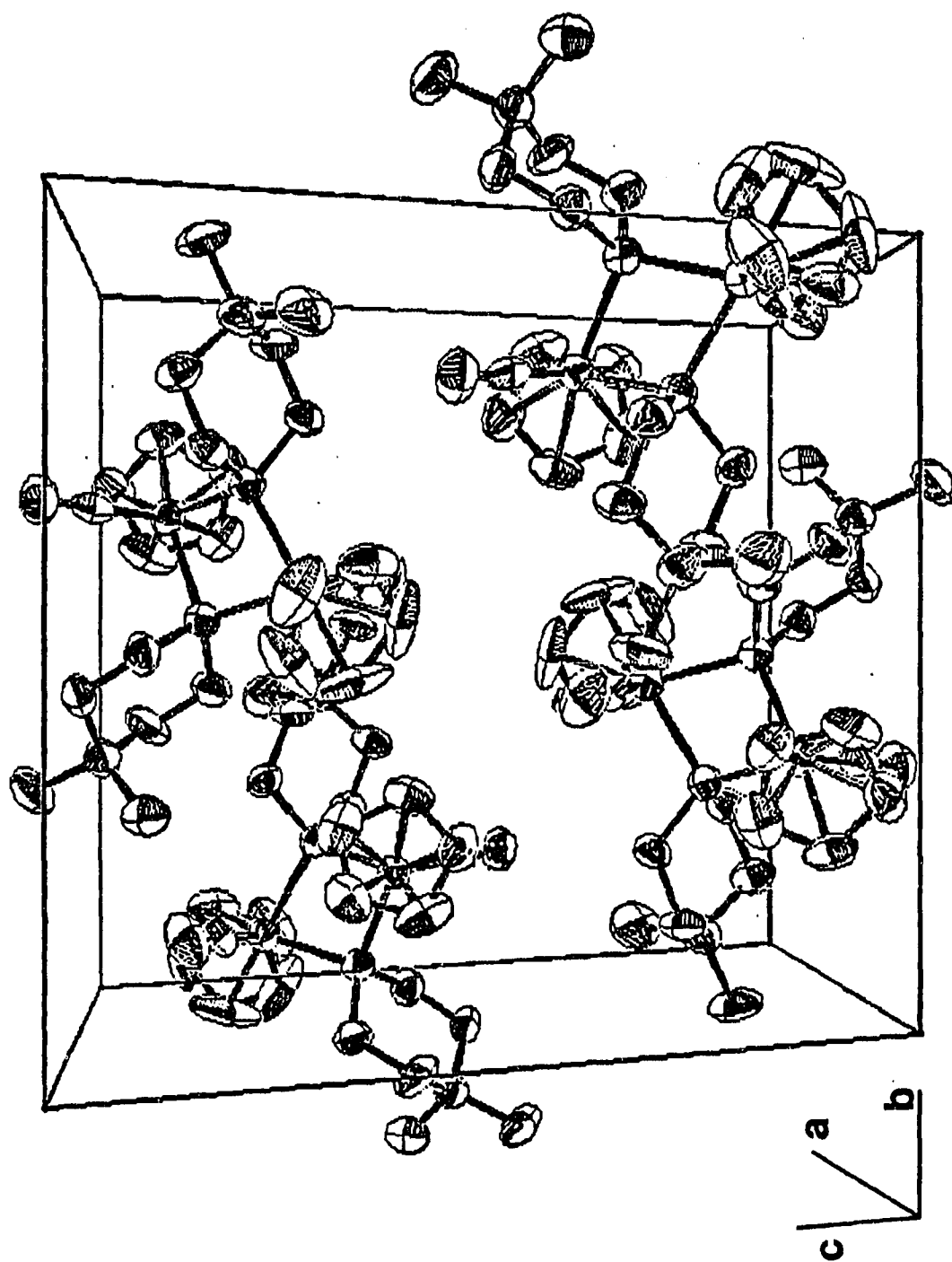


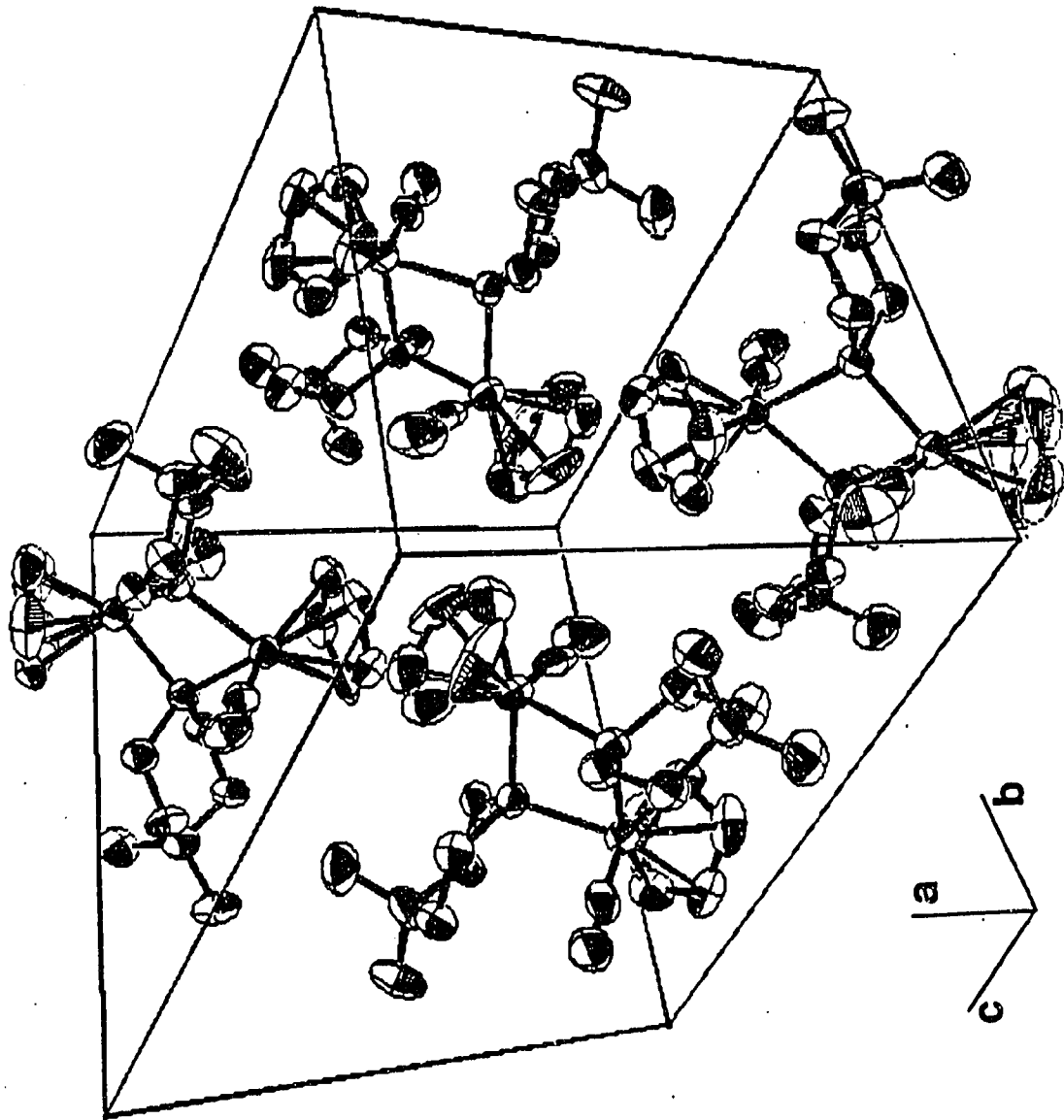
APPENDIX II

Stereopair Drawings and Unit Cell Drawings of
 $\text{trans-}[\text{Fe}(\eta^5\text{-Cp})(\text{CO})(\mu\text{-5,5-dimethyl-1,3,2-dioxaphosphorinane})]_2$









APPENDIX III

Stereopair Drawings and Unit Cell Drawing of

